Identification of molecular events associated with evolution of multifocal and metastatic urothelial cancer

Rafal Kamil Turo

MRCS

Submitted in accordance with the requirements for the degree of Doctor of Medicine

The University of Leeds

School of Medicine

October, 2014

The candidate confirms that the work submitted is his/her own and that appropriate credit has been given where reference has been made to the work of others.

Acknowledgements

This work was supported by Cancer Research UK.

Tumour tissue sectioning in preparation for DNA extraction was performed by Joanne Brown and Fiona Platt. Assessment of tumour's purity was performed by myself and Fiona Platt.

TMA slides for IHC were processed by Filomena Esteves. IHC was performed by myself on samples not included in the study to acquire the skills and learn the technique.

TMA slides were provided by Institute of Pathology (Professor Achim Fleischmann) and Department of Urology (Professor George N. Thalmann), University of Bern (Professor Roland Seiler), Bern, Switzerland

Immunohistochemistry scoring of TMAs was performed by myself, Dr Patricia Harnden, Consultant Histopathologist, St James's University Hospital, Leeds and Professor Maggie Knowles.

Ms Fiona Platt performed the TuMult analysis. Ms Fiona Platt and Dr Carolyn Hurst have helped me to perform clustering and Nexus analysis. These analyses have been performed initially by myself with supervision. Repeated analyses were performed by Ms Fiona Platt and Dr Carolyn Hurst.

aCGH and SNaPshot experiments were performed by myself.

Statistical analyses were performed by Helene Thygesen, Section of Epidemiology and Biostatistics, Leeds Institute of Cancer Studies and Pathology, St James's University Hospital, Leeds.

Personal acknowledgments

I would like to thank the following people for helping me during the course of this research:

My supervisors, Professor Maggie Knowles, Mr William Cross and Dr Patricia Harnden, for their unlimited support, patience and advice; Dr Carolyn Hurst and Ms Fiona Platt for teaching me all laboratory experiments and techniques; and everyone else in Lab 5 for their support and friendship during my time at CRUK.

I would like to thank my wife Ania for her caring encouragement and tolerance and my parents and sister for their endless support.

Abstract

Urothelial cell carcinoma of the bladder is characterized by multifocality. Identification of molecular events associated with multifocal disease will increase understanding of disease pathogenesis, aid development of targeted therapies and ultimately lead to reduced morbidity, mortality and healthcare costs. In the first part of the project, I determined genome-wide copy number alterations and mutations in key genes in synchronous multifocal non-invasive tumours in order to:

• Assess monoclonal or oligoclonal origin.

• Assess molecular heterogeneity of tumours within one patient as this might imply differential response to treatment.

• Identify specific features of multifocality i.e. is multifocal disease different from solitary disease matched for grade and stage.

One-way hierarchical cluster analysis of copy number and mutational data of *FGFR3*, *PIK3CA* and RAS genes from 66 tumours was performed to assess the relationships between the individual tumours of each patient. Tumours separated into 3 main clusters with tumours from the same patient tending to group together. The majority of tumours from the same patient shared at least a few copy number alterations indicating monoclonal origin.

Comparison of multifocal and solitary tumours of the same grade and stage revealed that multifocal tumours exhibited higher frequencies of chromosomal alterations than solitary counterparts.

In the second part of the project I used immunohistochemistry on tissue microarrays to assess whether the FGFR3 expression status of a primary bladder tumour can serve as a surrogate for the related metastases.

Expression levels in two evaluable tissue spots from the primary tumour (n= 97) or the lymph node metastases (n = 90) showed a high level of concordance (primary tumour: OR=8.6, p=0.000003; metastases: OR=16.7, p=0.0000002).

With few exceptions, the levels of FGFR protein expression were the same in matched primary and metastatic lesions (p=0.78), suggesting that expression in the primary tumour can be used to select FGFR-targeted therapy for disseminated disease.

Table of Contents

List of Tables

List of Figures

Abbreviations

aCGH	array Comparative Genomic Hybridization
amp	amplicon
bp	base pairs
Cis	Carcinoma *in situ*
CT	cancer-testis
DAB	3,3- diaminobenzidine terahydrochloride
ddNTPs	dideoxynucleotides
dH_2O	distilled water
DNA	Deoxyribonucleic acid
dNTP	Deoxyribonucleotide triphosphate
dsRNA	Double stranded RNA
EBV	Epstein-Barr virus
EDTA	Ethylenediamine tetraacetic acid
EGFR	epidermal growth factor receptor
EORTC	The European Organization for Research and Treatment of Cancer
F&T	freeze-thaw
FFPE	formalin-fixed paraffin wax-embedded
FISH	fluorescence in situ hybridization
GAP	guanosine triphosphatase activating protein
GAPDH	glyceraldehyde-3-phosphate dehydrogenase
GC	gemcitabine and cisplatin
GDI	guanine nucleotide dissociation inhibitor
GDP	guanosine diphosphate
GEF	Guanine nucleotide exchange factor
GTP	guanosine triphosphate
h	Hour

HER2	human epidermal growth factor receptor-2
IHC	immunohistochemistry
Kb	Kilo-bases
LOH	Loss of heterozygosity
M	molar
MAPK	Mitogen-activated protein kinase
MAPK	mitogen-activated protein kinases
Mb	megabase
$MgCl_2$	Magnesium chloride
Min	Minute
miRNA	micro RNA
mM	miliM
MMP	Matrix metalloproteinases
MMR	Mismatch repair
mRNA	Messenger RNA
MSI	microsatellite instability
mut	mutation
MVAC	methotrexate, vinblastine, doxorubicin and cisplatin
NaAc	Sodium acetate
OS	overall survival
PBS	Phosphate buffered saline
PCR	Polymerase chain reaction
PDGFR	Platelet-derived growth factor receptors
PI3K	phosphatidylinositol 3-kinase
PI3K	Phosphatidylinositol-4,5-bisphosphate 3-kinase
PIP2	Phosphatidylinositol 4,5-bisphosphate
PIP3	Phosphatidylinositol (3,4,5)-trisphosphate
PLC-γ	phospholipase C-gamma
PUNLMP	papillary urothelial neoplasm of low malignant

	potential
RALGDS	Ral guanine nucleotide dissociation stimulator
RFS	recurrence free survival
RNA	Ribonucleic acid
s	Seconds
S	stroma
SDS	Sodium dodecyl sulphate
SSC	saline-sodium citrate buffer
SSCP	single-stranded conformation polymorphisms
SSO	Senior Scientific Officer
ssRNA	Single stranded RNA
st	same transition
T	tumour
TBE	Tris borate EDTA
TCC	transitional cell carcinoma
TKI	Tyrosine Kinase Inhibitors
TMA	tissue microarray
Tris-HCl	Tris hydrochloride
TSG	Tumour suppressor gene
U	Units
UC	urothelial cancer
UV	Ultraviolet
V	Volt
v/v	Volume per volume
VEGFR	Vascular Endothelial Growth Factor Receptor
w/v	Weight per volume
WHO	World Health Organisation
WT	Wild type

Aims

Bladder cancer is commonly characterized by development of multifocal tumours in the same patient and tumour multifocality is associated with poorer outcomes. Cytogenetic studies have provided evidence of non-random chromosomal aberrations, which can vary from few changes in low stage and/or grade tumours to highly deranged karyotypes in advanced, muscle-invasive disease [1]. Strong association between tumour's karyotypic complexity and stage and grade has been noted in multiple studies [2]. This might indicate that tumours progressively accumulate genetic alterations on bladder carcinogenesis pathway. Analysis of bladder tumours and cell lines with aCGH described multiple genomic changes underlying neoplastic development [3-5]. These studies provided detailed evidence on deleted or amplified regions of tumours of different stage and grade with no distinction of tumours multifocality. In our study I aimed to determine genome-wide copy number alterations and mutations in key genes in synchronous multifocal tumours in order to: assess tumour monoclonality or oligoclonality; assess the molecular heterogeneity of tumours; identify unique features related to multifocality as opposed to solitary disease matched for grade and stage. I hypothesise that tumours multifocality might represent a significant risk factor for tumours progression and/or recurrence in superficial bladder cancers. Non-muscle invasive multifocal tumours at the cytogenetic level might resemble more advanced disease than non-multifocal tumours matched for stage and grade. One of the methods chosen to test the hypothesis was aCGH. This technique enables the characterisation of large chromosomal aberrations as well as amplified and deleted regions to the level of specific candidate genes.

In the second part of the project I used immunohistochemistry on tissue microarrays to assess whether the FGFR3 expression status of a primary bladder tumour can serve as a surrogate for the occurrence of related metastases.

Chapter 1
Introduction

1.1 Bladder cancer

Bladder cancer is the most frequently occurring tumour of the urinary tract. Worldwide an estimated 386,000 new cases of bladder cancer were diagnosed in 2008 representing about 3.2% of all cancers. Transitional cell carcinoma is the most common type of bladder cancer in Europe, comprising 90-95% of cases in the UK, bladder cancer is the seventh most common cancer, accounts for approximately 1 in 30 new cases of cancer each year. It is more common in males than in females (3.7:1) and represents the sixth cause of death in males and the thirteenth in females [6]. The high incidence rates of bladder cancer are observed in Western Europe, North America and Australia. The areas associated with endemic schistosomiasis in Africa and the Middle East are also reported to have a high incidence rate of bladder cancers, majority of which are squamous cell carcinomas. The median age for diagnosis is 65 years old, and the disease is seldom diagnosed before 40 years old.

1.1.1 Histology, presentation and survival

At initial presentation over 70% of patients have low-grade tumours confined to the urothelium or submucosa (Ta, T1, Cis). This is depicted in Figure 1.1 and 1.2 and described in text below. The primary treatment for these patients consists of transurethral resection and in the majority cases

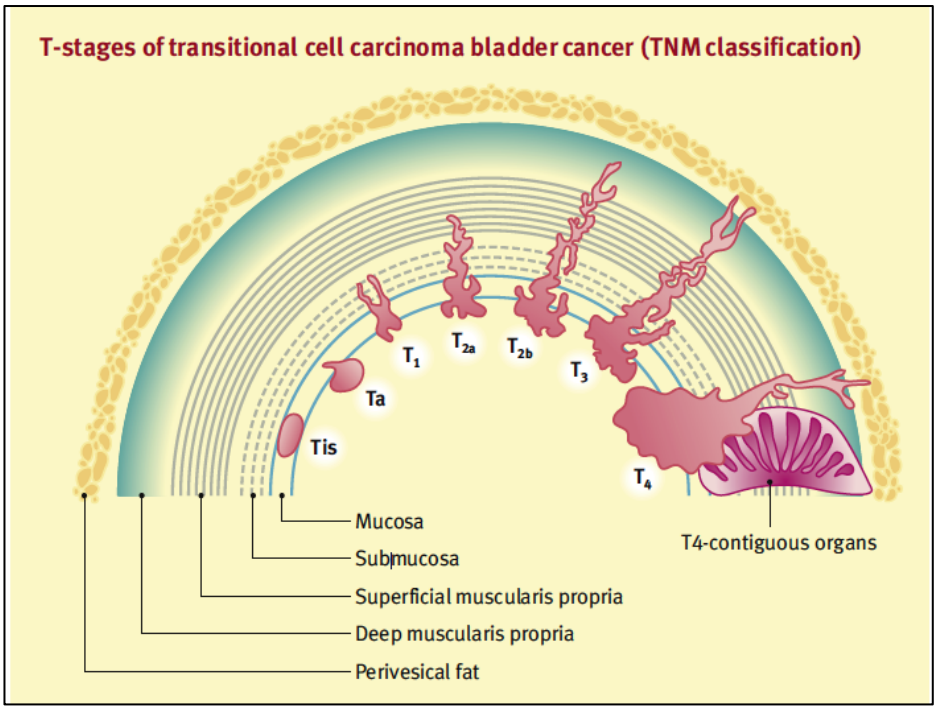

Figure 1.1: The staging of TCC
Ta: Superficial papillary tumour that has not invaded the lamina propria (i.e. not breached the basement membrane)
T1: Invasion of the lamina propria
T2: Tumour invades the superficial (T2a) or deep muscle (T2b)
T3: Tumour invades the peri-vesical fat microscopically (T3a) or macroscopic (T3b)
T4: Invades the pelvic viscera (T4a invade the prostatic stroma, rectum, vagina or uterus; T4b tumours extend to the pelvic sidewall or abdominal walls). Adapted from Turo, 2012 [7]

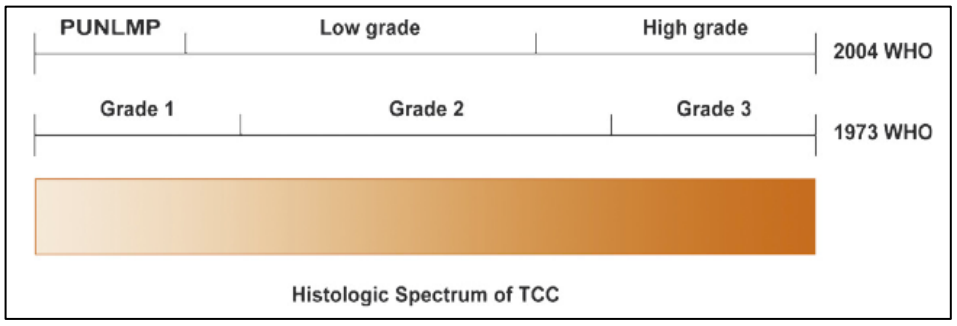

Figure 1.2: Comparison of the 1973 and 2004 WHO grading system [8, 9]. The 1973 WHO grade 1 and grade 2 carcinomas are not interchangeable with the 2004 WHO PUNLMP and low grade carcinoma category. Some grade 1 carcinomas are assigned to the PUNLMP category, and some to the low-grade carcinoma category. Similarly, grade 2 carcinomas are assigned, some to the low-grade carcinoma category, and others to the high-grade carcinoma category. All grade 3 tumours are assigned to the high-grade carcinoma category. WHO = World Health Organization; PUNLMP = papillary urothelial neoplasm of low malignant potential. Adapted from MacLennan, 2007 [8]

additional administration of intravesical immuno- or chemo-therapy to reduce the risk of disease recurrence and/or progression. Fifteen to thirty per cent of these tumours show grade and stage progression, eventually requiring radical treatment [10]. However, these tumours despite being classified as ‘lower risk’ tumours tend to re-occur after primary treatment and therefore require intensive clinical follow up, in the form of cystoscopic surveillance . The risk of recurrence in these patients with superficial disease can be as high as 70% [11]. Due to an extensive follow up regime , transurethral resections of recurrences and treatment with intravesical instillations bladder cancer is the most expensive malignancy to treat per patient [12]. Two large studies identified that the average cost of treatment per patient was $65,158 (US dollars).The estimated lifetime costs for patients averaged $99,270 in the best-case scenario and$120,684 in the worst-case scenario [13].The calculated 5-year net cost of bladder cancer was one billion dollars (one of the highest among all cancers) in 2008 [14]. Therefore bladder cancer is a major public health issue and development of diagnostic, treatment and surveillance methods is required. The need for better prognostic tools to individualize management and care is also of high priority.
Twenty to thirty per cent of patients with bladder cancer present with muscle invasive disease, which has a less than 50% disease specific survival at 5 years. Lymph node involvement reduces the 5- and 10-year recurrence-free survival rates to 35 and 34%, respectively [15, 16].

Current gold standard treatment for muscle invasive bladder cancer is bilateral pelvic lymphadenectomy and radical cystoprostatectomy in men and anterior exenteration in women. This treatment can offer long-term disease free survival in up to 70% in patients with organ-confined disease [17].

Pelvic lymphadenectomy is performed for staging and prognostic purposes, but also potentially offers a therapeutic role. It has been reported that up to 30% of patients with pelvic lymph node metastasis remained recurrence free 5 years after cystectomy and pelvic lymphadenectomy. The optimal extent of lymphadenectomy still has not been determined and numerous approaches to assess the subject have been applied (overall lymph node count, number of positive lymph nodes, lymph node density) [18-23].

In the majority of cases of muscle invasive bladder cancer or lymph node positive bladder cancer surgical resection is not sufficient and additional systemic therapy is required. Therefore, from the therapeutic point of view, it is more important to eradicate the micro-metastasis that often cannot be identified by preoperative imaging rather than increase local curability by improving radical cystectomy results. Systemic chemotherapy using drug combination regimens is the standard therapy for metastatic transitional cell carcinoma of the bladder. The gold standard treatment was considered the combination of four drugs: methotrexate, vinblastine, doxorubicin and cisplatin (MVAC) as described by Sternberg *et al* [24] and Chester *et al* [25]. The median survival for patients on this regime is 11-13 months with a 5 year progression free survival of only 3% [26]. Subsequent studies revealed significant toxicity associated with MVAC including serious complications of neutropenia, mucositis and toxic death in 3-4% of cases. Therefore MVAC regime has subsequently been replaced with the combination of gemcitabine and cisplatin (GC) [24, 27-29]. A large randomized study comparing both regimes demonstrated similar response rates (GC, 49% and MVAC, 46%; $p = 0.51$), progression-free survival (GC, 7.7 months and MVAC, 8.3 months; $p = 0.63$), and median survival (GC, 14 months and MVAC, 15.2 months; $p = 0.66$), with significantly improved tolerability and safety profile for the GC-treated patients with locally advanced or metastatic TCC. However, cisplatin-containing chemotherapy is only suitable for patients with good performance, adequate renal function and no comorbidity that prevents high-volume hydration [30, 31].

1.1.2 Prognostic factors

At present there are limited number of established prognostic factors for recurrence, progression, and overall survival based on histological and anatomical appearance of the bladder cancer. These include: tumour grade, T stage classification, associated carcinoma *in situ* (Cis), multifocality and the presence of lymph node metastasis. Based on these factors, the European Organization for Research and Treatment of Cancer (EORTC)

has published risk tables to assist clinicians in creation of individualised management plans and surveillance protocols according to calculated risk of recurrence and progression [32]. Despite the efforts to identify patients that are at high risk of progression and/or recurrence and reduce the frequency of patients' clinical visits, nearly 75% of cystoscopies at follow up are normal [33]. As a consequence there is an on-going search for novel markers to predict the chance of recurrence and guide therapeutic interventions on an individual basis.

1.1.3 Molecular features of bladder cancer

Bladder cancer is a heterogenous disease that significantly differs with regards to histopathological characteristics and clinical presentation. Improvements in classification that lead to better bladder cancer management, together with extensive characterization of the molecular alterations will lead to improved understanding of this disease and ultimately enhance prognostication and treatment modalities. There has already been significant progress in identification of various epigenetic and genetic alterations that are involved in the development and progression of bladder tumours [34]. Our knowledge has been improved on the nature of different molecular events that occur most frequently and are associated with a specific type of tumour. Based on tumours' molecular characteristics a new subcassification can be achieved in the near future.

Molecular features of invasive and non-muscle invasive bladder (NMIBC) cancer are distinct and commonly present different spectrum of genetic and epigenetic changes. Alterations identified and correlated with NMIBC include those involving oncogenes NRAS (1p13), HRAS (11p15), KRAS2 (12p12), FGFR3 (4p16), PIK3CA (3q26), CCND1 (11q13), MDM2 (12q13) and tumour suppressor genes DBC1 (9q32–33), PTCH (9q22), CDKN2A (9p21). Genomic alterations reported in MIBC frequently involve *CDKN2A* (9p21), *PTEN* (10q23), *RB1* (13q14), *TSC1* (9q34) and *TP53* (17p13).

1.1.4 Role of FGFR3 receptor in bladder cancer

Over 50% of primary bladder tumours harbour activating mutations in the *FGFR3* gene [35, 36]. The majority of these somatic mutations are similar to germ line mutations responsible for skeletal disorders such as achondroplasia, hypochondroplasia, severe achondroplasia with developmental delay and acanthosis nigricans (SADDAN) and thanatophoric dysplasia [37]. The early study of *FGFR3* mutations in bladder cancer, was performed by Capellen and colleagues who identified mutations in 35% of bladder carcinomas that were identical to two lethal forms of dwarfism [35]. This rather unexpected finding led to further extensive investigations on *FGFR3* receptor in bladder cancer and associated mutations of *FGFR3*. To date, studies have identified 11 mutations of this receptor [35, 38-47]. It has also become evident that these are associated with superficial bladder cancer rather than muscle invasive disease [39, 45]. The overall frequency and distribution of these is shown in Table 1.1. Among the most frequent mutations are S249C (66.6%) and Y375C (15.1%); and the least frequent are: S373C (0,1%), G282R (0,1%), K652Q (0,1%).

The mutation S249C causes ligand independent dimerization and signalling by producing cysteines in the extracellular domain of the receptor. This process is mediated by conversion of a serine residue between immunoglobulin domains II and III and thus preventing the formation of normal disulphide bonds within the chains or by enabling the formation of bonds between chains [48]. *FGFR3* mutations are also found in benign skin conditions, including seborrheic keratoses, benign skin lesions commonly seen in elderly patients [49, 50] and in epidermal nevi [51], and seem to be absent in other studied malignancies such as breast, prostate, skin, brain, ovarian, lung, renal, oesophageal and stomach. The only other malignancy where *FGFR3* mutations were found is multiple myeloma and cervical carcinoma [51, 52].

Mutation	Frequency (%)	Exon	Part of receptor
S249C	66.6	7	Extracellular
R248C	9.7	7	Extracellular
G372C	4.3	10	Transmembrane
S373C	0.1	10	Transmembrane
Y375C	15.1	10	Transmembrane
G282R	0.1	10	Transmembrane
A393E	1.2	10	Transmembrane
K652M	1.0	15	Kinase domain
K652Q	0.1	15	Kinase domain
K652E	1.4	15	Kinase domain
K652T	0.4	15	Kinase domain

Table 1.1 Relative frequencies and positions of *FGFR3* mutations in bladder cancer (all grades and stages). Frequencies are the percentage of all *FGFR3* mutations described to date. Adapted from Knowles, 2005 [53]

Four out of five family members of FGF receptors (FGFR1-5) harbour tyrosine kinase function. They play a significant role in cells differentiation, apoptosis, growth, adhesion and mobility [54] and activation of these receptors by gene overexpression or mutation may lead to tumour development. Once FGFR is activated, signal is transduced through three pathways: phosphatidylinositol 3-kinase (PI3K), mitogen-activated protein kinases (MAPK) and phospholipase C-gamma (PLC-γ); and this leads to the regulation of critical processes within the cell such as migration, survival, growth and differentiation [55]. (Figure 1.3).

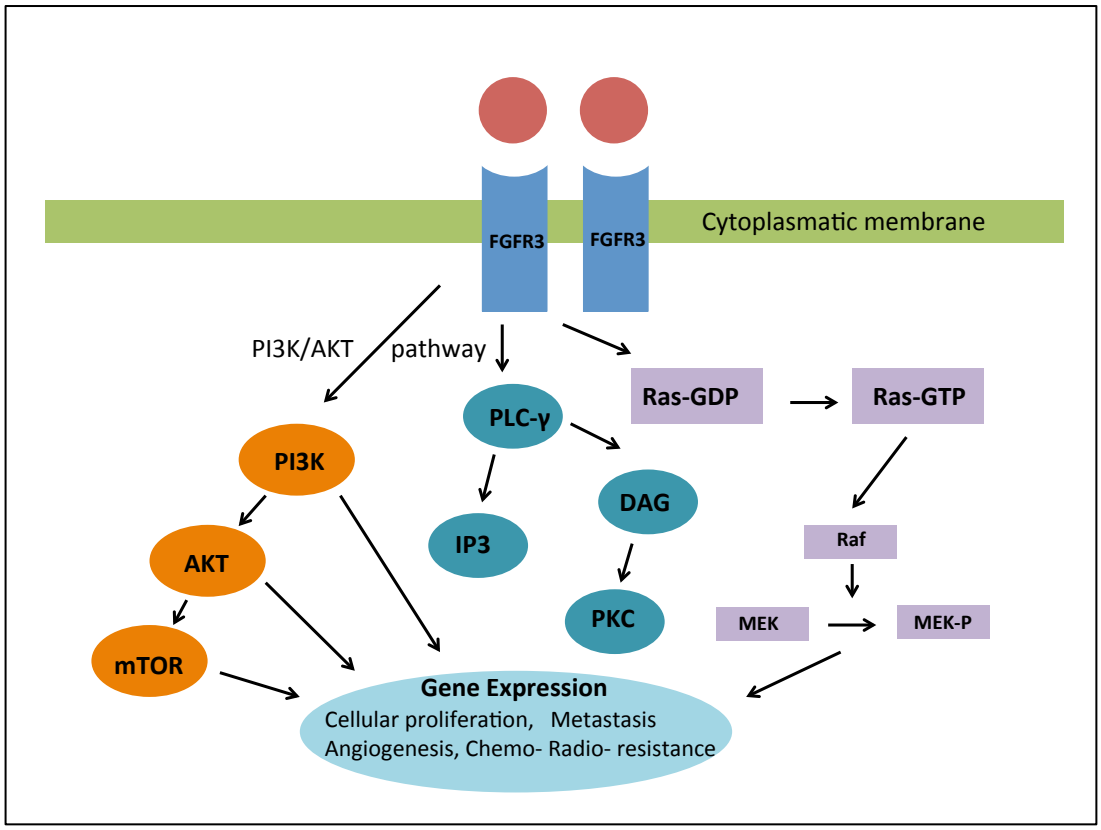

Figure 1.3: The FGFR signaling pathway. Once FGFR3 is activated by ligand binding, signal is transduced through three pathways: phosphatidylinositol 3-kinase (PI3K), mitogen-activated protein kinases (MAPK) and phospholipase C-gamma (PLC-γ), which then activates RAS and downstream RAF and MAPK pathways

FGFRs consist of an extracellular domain that includes an amino terminal hydrophobic signal peptide, three immunoglobulin-like domains, a hydrophobic transmembrane domain, and an intracellular tyrosine kinase domain, Figure 1.3 [56]. The FGFR family is highly conserved throughout evolution. The receptor's ligands (fibroblast growth factors) bind to extracellular Ig-like domains II and III, leading to downstream signalling [57]. It has been confirmed that the ligand-receptor binding is not only dependent on the specific receptor but also by alternative RNA splicing of FGF receptors in the Ig domain. This generates to two alternative isoforms 3b and 3c [56, 58-60].

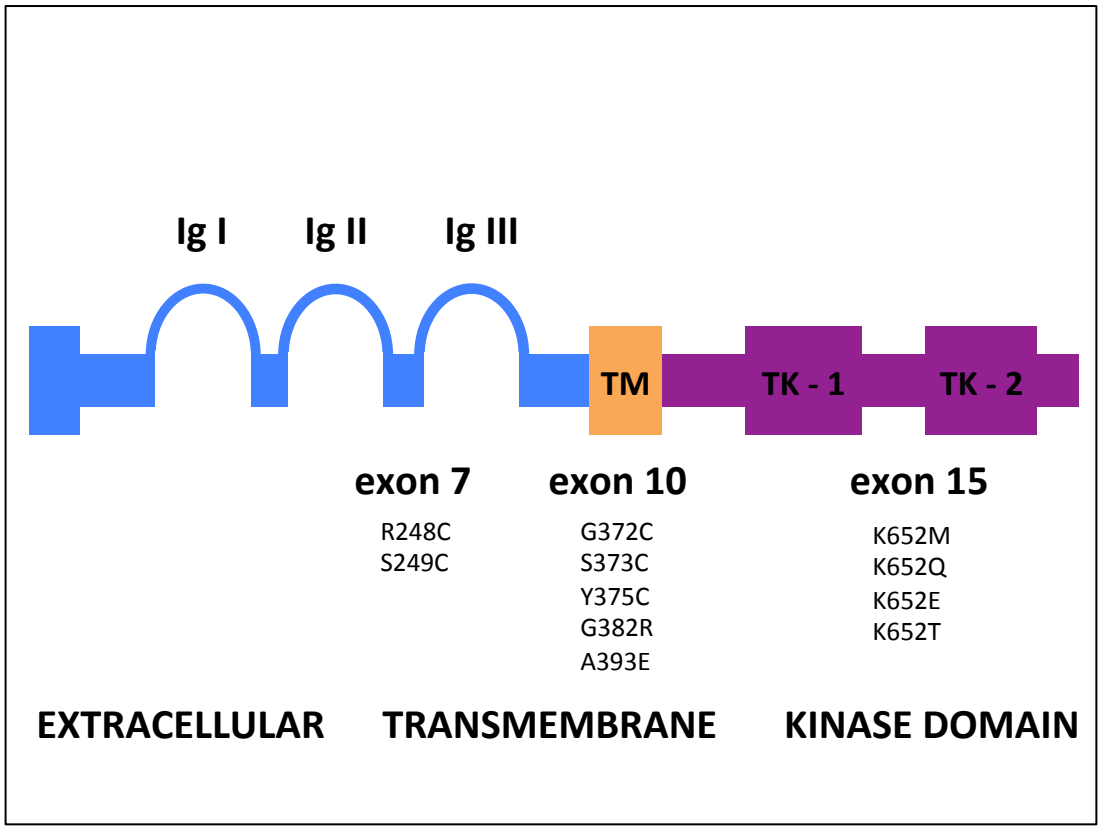

Figure 1.4: FGFR3 receptor structure. IgI, IgII, IgIII, immunoglobulin-like domains; TK-1, TK-2, split tyrosine kinase domain, TM Transmembrane. Frequent mutations occur in three regions of the *FGFR3* gene, located in exons 7, 10 and 15

Studies explaining the role of *FGFR3* mutation status in tumour development have been performed in urothelial hyperplasia, which is thought to be an early bladder cancer precursor. Hyperplastic lesions are commonly found adjacent to bladder cancer of different stages and grades.The study examining these lesions in 30 patients with simultaneous or consecutive papillary tumours, it was found that *FGFR3* mutation was present in 23% of hyperplasias and simultaneous chromosome 9 LOH in 30%. In 7% of patients, *FGFR3* mutation alone was present, and in 20% of cases chromosome 9 LOH alone was found. The authors of this study concluded that chromosome 9 losses might occur earlier than *FGFR3* mutation during the development of papillary TCC [61]. Further evidence confirming an early role of *FGFR3* mutation in bladder tumorigenesis has come from studies examining papillomas, which are considered by the majority of

histhopathologists regarded as precursors of TCC. In one study, examining 12 samples of urothelial papillomas, *FGFR3* mutation was found in 75% [46]. Another way of assessing the role of *FGFR3* mutation status and examining its time of appearance along the tumour development pathway, is the examination of different areas that represent different tumour stages within the same tumour from the same patient. Knowles and colleagues showed that mutation status was found to be different in different regions of tumour blocks from 8 of 158 patients [62]. Interestingly in most of the cases the mutation was found in the non-invasive component of the tumour. Two out of 8 samples were also reported as multifocal. It might be suggested that *FGFR3* mutations occur early in tumour development and the allele containing the *FGFR3* mutation is lost in the high stage region at later stage or that a small subset of *FGFR3* wild-type cells present in the low stage tumour had progressed and overgrown the remaining part of the tumour.

When the presence of *FGFR3* mutation was examined in relation to other molecular abnormalities it was found that RAS gene mutations and *FGFR3* mutations are mutually exclusive [63]. This mutual exclusivity phenomenon of both mutations may be explained by activation of the same RAS-MAPK pathway by either event [64] and this may represent an alternative means of contributing to the same phenotype on urothelial cancer cells.

1.1.5 Role of RAS genes in bladder cancer

In humans more than 100 members of small Ras proteins have been identified [65]. The majority of them do not exceed 30 kDa and they bind and hydrolyze guanosine triphosphate (GTP), cycling between a GTP active state and an inactive guanosine diphosphate (GDP) state, Figure 1.5. In cells they act as mediators in signal transduction and membrane trafficking playing important role in cell cycle control, apoptosis regulation, involvement in endocytosis and exocytosis, adhesion regulation, cell cycle progression

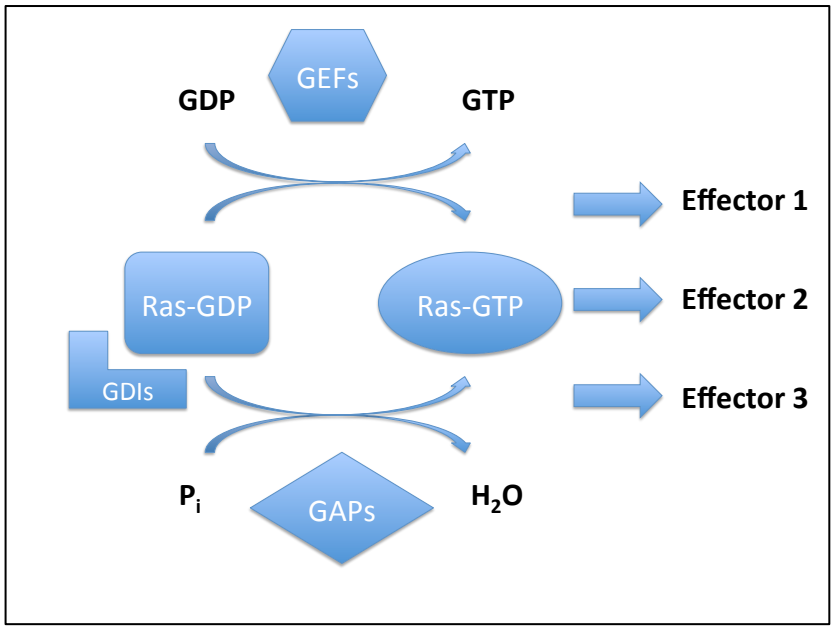

Figure 1.5: GTP/GDP cycle of Ras proteins. Monomeric G proteins cycle through GTP bound and GDP bound. This cycle is regulated by GEFs, which stimulate exchange of GDP for GTP, by GAPs, which stimulate hydrolysis of GTP, and by GDIs, which bind to GDP bound form and inhibit nucleotide exchange. GTP bound form is capable of stimulating various downstream effectors. Guanine nucleotide exchange factors (GEFs), guanosine triphosphate (GTP), guanosine diphosphate (GDP), guanine nucleotide dissociation inhibitors (GDIs), guanosine triphosphatase activating proteins (GAPs). Effectors regulate: cell cycle, apoptosis, involvement in endocytosis and exocytosis, adhesion, cell cycle progression and cell motility.

and cell motility [66]. The RAS family is divided into 11 members, including 5 RAS (N-RAS, K-RAS2, H-RAS, M-RAS, and R-RAS), 4 Rap and 2 Ral proteins. RAS proteins in mutated and/or overexpressed form are relatively common in human cancers, present in about 30% of tumours [67]. Activating mutations in RAS genes result in a constitutively active GTP bound form of the protein. Three RAS genes (H-RAS, K-RAS and N-RAS) encode highly homologous proteins with only significant amino acid differences at the C-terminal (40 amino acids). The function of this region is primarily in localizing these proteins inside the cell. All 3 proteins, encoded by these genes are associated with the plasma membrane. H-RAS and N-RAS are also found in significant amounts on endomembranes [68]. The three well characterized

effectors of RAS are RAF - protein kinases involved in mitogen activated protein (MAP) kinase signalling cascades, PI3 - lipid kinases that play role in inositol phospholipid signalling by generating PIP3 from PIP2 and a family of GEFs (RALGDS) (Figure 1.6). Point mutation of RAS gene leads to subsequent oncogenic activation of the phosphatidylinositol 3-kinase (PI3K) signalling pathway through the interaction of RAS with p110α unit [69].

Activating *HRAS* mutations were first discovered in bladder cancer [70]. The frequency of *HRAS* mutations in bladder cancer has been assessed in multiple studies, which reported a widerange of frequencies from 3% to 84% [70-73]. This range may be potentially due to various methods involved, differences of sensitivities or potential methodology errors. It is generally accepted that activating mutations in *HRAS* or *KRAS2* occur in approximately 13% of human bladder tumours [63, 74].

There was no correlation between tumour's stage/grade and RAS mutation status. To my knowledge there is no reported literature on the RAS mutation status in multifocal bladder cancer.

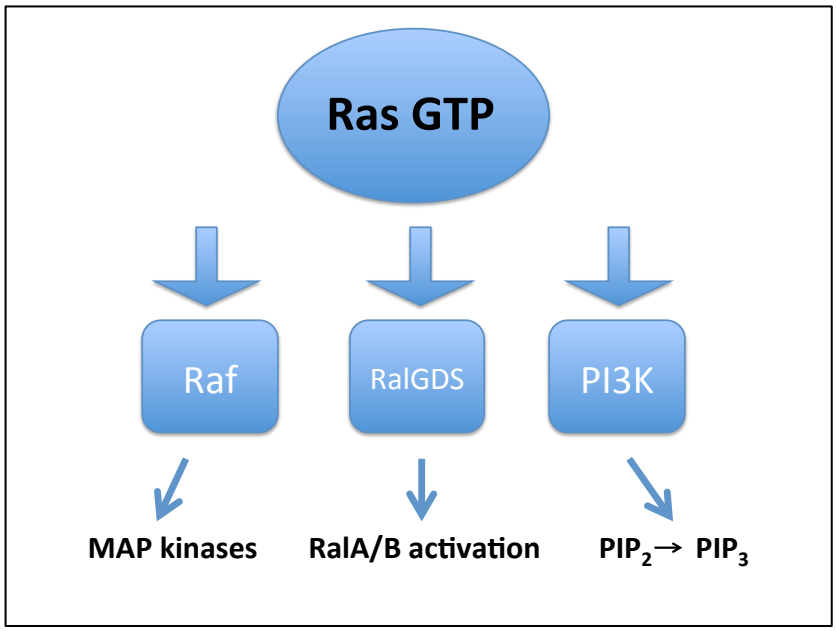

Figure 1.6: Common Ras effectors. Three best characterized effectors stimulated by Ras-GTP are Raf, which is protein kinase linked to MAP kinase cascades; RalGDS, exchange factor (GEF) for RalA and RalB, which stimulates their activation to GTP bound form, and lipid kinase

PI3K, which drives production of PIP3, contributing to activation of many cellular proteins by recruiting them to plasma membrane

1.1.6 Role of PI3K pathway and PIK3CA in bladder cancer

The PI3K pathway plays a significant role in cell proliferation, growth, and survival [75]. Multiple genes altered along this pathway are involved in tumorigenesis, including tumour suppressor genes (eg. *PTEN*) and proto-oncogenes (eg. *PIK3CA*) [76-81]. Commonly signalling is up-regulated in this pathway by mutation, deletion or amplification in sporadic cancers [82, 83]. Mutations of *PIK3CA* have been recently discovered in bladder cancer, which seems to correlate with low stage and grade tumours [84]. *PIK3CA* and Ras commonly interact with each other [69, 85] and when both mutations are present two pathways, mitogen-activated protein kinase and PI3K pathway, are activated [39]. When Knowles and colleagues analysed mutation frequencies of *PIK3CA*, it was discovered that the overall mutation frequency was 25.3% in tumours and cell lines [86]. In previous studies the overall frequency rate was reported as 13% and the mutation presence correlated with tumour stage: 65.5% of Ta, 11.5% of T1 and 23% of ≥T2 stage tumours [84]. The most frequent mutations in bladder cancer were E545K and E542K as opposed to several other types of cancer, where H1047R was most common [87]. Similarly, a study performed by Sjödahl *et al.* found 17% of mutated cases in the extended series of tumours (n = 218) [88] with a significantly higher proportion of *PIK3CA* mutations seen in Ta cases compared to T1 ($p=0.05$). However there was no difference observed between T1 and ≥T2. Also positive association was noted with low-grade tumours ($p=0.01$).

The PI3K pathway is altered through several different mechanisms in bladder tumorigenesis. As suggested by Platt *et al.* different pathway members may have additive or synergistic effects through non-canonical functions and therefore a single-agent PI3K-targeted therapy may not be successful in these cancers [86]. Structural studies defined that PI3Ks are heterodimeric lipid kinases composed of a catalytic (p110) and a regulatory

subunit (p85) and 110α. The 110α subunit is regulated through an inhibitory effect of p85. However this effect may be lost by the stimulation of upstream receptors and thus bringing PI3K to the membrane. The inhibition of p110α by p85 seems to be mediated by interaction of the N-terminal domain of p85 with the helical domain of p110α [89, 90]. A study recently performed by Zhao *et al*. has revealed that helical domain and kinase domain mutations (E545K, E542K, H1047R) in p110α of PI3K induce gain of function by different mechanisms and through interaction with RAS [91]. However, it is not clear why there is predominance of helical mutations in bladder cancer. It might be related to the dual activation of the RAS–mitogen-activated protein kinase pathway either through RAS mutation or signalling though epidermal growth factor receptor during tumorigenesis or through other mechanisms [86]. The coexistence of both RAS and PIK3CA mutations in the same tumour might be compatible with this hypothesis. In one study, 7 out of 92 tumours showed both mutations in the same patient [86].

1.1.7 Molecular features of muscle invasive bladder tumours

In muscle invasive bladder tumours both p53 and Rb pathways are more frequently inactivated [92-94]. Inactivation of TP53 commonly occurs by missense point mutations (80%), which leads to production of non-functional protein. p53 nuclear overexpression is often associated with a wide distribution of reported different mutations (more than 1000). There is mounting evidence from large, multi-institutional analyses that the p53 overexpression is associated with high stage and grade bladder tumours [95, 96]. Study performed by George *et al.* on *TP53* mutation and protein status showed that p53 molecular information was an independent predictor in lymph node negative disease [97]. Upregulation of Rb protein expression and associated loss of the p16 tumour suppressor [98], has been found in over half of the muscle invasive bladder tumours [99]. These finding are infrequent in non-muscle invasive bladder tumours [100, 101]. Together with inactivation of Rb pathway there is coexistent overexpression of genes on 6p22, seen in 9% of T2 bladder cancers [102]. Two candidate genes were

identified within the minimum region of amplification *E2F3* and *CDKAL1* [102-105]. Multiple studies showed that over 30% of muscle-invasive tumours show loss of expression of Rb [100, 101, 106].

Another alterations commonly associated with MIBC are losses, amplifications and rearrangement of chromosome arm 8p [107-110], and less frequently involving short arm 8q [4].

Deletions of 10q, including region of the tumour suppressor gene *PTEN,* are found frequently in higher stage and grade bladder cancers [111-113]. Studies on bladder tumour cells reported that *PTEN* has a significant effect on the invasive properties of bladder tumour cells in a mouse model [114].

Commonly associated with more aggressive and muscle invasive bladder tumours is the receptor tyrosine kinase gene *HER2* [115-119], which is amplified and/or overexpressed at the protein level in many bladder tumours.

There is emerging evidence for a tumour suppressor role of the tuberous scle- rosis gene *TSC1* in bladder cancer. *TSC1* mutations show no clear correlation with tumour's stage and grade, however Hirao and colleagues reported that LOH at the region close to *TSC1* has been associated with tumour invasion [120]. Chromosome 9 alterations are very frequent (>50%) in bladder cancer [121-123]. Chromosome 9 is the most studied genomic region in bladder tumours and its deletion was one of the first alterations identified cytogenetically in bladder cancer. On the short arm of chromosome 9, there is a single region including the known cell-cycle regulators and tumour suppressor genes *CDKN2A* and *CDKN2B* [123-127]. This locus is frequently homozygously deleted in bladder tumours and associated with high stage and grade tumours [128].

1.1.8 Targeted therapies

During the last decade cancer therapy has rapidly evolved. Limited effectiveness and side effects of systemic chemotherapy resulted in interest in developing drugs that would interfere specifically with pathways that are genetically altered in tumour cells only. This would allow sparing normal cells

that do not display the tumour-specific target. As opposed to cytotoxic therapies where mechanisms of action are based on the theory that cancer is basically a disease of growing cells, targeted therapies interfere in specific pathways altered in tumour cells only [129]. To predict response to such therapies, the molecular profile of the target cells needs to be characterised. For example, the selective application of anti-HER2 therapy in breast cancer patients requires the identification of human epidermal growth factor receptor-2 (HER2) amplification.

1.1.8.1 Receptor Tyrosine Kinase Inhibitors (TKIs)

One of the receptors commonly used as a target in many cancers including colorectal and head and neck cancers, is EGFR [130]. It has been shown that EGFR is also overexpressed in TCC and it is associated with poor prognosis [131]. In preclinical studies it was demonstrated that cetuximab (anti-EGFR monoclonal antibody) inhibited tumour expansion and metastasis in combination with paclitaxel by blocking neovascularization and inducing apoptosis [130]. Currently a randomised phase two trial is evaluating cetuximab in combination with gemcitabine and cisplatin in patients with locally advanced or metastatic urothelial carcinoma [132]. A group of drugs (gefitinib, erlotinib, lapatinib) targeting EGFR has been evaluated as a treatment option in many cancers with good response. The phase two trial of Cancer and Leukemia Group (NCT00041106), sought to determine the efficacy of cisplatin, standard infusion of gemcitabine and gefitinib in patients with advanced urothelial carcinoma. The results of this trial showed 40% of objective responses, the median survival time was 15.1 months (95% CI 11.1–21.7 months) and the median time to progression was 7.4 months (95% CI 5.6–9.2 months) [133]. Another oral EGFR TKI used commonly in the treatment of non-small cell lung cancer has been assessed in treatment of muscle invasive bladder cancer in the neoadjuvant setting before cystectomy (NCT00749892). Patients are scheduled to receive erlotinib for four weeks and undergo cystectomy, followed by adjuvant erlotinib. Effects on targeted pathways are examined by detailed evaluation

of tumour tissue together with microarray analysis to define predictive factors and to determine the effects of therapy on gene expression.

Successful reports of treatment of breast cancer patients with an oral TKI which targets both EGFR and HER2 (lapatinib), has led to a phase two trial in advanced urothelial cancer [134]. Preliminary report of 59 patients with EGFR and/or HER2 overexpression, showed activity of lapatinib as salvage therapy for advanced UC, with partial responses in 3% and clinical benefit in 12% of patients. The median time to progression was 8.6 weeks and there was also a trend towards clinical benefit in those in whom overexpressed EGFR or HER2. Similarly a UK based trial with lapatinib (NCT00949455) in patients with advanced bladder cancer is currently on-going and finished recruiting patients [135].

The expression of HER2 oncoprotein in invasive bladder cancer was examined by immunohistochemical staining in a study performed by Matsubara *et al.* who found that 50% of lymph node positive patients were HER-2 positive. These patients also had corresponding HER 2-positive primary tumours [136]. In a more recent study, 42 paired lymph node metastases where examined to determine frequency of HER2 overexpression, *HER2/MYC* coamplification, and association between HER2 and MYC status and clinicopathologic features. The results revealed that HER2 overexpression occurred in 19 primary tumours (36%) and 14 metastases (30%), with an 88% concordance rate between primary and matched metastases [137]. The results of this study also indicate that HER2-targeted therapy may be a valuable treatment option for metastatic bladder cancer. Furthermore, studies in other cancer types have shown that coamplification of *HER2* and *MYC* may impact tumour growth and influence response to HER2- directed therapy and this could be relevant in bladder cancer [137, 138].

Sorafenib is another drug that is currently being assessed in treatment of advanced UC as a second line therapy and also as a first line therapy in combination with chemotherapeutic agents. It has got multitargeting properties, inhibiting BRAF and CRAF in the RAS/MAPK signalling pathway inhibiting tumour cell proliferation and angiogenesis (targeting VEGFR and

PDGFR). Sorafenib also blocks other TKs receptors including VEGFR-2, platelet-derived growth factor receptor (PDGFR)-β, c-KIT and Flt-3.

Another multitargeted receptor TKI is drug called sunitinib which is currently approved for the treatment of renal cell carcinoma. It work is mainly based on targeting VEGFR-2, PDGFR-β, KIT and Flt3 receptors. There is evidence emerging from preclinical studies that it is effective as a single agent and in combination with cisplatin [139, 140]. There are few phase two trials currently undergoing with sunitinib either as a the salvage therapy [141], in patients with stable disease [142], in combination with GC [143] or in neoadjuvant setting [144]. To some extent similar in action multitargeted receptor TKI-axitinib, showed some promising pre-clinical results. Axitinib on xenografts revealed inhibition of angiogenesis and VEGFR-2 and PDGFR-α phosphorylation together with overall regression of the graft [145].

1.1.8.2 VEGF targeted therapy

Vascular endothelial growth factor (VEGF) is responsible for mediating angiogenesis in TCC of bladder. Several studies have shown that its levels are associated with bladder tumour stage, grade, vascular invasion and carcinoma *in situ* [146-149]. Patients with metastatic disease also had a significantly higher levels of VEGF than those with localized disease [150]. Based on the rationale that antiangiogenic drugs in urothelial cancer may play a significant role, a phase two trial was designed to assess the activity of sunitinib as first-line treatment in patients with metastatic urothelial cancer ineligible for cisplatin [151]. Sunitinib is a multitargeted tyrosine kinase inhibitor that selectively inhibits VEGF receptors -1, - 2, and - 3; platelet-derived growth factor (PDGF) receptors -α and -β; stem cell receptor (kit); Fms-like tyrosine kinase-3 receptor (FLT3); the receptor tyrosine kinase encoded by the ret proto-oncogene (RET); and the receptor for M-CSF (CSF-1R) [141]. It showed promising initial results: on intention-to-treat analysis, 3 out of 38 patients (8%) showed partial responses and 19 (50%) presented with stable disease, 17 (45%) of them at 3 months. Clinical benefit was estimated at 58%. Median time to progression was 4.8 months and

median overall survival 8.1 months. Relying on preclinical evidence that supports the antitumour efficacy of targeting VEGF receptors expressed on bladder cancer in combination with chemotherapy [152], several other phase two trials have been initiated with bevacizumab [153].

1.1.8.3 FGFR3 targeted therapy

The FGFR family of receptors are considered potential theraupetic targets in bladder cancer. FGFR3 mutations in bladder carcinogenesis [61, 74] are strongly associated with low stage and grade [74]. While FGFR3 mutations are not associated with invasive bladder tumours, FGFR3 protein expression is significantly increased in muscle invasive disease [62]. FGFR1 is over-expressed in human bladder cancer cell lines and tumour samples, independently of the stage and grade [154]. In pre-clinical studies FGFR1 knock-down inhibited tumour growth, suggesting FGFR1 as a potential therapeutic target in UC. Small molecules work against the cytoplasmic domain containing the tyrosine kinase site (small molecule) or against the extracellular domain (mAb) of the receptor [155]. These small molecules induce direct cytostatic effect in FGFR3 mutant cells. It has been also discovered that human antibody anti-FGFR3 (PRO-001) inhibits the proliferation of cells and induces apoptosis [156]. PRO-001 binds to FGFR3 expressed cells and inhibits FGFR3 autophosphorylation and downstream signalling. It potently inhibited FGFR3-dependent solid tumour growth in a mouse xenograft model. An antibody (R3Mab) developed by Qing *et al* inhibited WT FGFR3 and various mutants of the receptor [157]. By binding to FGFR3 receptor it exerted potent antitumor activity against bladder carcinoma and multiple myeloma xenografts in mice. Also the inhibition of FGFR3 expression has been reported by interference with iRNA by decreasing the levels of proteins MCL-1 and Bcl-2, which play anti-apoptotic role in the cell [155]. The anti tumour activity of mAb has been also shown in both multiple myeloma xenograft tumour models (harbouring either WT or mutant FGFR3) and in vitro, in human bladder cancer [157, 158]. Several FGFR3 small molecule inhibitors have been recently tested *in vivo* and *in*

vitro. Examples are PD173074, TKI258 and SU5402 inhibitors [159]. PD173074 selectively inhibits FGFR3 and FGFR1 competing for ATP binding and inhibiting autophosphorylation [160]. TKI258 and SU5402 are inhibitors, which target both FGFRs and VEGFR [161, 162]. All three inhibitors were shown to be cytoxic and/or cytostatic on bladder cancer cell lines [163, 164]. However, only PD173074 revealed no toxicity on normal bladder cells. When tested *in vivo* it inhibited tumour growth and induced regression and the response seemed to be related to the level of FGFR expression and dependence [163, 164]. These investigations imply that anti-FGFR3 treatment should be considered for targeted therapy of cancer and possibly other diseases where the receptor is involved. Currently Hoosier Oncology Group is recruiting patients to a phase two trial of dovitinib in Bacillus Calmette-Guerin (BCG) refractory urothelial carcinoma in patients with tumour *FGFR3* mutations or over-expression (Trial: NCT01732107) [165]. Dovitinib (TKI258) is an inhibitor of FGFR1, FGFR2, and FGFR3, and has shown antitumor activity in FGFR-amplified breast cancers [166]. The results of a multicentre phase two study with dovitinib in *FGFR3* mutated and WT advanced UC are awaited (Trial: NCT00790426) [167]. Although the majority of these studies are preliminary, the interim findings from these trials are encouraging. Despite the fact that no targeted therapy agents are ready for routine use in advanced bladder cancer these trials are exceptionally important and may lead in future to significant improvement in bladder cancer management.

1.1.9 Targeted therapies and relationship of primary and matched metastasis

As more research is being conducted on targeted cancer therapies we have learned the need to understand the molecular features of cancer in order to predict response to specific agents. For example, one of prerequisites for an anti-EGFR antibody response is prior knowledge of the molecular activation of the EGF-receptor pathway either by mutation or amplification as well as absence of *KRAS*, *BRAF* or PI3K mutations [168-170].

Similarly, prior to breast cancer treatment with trastuzumab or lapatinib, the status of HER2 must be examined [171, 172]. However the major target tissue in disseminated disease is metastatic tumour and a potential problem is the possibility that systemic tumour differs at the molecular level from the primary tumour that is available for analysis. Whilst this is widely acknowledged, few studies to date have assessed metastatic tumours tissues or compared primary tumours with related metastatic lesions. Studies comparing primary and matched metastasis were performed on non-bladder cancers and have demonstrated similarities between them [173-175].

One of the widely used methods to characterize human cancers is gene expression analysis based on genome-wide microarrays. MicroRNAs (miRNAs) are a class of non-coding RNA molecules contributing to cancer onset and progression. A miRNA array study performed on breast, lung and bladder cancer and their corresponding metastases overexpression of miR-148a was found in lung and breast, miR-148b in lung, and miR-126 in bladder cancer metastases, and down-regulation of miR-373 in lung and miR-143 in bladder cancer metastases. The signature analysis of miRNAs may also help to identify the organ of origin, in difficult cases of unknown metastases [176]. A study that characterized primary and metastatic bladder cancer defined MAGE-A4 and MAGE-A9 expression. It was discovered that expression of both antigens was high in primary tumours compared to metastases. Characterization of the expression of various cancer-testis (CT) genes in bladder cancer has shown that members of the MAGE-A family are frequently expressed in these tumours making them a target of choice for bladder cancer immunotherapy [177].

Recent molecular studies of bladder cancer indicate that FGF receptors together with PI3K pathway components may be important therapeutic targets [178-180]. However, no studies to date have compared the expression and/or mutation of these targets in paired primary and metastatic cancers.

1.1.10 Molecular analyses of matched primary and metastatic bladder cancer

Metastasis is the major cause of death in bladder cancer patients. The spread of tumour cells from a primary tumour to secondary sites within the body is a complex process and involves: cell migration, invasion, adhesion, proliferation and angiogenesis. An understanding of metastasis at the cellular and molecular levels is an important objective in cancer research. Detailed molecular and genetic ships between primary tumours and their paired metastatic lesions have not been characterized well in patients with urothelial carcinoma.

Understanding of the relationship between primary and matched bladder tumours may become significantly more important in the near future as targeted therapies become widely used in clinical practice.

The majority of published data on bladder cancer has described studies performed on primary bladder tumours. Relatively few molecular studies have analysed metastatic bladder cancer lesions. It is unknown whether distant or lymph node bladder metastases originate from separate, genetically different subclones from within the primary tumour, whether these metastatic lesions arise from an identical cell of origin and whether changes in expression of therapeutic targets occur in metastatic sites. In the past it has been hypothesized that metastases were due to a small set of cells within the primary neoplasm that acquired a set of genetic modifications allowing them to leave the original site and grow in another organ. The findings of recent studies using DNA array analysis suggest that most of the cells in a primary tumour are capable of metastasizing [181, 182]. This may indicate that metastatic potential is determined by the bulk of the primary tumour [183]. Compatible with this Hovey *et al.* performed CGH on matched urothelial cancer primary and metastasis samples and revealed that there is minimal clonal evolution occurring in the metastatic tumour cell population after the metastatic event [184]. There is an on going debate addressing the mechanisms of metastatic progression, which has resulted in various models [185, 186]. In relation to targeted therapy, a critical issue is whenever primary tumours may serve as surrogates for the genetics and expression

profile of disseminated metastases. Currently there are two fundamental concepts of systemic cancer progression, which aim to find an explanation to this question [187]. The first model of *linear progression* is based on the concept that metastasis founder cells within the primary tumour disseminate as fully malignant cells. Once at the secondary sites they grow, expand and go through the process of adaptation to the new microenvironment. During this adaptation process these cells 'adjust' to the new ectopic microenvironment and hence no new genetic development is necessary though changes in gene expression may occur. In the second *parallel progression* model, less genetically evolved cells within the primary tumours disseminate at the earlier stage and undergo extensive somatic progression at the ectopic site. This adaptation is fundamental to 'survival' at the ectopic site and includes mutation, selection and inheritance [188]. Both models could potentially co-exist and play simultaneous roles in systemic cancer progression, however it is important to note the key difference in both of them. According to the *linear progression* model it is possible to predict the genotype of the metastasis by characterizing the primary tumour. In contrast, the *parallel progression* model emphasises the genetic disparity between primary and metastasis, making it almost impossible to find any similarities between primary and matched metastases. This could have important clinical implications. The ability to predict genotype and phenotype by sampling and characterization of the primary tumour may allow selection of targeted therapies, so that therapy can be limited only to patients with the potential for effectiveness and responsiveness to the drug.

In a study performed on cystectomy samples and their matched lymph node metastases obtained from 24 patients, LOH and X-chromosome inactivation assays showed that they had the same clonal origin [189]. Eleven tumours demonstrated identical allelic loss patterns at all DNA loci for 3 microsatellite polymorphic markers on chromosome 9p21, 9q32 and 17p13 (*TP53*, the p53 locus) both in the primary carcinoma and in all corresponding lymph node metastases. Unfortunately the results of this study do not explain whether each focus of lymph node metastasis originated from independent cell populations in the primary tumour or metastases were descendants of one, single altered cell population in the primary [189]. In a similar study, the

authors examined the pattern of allelic loss with polymorphic microsatellite markers on chromosome 9p21, a region which contains the tumour suppressor gene p16, and on chromosome 17p13, and found an identical pattern of allelic imbalance (allelic loss or retention) at multiple DNA loci in 8 (88%) cases [190]. These findings suggest that allelic loss of these chromosome regions most likely occurs prior to the metastatic spread. Miyao *et al*. performed experiments on 14 paired samples of primary and metastases of the bladder and found complete concordance between genetic defects in the primary and metastatic sites [191]**.** Shariat *et al.* evaluating the association between p53, p21, p27 and Rb expression and pathological features and clinical outcomes of advanced bladder cancer, concordance between marker expression in the lymph nodes and matched radical cystectomy specimens was 92, 82, 70 and 86% for p53, pRB, p21 and p27, respectively. It was also reported that p27 expression was strongly associated with bladder cancer presence, progression, metastasis and mortality [192].

A study performed by Byrne *et al.* analysed the expression of E-cadherin in bladder TCC, areas of carcinoma *in situ* and corresponding lymph node metastases [193]. In this study samples were obtained from 77 patients including 17 patients with lymph node metastasis. They found high (88% and 85%) concordance of E-cadherin status in metastatic lymph nodes and carcinoma *in situ* areas with the primary tumours. They also reported that E-cadherin expression was significantly associated with disease progression ($p=0.0219$) and bladder cancer specific survival ($p=0.037$) and suggested that loss of expression of this protein plays an important role in increased cellular invasiveness and metastasis.

An interesting study characterizing early metastatic progression of bladder cancer from the primary tumour to the first lymph node was performed by Malmström *et al.* [194] In this study, 8 patients were included with sentinel lymph node metastasis and underwent immunohistochemical analysis of p53, pRB, Ki67 and E-cadherin expression. The sentinel lymph node metastasis had very similar molecular profile. However, in half of the cases signs of clonal evolution appeared and immunohistochemical non-concordance was observed between primary and corresponding metastasis.

Two studies compared expression profiles of HER2 in the primary tumour and corresponding metastasis and found contradictory results [195, 196]. The study conducted by Jimenez *et al* on 39 patients with evaluable histological material from both locations showed that over-expression in the primary tumour predicted over-expression in regional or distant metastasis [195]. Researchers also noted that HER2-negative primary tumours may show over-expression in their corresponding metastasis (45% of lymph nodes and 67% of distant metastases). However, the other study performed on large cohort of patients and using HercepTest™ (Dako Ltd, Ely, UK) staining revealed that 36% of the patients had negative metastases despite positive primary tumours, and in 5% the metastases were positive even though the primary tumours were negative. Differences in obtained results may be attributed to different immunohistochemical retrieval and staining protocols that were used in both studies.

Recently, a group from Switzerland performed analysis of over 150 patients with bladder TCC and matched metastasis [197]. They have determined HER2 status at the gene level by FISH and at the protein level by IHC. They showed that HER2 amplification was significantly more frequent in lymph node metastases (15.3%) than in matched primary bladder cancers (8.7%; $p = 0.003$) and there was a high concordance in HER2 FISH results between the primary tumour ($\kappa = 0.853$) and metastases ($\kappa = 0.930$). However, IHC results were less concordant ($\kappa = 0.539$ and 0.830, respectively). The same group evaluated expression of MMP-2 and MMP-9 in tissue microarrays constructed of corresponding samples from primary tumours and lymph-node metastases [198]. Matrix metalloproteinases (MMP) participate in tumour progression and metastasis in various cancers. The results of this study however, failed to show positive correlation between expression levels of the primary tumour and metastasis suggesting an infiltration strategy independent of MMP-2 and MMP-9 activity. The same cohort of patients was investigated for CCND1 amplification and CyclinD1 expression with regard to tumour heterogeneity, correlation of amplification and protein expression as well as association with histopathological tumour characteristics, survival and response to chemotherapy [199]. The results showed that CCND1 amplification status and the percentage of IHC positive cancer cells were

correlated with histopathological tumour characteristics, cancer-specific survival and response to adjuvant chemotherapy. CyclinD1 expression and CCND1 amplification status were independent risk factors in metastasizing bladder cancer. Also, high CyclinD1 expression in lymph node metastases predicted favorable response to chemotherapy.

1.2 Multifocal bladder cancer

1.2.1 Multifocal bladder cancer and its origin

Bladder cancer is commonly characterized by development of multifocal tumours in the same patient. Approximately 30% of all patients with urothelial carcinoma present with multifocal tumours [200]. Tumour multifocality is associated with poorer outcomes. Patients presenting with multiple, separate tumours are at higher risk for recurrence, progression and cancer-specific death [201]. During recent years, two theories have been proposed to explain urothelial tumour multifocality, the monoclonal and polyclonal theories. The monoclonal theory suggests that all of the coexisting tumours are descendants of a single progenitor cell that has undergone malignant transformation [202]. This cell proliferates and spreads throughout the urothelium by intra-epithelial spread or intraluminal seeding with secondary implantation at different sites within the urinary tract resulting in genetically related tumours. The second concept of field-cancerization suggests that multifocal tumours are derived from multiple cells that become transformed as a result of carcinogenic insults and acquire independent genetic alterations leading to the development of genetically unrelated tumours. The establishment of clonal origin of multifocal bladder cancer may have significance in the application of different therapeutic approaches such as targeted gene therapy. These new treatments may be more efficacious against a monoclonal population of cells all expressing the relevant target than against cells in tumours that are not genetically related. Whatever the

clonal origin, subclonal evolution may lead to diversity in expression of therapeutic targets.

The difficulty in interpreting published results on multifocal disease is associated with the fact that clonality has not always been defined in the same way. For example, clonality could mean that two tumours A and B share common origin and evolved from single progenitor cell or they could have evolved from each other later during pathogenesis (e.g. because they share the same *FGFR3* mutation) (Figure 1.7). In studies involving only a few markers, unless markers that identify events that occur early in tumour development are used, it is difficult to exclude monoclonality. The more detailed the analysis e.g. genome wide, the easier it is to assess clonality.

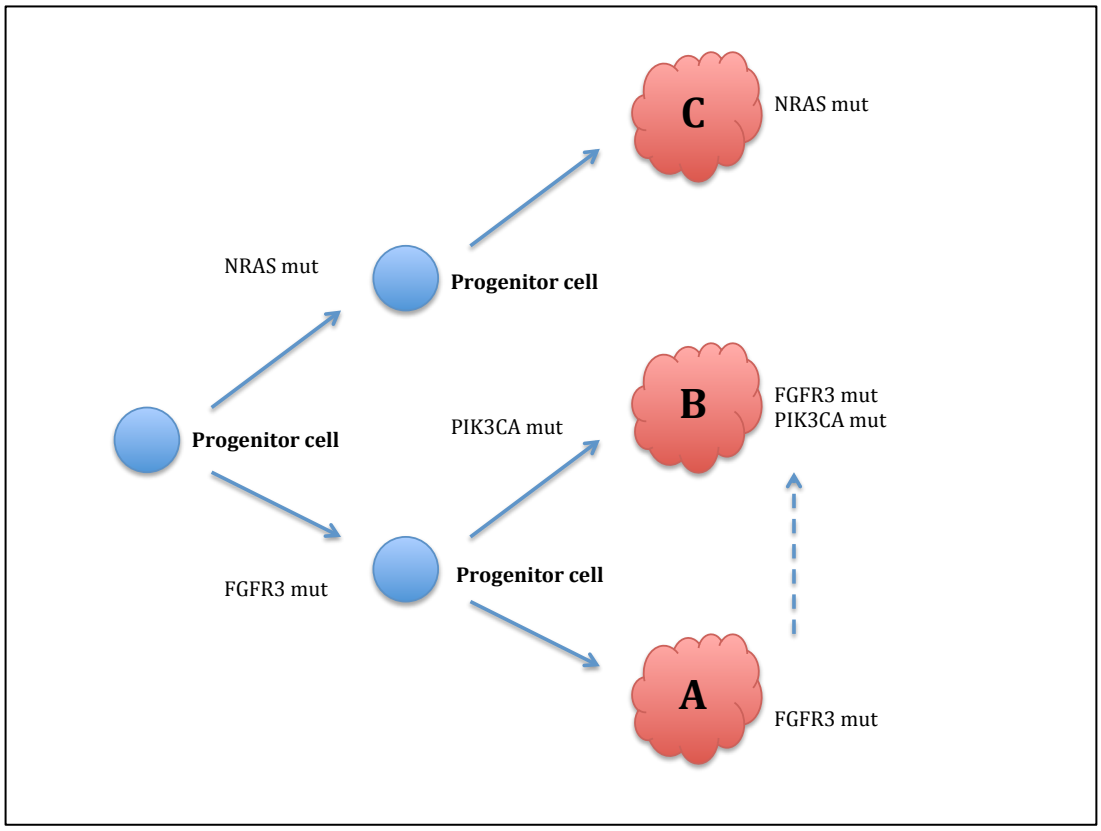

Figure 1.7: Different clonality interpretations described in literature. Clonality could mean that tumours A,B and C have clonal origin as all are descendants of common progenitor cell. Alternatively the term may be used to denote that tumour B has evolved from tumour A thus sharing the same *FGFR3* mutation.

1.2.2 Multifocal bladder cancer as a monoclonal disease

One of the early studies investigating clonality of multifocal tumours was performed by Sidransky *et al.* [203] where the authors analysed by chromosome X-inactivation analysis in 13 tumours from four different female patients. X-chromosome inactivation occurs early in female development and as it is a random process can be used as a marker for determining common origin of transformed cells. Once an X chromosome's DNA is inactivated by methylation, all its daughter cells remain inactivated throughout their life span. Sidransky and colleagues reported that for each patient all the tumours had inactivation of the same X chromosome indicating tumours monoclonal origin. Studies using these techniques were performed by Li *et al.* [204] and Cheng *et al.* [205] and they both determined monoclonal origin of the majority of synchronous multifocal tumours. However Cheng *et al.* in two cases showed different non-random X-chromosome inactivation patterns in different sites suggesting an oligoclonal origin. The majority of accumulated published data on chromosomal changes, and gene mutations indicates that most of multifocal bladder tumours are of monoclonal origin. However, multifocal tumours may have undergone significant changes during tumorigenesis with extensive subclonal evolution. Takahashi *et al.* examined LOH at 10 microsatellite loci in pathologically normal mucosa and associated multifocal bladder tumours from six patients. Findings of this study indicated that multifocal bladder cancer derived from single cell in monoclonal fashion. Multifocal tumours originated from single foci that had spread along normal urothelium rather than occurred as independent polyclonal events [206, 207].

Researchers who were not able to definitely determine the clonal origin of all syn- or metachronous multifocal tumours were mostly using LOH analysis as primary method [202, 205, 208, 209]. Because LOH of some genomic regions can occur late in the tumour development findings of these studies cannot totally exclude a clonal relationship among these tumours. LOH reveals regions carrying tumour suppressor genes. An interesting study, which combined three methods, FISH, LOH and genomic sequencing was

performed by Denzinger *et al.* with the aim of determining the clonality status of multifocal lesions within cystectomy specimens [210]. In addition, it used extensive histopathologic whole-organ mapping of the cystectomy specimens as an important prerequisite for a comprehensive molecular characterization of multifocal tumours and adjacent normal and dysplastic urothelium. In all 7 analysed tumour samples LOH analysis showed losses of the same alleles and identical *TP53* mutation. The mapping of *TP53* mutated samples revealed continuous spread and outgrowth of the tumour within the bladder. This study supported not only monoclonality of tumours but also supported the hypothesis of extensive intraurothelial migration of preneoplastic and tumour cells rather than intraluminal seeding. In intraluminal seeding a random distribution of mutant patches instead of *TP53* mutant patches in adjacent regions, would be evident.

One of the criticisms of studies performed in the past using chromosomal alteration and single gene mutation in clonality analysis was the fact that they detected alterations that may not be clone specific and could arise in unrelated tumours under similar carcinogenic pressures. In an attempt to overcome these problems, a study using microsatellite instability (MSI) was performed by Catto *et al.* [211]. There are multiple detectable mutations in tumours with high MSI, which persist during tumour development due to mismatch repair deficiency [212]. These mutations include the development of new alleles or alterations in the number of DNA repeats in an allele and are best observed in the repetitive microsatellite regions. MSI arises in the daughter cell during cell replication therefore it represents a reliable measure of clonal expansion. By characterizing MSI (its predictability and prevalence) it is also possible to estimate a tumour's age in cell divisions [213]. In the study performed by Catto *et al.* researchers investigated 32 lower and upper urinary tract TCCs with high MSI [211]. The results suggested that in all patients there was a single progenitor cell with subsequent expansion of one or more tumour subclones. MMR deficiency (the first event on the MSI carcinogenic pathway) was a characteristic feature of the progenitor cell. Normal urothelium and multifocal TCCs were also found to show MMR deficiency. Methylation analysis along with the distribution of MSI, all suggested monoclonality. For four of the patients with multifocal tumours

they were able to draw phylogenetic trees. Interestingly, these trees showed that the order in which the tumours were detected clinically did not match with the order in which they developed molecularly. Similar findings were also reported by van Tilborg *et al.* [214] with LOH and *FGFR3* mutation analysis. The disparities between clinical presentation of bladder cancer and evolutionary development occurred also in a study performed by Catto *et al* [211]. In one patient, MSI was greater in extent and frequency in the ureteric tumour than in the bladder cancer. Clinically bladder cancer presented several months after the ureteric tumour was removed. However, it is apparent that malignant cells were already present in the bladder at the time of nephroureterectomy despite having normal cystoscopy 3 months postoperatively. In another patient, tumours that were considered to be earliest on the evolutionary tree, with fewest alterations, did not present until a few years after the initial tumour. Findings of this important study may also suggest that all of these patients had a population of tumour cells *in situ* despite surgical removal of the primary lesion. It may have important clinical implications. Currently the administration of post-operative intravesical adjuvant chemotherapy is only used routinely after transurethral resection of bladder tumours as it has been shown to decrease recurrence rates [215]. However, this is not standard practice following nephroureterectomy. The data of this study suggest that intravesical chemotherapy given after nephroureterectomy may be of benefit in an attempt to treat residual tumour cells in the bladder, which are clonally related to the primary tumour.

In a study performed by Steidl *et al*. the authors examined the urothelium surrounding tumours and the role it might play in spreading the cancer cells. They performed FISH for common genetic changes on chromosomes 1, 8, 9, 11 and 17 [216] and detected chromosomal aberrations in 73% of normal or dysplastic samples. In these samples the highest number of aberrations were observed in samples adjacent to high-grade tumours. Moreover, the level of genomic instability was proportional to the stage and grade of the tumour. This finding may support the hypothesis that high-grade tumours do not develop directly from low-grade tumours. Another interesting finding of this study was the presence of chromosomal aberrations in urothelial cells but not in adjacent tumours. This may indicate that clonal evolution is

already happening in clinically normal looking urothelium and leading to creation of different sub-clones. However, only one of these sub-clones becomes a source of the tumour. Similar findings were confirmed by other groups [217-219]. Using FISH, Hartmann *et al.* found copy number variations in 50% of histopathologically normal urothelium and in 71% of hyperplasias [217]. By examining these results one may hypothesize that the area of clonally related aberrant cells surrounds and precedes bladder cancer development. Similar hypothesis were made when examining other cancers such as lung and oral cavity [220-223].

1.2.3 Bladder cancer characterized by aCGH

To date most studies of multifocal bladder cancer have examined only a few molecular characteristics in each tumour. The most complex analysis was performed by Simon *et al*. [224] using conventional CGH to metaphase chromosomes,*TP53* mutation and IHC analyses to examine 32 multifocal tumours from six patients. Typically the resolution of conventional CGH is between 5-10 Mb depending on how condensed the chromosomes are. Array comparative genomic hybridization (aCGH) is a microarray based technique for the detection of genome wide copy number alterations in the tumour genome. This method enables detection of whole chromosome gain or loss, partial or complete chromosome arm changes, high-level amplification, and homozygous deletions at high resolution. The resolution of aCGH is limited only by the clone insert size and the density of the mapped sequences used. For a resolution of 1Mb approximately 3,500 clones are required.

aCGH has allowed the high-resolution mapping of DNA copy number alterations in TCC of bladder and in other malignancies [3, 5, 225, 226]. This technology has been successfully applied in clinical research to identify new therapeutic targets and has been shown to be a robust method for identifying new oncogenes and tumour suppressor genes. High throughput technologies also have been recently applied in routine clinical practice for a more comprehensive assessment of biological characteristics of each

individual tumour [227, 228]. The unique arrangements of copy number alterations identified by aCGH have been reported to aid in differentiating tumours into more clinically and biologically relevant subtypes. Moreover, the higher resolution of aCGH has led to precise mapping of the boundaries of amplified and deleted regions indicating potential candidate genes relevant to cellular control pathways. The degree, type, and locations of chromosomal changes identified by aCGH may have prognostic and therapeutic implications, and thus the next wave of medical advances in oncology might come from the use of these technologies and from the development of new software to aid in identification which molecular aberrations should be targeted in each patient. Among other advantages of aCGH is that it allows a unique and precise view of the genomic instability in a tumour with both the amount of genomic copy number alteration and the specific loci involved defined in one relatively quick analysis. Therefore aCGH enables the detection of multiple genomic events in a single sample. However, the high diversity of genetic changes encountered by aCGH in one sample makes it almost impossible to analyse steps of bladder tumorigenesis with a simple algorithm.

The majority of published literature on evolutionary processes in cancer has been based only on data from a single time point in cancer progression (the time of surgery) and therefore it was the standard to reveal different steps in tumorigenesis by comparing genetic alterations in tumours from various patients with cancers of different histological stages and grades. This was based on the hypothesis that chromosomal aberrations and mutations that occur are consistent with a model of clonal evolution [218]. The changes characteristic for all stages were defined as early alterations, whereas the late events were associated exclusively in advanced stages of tumour development. One of the first models based on this hypothesis was proposed in 1990 in colorectal cancer [229] and it included only 5 general steps. Currently, in view of whole genome analyses with extremely high numbers of genomic alterations encountered, computational methods were developed to aid in identification of unique pathways and subgroups of tumours during tumour development. In this project we have utilised the computational method TuMult to reveal the succession of steps in cancer

development and analysed samples from a single patient at different locations or different time points during the disease process. This type of approach allows reconstruction of the sequence of alterations occurring in an individual, rather than a theoretical model generated by the comparison of heterogeneous samples. This sort of analysis is only possible in two scenarios: if several biopsy specimens are available for the same patient either because neoplastic condition led to prospective biopsies or because of availability of multiple recurrences following excision of the primary tumour. Bladder cancer seems to be a particularly useful model for such an approach due to its frequent multifocal recurrences. In the past, authors were able to conclude the monoclonal origin of tumours based on chromosomal aberrations common to several samples, and manually reconstruct the relationships between samples. This was possibly due to the fact that only few events were involved. However, nowadays with high definition copy number analyses on several samples automated approaches are required.

1.2.4 Bladder cancer characterized by SNaPshot

At present, investigations of bladder cancer are expensive, time consuming and invasive and usually involve cystoscopy, ultrasound and CT urography and cytology. Therefore, there is an urgent need for development of quick, non-invasive, inexpensive and simple investigation, which at the same time is highly specific and sensitive for detection of bladder cancer. Numerous molecular assays have been developed to aid in detection, monitoring urothelial cancer and to predict tumour progression, recurrence, development of metastasis, response to therapy or patient survival. To enhance the sensitivity of cytology the analysis of *FGFR3* gene has been performed [42, 44]. In order to facilitate application of *FGFR3* mutation analysis in clinical practice, quick and reliable test needed to be developed. One of the methods which easily identifies common bladder hot spot mutations, in relatively labour-free manner, is a SNaPshot assay. Some investigators have reported it to be a more sensitive method than analysis by

single-stranded conformation polymorphisms (SSCP) or sequencing [42]. This method allows simultaneous detection of nine common *FGFR3* mutations, four *PIK3CA* and all mutations in hotspot codons 12, 13 and 61 of the *HRAS*, *KRAS* and *NRAS* genes. It is also fast and relatively inexpensive. In one cost analysis it has been estimated to be nine times cheaper when compared to sequencing methodology [230]. It can be applied on both fresh and archival samples with very little DNA required. It has been proven to be more sensitive than SSCP and mutations are easy to score, with no interobserver variability [230, 231]. In comparison to other PCR-based mutation screening methods such as high resolution melting analysis, ARMS/Scorpion assays and direct sequencing of PCR products, SNaPshot provides high turnover of samples in a short space of time [231]. The other advantage of this assay is its high sensitivity. Researchers from our group were able to detect *PIK3CA* mutations when mutant DNA represented 5–10% of the total input DNA with the observed sensitivity results equate to being able to detect one mutant allele in a background of 5% or 10% wild type alleles in bladder cancer [231]. Similar sensitivity results were reported by other group using SNaPshot assay for detection of *FGFR3* mutations, where they showed that one mutant allele could still be detected against a background of up to 39 wild-type alleles [232].

Chapter 2
Materials and Methods

Multifocal Study

2.1 Study participants, sample collection and clinical information

2.1.1 Study participants and consent procedure

The study was approved by the Local Research Ethics Committee (Leeds-East 99/156), and informed consent was obtained from all patients. Study participants were selected from patients listed for transurethral resection of bladder tumour (TURBT), cystoscopy and/or bladder biopsy and cystectomy. Patients were recruited to the study if they had multifocal disease classified as superficial transitional cell carcinoma (TCC) of the bladder and the samples collected met the following selection criteria:

- samples collected from at least two visually separate tumours from consented adults
- sufficient quantity of the tissue collected to perform experiments described in the study
- confirmed superficial (stage < T2) TCC on pathological examination

All operative lists from Pyrah Urology Department (St James's University Hospital, Leeds) were accessed one-week prior to the procedure and reviewed by a Senior Scientific Officer (SSO) and Rafal Turo (RT) on a daily basis. Patients' clinical information was reviewed with particular emphasis on information obtained from flexible cystoscopy procedure (i.e. number and characteristics of bladder tumours). Informed consent and a discussion with the patient regarding the research were carried out on the morning of

surgery and/or one day prior to the procedure. At consultation patients were supplied with a descriptive protocol of the study and all necessary contact details of the persons involved. A copy of informed consent was always offered to the participants together with an occupational risk factor and smoking questionnaire (Appendix 2.1). Once consent was obtained, the surgeon carrying out the procedure and operating theatre (OT) staff were informed about participants.

2.1.2 Sample collection and transportation of tissue from the OT to the sample processing department

Initially we have encountered problems in collecting sufficient number of samples. However, after improved communication with clinicians our recruitment rate improved significantly. Due to difficulties in obtaining large number of samples statistical power calculations were not performed.

The sample collection procedure (Figure 2.1) was explained to clinicians and nursing staff in detail by RT. All clinicians and nursing staff were informed and the study protocol was presented to them during two departmental audit meetings held on 09.12.2010 and 12.02.2010.

Nursing staff placed each resected tumour sample in a separate container containing 10 ml RPMI 1640 (Sigma R0883) and a protease inhibitor tablet (Roche 1836153) and labelled it accordingly. Immediately after being notified by OT, the SSO retrieved the specimen from the OT suite and delivered the specimen to the sample processing department. When transporting tissue, the samples were kept cool by placing the specimens on ice. At the same time tissue from the same tumours were sent to the pathology department for assessment via the standard diagnostic procedures for this hospital. A blood sample (3-5 mls) was also collected from each patient in ethylenediamine tetraacetic acid (EDTA) tubes and stored at -20°C until DNA was extracted (Figure 2.1).

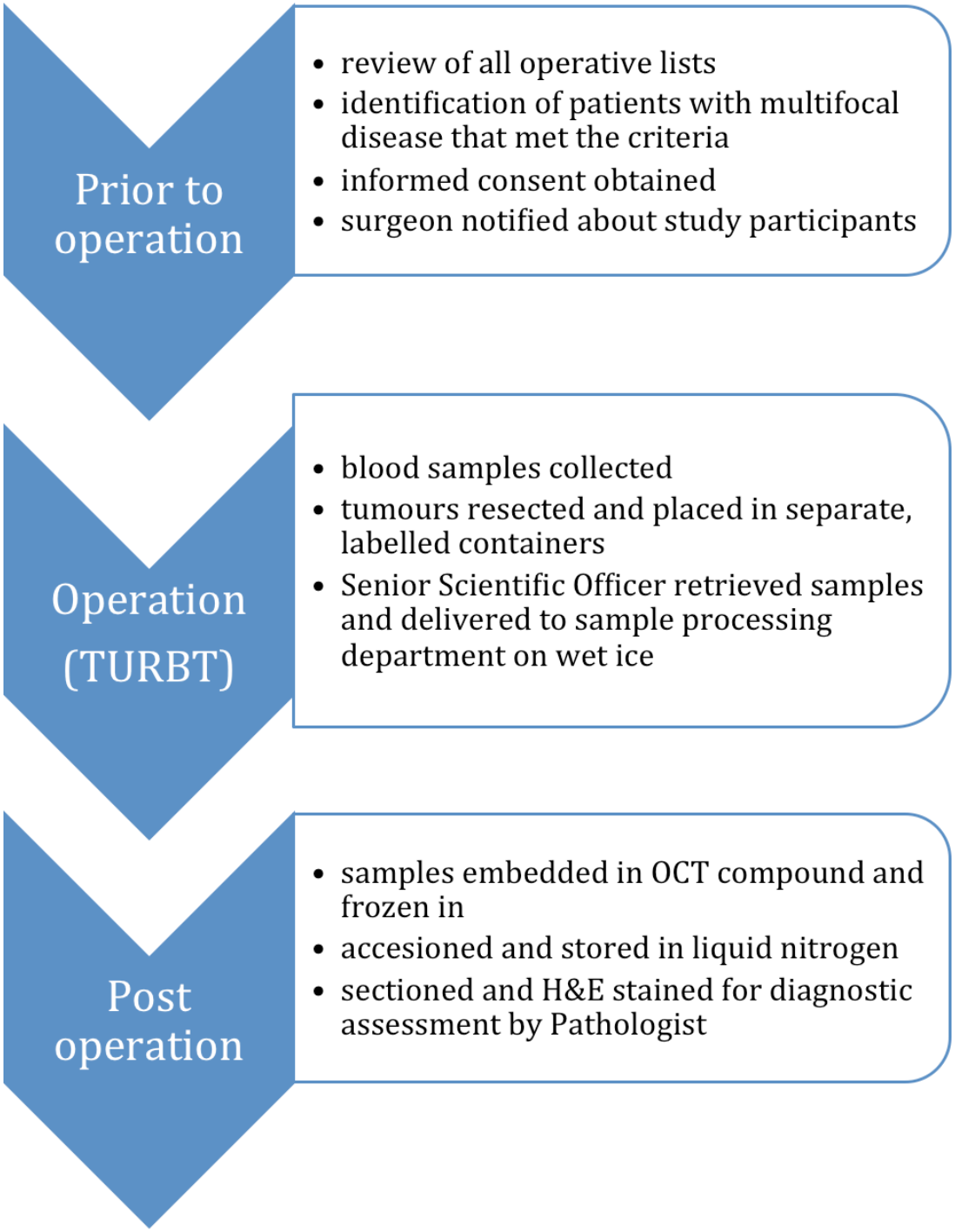

Figure 2.1. Flow chart of the sample collection procedure. TURBT – transurethral resection of bladder tumour, OCT compound – optimal cutting temperature compound.

2.1.3 Tumour sample processing

All specimens were generally processed/frozen within 20-30 min from resection. Once accessioned, the bladder tumour specimen was handled according to conventional sample processing techniques for our institution. At our institution, the SSO performed processing. Cold cup biopsies were rinsed in Dulbecco's PBS (Sigma D8537). Each biopsy was then embedded in optimal cutting temperature compound (OCT) on a specimen chuck cooled on dry ice, wrapped in labelled foil and snap-frozen in liquid nitrogen. A 5 μm section was taken using a cryostat and haematoxylin and eosin (H&E) stained for stage and grade assessment by an experienced Pathologist (Dr Patricia Harnden) according to the WHO 1973 and UICC, 1978 classification systems. The biopsies were stored in liquid nitrogen until used.

2.1.4 Patient information

A summary of patient information is given in Table 2.1. Twenty-two patients were recruited. The median age for all patients was 77 years. The majority of patients (19 patients) were referred to the flexible cystoscopy clinic for diagnosis of macroscopic haematuria. There were sixteen male patients and 6 female. Seventeen patients were smokers with a median of 20 pack-years of smoking (smoking pack history range: 3-75 per patient). Four patients were exposed to occupational hazards such as printing, dyes, paints and diesel fumes.

Patient Number	Stage/Grade	Number of tumours	Sex (Age)	Smoker (S) / Non-smoker (N) /Occupational hazards	Smoking -pack-years	Primary (P) / Recurrent (R)
1	TaG2 all tumours	3	Male (69)	S / Printing, Diesel fumes	75	R
2	TaG2 all tumours	3	Female (81)	S	45	R
3	T1G3 all tumours	3	Male (74)	S	3	R
4	TaG3 all tumours	6	Male (72)	S	20	R
5	TaG2 all tumours	2	Male (90)	S / Laboratories	35	P
6	T1G3 all tumours	3	Male (79)	S	15	P
7	TaG2 all tumours	2	Male (81)	S	26	R
8	TaG2 all tumours	3	Female (69)	S / Printing, Dyes & Paints	30	R
9	T1G3 all tumours	2	Male (94)	N	-	P
10	TaG3 all tumours	2	Male (75)	S	10	P
11	TaG2 tumour 1 T1G3 tumour 2	2	Female (79)	N	-	R
12	T1G3 tumour 1-3 TaG3 tumour 4	4	Female (81)	N	-	P
13	TaG3 all tumours	4	Male (60)	S	23	P
14	TaG3 all tumours	4	Female (89)	S	5	P
15	TaG2 all tumours	2	Male (70)	S	5	P
16	TaG2 all tumours	4	Male (50)	N	-	R
17	TaG2 all tumours	3	Male (81)	N	-	R
18	T1G3 all tumours	4	Male (81)	S	10	P
19	TaG2 all tumours	3	Female (66)	S	11	P
20	TaG2 tumour 1 T1G3 tumour 2-3	3	Male (85)	S / Printing	10	P
21	TaG2 all tumours	2	Male (69)	S	20	R
22	TaG2 all tumours	2	Male (69)	S	35	P

Table 2.1. Patients' characteristics. The histopathological stages and grades of all initial multifocal tumours used in the study are shown. For each patient, it was also noted whether multifocal disease was primary or recurrent. Patients' sex, age, smoking status and history of occupational exposure to risk factors are also shown.

2.1.5 Histopathological details

A summary of the histopathological details of tumours collected in this study is presented in Table 2.1. Sixty-six bladder tumours of transitional histology were collected from twenty-two patients. These included 14 stage pTa (3 grade 3 and 11 grade 2) and eight stage T1 (all grade 3). In two patients (11 and 20) tumours of different stage and/or grade were present in the same patient. The number of tumours from a single patient varied from 2 to 6. Tumours from twelve patients were primary and tumours from 10 patients were recurrent. Tumours from one patient (patient 12) recurred twice during the course of the study and samples were available for comparisons with the initial tumours (Table 2.2).

Patient number	Stage / Grade	Number of tumours
second recurrence of patient 12	T1G3 all tumours	2
third recurrence of patient 12	T1G3 all tumours	5

Table 2.2. Histopathological stage and grade of recurrences that occurred in multifocal bladder cancer patients during the course of the study.

2.2 Extraction and quantification of DNA

2.2.1 Extraction of DNA from tumour tissues

Tumour biopsies embedded in OCT were sectioned in a cryostat (Leica Microsystems Ltd, Milton Keynes, UK). An initial 5 μm section was stained with haematoxylin and inspected for at least 70% tumour purity, then 10 x 20 μm sections were cut and transferred into a 1.5 ml micro-centrifuge tube for DNA extraction. A 5 μm section was cut after each set of 10 sections and stained with haematoxylin and eosin to ensure the purity of the sample was maintained throughout.

DNA was extracted using the QIAamp DNA Mini Kit (Qiagen, Crawley, UK) tissue protocol according to the manufacturer's instructions. The method is based on specific binding of DNA to a silica-gel membrane in the QIAamp Mini spin column while contaminants pass through. Briefly, 180 μl of ATL buffer was added to 10 x 20 μM tissue sections in a 1.5 ml microcentrifuge tube and mixing was performed using a vortex. 20 μl of proteinase K was then added and the sample was incubated at 56°C until the tissues were completely lysed (2 – 3 hours). 200 μl of AL buffer was added and the samples were mixed using a vortex then incubated at 70°C for 10 min. Samples were then mixed with 200 μl of 96% ethanol, and applied to a QIAamp Mini spin column. The column was subsequently centrifuged at 8,000 rpm for 1 min then washed with 500 μl of AW1 buffer and re-centrifuged at 8,000 rpm for 1 min. Then, 500 μl of AW2 buffer was applied and the column was centrifuged at 14,000 rpm for 3 min. To remove residual wash solution, the column was then placed in a fresh collection tube and centrifugation was performed at 13,000 rpm for 1 min. Finally, to elute the DNA from the column 20 μl of AE buffer was added and the column was incubated at room temperature for 5 min. The DNA containing solution was then collected by centrifugation (8,000 rpm for 1 min). The elution step was

repeated using another 20 μl of AE buffer and the combined eluates were stored at -80°C.

2.2.2 Extraction of DNA from blood samples

DNA was extracted from venous blood samples using a Nucleon DNA extraction kit (Nucleon Biosciences, Lanarkshire, UK) or by a salt-precipitation method carried out in the DNA Laboratory at St. James's University Hospital. The extracted DNA samples were stored at -20°C.

2.2.3 Extraction of DNA from laser capture micro-dissected tumour

When samples consisted of less than 70% tumour cells on examination of hematoxylin stained fresh samples, laser-assisted microdissection of the neoplastic cells was performed. H&E stained 10 μm sections mounted on polyethylene naphthalate (PEN) membrane slides (Arcturus Engineering, Mountain View, USA) were dissected using a Pix-Cell II Laser-Capture Microdissection (LCM) system (Arcturus Engineering, Mountain View, USA). Neoplastic cells from each tumour tissue section were captured on CapSure® Macro LCM (0211) Caps (Applied Biosystems, Warrington, UK) by LCM and using a 7.5-mm laser beam at 50 to 100 mV. The laser causes the film on the cap to melt adhering to targeted cells. In each cap multiple area of neoplastic cells were collected from individual tumours. Films containing the cells were removed from the caps and transferred to 1.5 ml micro-centrifuge tubes. The DNA was extracted using a QIAamp DNA Mini kit (Qiagen, Crawley, UK) according to manufacturer's instructions except that after the overnight lysis step and prior to addition of buffer AL, the lysate was transferred away from the film into a fresh 1.5 ml micro-centrifuge tube (empty films were discarded). DNA was eluted in 2 x 20 μl of buffer AE. The DNA samples were stored at -80°C until required.

2.2.4 Quantification of DNA

A PicoGreen dsDNA Quantitation kit (Invitrogen Ltd. Paisley, UK) was used to quantify DNA extracted from tumour and blood samples according to the manufacturer's instructions. PicoGreen is an ultrasensitive fluorescent nucleic acid stain that binds selectively to dsDNA thus circumventing problems associated with contaminating proteins, free nucleotides and RNA.

A high range assay was performed to detect DNA at a concentration between 1 ng/ml and 1000 ng/ml. The provided λ DNA standard was diluted with 1x TE to a concentration of 2 ng/ml, 20 ng/ml, 200 ng/ml and 2000 ng/ml. Dilutions of tumour DNA samples were prepared by transferring 1 μl DNA into 999 μl of 1 x TE. Duplicate aliquots of 100 μl of each tumour DNA sample and standard were transferred into wells of a 96 well optical plate (BMG Labtech Ltd., Aylesbury, UK). A blank sample consisting of 1 x TE was also applied to the plate. PicoGreen reagent was diluted 100 fold in 1 x TE then 100 μl of diluted reagent was added to each well. The plate was covered and incubated for 2-5 min in the dark. Fluorescence intensity was measured on a FLUOstar Galaxy fluorescence plate reader (BMG Labtech Ltd., Aylesbury, UK) at an emission wavelength of 520 nm and excitation of 480 nm. The accuracy of the standard curve was assessed. The DNA concentration of the sample was then determined from the standard curve and by taking the initial dilution factor into account.

2.3 Whole genome DNA amplification

Low yields of genomic DNA were obtained for three tumour samples (11 tumour 1, 10 tumour 1, 4 tumour 2). In order to generate sufficient genomic DNA for the analysis of these samples, whole genome amplification was performed using a REPLI-g® Mini Kit (Qiagen, Crawley, UK). This method allows the generation of high yields of genomic DNA from a low amount of template DNA. It is a one-temperature amplification method employing the

use of exonuclease-resistant random primers and Phi 29 DNA polymerase that has great processivity. Figure 2.2 illustrates the mechanism of action of Phi 29 DNA polymerase. The process consists of three major steps: 1) a denaturation step in order to open up the helix to allow the random primers to access DNA; 2) a neutralisation step involving the addition of a neutralising buffer which enables primer annealing; 3) a polymerisation step during which polymerase and buffers are added to allow the process of amplification to start.

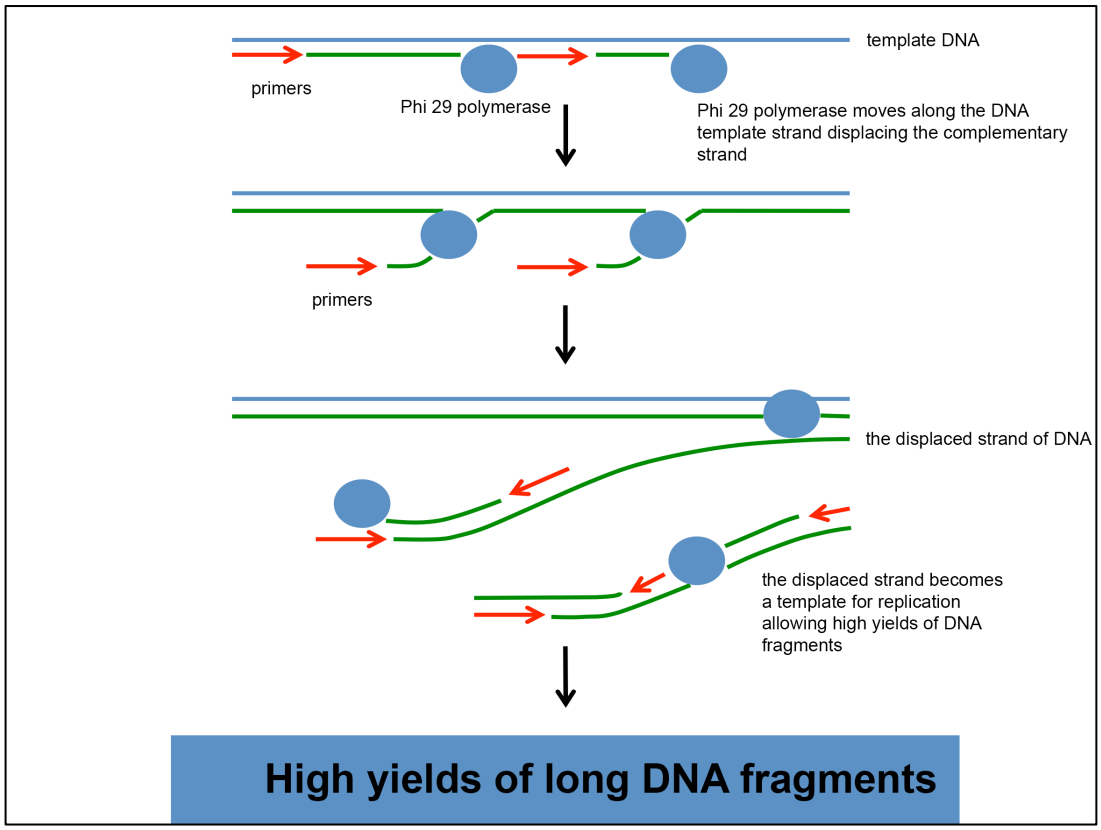

Figure 2.2: Mechanism of action of Phi 29 polymerase during WGA. Primers (red arrows) anneal to the template DNA and are extended by Phi 29 polymerase. The polymerase moves along the DNA template strand, displacing the complementary strand, which then becomes a template itself for replication. Adapted from Dean, 2001[233].

Whole genome amplification was performed according to the manufacturer's instructions. Briefly, 2.5 μl of the sample (containing 25ng of the tumour template DNA) was mixed with 2.5 μl of denaturation buffer and incubated at room temperature for 3 min. Five microliters of neutralization buffer was added, and finally, 40 μl of master mix consisting of 1 μl REPLI-g Mini DNA Polymerase and 39 μl Mini Reaction Buffer was added to the neutralised, denatured sample DNA. The mixture was incubated at 30°C overnight (10–16 hours). At the end of the incubation, the DNA polymerase was inactivated by heating the sample at 65°C for 3 min. One microlitre of the whole genome amplified sample diluted 1:100 with water was used in each subsequent polymerase chain reaction (PCR). For array comparative genomic hybridization (aCGH) 2 μl of neat whole genome amplified product (tumour and reference) was used for each array.

2.4 SNaPshot-based mutation detection assays

Three separate SNaPshot assays for the detection of hotspot codon mutations in *FGFR3*, *PIK3CA* and the three RAS genes (*HRAS*, *KRAS* and *NRAS*) were used in this study. The SNaPshot assay combines a single or multiplex PCR amplification with a multiplex primer extension assay to allow targeted detection of several mutations in one reaction. The SNaPshot assay workflow is shown in Figure 2.3.

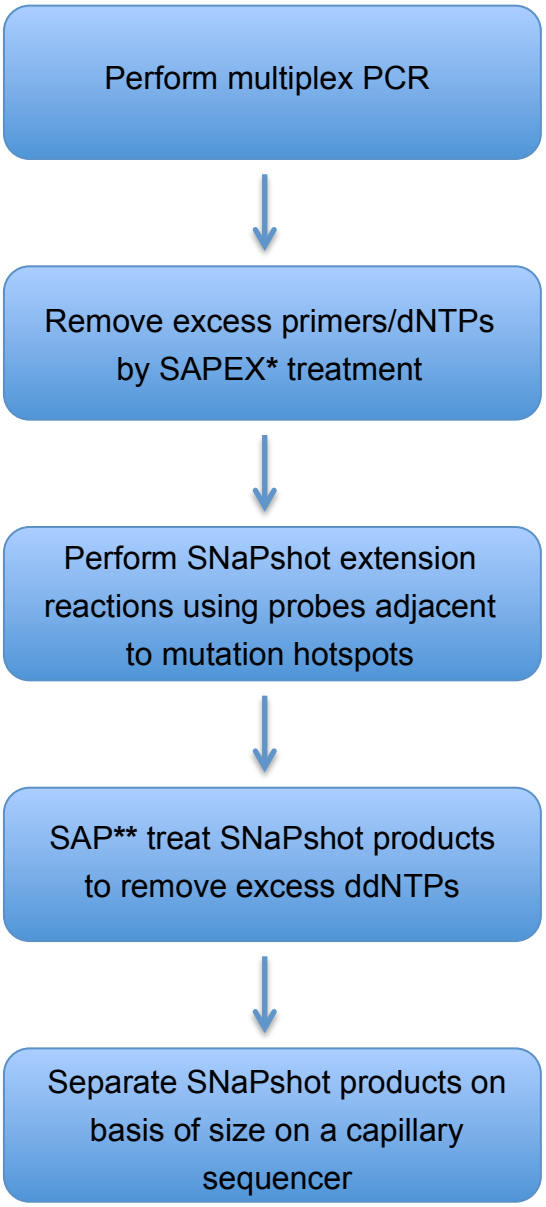

Figure 2.3: The SNaPshot assay workflow.

* SAPEX treatment = treatment with Shrimp Alkaline Phosphatase and Exonuclease I

** SAP treatment = treatment with Shrimp Alkaline Phosphatase

2.4.1 Multiplex PCR primers and SNaPshot probes

Multiplex PCR primers and SNaPshot probes used in these assays, were as described in van Oers *et al*. and Hurst *et al.* [231, 232]. Primers were selected for multiplex PCR amplification of exon 9 and exon 20 of *PIK3CA* (Table 2.3). SNaPshot probes for the detection of *PIK3CA* hotspot codon mutations (E542K, E545G, E545K and H1047R/L) were designed to anneal on the sense strand immediately adjacent to the mutation site. Each probe was synthesised with a different length of poly(dT) tail to allow separation of SNaPshot products on the basis of size (Table 2.4). Similarly, primers were designed for the amplification of three regions of the *FGFR3* gene, located in exons 7, 10, and 15 (Table 2.3). These regions cover the following potential codon mutations: R248C and S249C (exon 7), G372C, Y375C, G382R, and A393E (exon 10), and K652E, K652Q, K652M, and K652T (exon 15). The sequences of the probes designed to detect these hotspot mutations are shown in Table 2.4. In a third assay, primers were selected for multiplex amplification of exons 1 and 2 of the *HRAS*, *KRAS* and *NRAS* genes (Table 2.3). These regions cover potential mutations in hotspot codons 12, 13 and 61 of each gene. Two sets of probes were designed to detect hotspot codon mutations in the three RAS genes (Table 2.4).

Gene	Primer ID	Sequence (5'->3')	Strand	Concentration in primer mix (μM)	PCR product sizes (bp)
PIK3CA	Exon 9 F	AGTAACAGACTAGCTAGAGA	Forward	10	138
	Exon 9 R	ATTTTAGCACTTACCTGTGAC	Reverse	10	
	Exon 20 F	GACCCTAGCCTTAGATAAAAC	Forward	10	109
	Exon 20 R	GTGGAAGATCCAATCCATTT	Reverse	10	
FGFR3	Exon 7 F	AGTGGCGGTGGTGGTGAGGGAG	Forward	18	115
	Exon 7 R	GCACCGCCGTCTGGTTGG	Reverse	18	
	Exon 10 F	CAACGCCCATGTCTTTGCAG	Forward	7.5	135
	Exon 10 R	AGGCGGCAGAGCGTCACAG	Reverse	7.5	
	Exon 15 F	GACCGAGGACAACGTGATG	Forward	10	161
	Exon 15 R	GTGTGGGAAGGCGGTGTTG	Reverse	10	
RAS	HRAS exon 1 F	CAGGAGACCCTGTAGGAGG	Forward	9	139
	HRAS exon 1 R	TCGTCCACAAAATGGTTCTG	Reverse	9	
	HRAS exon 2 F	GGAGACGTGCCTGTTGGA	Forward	5	140
	HRAS exon 2 R	GGTGGATGTCCTCAAAAGAC	Reverse	5	
	KRAS exon 1 F	GGCCTGCTGAAAATGACTG	Forward	5	163
	KRAS exon 1 R	GGTCCTGCACCAGTAATATG	Reverse	5	
	KRAS exon 2 F	CCAGACTGTGTTTCTCCCTT	Forward	5	155
	KRAS exon 2 R	CACAAAGAAAGCCCTCCCCA	Reverse	5	
	NRAS exon 1 F	GGTGTGAAATGACTGAGTAC	Forward	5	128
	NRAS exon 1 R	GGGCCTCACCTCTATGGTG	Reverse	5	
	NRAS exon 2 F	GGTGAAACCTGTTTGTTGGA	Forward	5	103
	NRAS exon 2 R	ATACACAGAGGAAGCCTTCG	Reverse	5	

Table 2.3. Primers for multiplex PCR amplification of *PIK3CA* (exons 9 and 20), *FGFR3* (exons 7, 10 and 15) and the three genes RAS (exons 1 and 2)

Gene	Probe*	Sequence (5'->3')	Size (bp)	Mutation	Concentration in probe mix (μM)
PIK3CA	E542K	T(19)TACACGAGATCCTCTCTCT	38	G->A	0.8
	E545G	T(29)TCCTCTCTCTGAAATCACTG	49	A->G	2.3
	E545K	T(34)ATCCTCTCTCTGAAATCACT	54	G->A	1.5
	H1047R/L	T(46)TGAAACAAATGAATGATGCAC	67	A->G/T	1.5
FGFR3	R248C	T(46)CGTCATCTGCCCCCACAGAG	66	C->T	2
	S249C	T(36)TCTGCCCCCACAGAGCGCT	55	C->G	1.2
	G372C	T(29)GGTGGAGGCTGACGAGGCG	48	G->T	0.4
	Y375C	T(43)ACGAGGCGGGCAGTGTGT	61	A->G	1.2
	A393E	T(34)CCTGTTCATCCTGGTGGTGG	54	C->A	2.4
	K652M/T	T(20)CACAACCTCGACTACTACAAGA	42	A->T/C	0.8
	K652E/Q	T(50)GCACAACCCGACTACTACAAG	72	A->G/C	0.6
	S373C	T(19)GAGGATGCCTGCATACACAC	39	T->A	0.5
	G382R	T(56)GAACAGGAAGAAGCCCACCC	76	C->T	1.2
RAS Set 1	HRAS pos.34	T(17)CTGGTGGTGGTGGGCGCC	35	G->C/T/A	0.5
	HRAS pos.182	T(18)GCATGGCGCTGTACTCCTCC	38	T->G/C/A	1
	HRAS pos.35	T(31)CGCACTCTTGCCCACACCG	50	C->G/A/T	0.5
	HRAS pos.37	T(55)CAGCGCACTCTTGCCCACAC	75	C->G/A/T	7
	HRAS pos.181	T(46)CATCCTGGATACCGCCGGC	65	C->C/T	0.4
	KRAS pos.34	T(25)GGCACTCTTGCCTACGCCAC	45	C->G/A/T	2
	KRAS pos.181	T(41)CTCATTGCACTGTACTCCTCTT	63	C->A/G	0.4
	KRAS pos.35	T(49)AACTTGTGGTAGTTGGAGCTG	70	G->C/T/A	0.5
	NRAS pos.182	T(33)GACATACTGGATACAGCTGGAC	55	A->G/C/T	0.2
	NRAS pos.34	T(62)CTGGTGGTGGTTGGAGCA	80	G->C/T/A	0.5
RAS Set 2	KRAS pos.37	T(15)CAAGGCACTCTTGCCTACGC	35	C-> G/A/T	7
	NRAS pos.181	T(18)CTCATGGCACTGTACTCTTCTT	40	G->T/C	0.2
	NRAS pos.37	T(26)GGTGGTGGTTGGAGCAGGT	45	G->C/T/A	0.1
	KRAS pos.183	T(29)CCTCATTGCACTGTACTCCTC	50	T->A/G	0.4
	KRAS pos.38	T(33)CTTGTGGTAGTTGGAGCTGGTG	55	G->C/T/A	0.5
	NRAS pos.183	T(38)CTCTCATGGCACTGTACTCTTC	60	T->G/C/A	0.7
	NRAS pos.38	T(44)GTCAGTGCGCTTTTCCCAACA	65	C->G/A/T	0.5
	NRAS pos.180	T(49)GGACATACTGGATACAGCTGG	70	A->T	0.3
	KRAS pos.182	T(56)ATTCTCGACACAGCAGGTC	75	A->T/C/G	1
	HRAS pos.183	T(62)CCTGGATACCGCCGGCCA	80	G->C/T/A	0.4
	HRAS pos.38	T(64)GTCAGCGCACTCTTGCCCACA	85	C->A/T	0.5
	NRAS pos.35	T(71)CTGGTGGTGGTTGGAGCAG	90	G->C/A/T	0.3

Table 2.4. SNaPshot probes for the detection of *PIK3CA*, *FGFR3* and RAS mutations. * Position refers to nucleotide position in the cDNA with numbering from the first base of the ATG start codon.

2.4.2 Multiplex PCR amplification

Multiplex PCR was performed in a volume of 15 μl containing 1 × PCR buffer, 1.5 mM $MgCl_2$, 0.17 mM dNTPs, 1 μl of primer mix (see Table 2.3 for primer concentrations in each of the primer mixes), 5% glycerol, 1 unit GoTaq DNA polymerase and 20 ng of template DNA. Thermal cycler conditions for *FGFR3* and *PIK3CA* were: 95°C for 5 min then 35 cycles of 95°C for 45 sec, 60°C for 45 sec, then 72°C for 45 sec followed by 72°C for 10 min. Thermal cycler conditions for RAS were essentially the same except an annealing temperature of 55°C was used.

2.4.3 Agarose gel electrophoresis of PCR products

Multiplex PCR products were checked for quality and yield by agarose gel electrophoresis, using Sub-Cell Systems electrophoresis tanks (Bio-Rad, Hemel Hempstead, UK) containing 1 x Tris Borate EDTA running buffer (0.089M Tris, 0.089 M Boric Acid, 0.0025 M EDTA, pH 8.3; MP Biomedicals, LCC). Three microliters of PCR product were mixed with 6 μl water and 1 μl loading buffer (40% w/v sucrose, 0.25% w/v bromophenol blue) and loaded onto 2% w/v agarose gels, containing 0.7 μg/ml ethidium bromide (Severn BioTech Ltd, Kidderminster, UK). Samples were electrophoresed at 6 V/cm for 30 min alongside 0.5 μg of a 100 bp DNA ladder (New England Biolabs, Hitchin, UK). Fractionated PCR products were visualized under short-wavelength UV illumination using a ChemiDoc XRS system (Bio-Rad, Hemel Hempstead, UK) and imaged with Quantity One software (Bio-Rad). The sizes of the fractionated amplicons were compared to the anticipated PCR product sizes (Tables 2.3 and 2.4).

2.4.4 SNaPshot probe extension reactions

The remaining PCR products (12 μl) were treated with 3 units of shrimp alkaline phosphatase (GE Healthcare Life Sciences, Buckinghamshire, UK) and 2 units of exonuclease I (GE Healthcare Life Sciences) to dephosphorylate unincorporated deoxyribonucleotide triphosphates (dNTPs) and degrade residual primers, respectively, that might interfere with subsequent steps. Samples were incubated at 37°C for 60 min, followed by 15 min at 72°C.

SNaPshot probe extension reactions were performed using an Applied Biosystems SNaPshot Multiplex Kit. The SNaPshot probe extension step is illustrated in Figure 2.4. Reactions were performed in a volume of 9 μl containing 2.5 μl of SNaPshot Multiplex Ready Reaction Mix, 1 × BigDye sequencing buffer, 1 μl of probe mix (see Table 2.4 for probe concentrations) and 1 μl of shrimp alkaline phosphatase/ exonuclease I-treated multiplex PCR product. Extension reactions were performed in a thermal cycler and consisted of 35 cycles of denaturation at 95°C for 10 sec and annealing/extension at 58.5°C for 40 sec. Labelled extension products were treated with shrimp alkaline phosphatase (1 unit per sample) to dephosphorylate unincorporated dideoxynucleotides (ddNTPs) then diluted 1 in 10 with water. One microlitre of the diluted extension product was mixed with 9.8 μl of HiDi™ formamide and 0.2 μl of GeneScan-120LIZ® size standard (Applied Biosystems). Products were denatured at 95°C for 5 min then separated using an ABI PRISM 3100 Genetic Analyser with a 36 cm length capillary and POP-7™ polymer. Analysis was performed using GeneMapper 3.7 Software, which colour codes peaks according to the dye label on the incorporated ddNTP. Genotypes were scored manually based on the peak colour and position relative to the GeneScan™ 120 LIZ® internal size standards. Slight shifts in the molecular weights of mutant alleles are observed due to mobility differences in the fluorophores used to detect each of the bases.

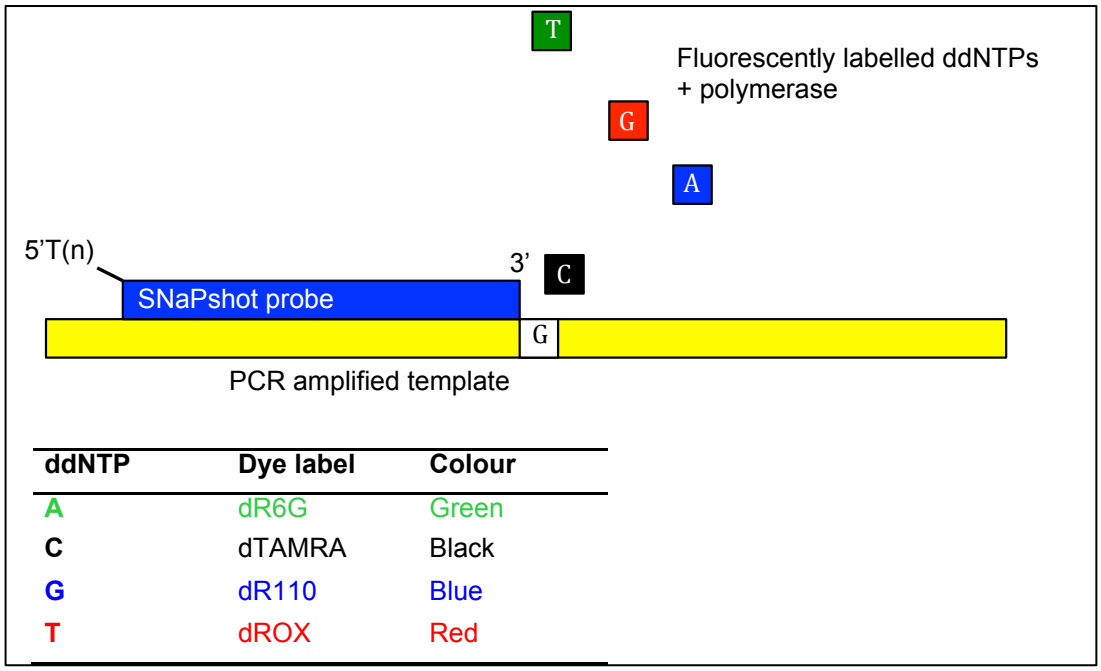

ddNTP	Dye label	Colour
A	dR6G	Green
C	dTAMRA	Black
G	dR110	Blue
T	dROX	Red

Figure 2.4: The SNaPshot probe extension step. SNaPshot probes are designed to anneal adjacent to hotspot mutations and are extended by one base only. They are tailed with differing lengths of Ts at their 5'-terminus to allow separation of SNaPshot products according to size. The dye labels on each of the ddNTPs are shown in the table.

2.5 Array Comparative Genomic Hybridization

Array Comparative Genomic Hybridization (aCGH) is a microarray-based technique used for genome-wide screening of DNA copy number alterations. The microarrays are created by positioning and immobilising fragments of DNA (probes) on a solid support (glass slide) in a predetermined, ordered fashion. The level of resolution is determined by both probe size and genomic distance between DNA probes. The basic methodology is illustrated in Figure 2.5.

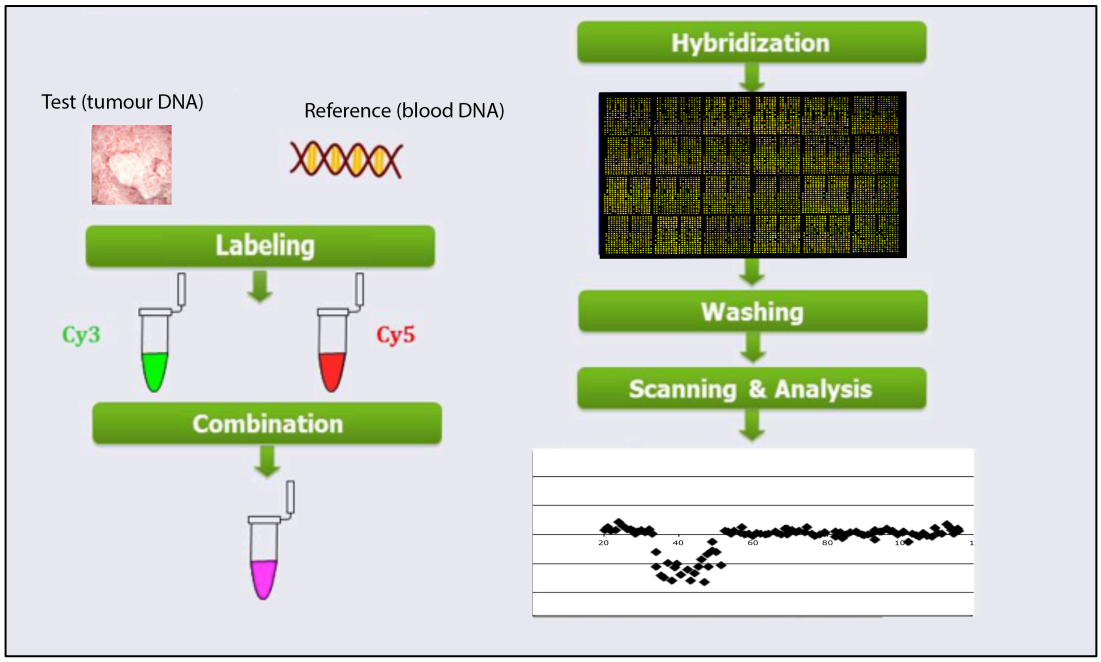

Figure 2.5. Diagram illustrating the aCGH process. In aCGH, DNA from a tumour sample (green) and a normal reference sample (red) are labelled differentially, and co-hybridized to probes which are printed onto a glass slide. The fluorescence intensities of the test and reference samples is measured and the ratio (test/reference) is used to determine copy number alterations in the tumour sample. Adapted from Memorial Hospital, Turkey, 2014

In the current study, BAC (Bacterial Artificial Chromosome) arrays with 1-Mb resolution (Centre for Microarray Resources, Department of Pathology, University of Cambridge, Cambridge, UK) were used. The BACs contain copies of human DNA, the positions of which are known. 1-Mb resolution means that the human sequences represented on the array are spaced at approximately 1-Mb intervals throughout the genome. DNA extracted from a tumour sample (test) and the corresponding blood sample (reference) are differentially labelled with the fluorescent dyes Cy5 and Cy3, respectively. Both the microarray and labelled DNA samples are pre-treated using herring sperm DNA and COT1 DNA to reduce general non-specific hybridisation and binding to repetitive sequences that are found at numerous locations throughout the genome, respectively. The differentially-labelled genomic DNAs from tumour and blood samples are then mixed together, denatured

and allowed to competitively hybridise to the single-stranded probes on the microarray. Following a series of washing steps to remove unincorporated and non-specifically bound labelled DNAs, slides are scanned using a high resolution microarray laser scanner. The scanner measures the intensity of the two dyes on the labelled DNAs simultaneously allowing the relative fluorescence intensity of hybridisation at each probe to be determined. Thus, the ratio of fluorescence signals from the test and reference is determined at different positions along the genome, thereby providing information on the relative copy number of sequences in the tumour genome as compared to the control genome.

In the current study, hybridization to arrays was essentially as described by Fiegler *et al.* and Hurst *et al.* [5, 234]. Reference samples were matched blood DNA or DNA extracted from an EBV immortalized lymphocyte cell line (J82 EBV) where blood was not available (patient 5, 7, 9, 13, 22). Briefly, tumour and reference genomic DNAs were labelled with Cy5-dCTP or Cy3-dCTP respectively, using random-primer labelling (BioPrime DNA Labelling Kit, Invitrogen Ltd, Paisley, UK) (Figure 2.6). A reaction mix consisting of random-primers (20μl), Cy5-dCTP or Cy3-dNTP (5 μl), template DNA (400ng) and molecular biology grade water to a total volume 45 μl was heat-denatured for 5 mins at 94°C, then snap-cooled on ice. Next, 1μl of Klenow was added to each tube and the reactions were incubated at 37°C for 16-20 hrs.

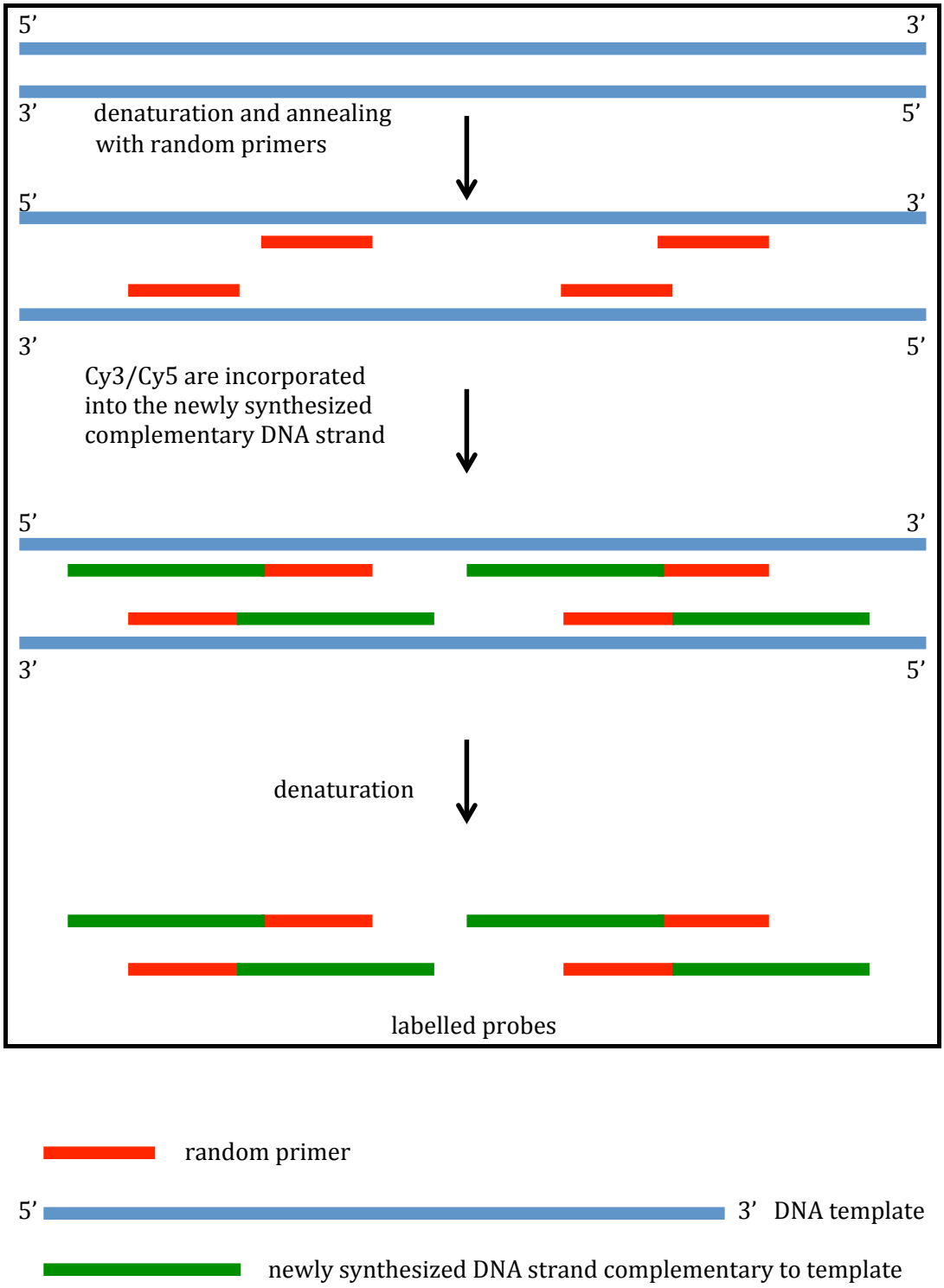

Figure 2.6. DNA labelling by the random primer method. Double-stranded DNA (blue) is heat denatured then snap-cooled allowing annealing of random primers (red). New strands are then synthesized by Klenow DNA polymerase. During the synthesis step, labelled dNTPs such as Cy3-dNTP

or Cy5-dNTP (green) are incorporated resulting in uniformly labelled DNA on both DNA strands. Adapted from Invitrogen Ltd, 2014.

Unincorporated nucleotides were separated from labelled DNA using Micro-spin G50 columns (GE Healthcare, Buckinghamshire, UK) according to manufacturer's instructions. Unincorporated dye adheres to the resin whilst labelled DNA passes through the column into the collection tube. The labelled genomic DNAs from tumour and reference sample were then combined, giving a total volume of 100 μl, then precipitated using 10 μl of 3 M sodium acetate (pH 5.5) and 250 μl of ice-cold absolute ethanol. Samples were centrifuged and the supernatant removed. The pellets were dried and re-suspended in 25 μl of hybridization buffer (50% formamide, 10% dextran sulphate, 0.1% Tween 20, 2 x SSC, 10 mM Tris-HCl pH 7.5) containing 62.5 μg Cotl I DNA and 375 μg herring sperm DNA then left to prehybridize at 37°C for 2h. This prehybridization step enables the blocking of repetitive sequences by Cotl I DNA and blocking of general non-specific binding by herring sperm DNA.

Slides containing arrays were prehybridized to block non specific binding by the addition of 30 μl of hybridization buffer containing denatured herring sperm DNA (9-12 μg/ml, Sigma-Aldrich Company Ltd., Dorset, UK). A Hybri-Slip was placed on top of the array to prevent drying out. The slides were then incubated at 37°C for 2h in a humid chamber containing tissues saturated with 2 x saline-sodium citrate buffer (SSC) (3 M NaCl in 0.3 M sodium citrate, pH 7.0) and 50% formamide. Slides were then washed twice in Phosphate Buffered Saline (PBS) solution (H_2O, 137 mM NaCl, 2.7 mM KCl, 10 mM Na_2HPO_4, 1. 8 mM KH_2PO_4, pH 7) (Sigma-Aldrich Company Ltd., Dorset, UK) and dried by centrifugation at 150 x g for 3 min.

The prehybridized labelled DNA was then added to the prehybridized slide, a Hybri-Slip was placed on top and the slides were incubated for 20-24h at 37°C in a humid chamber to prevent drying out. Slides were washed in PBS/0.05% Tween 20 for 10 min at room temperature, then 50% formamide/

2 x SSC for 30 min at 42°C, and finally PBS/0.05% Tween 20 for 10 min at room temperature, and then dried by centrifugation at 150 x g for 3 min.

2.5.1 Image acquisition and data processing

Slides were scanned at 532 nm and 633 nm with a resolution of 10 µm using an Agilent G2565CA Microarray Scanner (Agilent Technologies, Stockport, UK). High-resolution TIFF images were generated and these were used as input for analysis using BlueFuse software (BlueGnome, Cambridge, UK).

BlueFuse software was used to define spots, subtract background, and calculate normalised fluorescence intensities. The software (1) excludes data values below the fluorescence intensity values of Drosophila control spots and empty buffer spots on the array, (2) adjusts for differences in overall signal intensity between Cy3 and Cy5 channels by normalizing all signal intensities to a 1:1 ratio on autosomal chromosome clones, (3) calculates mean $\log_2$ (test/reference) ratios for triplicates spots, and (4) excludes controls, excludes replicate clones >0.2 SD apart and excludes spots with <0.1 confidence (i.e. poor quality spots).

BlueFuse produces a $\log_2$ ratio (test/reference) value for each clone on the array which can be exported. This $\log_2$ ratio data was transferred to an Excel spreadsheet to produce graphical outputs in the form of individual chromosome plots of mean $\log_2$ ratio (y-axis) against distance along the chromosome (Mb) (x-axis). Physical positions were according to hg19/NCBI Build 37. The same data was also transferred to another Excel spread sheet and presented as a graph where the whole genome of each tumour could be visualized. This graphical presentation (tiled data) of the whole genome allowed tumours from the same patient to be aligned thus enabling the comparison of breakpoints and altered regions between tumours (including the modified scoring mentioned below).

Normal thresholds of experimental variation for the array used in this study have been previously determined by observation of normal samples and samples with known changes by Hurst *et al* [235]. Regions of gain and loss and breakpoints were detected initially by the BlueFuse software aCGH-Smooth algorithm [236] with calling thresholds for copy number gains and losses set to +0.15 or -0.15 $\log_2$ ratio of test/reference respectively. The algorithm gives an average $\log_2$ score across regions defined as altered.

Subtle changes not scored by the BlueFuse software but relevant to the study were included manually upon visual inspection. Modified scoring criteria for the purpose of this study included incorporation of the alterations in tumours which were shared by other tumours in the same patient but did not reach the BlueFuse thresholds and low level single clone alterations below the BlueFuse threshold but common to all other tumours from the patient. In order to do this the whole genome plots for all tumours from a patient were tiled and used as a guide to modify the scoring where necessary.

2.5.2 Fraction of genome altered (FGA)

Fraction of genome altered (FGA) was calculated for each tumour sample. FGA provides a measure of chromosomal instability and was defined as the percentage of clones reporting significantly altered copy number. FGA was classified into four groups: A<1%, B 1≤10%, C 10≤30%, and D>30% of clones altered.

2.5.3 Constructing patient representative data

In order to facilitate comparisons of patients' copy number data, each patient had to have a single set of representative data from all of its tumours. To construct representative data (merged data) for each patient, data from all

tumours in a given patient were combined together so every copy number alteration within the patient was included to give a view of the total complexity Table 2.5. The only exception being if a given region was both gained and lost within the patient in different tumours in which case such conflicts were excluded from the analysis. Conflicts were reported as no change. The highest level gain/loss in the patient was reported for each clone. The merging of data for representative group could potentially have some disadvantages. This could have resulted in some small tumour differences being 'lost' in the representative profile. Differences in only a few clones could also have been under represented.

Prior to generating the merged data, the smoothed scored data for each tumour was manipulated using Excel formula work sheets so that each clone was assigned a copy number class (0 = no copy number aberration; 1 = gain; -1 = loss; 2 = high-level gain (>+1.2 $\log_2$ threshold) -2 = high-level loss (<-1.2 $\log_2$ threshold)). Conflicts, as described above, were assigned a value of 0.

For the purpose of merged data analysis, if multifocal tumours were of different stage and/or grade then the highest stage and/or grade within the patient was applied. A similar rule was applied in patients where there was a conflict with respect to mutation status. If one tumour was mutant then the patient was classified as mutant in merged data set. FGA value per patient was calculated based on merged copy number data for each patient.

Number	Stage and grade	FGA group	*FGFR3* mutation status	*PIK3CA* mutation status	*RAS* mutation status
1	TaG2	B	WT	Mutant	WT
2	TaG2	C	Mutant	WT	WT
3	T1G3	C	WT	WT	Mutant
4	TaG3	C	Mutant	Mutant	WT
5	TaG2	D	Mutant	WT	WT
6	T1G3	D	WT	WT	WT
7	TaG2	C	WT	WT	WT
8	TaG2	C	Mutant	Mutant	WT
9	T1G3	A	WT	WT	WT
10	TaG3	D	WT	WT	WT
11	T1G3	C	WT	WT	WT
12	T1G3	D	WT	WT	WT
13	T1G3	D	WT	WT	WT
14	TaG3	D	WT	WT	WT
15	TaG2	C	Mutant	Mutant	WT
16	TaG2	C	WT	WT	Mutant
17	TaG2	B	Mutant	Mutant	WT
18	T1G3	D	WT	WT	WT
19	TaG2	C	Mutant	WT	WT
20	T1G3	D	WT	WT	WT
21	TaG2	C	Mutant	WT	WT
22	TaG2	C	WT	WT	WT

Table 2.5. Representative data (merged data) for each patient.

2.5.4 Copy number frequency plot visualisation and statistical comparisons

The merged copy number class data described in section 3.5.2 was used as the input for frequency plot visualization and statistical comparisons performed within the Nexus Copy Number Professional 6 software package (BioDiscovery).

Using the Comparisons function of the Nexus software a Fisher's Exact test with a p-value cutoff of 0.05 and a differential threshold of 25% was performed to determine significant differences in the copy number data for specified sample sub-groups. Comparisons of copy number alterations were made with respect to:

- stage
- grade
- *FGFR3* mutation status
- smoking status
- *CDKN2A* copy number loss

2.5.5 Multifocal (merged) vs single tumour comparisons

aCGH data for 160 tumours from Hurst *et al.* [235] was available for comparison with the data from the current study. One hundred and three of these tumours were single. This subset consisting of 28 TaG2, 10 TaG3, 7 T1G2, 29 T1G3 and 29 ≥ T2G3 tumours had no known multifocality at the time of sample collection and were used in comparisons with the multifocal data from the current study.

The single tumour data of Hurst *et al*. was imported into Nexus for comparison with the multifocal data. For this to occur, multifocal tumour data had to be made compatible by converting it to hg18/NCBI Build 36 using Excel. Copy number alterations in the merged multifocal and single tumour datasets were compared with respect to:

- stage and grade,

- *FGFR3* mutation status and stage,
- *FGFR3* mutation status and stage and grade
- *CDKN2A* copy number loss

2.5.6 Other statistics

Associations between non-parametric data (stage and grade, mutation status, *CDKN2A* copy number loss, FGA) were tested using the chi-square (X^2) test within the Prism software package (GraphPad Software, Inc.). The chi-square test compares observed with expected numbers, with the null hypothesis being that there is no significant difference between the expected and observed result. Significance was taken as a probability value $P < 0.05$.

2.5.7 Clustering

One-way unsupervised hierarchical cluster analysis was performed to reveal relationships between samples using Partek Genomics Suite 6.6 (Partek Inc.). One-way unsupervised hierarchical cluster analysis was performed using copy number class data with Euclidean distance and the Ward method of linkage. Cluster analysis was performed for the individual multifocal tumours (n=66), for merged multifocal patient data (n=22) and for merged multifocal patient data combined with the single tumour data of Hurst *et al.* (n=74).

2.5.8 Construction of phylogenetic trees

For the analysis of copy number alterations and break points in tumour samples from the same patient and reconstruction of the relationships between them (both similarity and differences), the computational TuMult [237] algorithm was applied. During tumorigenesis cells that are descendants from one cancerous cell are characterized by having common genetic alterations and unique alterations characteristic only to the given cell. The common changes are hypothesised to occur before clone separation and the unique alterations after clone separation. Hence, the comparison of these changes can lead to the reconstruction of the sequence

of chromosomal events giving rise to each tumour. This concept is applied in the TuMult methodology, as is the reasoning that clones separating later in the tumorigenesis process should have more genetic events in common than those separating earlier in this process. Tumult uses an iterative grouping of the two closest nodes according to chromosome breakpoints, to reconstruct the tumour lineage from the leaves (tumours) to the root (normal cell).

The TuMult algorithm is implemented through the R software environment. The input data for TuMult was copy number class data (as described above) and $\log_2$ data for each tumour. All tumours from each individual patient were included in the analyses. For patients with prequel or recurrent tumours a second analysis was performed that included these samples. Phylogenetic trees produced by TuMult were exported in .dot format. Images were then generated from the .dot files using the open source graph visualization software Graphviz (http://www.graphviz.org).

Matched Primary and Metastatic Bladder Cancer Study

2.1 Patients, follow-up, surgical technique and pathology

The cohort comprised 150 bladder cancer patients without preoperative evidence of metastases (i.e., physical examination, chest x-ray, intravenous urography, bone scan, and pelvic computed tomography, when available) but with lymph node metastases on pathologic examination. All patients underwent extended pelvic lymphadenectomy with cystectomy as a single procedure between January 1985 and April 2008 at the Department of Urology, University of Bern according to standard protocols described previously in detail [238, 239]. The surgical specimens were processed as described previously [239]. The tumours were staged according to the 7th Union Internationale Contre le Cancer classification [240]. No neoadjuvant therapy was given. Postoperatively, the patients were followed prospectively according to a standard protocol with examinations at the Department of Urology or by urologists in private practice at 3 months and 6 months, then

at 6-monthly intervals until 5 year, and then at yearly intervals thereafter. Patients' clinicopathological data included in the study is shown in Table 2.6.

Patient data (n = 150)	
Age at surgery, yr, median (range)	67 (35–89)
Female/male, No.	29/121
Follow-up, yr, median	7.1
Cystectomy data	
Tumour stage, No.	
pT1	4
pT2	17
pT3	92
pT4	37
Lymphadenectomy data	
Evaluated nodes per patient, median (range)	27 (10–56)
Positive nodes per patient, median (range)	3 (1–46)
Extracapsular extension of metastases, No.	
No	71
Yes	79

Table 2.6 Clinicopathologic data of patients included in the study

2.2 Construction of the tissue microarray (TMA)

The TMA was constructed in Bern, Switzerland by experienced technician. Briefly, the TMA [241] was constructed with six tissue cores (0.6-mm diameter) per patient: two each from normal urothelium, primary tumour (centre and invasion front), and a nodal metastasis. Biopsies were placed on slides with 17 columns and 9 rows with one liver biopsy as a control sample (Figure 2.7).

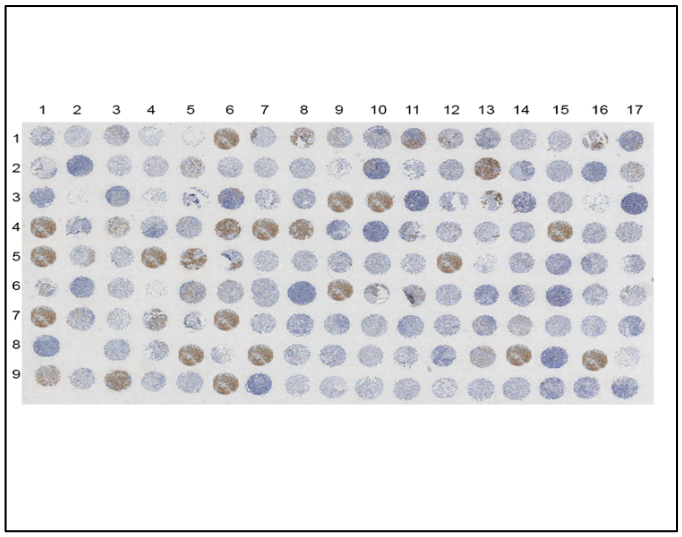

Figure 2.7: Tissue microarray. A microarray contains many small representative tissue samples from different patients assembled on a single slide. This allows high throughput analysis of multiple specimens at the same time.

2.3 Immunohistochemistry

FGFR3 protein expression was assessed in sections of TMAs of formalin-fixed paraffin wax-embedded tumours in two blocks. Briefly, 3 µm sections were deparaffinised in xylene (four times for 5 min.), rehydrated through graded ethanols (100%, 90%, and 70%, samples were immersed for 2 min.) and endogenous peroxidase activity blocked in 3% hydrogen peroxide (Sigma-Aldrich Company Ltd., Dorset, UK) for 20 min. The graded ethanols were in order: 100%, 90%, and 70% and samples were immersed for 2 min. Next, running cold tap water was used to rinse for 10 min. For antigen retrieval, sections were boiled in 10mM citric acid buffer (pH6) for 2 min, and non-specific binding was blocked for 15 min. with avidin/biotin solution (Vector Laboratories, Peterborough, UK) followed by 10% normal serum (Dako, Ely, UK) for 20 min. Primary antibody (FGFR3 B9, 1:100; Santa Cruz, CA, USA) was applied for 1 h at room temperature and detected with a biotinylated secondary antibody and 3,3- diaminobenzidine terahydrochloride (DAB; Vector Laboratories, Peterborough, UK). Slides were counterstained with Mayer's haematoxylin for 20 seconds, rinsed for 1 min with tap running water. Then dehydrated with absolute alcohol for 3 min.

dried for 5 min and immersed in Xylene for 2 min. Following this coverslips were mounted on the slides with DEPEX (Fisher Scientific UK Ltd, Loughborough, UK). Immunostaining was assessed by three independent observers (Prof. M. Knowles, Dr P. Harnden, Mr R. Turo), who were blinded to mutational status and clinical outcomes. A semi-quantitative scoring system was adopted: 0, all tumour cells negative; 1, faint but detectable positivity in some or all cells; 2, weak but extensive positivity; 3, strong positivity (regardless of extent). (Figure 2.8, 2.9, 2.10, 2.11). For the statistical analysis, tumours with the score 0 and 1 were grouped as low (L) and tumours scored 2 and 3 as high (H). Scanned images were viewed on a computer using different magnifications.

2.3.1 Statistical analysis of TMA

FGFR3 expression was tested for association with categorical clinical data using a Fisher's exact test, and overall survival (OS) and recurrence free survival (RFS) using Kaplan-Meier analysis. Significance of predictors in survival analysis was assessed using the log-rank test for univariate analysis. For analysis of metastatic tumour phenotype the ratios have been calculated of total and lower metastases' diameter, and total number of metastases. All statistical calculations were carried out with SPSS for Windows ® version 20.

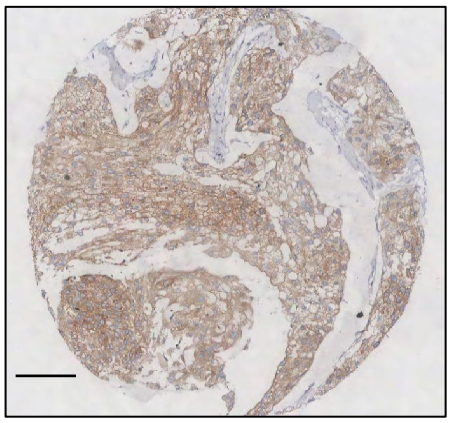

Figure 2.8: Detection of FGFR3 by IHC. Strong FGFR3 expression (score 3), (x10 magnification), Size bar = 100μm

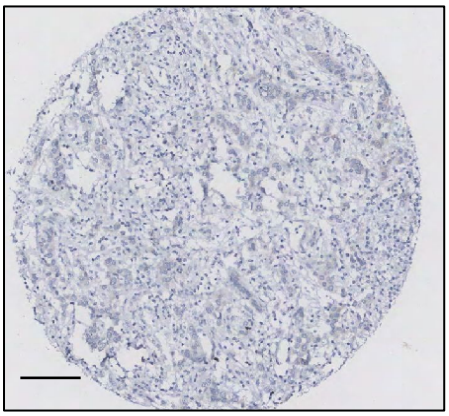

Figure 2.9: Detection of FGFR3 by IHC. Absence of staining (score 0), (x10 magnification), Size bar = 100μm

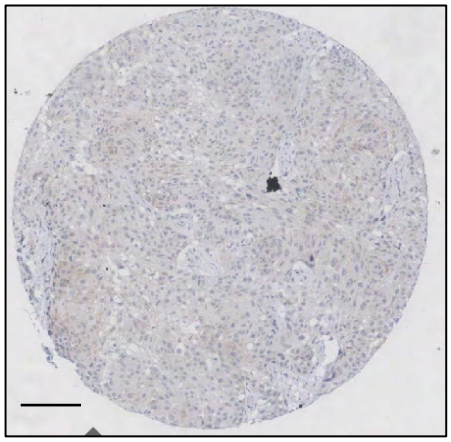

Figure 2.10: Detection of FGFR3 by IHC. Faint but detectable positivity (score 1), (x10 magnification), Size bar = 100μm

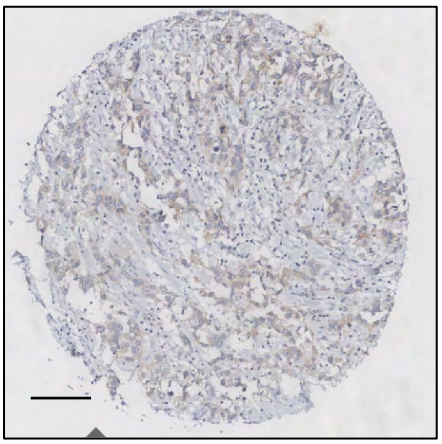

Figure 2.11: Detection of FGFR3 by IHC. Weak but extensive positivity (score 2), (x10 magnification), Size bar = 100μm

Chapter 3
Copy number alterations and mutation analysis

In this chapter we have aimed to describe detailed molecular characterization and comparison of genetic alterations in clinically and morphologically distinct multifocal tumour cell populations. This information would serve to reveal the clonal evolution of carcinoma of the urinary bladder. Also our enhanced knowledge of the molecular genetic characteristics of multifocal bladder tumours may offer a combined molecular and histo-pathological approach to classification and thus improve clinical management and the decision-making process of this common cancer. By combing copy number and mutation data we aimed to assess the molecular heterogeneity of tumours within and between patients, and to identify specific features related to multifocality. In most of the published studies on multifocal bladder cancer, conventional CGH, LOH analysis, FISH and mutation scanning of *TP53* and *FGFR3* have been applied to the study of small sets of tumours [184, 242-247]. To our knowledge, this study is the first to use aCGH to analyse such a large panel of superficial multifocal bladder tumours.

This chapter describes the results of experiments in which aCGH and SNaPshot analysis were used to determine copy number alterations and mutations, respectively, in 66 tumours from 22 patients with non muscle-invasive multifocal bladder cancer. As described in detail in the Materials and Methods (see Section 2), in order to facilitate comparisons of patients' copy number data, each patient had to have a single set of representative data from all tumours. To construct representative data (merged data) for each patient, data from all tumours in a given patient were combined together so every copy number alteration within the patient was included to give a view of the total complexity. Relationships between copy number alterations, mutation status and clinico-pathologic data have been assessed.

3.1 Copy number alterations

3.1.1 Frequencies of copy number alterations

1Mb-resolution aCGH was used to assess copy number alterations in 66 tumours from 22 patients. All copy number data is available in the Appendix 3.1. Copy number alterations involving whole chromosomes, chromosome arms and smaller regions were detected. Representative data (merged) data was constructed for each patient using the individual tumour copy number data. The frequencies of copy number alterations by chromosome arm were then calculated using the merged copy number data for each patient (Table 3.1). The most common region gained was 20q (68.2%), and the most common region lost was 9q (81.8%). The most frequent gains observed in ≥50% of the patients were on 8q (63.6%) and 1q (50%). The most frequent deletions were observed on 9p (77.3%), 10q (63.6%), 5q (54.5%), 8p (50%) and 2q (50%). The mean number of chromosomal gains per patient was 29.02 (range 0-66.7) and mean number of chromosomal deletions was 30.1 (range 0-56.4).

	Chromosome arm (frequency in patients %)
Gains	20q (68.2%), 8q (63.6%), 1q (50%), 20p (45.5%), 13q (45.5%), 10q (40.9%), 6p (40.9%), 17q (36.4%), 12q (36.4%), 9p (36.4%), 7q (36.4%), 2p (36.4%), 1p (36.4%), 15q (31.8%), 11q (31.8%), 5p (31.8%), 19q (27.3%), 14q (27.3%), 4p (27.3%), 3q (27.3%), 3p (27.3%), 21q (22.7%), 18q (22.7%), 18p (22.7%), 16p (22.7%), 7p (22.7%), 2q (22.7%), 4q (22.7%), 17p (18.2%), 16q (18.2%), 12p (18.2%), 10p (18.2%), 8p (18.2%), 22q (13.6%), 19p (13.6%), 11p (13.6%), 9q (13.6%), 6q (13.6%), 5q (9.1%)
Deletions	9q (81.8%), 9p (77.3%), 10q (63.6%), 5q (54.5%), 8p (50%), 2q (50%), 22q (40.9%), 17p (40.9%), 14q (40.9%), 13q (40.9%), 12q (36.4%), 11p (36.4%), 19p (31.8%), 16q (31.8%), 6q

	(31.8%), 19q (27.3%), 16p (27.3%), 11q (27.3%), 8q (27.3%), 4q (27.3%), 4p (27.3%), 3q (27.3%), 18p (22.7%), 17q (22.7%), 15q (22.7%), 7p (22.7%), 1q (22.7%), 1p (22.7%), 18q (18.2%), 12p (18.2%), 7q (18.2%), 2p (18.2%), 21q (13.6%), 10p (13.6%), 5p (13.6%), 3p (13.6%), 20q (4.5%), 6p (4.5%)

Table 3.1 The frequencies of copy number alterations by chromosome arm in 22 patients.

3.1.2 Copy number alterations and stage and grade

Genome-wide frequency plots of copy number alterations were constructed for all 22 patients and according to stage and grade (Figure 3.1). The proportions of the different types of copy number alterations (whole chromosome, chromosome arms or smaller regions) did not significantly differ between stages or grades, but the frequencies of copy number events increased with stage and grade (Figure 3.1).

The frequencies of copy number alterations by chromosome arm in stage Ta and T1 tumours are shown in Table 3.2. Ta and T1 tumours showed alterations on 18% and 30% of chromosome arms respectively. The most frequent alterations in Ta tumours were losses of 5q (50%), 9p (78.6%), 9q (85.7%) and gains of 8q (57.1%) and 20q (57.1%). In T1 tumours, frequent losses were observed of 2q (75%), 9p (75%), 9q (75%), 10q (87.5%), 22q (75%) and gains of 2p (75%), 6p (75%), 8q (75%), 20p (75%) and 20q (87.5%).

Using the Comparisons function of the Nexus software package, a Fishers Exact test (0.05 p-value cut off; 25% differential threshold) was used to compare the frequencies of copy number alterations in patients with Ta (n=14) versus T1 (n=8) tumours (Figure 3.1, Appendix 3.2). Gains on 1p, 2p, 6p, 7p, 7q, 9q, and 16p were significantly more frequent in stage T1 tumours. Deletions on 2q, 6q, 10q, 12p, 12q, 14q and 22q were also

significantly more frequent in patients with stage T1 tumours. The region showing the biggest difference in the frequency of deletion between Ta and T1 tumours was a region on 10q extending from 10q23.32 to 10q23.33 . This region contains the following genes: *CPEB3, SDHCP2, EIF4A1P8, NHP2P1, MARCH5, MARK2P9, IDE, KIF11, RPL11P4, EIF2S2P3, HHEX, EXOC6, CYP26C1, CYP26A1*, and *NIP7P1*.

Stage	**Losses (frequency %)**	**Gains (frequency %)**
Ta n=14	1p (21.4), 1q (21.4), 2p (21.4), 2q (35.7), 3p (14.3), 3q (21.4), 4p (21.4), 4q (21.4), 5p (7.1), 5q (50), 6q (21.4), 7p (28.6), 7q (28.6), 8p (42.9), 8q (35.7), 9p (78.6), 9q (85.7), 10p (7.1), 10q (50), 11p (28.6), 11q (21.4), 12p (7.1), 12q (28.6), 13q (35.7), 14q (28.6), 15q (14.2), 16p (21.4), 16q (28.6), 17p (35.7), 17q (35.7), 18p (21.4), 18q (14.3), 19p (21.4), 19q (28.6), 20q (7.1), 21q (14.3), 22q (21.4)	1p (28.6), 1q (42.9), 2p (14.3), 2q (14.3), 3p (21.4), 3q (28.6), 4p (28.6), 4q (14.3), 5p (28.6), 6p (21.4), 6q (7.1), 7p (7.1), 7q (21.4), 8p (14.3), 8q (57.1), 9p (35.7), 10p (28.6), 10q (35.7), 11p (7.1), 11q (21.4), 12p (7.1), 12q (28.6), 13q (42.9), 14q (21.4), 15q (28.6), 16p (7.1), 16q (14.3), 17 p (14.3), 17q (35.7), 18p (21.4), 18q (14.3), 19p (14.3), 19q (21.4), 20p (28.6), 20q (57.1), 21q (21.4), 22q (7.1)
T1 n=8	1p (25), 1q (25), 2q (75), 3q (37.5), 4p (37.5), 4q (37.5), 5p (25), 5q (62.5), 6q (50), 8p (62.5), 9p (75), 9q (75), 10p (25), 10q (87.5), 11p (50), 11q (37.5), 12p (37.5), 12q (50), 13q (50), 14q (62.5), 15q (37.5), 16p (37.5), 16q (37.5), 17p (50), 18p (25), 18q (25), 19 (50), 19q (25), 22q (75)	1p (50), 1q (62.5), 2p (75), 2q (37.5), 3p (37.5), 3q (25), 4p (25), 4q (37.5), 5p (37.5), 5q (25), 6p (75), 6q (25), 7p (50), 7q (62.5), 8p (25), 8q (75), 9p (37.5), 9q (37.5), 10q (50), 11p (25), 11q (50), 12p (37.5), 12q (50), 13q (50), 14q (37.5), 15q (37.5), 16p (50), 16q (25), 17p (25), 17q (37.5), 18p (25), 18q (37.5), 19q (37.5), 20p (75), 20q (87.5), 21q (25), 22q (25)

Table 3.2 Recurrent genomic alterations by chromosome arm in 22 patients according to stage.

The frequencies of copy number alterations by chromosome arm in grade 2 and grade 3 tumours are shown in Table 3.3. Grade 2 tumours showed a lower average frequency of alterations (10%) than grade 3 tumours (27%). Grade 3 tumours exhibited frequent losses of 2q (72.7%), 5q (72.7%), 9p (72.7%), 9q (81.8%), 10q (81.8%) and 22q (81.8%), and gains of 1q (63.6%), 2p (63.6%), 6p (63.6%), 8q (63.6%), 20p (63.6%) and 20q (90.9%). In grade 2 tumours, losses of 9p (81.8%) and 9q (81.8%), and gains of 8q (63.6%), 13q (45.5%) and 20q (45.5%) predominated.

Stage	Losses (frequency %)	Gains (frequency %)
G2 **n=11**	1q (9.1), 2p (18.2), 2q (27.3), 3q (18.2), 4p (9.1), 4q (18.2), 5p (9.1), 5q (36.4), 6q (18.2), 7p (9.1), 7q (27.3), 8p (36.4), 8q (27.3), 9p (81.8), 9q (81.8), 10p (9.1), 10q (45.5), 11p (18.2), 11q (9.1), 12p (9.1), 12q (9.1), 13q (36.4), 14q (18.2), 15q (18.2), 16p (27.3), 16q (36.4), 17p (27.3), 17q (27.3), 18p (27.3), 18q (18.2), 19p (9.1), 19q (18.2), 20q (9.1)	1p (27.3), 1q (36.4), 2p (9.1), 2q (9.1), 3p (9.1), 3q (18.2), 4p (18.2), 4q (9.1), 5p (18.2), 6p (18.2), 7q (18.2), 8p (9.1), 8q (63.6), 9p (36.4), 10p (27.3), 10q (36.4), 11q (9.1), 12q (27.3), 13q (45.5), 14q (18.2), 15q (18.2), 17p (18.2), 17q (27.3), 18p (18.2), 18q (9.1), 19p (9.1), 19q (18.2), 20p (27.3), 20q (45.5), 21q (18.2), 22q (9.1)
G3 **n=11**	1p (45.5), 1q (36.4), 2p (18.2), 2q (72.7), 3p (27.3), 3q (36.4), 4p (45.5), 4q (36.4), 5p (18.2), 5q (72.7), 6p (9.1), 6q (45.5), 7p (36.4), 7q (9.1), 8p (63.6), 8q (27.3), 9p (72.7), 9q (81.8), 10p (18.2), 10q (81.8), 11p (54.5), 11q (45.5), 12p (27.3), 12q (63.6), 13q (45.5), 14q (63.6), 15q (27.3), 16p (27.3), 16q (27.3), 17p (54.5), 17q (18.2), 18p (18.2), 18q (18.2), 19p (54.5), 19q (36.4), 21q (27.3), 22q (81.8)	1p (45.5), 1q (63.6), 2p (63.6), 2q (36.4), 3p (45.5), 3q (36.4), 4p (36.4), 4q (36.4), 5p (45.5), 5q (18.2), 6p (63.6), 6q (27.3), 7p (45.5), 7q (54.5), 8p (27.3), 8q (63.6), 9p (36.4), 9q (27.3), 10p (9.1), 10q (45.5), 11p (27.3), 11q (54.5), 12p (36.4), 12q (45.5), 13q (45.5), 14q (36.4), 15q (45.5), 16p (45.5), 16q (36.4), 17p (18.2), 17q (45.5), 18p (27.3), 18q (36.4), 19p (18.2), 19q (36.4), 20p (63.6), 20q (90.9), 21q (27.3), 22q (18.2)

Table 3.3 Recurrent genomic alterations by chromosome arm in 22 patients according to grade.

A comparison of the frequencies of copy number alterations in grade 2 and grade 3 patients was performed Appendix 3.3. Deletions on 2q, 4q, 4p, 10q, 11p, 14q, 19p, 22q and gains on 2p, 3p, 5p, 7p, 7q, 15q, 16p and 20q were more frequent in patients with grade 3 tumours (Figure 3.1). Only deletion of 9q was more frequent in grade 2 patients, however it was not statistically significant (p> 0.05) (Figure 3.1).

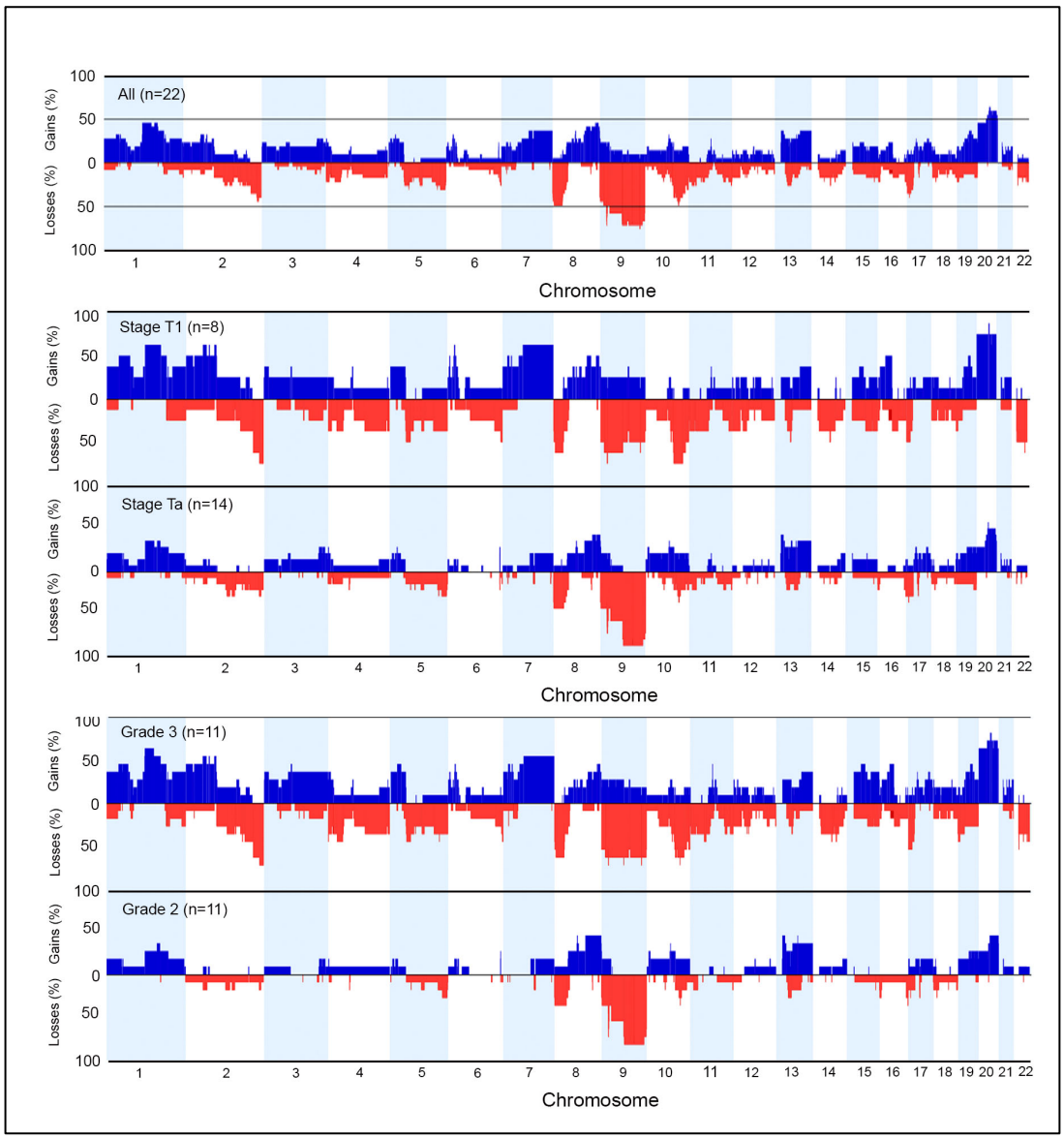

Figure 3.1: Genome-wide frequency plots of copy number alterations identified in all 22 patients. The *x*-axis corresponds to chromosomes 1 to 22 and the *y*-axis corresponds to the percentage of gains and losses. Copy number gains are shown in blue and losses in red. Frequencies of copy number alterations are shown for all 22 patients and according to stage and grade.

The frequencies of copy number alterations by chromosome arm were also calculated according to stage and grade (i.e. TaG2, TaG3 and T1G3 tumours). Copy number alterations that occurred at frequencies of ≥15% in TaG2, TaG3 and T1G3 tumours are shown in Table 3.4. The most frequent alterations in TaG2 tumours were losses of 9p (81.8%) and 9q (81.8%) and gains of 8q (63.4%), 13q (45.5%) and 20q (45.5%). Losses of 1p (100%), 5q (100%), 7p (100%), 9q (100%), 22q (100%) and gains of 1q (66.7%), 3p (66.7%), 4p (66.7%), 5p (66.7%), 11q (66.7%), 15q (66.7%), 16q (66.7%), 17q (66.7%) and 20q (100%) were the most frequent events in TaG3 tumours. In T1G3 tumours losses of 2q (75%), 9p (75%), 9q (75%), 10q (87.5%), 22q (75%) and gains of 2p (75%), 6p (75%), 8q (75%), 20p (75%), 20q (87.5%) were most frequent. Low-grade Ta and T1 tumours had fewer copy number alterations than high-grade tumours Table 3.4.

Stage/grade	Losses (frequency %)	Gains (frequency %)
TaG2 **(n=11)**	2p (18.2), 2q (27.3), 3q (18.2), 4q (18.2), 5q (36.4), 6q (18.2), 7q (27.3), 8p (36.4), 8q (27.3), 9p (81.8), 9q (81.8), 10q (45.5), 11p (18.2), 13q (36.4), 14q (18.2), 15q (18.2), 16p (27.3), 16q (36.4), 17p (27.3), 17q (27.3), 18p (27.3), 18q (18.2), 19q (18.2)	1p (27.3), 1q (36.4), 3q (18.2), 4p (18.2), 5p (18.2), 6p (18.2), 7q (18.2), 8q (63.4), 9p (36.4), 10p (27.3), 10q (36.4), 12q (27.3), 13q (45.5), 14q (18.2), 15q (18.2), 17p (18.2), 17q (27.3), 18p (18.2), 19q (18.2), 20p (27.3), 20q (45.5), 21q (18.2)
TaG3 **(n=3)**	1p (100), 1q (66.7), 2p (33.3), 2q (66.7), 3p (66.7), 3q (33.3), 4p (66.7), 4q (33.3), 5q (100), 6q (33.3), 7p (100), 7q (33.3), 8p (66.7), 8q (66.7), 9p (66.7), 9q (100), 10q (66.7), 11p (66.7), 11q (66.7), 12q (100), 13q (33.3), 14q (66.7), 17p (27.3), 17q (66.7), 19p (66.7), 19q (66.6), 21q (66.7), 22q (100)	1p (33.3), 1q (66.7), 2p (33.3), 2q (33.3), 3p (66.7), 3q (66.7), 4p (66.7), 4q (33.3), 5p (66.7), 6p (33.3), 6q (33.3), 7p (33.3), 7q (33.3), 8p (33.3), 8q (33.3), 9 p (33.3), 10p (33.3), 10q (33.3), 11p (33.3), 11q (66.7), 12p (33.3), 12q (33.3), 13q (33.3), 14q (3.33), 15q (66.7), 16p (33.3), 16q (66.7), 17q (66.7), 18p (33.3), 18q (33.3), 19p (33.3), 19q (33.3), 20p (33.3), 20q (100), 21q (33.3)
T1G3 **(n=8)**	1p (25), 1q (25), 2q (75), 3q (37.5), 4p (37.5), 4q (37.5), 5p (25), 5q (62.5), 6q (50), 8p (62.5), 9p (75), 9q (75), 10p (25), 10q (87.5), 11p (50), 11q (37.5), 12p (37.5), 12q (50), 13q (50), 14q (62.5), 15q (37.5), 16p (37.5), 16q (37.5), 17p (50), 18p (25), 18q (25), 19 (50), 19q (25), 22q (75)	1p (50), 1q (62.5), 2p (75), 2q (37.5), 3p (37.5), 3q (25), 4p (25), 4q (37.5), 5p (37.5), 5q (25), 6p (75), 6q (25), 7p (50), 7q (62.5), 8p (25), 8q (75), 9p (37.5), 9q (37.5), 10q (50), 11p (25), 11q (50), 12p (37.5), 12q (50), 13q (50), 14q (37.5), 15q (37.5), 16p (50), 16q (25), 17p (25), 17q (37.5), 18p (25), 18q (37.5), 19q (37.5), 20p (75), 20q (87.5), 21q (25), 22q (25)

Table 3.4 Recurrent genomic alterations by chromosome arm in 22 patients according to stage and grade. Only those alterations that occurred at frequencies > 15% are shown.

3.1.3 Whole genome profiles of all tumours from individual patients

Construction of whole genome plots for all tumours in a given patient enables the overall chromosomal instability to be assessed and the visualisation of genetic alterations that are unique to individual tumours. Analysis of whole genome profiles revealed that some patients had tumours that shared all or the majority of copy number events (patient 2, 3, 4, 7, 11, 13, 14, 17, 20, 21) (e.g. Figure 3.2), whilst others had tumours that shared some common copy number events but were otherwise highly divergent (patient 6, 10, 12, 15, 18, 19, 22) (e.g. Figure 3.3). In 6 patients (1, 5, 8, 9, 13, 16) there was at least one tumour in a given patient where a monoclonal origin could not clearly be confirmed. Patient 1 had two tumours with no copy number events while third synchronous tumour had copy number alterations (Figure 3.4). Patient 9 had no copy number alterations. Two tumours from patient 5 did not share copy number events. Genome plots for all tumours are available in Appendix 3.1.

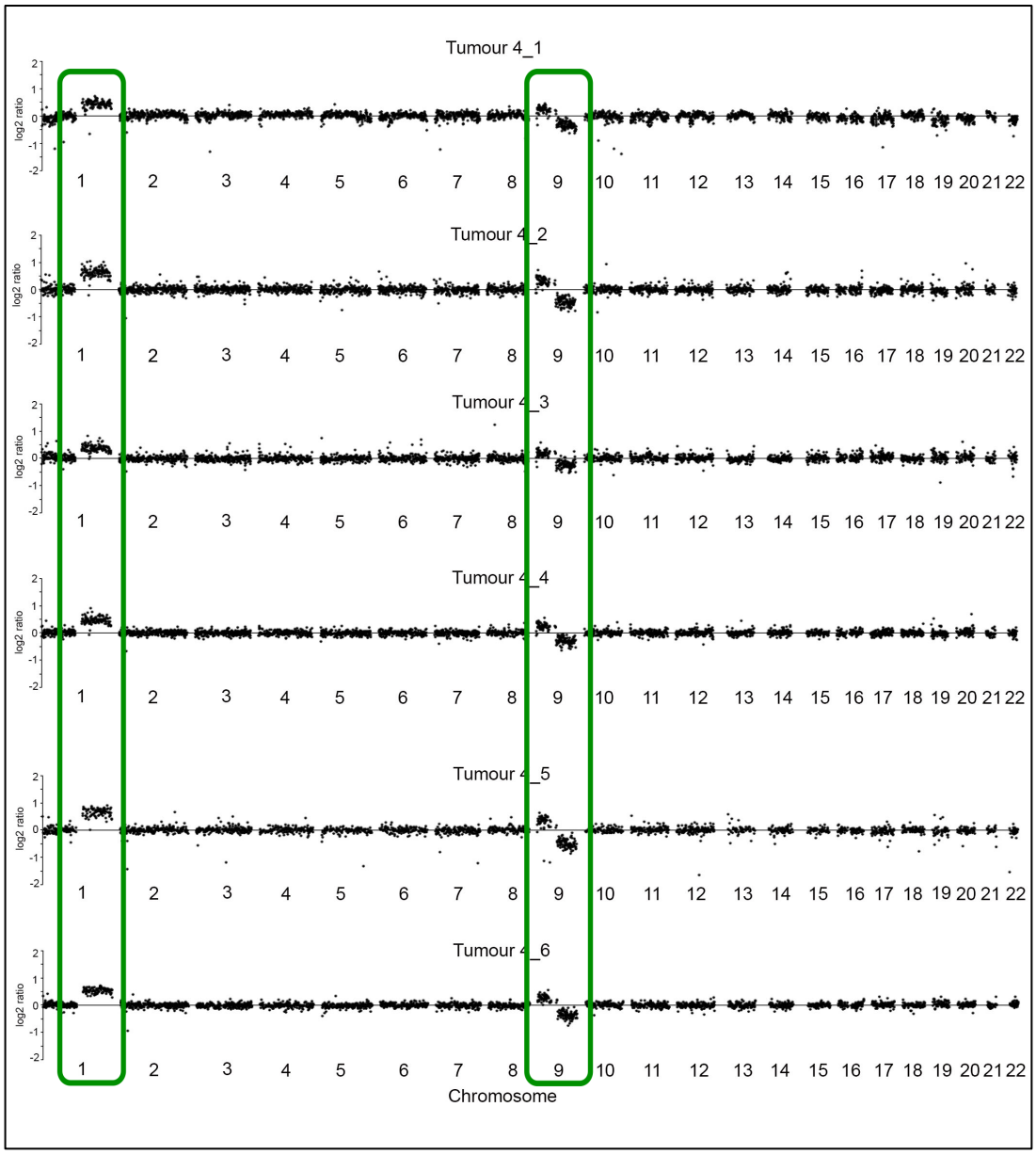

Figure 3.2: Whole genome plots of array CGH data for 6 tumours from patient 4 that shared the majority of copy number events. Shared copy number events on chromosomes 1 and 9 are highlighted in green. The Y-axis represents the log2 ratio (test / reference) for each BAC clone on the array. BAC clone genome order is plotted on the X-axis from chromosome 1 to chromosome 22.

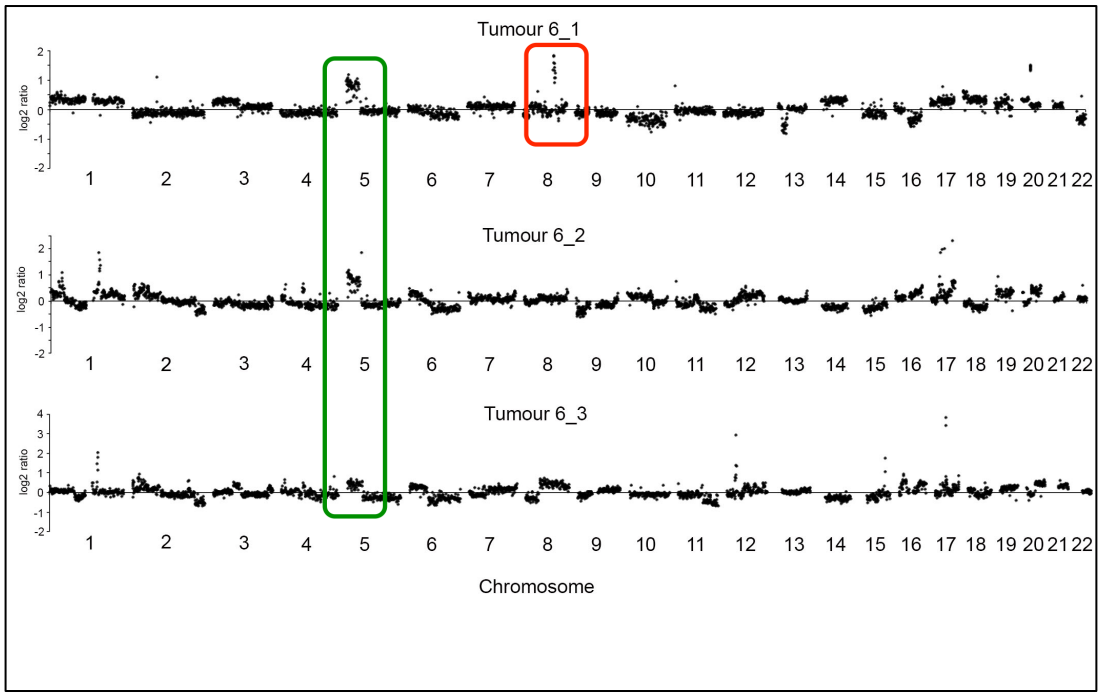

Figure 3.3: Whole genome plots of array CGH data for 3 tumours from patient 6 that shared some common copy number events but were otherwise highly divergent. Shared copy number events on chromosome 5 are highlighted in green and unique changes on chromosome 8 are highlighted in red.

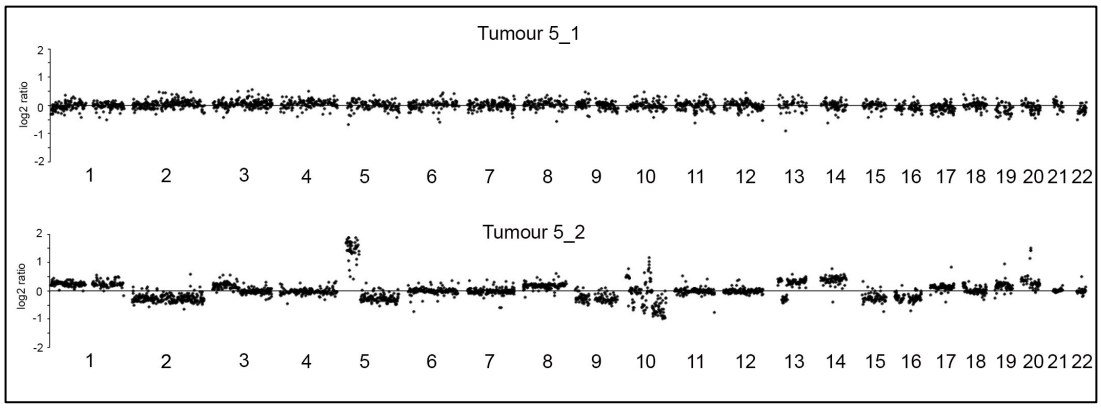

Figure 3.4: Whole genome plots of array CGH data for 2 tumours from patient 5 that did not share copy number events.

3.1.4 Transition of breakpoints

Whole genome plots for each tumour were aligned with others from the same patient, thus enabling the identification of breakpoints and alterations between tumours. The majority of identified breakpoints had the same transition from loss of copy number to gain or from gain to loss. In some patients a difference in the transition of breakpoint regions was seen in different tumours i.e. in some tumours the transition was up whilst in others the transition was down. Figure 3.5. This was identified in 15 patients.

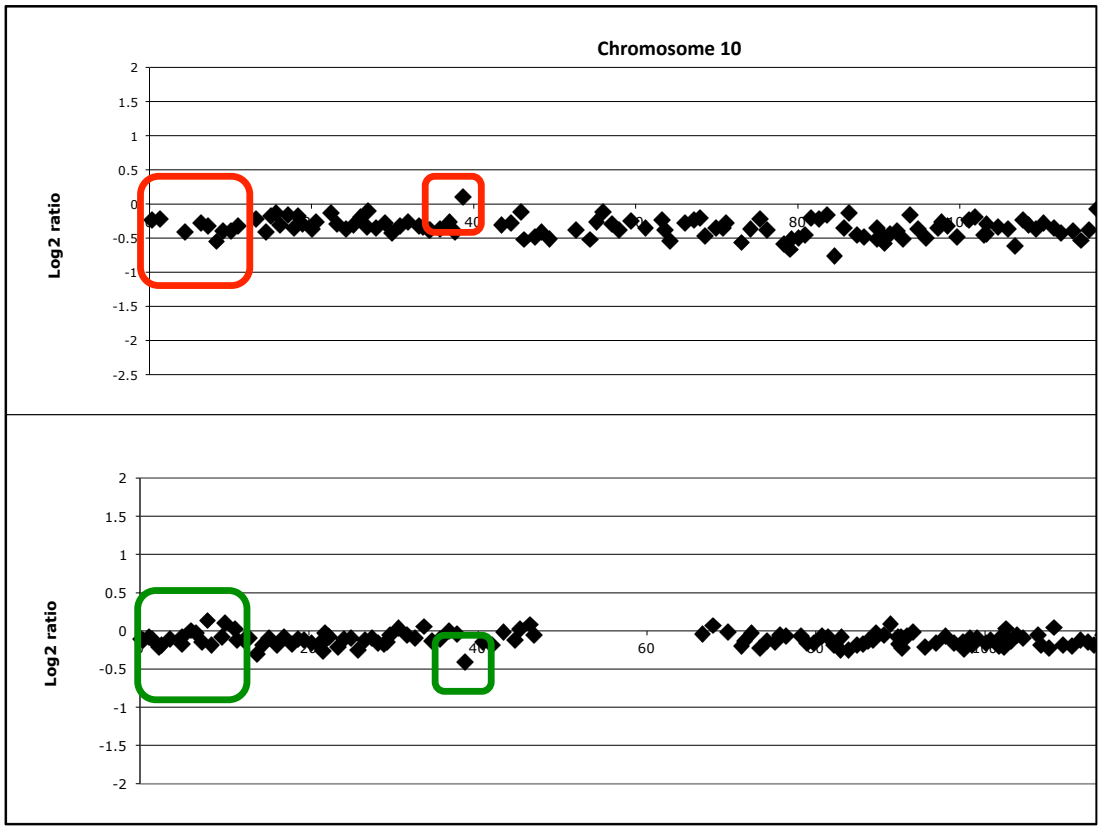

Figure 3.5: Difference in the transition of breakpoint regions (marked in red and green) between tumours from the same patient. Y-axis: $\log_2$ ratio (test / reference), X-axis: distance along chromosome (Mb)

3.1.5 Tumours exhibiting no copy number alterations

The majority of tumours exhibited at least some chromosome alterations. Seven tumours (patient 1 tumours 2 and 3; patient 8 tumour 3; patient 9 tumours 1 and 2; patient 16 tumours 1 and 3) exhibited no copy number alterations. Among these tumours with 'flat' profiles tumours 8_3, 1_1, 1_3 and 16_3 had been deemed not 'pure' enough and these had been laser micro-dissected prior to performing aCGH to ensure >70% tumour purity (Figure 3.6). The other tumours with 'flat' profiles were specifically visually re-checked for tumour purity in the resected samples. On visual inspection it was confirmed that these samples consisted of > 70% tumours cells. Figure 3.7.

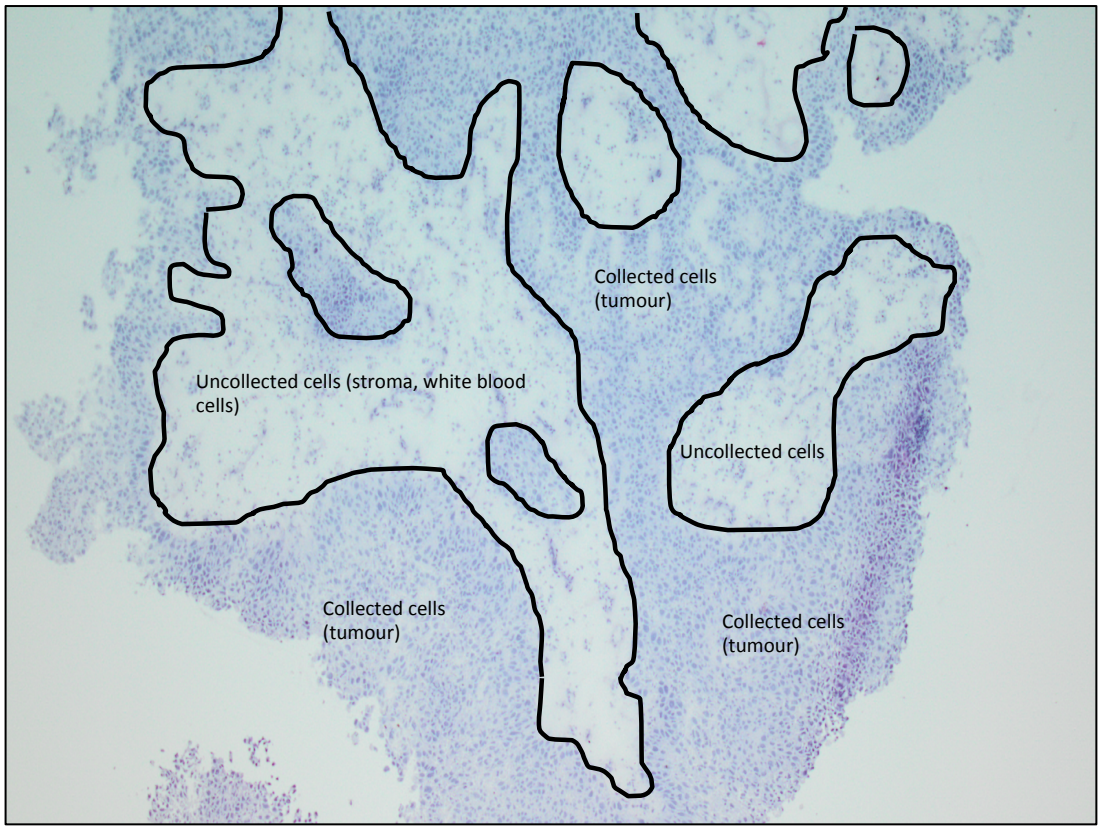

Figure 3.6: Laser micro-dissection of tumour 3 from patient 8. The black line distinguishes between the collected (pure tumour cells) and uncollected parts of the tissue sample.

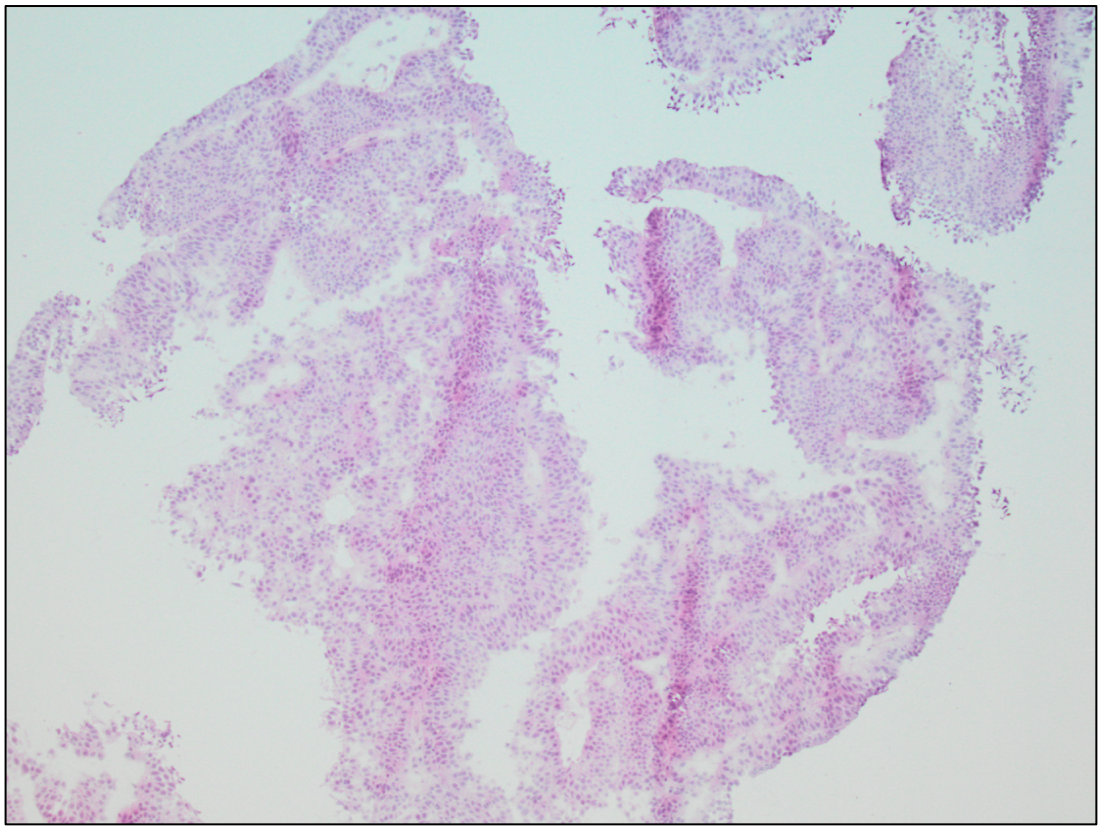

Figure 3.7: A representative example of a tumour (9_1) which showed no copy number alterations by aCGH but demonstrated >70% tumour purity.

3.1.6 Regions of homozygous deletion (HD) and high-level amplification

Sixty-nine high-level amplifications were detected in 66 tumours from 22 patients. The number of amplicons per tumour ranged from 1 to 9. Amplifications were more common in higher stage and grade tumours (p=0.0014) (Figure 3.8). Those found in two or more patients are shown in Appendix 3.4.

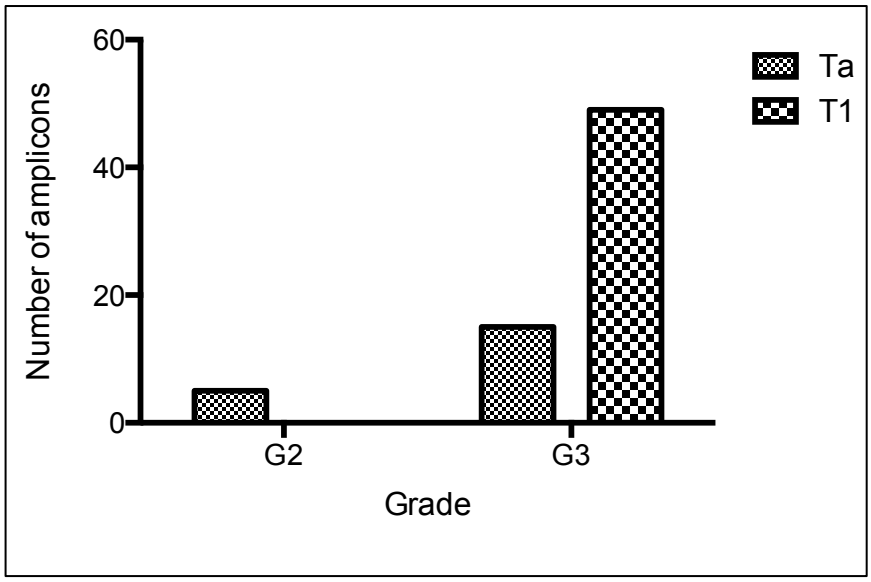

Figure 3.8: Numbers of amplifications in each stage according to grade for all 66 tumours. The y-axis corresponds to the number of amplicons and the x-axis corresponds to tumour grade.

The most frequently amplified regions were 11q13.2 - q13.4 and 6p22.3 - p22.2. Amplification of 11q13.2 - q13.4 (containing *MYEOV, CCND1, ORAOV1, FGF19, FGF4, FGF3*) was detected in 10 tumours (3_1, 12_1, 12_2, 12_3, 12_4, 14_1, 14_2, 14_3, 14_4, 18_3) from four different patients (patient 3, 12, 14, 18). Amplification of 6p22.3 - p22.2 (containing *MBOAT1, E2F3, CDKAL1, SOX4, PRL*) was detected in 8 tumours (12_1, 12_2, 12_3, 12_4, 13_1, 13_2, 13_3, 18_2) from three patients (patient 12, 13, 18). Other regions of amplification were 12q14.3 - q21.1 and 17q11.2 - q12, with amplifications being detected in 7 (12_1, 12_2, 12_3, 12_4, 20_1, 20_2, 20_3) and 5 (6_2, 14_1, 14_2, 14_3, 14_4) tumours respectively of two different patients (patient 12 and 20) and (patient 6 and 14). Amplification of p16.3 - p16.1 (containing *FGFR3*) on chromosome 4 was detected in two tumours (10_2, 21_2). The full lists of genes in these regions are shown in Appendix 3.4.

Forty-four homozygous deletions were detected in 15 tumours (2_1, 2_3, 4_1, 4_5, 10_2, 12_1, 12_2, 12_3, 14_1, 14_2, 14_3, 17_1, 17_2, 17_3, 21_2) from seven different patients (patient 2, 4, 10, 12, 14, 17, 21). Those found in two or more patients are shown in Table 3.5. A region on

chromosome 10 (103.28-104.34Mb) was HD in five tumours (tumour 4_1, 14_1, 14_2, 14_3, 17_3) from three different patients (patient 4, 14, 17). It contained 29 possible candidate genes: *ACTR1A, BTRC, C10orf76, C10orf95, CUEDC2, DPCD, ELOVL3, FBXL15, FBXW4, FGF8, GBF1, HPS6, KCNIP2, KCNIP2-AS1, LDB1, LOC101927445, MGEA5, MIR146B, MIR3158-1, MIR3158-2, NFKB2, NOLC1, NPM3, PITX3, POLL, PPRC1, PSD, RPARP-AS1, SUFU, and TMEM180*.

Chromosome	Cytoband	Position[1] (Mb)	No of genes	Candidate genes	Tumours[2]	Deletion frequency of patients (%)[3]	Number of tumours with a deletion
3	p21.2 - p21.1	51.56 - 52.66	39	ABHD14A, ABHD14A-ACY1, ABHD14B, ACY1, ALAS1, ALDOAP1, BAP1, DNAH1, DUSP7, GLYCTK, GPR62, GRM2, IQCF1, IQCF2, IQCF3, IQCF4, IQCF5, IQCF5-AS1, IQCF6, LINC00696, LOC101929029, LOC101929054, LOC101929702, MIR135A1, MIRLET7G, NISCH, NT5DC2, PARP3, PCBP4, PHF7, POC1A, PPM1M, PPP2R5CP,	4_1, 14_2	4.55	2
7	p21.1	16.21 - 17.76	10	AGR2, AGR3, AHR, ANKMY2, BZW2, ISPD, ISPD-AS1, LOC317727, LOC100131425, LOC100287613, LOC101927585, LOC101927609, LOC101927630, LRRC72, RAD17P1, RPL36AP29, SOSTDC1, TSPAN13	4_1, 14_1	9.1	2
10	q24.32	103.28 - 104.34	29	ACTR1A, BTRC, C10orf76, C10orf95, CUEDC2, DPCD, ELOVL3, FBXL15, FBXW4, FGF8, GBF1, HPS6, KCNIP2, KCNIP2-AS1, LDB1, LOC101927445, MGEA5, MIR146B, MIR3158-1, MIR3158-2, NFKB2, NOLC1, NPM3, PITX3,	4_1, 14_1, 14_2, 14_3,	4.55	5
12	q21.31	78.75 - 80.26	11	LOC642550, LOC100420794, LOC100507498, LOC101928252, MIR1252, MRPL11P3, PAWR, PPP1R12A, SYT1	4_5, 17_1, 17_2	9.1	3

Table 3.5 Recurrent regions of homozygous deletions detected in all 66 tumours.

[1]Physical position is according to hg19/NCBI build 37.

[2]Deletions were classified as those regions where the normalized $\log_2$ ratio was ≤1.2 detected in 2 or more tumours are listed.

[3]The frequency of loss across candidate regions was estimated as the percentage of samples with $\log_2$ratio ≤0.15

3.1.7 Fraction of genome altered

Fraction of genome altered (FGA) (the percentage of clones reporting significantly altered copy number) provides a measure of chromosomal instability. FGA was calculated using the individual copy number data for all 66 tumours and the merged copy number data for each patient. Samples were assigned to FGA groups A (≤1%), B (1-≤10%), C (10-<30%) or D (≥30%). The majority of the individual tumours fell into FGA groups C or D (Table 3.6). Only 10 of the individual tumours had an FGA value of ≤1%. When FGA was examined within patients, the majority (8 patients in group D, 11 in group C, 2 in group B and 1 patient in group A) were in group C or D (Table 3.6). Three patients belonging to groups A (patient 9) and B (patient 1 and 17) revealed minimal (FGA 4.9%) or no copy number alterations. Within this group 4 tumours (1_2, 1_3, 9_1, 9_2) had no copy number alterations.

Patient	Stage and grade	FGA group	Patients FGA	Tumour	Tumours FGA	FGA
1	TaG2	B	4.9	1_1	5	B
				1_2	0	A
				1_3	0	A
2	TaG2	C	10.7	2_1	10.1	C
				2_2	7.7	B
				2_3	7.4	B
3	T1G3	C	19.1	3_1	13.1	C
				3_2	12.4	C
				3_3	11.4	C
4	TaG3	C	14.5	4_1	12.9	C
				4_2	8.44	B
				4_3	9.01	B
				4_4	8.17	B
				4_5	8.44	B
				4_6	7.92	B
5	TaG2	D	60.1	5_1	0	A
				5_2	60.07	D
6	T1G3	D	72.4	6_1	57.77	D
				6_2	63.42	D
				6_3	69.58	D
7	TaG2	C	11.9	7_1	11.7	C
				7_2	12.1	C
8	TaG2	C	12.7	8_1	0.39	A
				8_2	12.4	C
				8_3	0	A
9	T1G3	A	0.03	9_1	0	A
				9_2	0	A
10	TaG3	D	60.7	10_1	28.38	C
				10_2	53.58	D
11	T1G3	C	19	11_1	16.51	C
				11_2	15.42	C
12	T1G3	D	61.6	12_1	42.68	D
				12_2	45.26	D
				12_3	58.95	D
				12_4	40.59	D
13	T1G3	D	63.1	13_1	57.13	D
				13_2	48.18	D
				13_3	56.43	D
				13_4	0.36	A
14	TaG3	D	54.7	14_1	49.57	D
				14_2	42.38	D
				14_3	39.58	D
				14_4	44.29	D
15	TaG2	C	18.2	15_1	15.85	C
				15_2	7.44	B
16	TaG2	C	20	16_1	15.76	C
				16_2	7.95	B
				16_3	0	A
				16_4	0.15	A
17	TaG2	B	3.1	17_1	1.21	B
				17_2	2.19	B
				17_3	1.28	B

Patient	Stage and grade	FGA group	Patients FGA	Tumour	Tumours FGA	FGA
18	T1G3	D	70.5	18_1	47.87	D
				18_2	45.02	D
				18_3	40.47	D
				18_4	50.49	D
19	TaG2	C	18	19_1	3.34	B
				19_2	6.16	B
				19_3	13.4	C
20	T1G3	D	73.3	20_1	45.69	D
				20_2	52.82	D
				20_3	54.28	D
21	TaG2	C	15.3	21_1	13.81	C
				21_2	13.33	C
22	TaG2	C	17.9	22_1	16.39	C
				22_2	5.19	B

Table 3.6 Stage, grade and FGA in patients and tumours

3.1.8 Relationship of FGA to stage and grade

The relationship of FGA to stage and grade was examined for the 66 individual tumours and for the 22 patients.

Overall, grade 3 tumours had a higher median FGA than grade 2 tumours (grade 2 = 7.4 and grade 3 = 42.4, p=0.0001, X^2 analysis) (Figure 3.9). Stage Ta tumours had lower median FGA than stage T1 tumours (stage Ta = 9.6 and stage T1 = 45.14, p=0.0001, X^2 analysis) (Figure 3.10).

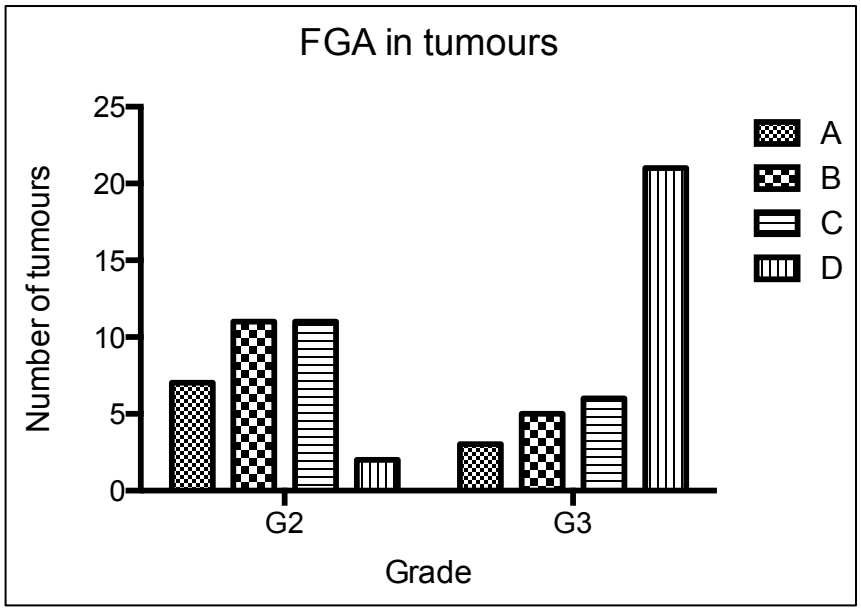

Figure 3.9: Numbers of tumours in each FGA group according to grade for all 66 tumours. The y-axis corresponds to the number of tumours and the x-axis corresponds to tumour grade.

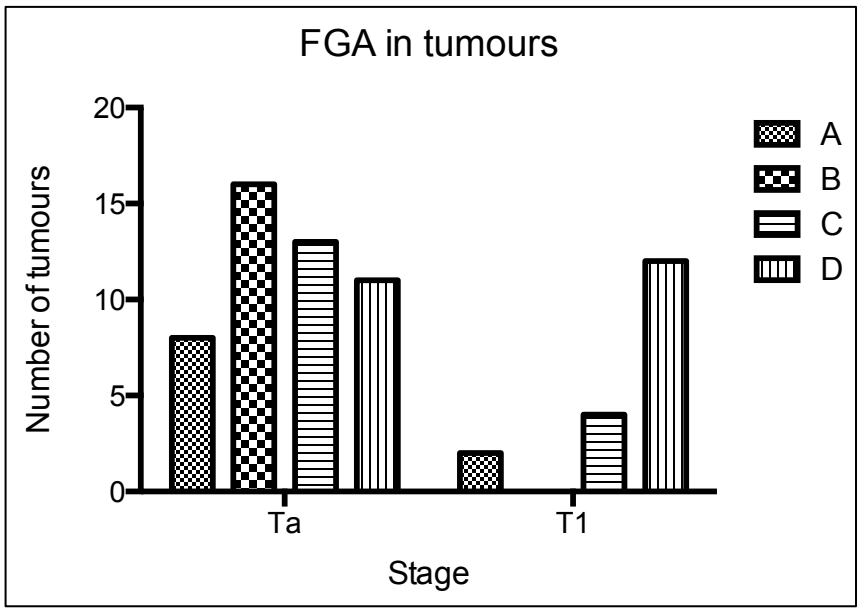

Figure 3.10: Numbers of tumours in each FGA group according to stage for all 66 tumours. The y-axis corresponds to the number of tumours and the x-axis corresponds to tumour stage.

Table 3.7 and Figure 3.11 show the numbers of tumours in each of the FGA groups according to combined stage and grade for the 66 individual tumours. TaG2 tumours were predominantly FGA groups A and B. The majority of TaG3 and T1G3 tumours were FGA group D.

FGA / Stage/grade	A (<1%)	B (1-<10%)	C (10-<30%)	D (≥30%)	Total
TaG2	7	11	11	2	**31**
TaG3	1	5	2	9	**17**
T1G3	2	0	4	12	**18**
Total	**10**	**16**	**17**	**23**	**66**

Table 3.7 FGA group according to stage and grade for 66 tumours.

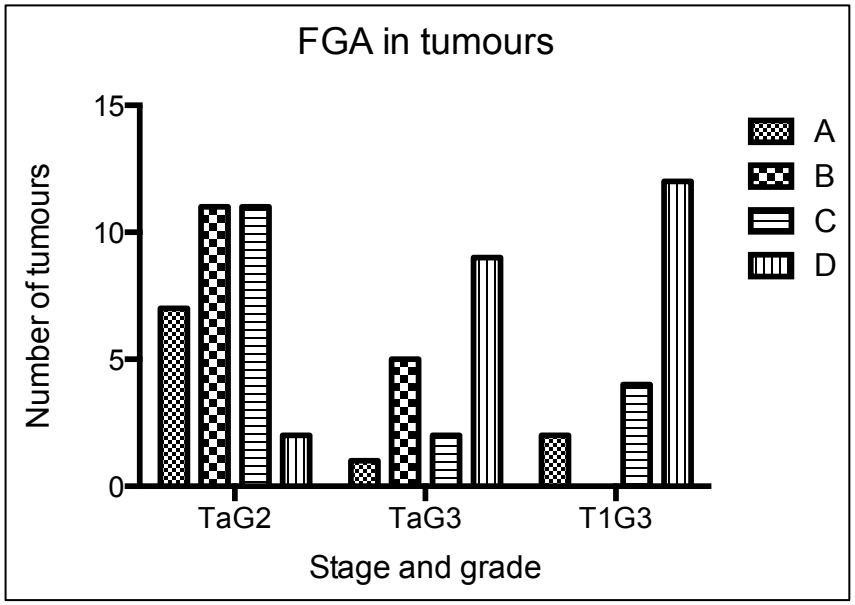

Figure 3.11: Numbers of tumours in each FGA group according to stage and grade for all 66 tumours. The y-axis corresponds to the number of tumours and the x-axis corresponds to tumour stage and grade.

Median FGA was also examined in the 66 tumours. TaG2 tumours had a lower median FGA (7.4%) than TaG3 (39.6%; p=0.001, X^2 analysis) and T1G3 (59.6%; p<0.001, X^2 analysis) tumours Figure 3.12.

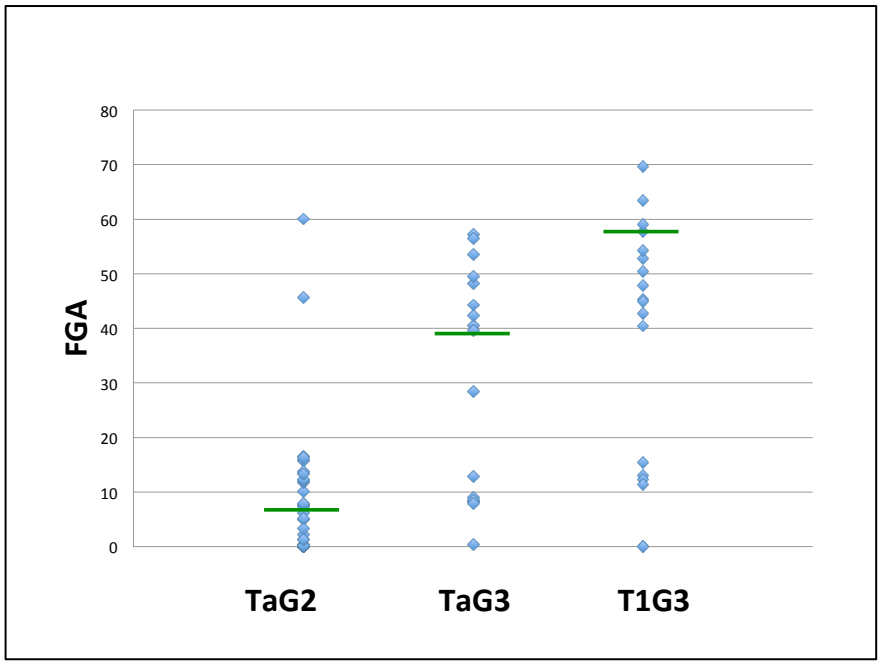

Figure 3.12: FGA (%) in all 66 multifocal tumours according to stage and grade. The y–axis corresponds to FGA (%) and the x–axis corresponds to stage and grade. Green lines indicate median FGA values (%) for TaG2 (7.4%), TaG3 (39.6 %) and T1G3 (59.6 %).

Some tumours exhibited few or no copy number alterations and these tumours had correspondingly low FGA values. Fifteen tumours (1_1, 1_2, 1_3, 5_1, 8_1, 8_3, 9_1, 9_2, 13_4, 16_3, 16_4, 17_1, 17_2, 17_3, 19_1) had <5% FGA and 10 of these (1_2, 1_3, 5_1, 8_1, 8_3, 9_1, 9_2, 13_4, 16_3, 16_4) had <1% FGA. The majority of these genomically stable tumours were of low stage and grade (TaG2 n=12; TaG3 n=1; T1G3 n=2).

Next, we examined FGA according to stage and grade in merged data for the 22 patients. Most of the patients with grade 2 disease were FGA group C (Figure 3.13). Patients with grade 3 tumours were mainly FGA group D with no patients in group B. Most of the patients with stage Ta disease were FGA group C (Figure 3.14). Stage T1 patients were mainly FGA group D. Table 3.8 and Figure 3.15 show the numbers of patients in each of the FGA groups according to combined stage and grade for the 22 patients. One patient with T1G3 was FGA Group A and two patients with TaG2 tumours were FGA

group B. The majority of TaG3 and T1G3 tumours were FGA group D. The majority of patients with TaG2 tumours were FGA group C.

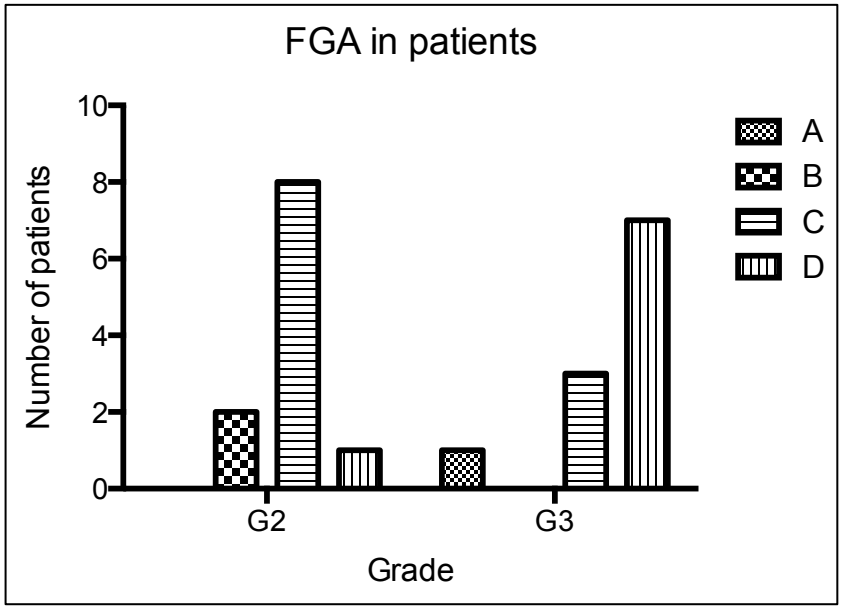

Figure 3.13: Numbers of tumours in each FGA group according to grade for 22 patients. The y-axis corresponds to the number of tumours and the x-axis corresponds to tumour grade.

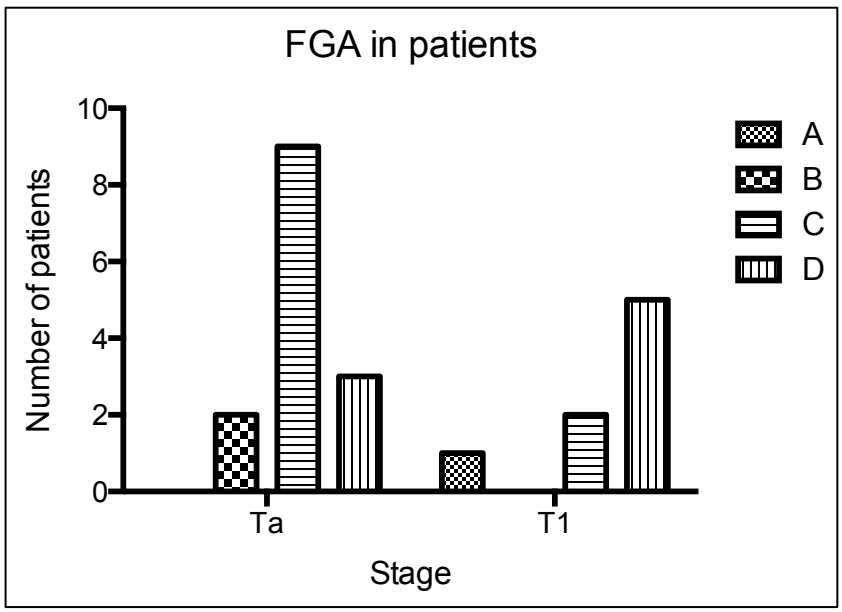

Figure 3.14: Numbers of tumours in each FGA group according to stage for 22 patients. The y-axis corresponds to the number of tumours and the x-axis corresponds to tumour stage.

FGA / Stage/grade	A (<1%)	B (1-<10%)	C (10-<30%)	D (≥30%)	Total
TaG2	0	2	8	1	**11**
TaG3	0	0	1	2	**3**
T1G3	1	0	2	5	**8**
Total	**1**	**2**	**11**	**8**	**22**

Table 3.8 FGA group according stage and grade for 22 patients.

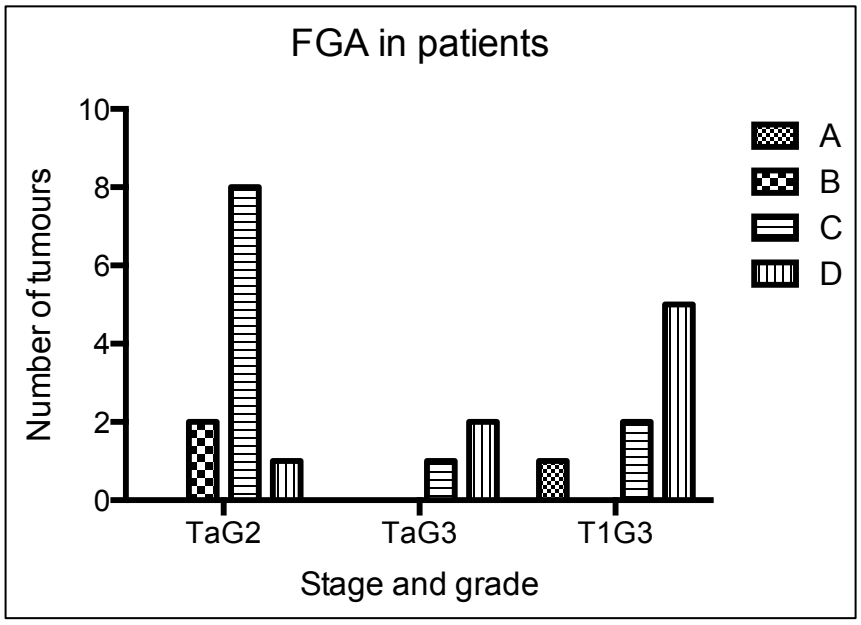

Figure 3.15: Numbers of tumours in each FGA group according to stage and grade for 22 patients. The y-axis corresponds to the number of tumours and the x-axis corresponds to tumour stage and grade.

3.2 Mutation analysis

The mutation status of *FGFR3, PIK3CA* and the 3 RAS genes *(HRAS, KRAS* and *NRAS)* was determined for all 66 tumours by SNaPshot analysis (Table 3.9, Figure 3.16). These genes play an important role in many cellular processes. Mutations in *FGFR3, PIK3CA and Ras* genes have been identified in a variety of human cancers including bladder cancer. The assays used covered all hotspot mutation codons.

FGFR3 mutations were detected in 23 of 66 tumours (34.8%). S249C mutations were detected in 16 tumours from 5 patients (Figure 3.17). The second commonest *FGFR3* mutation was Y375C which was detected in 5 tumours from 2 patients. K652T mutations were detected in two tumours from 1 patient. *PIK3CA* mutations were detected in 16 (24.2%) tumours. The most common mutation was E542K, which was detected in 7 tumours from 3 patients. An E545Q mutation was detected in all 6 tumours from 1 patient (Figure 3.18). In three tumours from one patient, H1047R mutations were detected. *RAS* gene mutations were detected in 7 tumours (10.6%). *HRAS* Q61R mutations were detected in three tumours from 1 patient, and *HRAS* G12C mutations were detected in four tumours from 1 patient.

In eleven patients none of the screened mutations were detected. Eleven patients had at least one mutation detected. All tumours from the same patient shared the same mutation status except in two cases (patient 1 and patient 19) where *PIK3CA* and *FGFR3* mutations, respectively, were not present in all tumours from the same patient. Where RAS mutations were detected, they were shared by all tumours from the same patient. RAS and *FGFR3/PIK3CA* mutations were mutually exclusive. Four patients had concomitant mutation of both *FGFR3* and *PIK3CA*. In one patient (4), two tumours shared mutations in *FGFR3* (S249C) and *PIK3CA* (E545Q) and shared the majority of copy number alterations (Table 3.9 and 3.10).

Table 3.9 *FGFR3*, *PIK3CA* and RAS gene mutations detected in 66 individual tumours from 22 patients with multifocal bladder cancer.

Tumour Number	Stage & grade	Primary/ Recurrent	*FGFR3* Mutation Status	*PIK3CA* Mutation Status	Ras gene Mutation Status
1_1	Ta G2	Recurrence	WT	E542K	WT
1_2	Ta G2	Recurrence	WT	E542K	WT
1_3	Ta G2	Recurrence	WT	WT	WT
2_1	Ta G2	Recurrence	S249C	WT	WT
2_2	Ta G2	Recurrence	S249C	WT	WT
2_3	Ta G2	Recurrence	S249C	WT	WT
3_1	T1 G3	Recurrence	WT	WT	HRAS:Q61R
3_2	T1 G3	Recurrence	WT	WT	HRAS:Q61R
3_3	T1 G3	Recurrence	WT	WT	H:Q61R
4_1	Ta G3	Recurrence	S249C	E545Q	WT
4_2	Ta G3	Recurrence	S249C	E545Q	WT

Tumour Number	**Stage & grade**	**Primary/ Recurrent**	***FGFR3* Mutation Status**	***PIK3CA* Mutation Status**	***Ras* Mutation Status**
4_3	Ta G3	Recurrence	S249C	E545Q	WT
4_4	Ta G3	Recurrence	S249C	E545Q	WT
4_5	Ta G3	Recurrence	S249C	E545Q	WT
4_6	Ta G3	Recurrence	S249C	E545Q	WT
5_1	Ta G2	Primary	S249C	WT	WT
5_2	Ta G2	Primary	S249C	WT	WT
6_1	T1 G3	Primary	WT	WT	WT
6_2	T1 G3	Primary	WT	WT	WT
6_3	T1 G3	Primary	WT	WT	WT
7_1	Ta G2	Recurrence	WT	WT	WT
7_2	Ta G2	Recurrence	WT	WT	WT
8_1	Ta G2	Recurrence	S249C	H1047R	WT
8_2	Ta G2	Recurrence	S249C	H1047R	WT
8_3	Ta G2	Recurrence	S249C	H1047R	WT

Tumour Number	**Stage & grade**	**Primary/ Recurrent**	***FGFR3*** **Mutation Status**	***PIK3CA*** **Mutation Status**	***Ras*** **Mutation Status**
9_1	T1 G3	Primary	WT	WT	WT
9_2	T1 G3	Primary	WT	WT	WT
10_1	Ta G3	Primary	WT	WT	WT
10_2	Ta G3	Primary	WT	WT	WT
11_1	Ta G2	Recurrence	WT	WT	WT
11_2	T1 G3	Recurrence	WT	WT	WT
12_1	T1 G3	Primary	WT	WT	WT
12_2	T1 G3	Primary	WT	WT	WT
12_3	T1 G3	Primary	WT	WT	WT
12_4	Ta G3	Primary	WT	WT	WT
13_1	Ta G3	Primary	WT	WT	WT
13_2	Ta G3	Primary	WT	WT	WT
13_3	Ta G3	Primary	WT	WT	WT
13_4	Ta G3	Primary	WT	WT	WT

Tumour Number	**Stage & grade**	**Primary/ Recurrent**	***FGFR3* Mutation Status**	***PIK3CA* Mutation Status**	***Ras* Mutation Status**
14_1	Ta G3	Primary	WT	WT	WT
14_2	Ta G3	Primary	WT	WT	WT
14_3	Ta G3	Primary	WT	WT	WT
14_4	Ta G3	Primary	WT	WT	WT
15_1	Ta G2	Primary	S249C	E542K	WT
15_2	Ta G2	Primary	S249C	E542K	WT
16_1	Ta G2	Recurrence	WT	WT	HRASG12C
16_2	Ta G2	Recurrence	WT	WT	HRASG12C
16_3	Ta G2	Recurrence	WT	WT	HRASG12C
16_4	Ta G2	Recurrence	WT	WT	HRASG12C
17_1	Ta G2	Recurrence	Y375C	E542K	WT
17_2	Ta G2	Recurrence	Y375C	E542K	WT
17_3	Ta G2	Recurrence	Y375C	E542K	WT
18_1	T1 G3	Primary	WT	WT	WT

Tumour Number	**Stage & grade**	**Primary/ Recurrent**	***FGFR3*** **Mutation Status**	***PIK3CA*** **Mutation Status**	***Ras*** **Mutation Status**
18_2	T1 G3	Primary	WT	WT	WT
18_3	T1 G3	Primary	WT	WT	WT
18_4	T1 G3	Primary	WT	WT	WT
19_1	Ta G2	Primary	Y375C	WT	WT
19_2	Ta G2	Primary	Y375C	WT	WT
19_3	Ta G2	Primary	WT	WT	WT
20_1	Ta G2	Primary	WT	WT	WT
20_2	T1 G3	Primary	WT	WT	WT
20_3	T1 G3	Primary	WT	WT	WT
21_1	Ta G2	Recurrence	K652T	WT	WT
21_2	Ta G2	Recurrence	K652T	WT	WT
22_1	Ta G2	Primary	WT	WT	WT
22_2	Ta G2	Primary	WT	WT	WT

Patient	Tumour number	FGFR3	PIK3CA	RAS
1	TaG2 1		E542K	
	TaG2 2		E542K	
	TaG2 3			
2	TaG2 1	S249C		
	TaG2 2	S249C		
	TaG2 3	S249C		
3	T1G3 1			HRASQ61R
	T1G3 2			HRASQ61R
	T1G3 3			HRASQ61R
4	TaG3 1	S249C	E545Q	
	TaG3 2	S249C	E545Q	
	TaG3 3	S249C	E545Q	
	TaG3 4	S249C	E545Q	
	TaG3 5	S249C	E545Q	
	TaG3 6	S249C	E545Q	
5	TaG2 1	S249C		
	TaG2 2	S249C		
6	T1G3 1			
	T1G3 2			
	T1G3 3			
7	TaG2 1			
	TaG2 2			
8	TaG2 1	S249C	H1047R	
	TaG2 2	S249C	H1047R	
	TaG2 3	S249C	H1047R	
9	T1G3 1			
	T1G3 2			
10	TaG3 1			
	TaG3 2			
11	TaG2 1			
	T1G3 2			
12	T1G3 1			
	T1G3 2			
	T1G3 3			
	TaG3 4			

Patient	Tumour number	FGFR3	PIK3CA	RAS
13	TaG3 1			
	TaG3 2			
	TaG3 3			
	TaG3 4			
14	TaG3 1			
	TaG3 2			
	TaG3 3			
	TaG3 4			
15	TaG2 1	S249C	E542K	
	TaG2 2	S249C	E542K	
16	TaG2 1			HRASG12CT
	TaG2 2			HRASG12CT
	TaG2 3			HRASG12CT
	TaG2 4			HRASG12CT
17	TaG2 1	Y375C	E542K	
	TaG2 2	Y375C	E542K	
	TaG2 3	Y375C	E542K	
18	T1G3 1			
	T1G3 2			
	T1G3 3			
	T1G3 4			
19	TaG2 1	Y375C		
	TaG2 2	Y375C		
	TaG2 3			
20	TaG2 1			
	T1G3 2			
	T1G3 3			
21	TaG2 1	K652T		
	TaG2 2	K652T		
22	TaG2 1			
	TaG2 2			

Figure 3.16: Heatmap of mutations detected in all 66 tumours. Orange: mutant, green: WT.

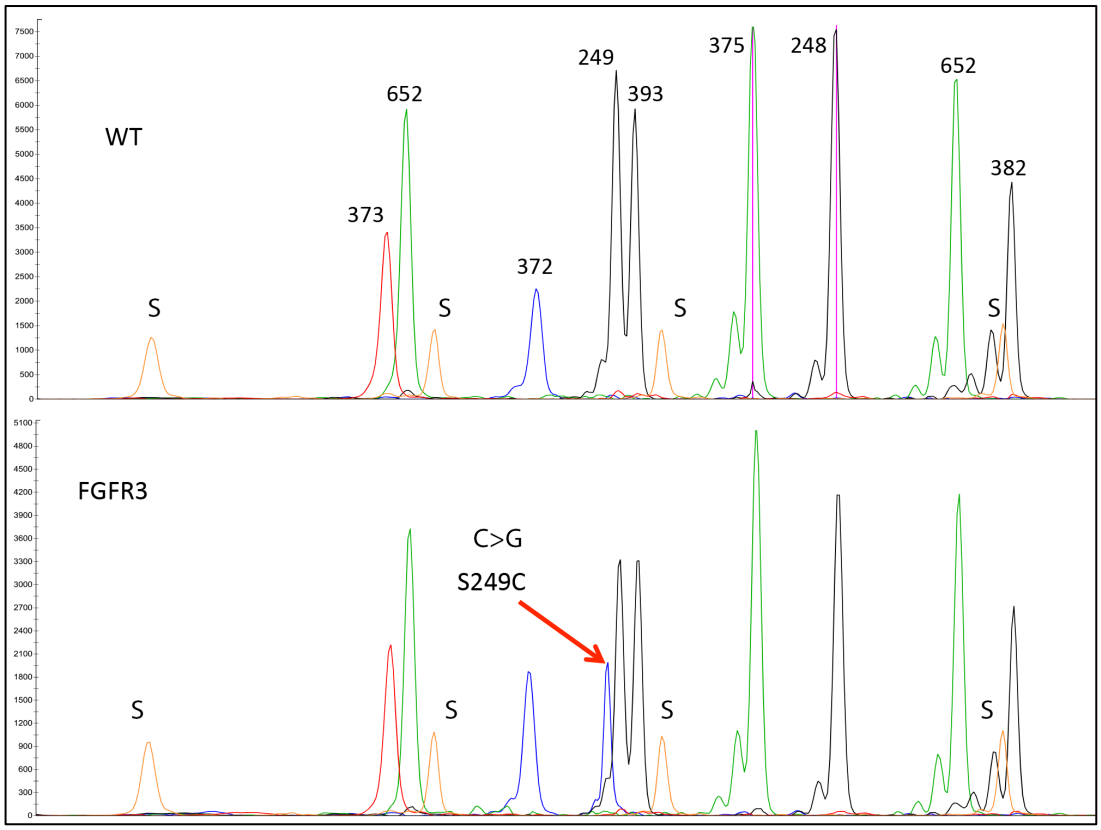

Figure 3.17: SNaPshot detection of a *FGFR3* S249C mutation in a tumour from patient 4. Top panel: Wildtype SNaPshot profile obtained using DNA extracted from patient 4's blood sample. Bottom panel: Profile showing a *FGFR3* S249C mutation (indicated by the red arrow). Bases are represented by the following colours: A = green; C = black; G = blue; T = red. Positions of codons are indicated next to peaks. Orange peaks (S) represent the internal size standard (Genescan-120LIZ).

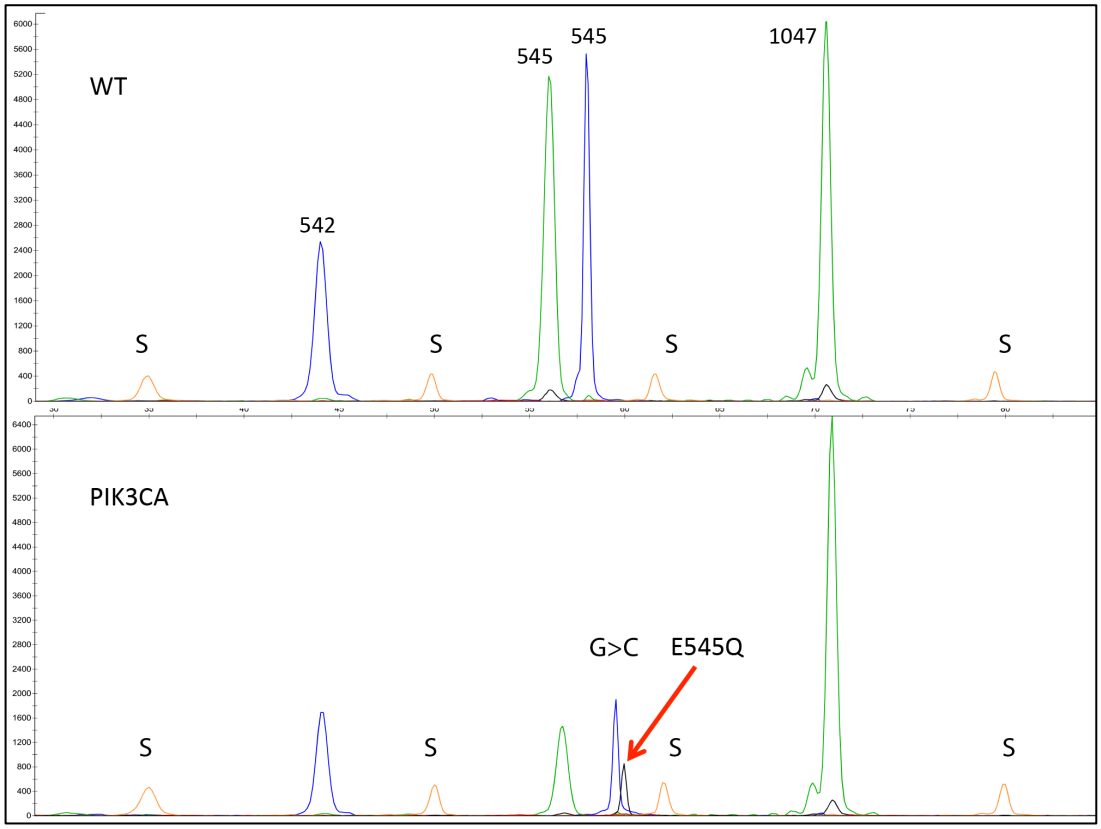

Figure 3.18: SNaPshot detection of a *PIK3CA* E545Q mutation in a tumour from patient 4. Top panel: Wildtype SNaPshot profile obtained using DNA extracted from patient 4's blood sample. Bottom panel: Profile showing a *PIK3CA* E545Q mutation (indicated by the red arrow).

3.2.1 Mutation status and stage and grade

X^2 tests were conducted to test for associations of mutation status with stage and grade in all 66 tumours. *FGFR3* mutation was associated with low stage and grade (p=0.0001) (Figure 3.19). *PIK3CA* mutation was associated with low stage and grade (p=0.02) and RAS gene mutations were associated with high stage and grade tumours (p<0.0001) (Figure 3.20 and Figure 3.21).

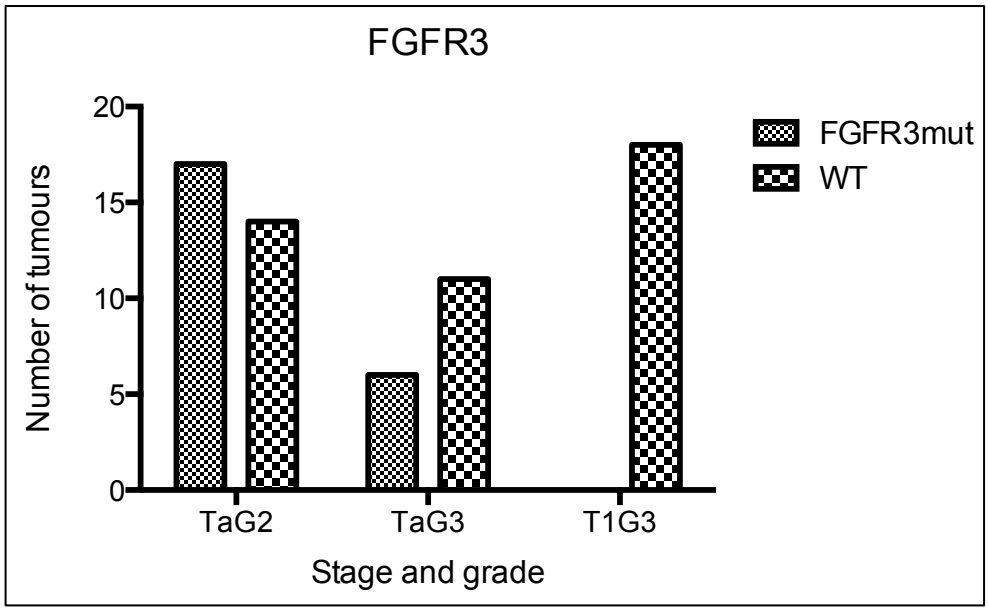

Figure 3.19: *FGFR3* mutations in all 66 tumours according to stage and grade. The y-axis corresponds to the number of tumours and the x-axis corresponds to tumour stage and grade.

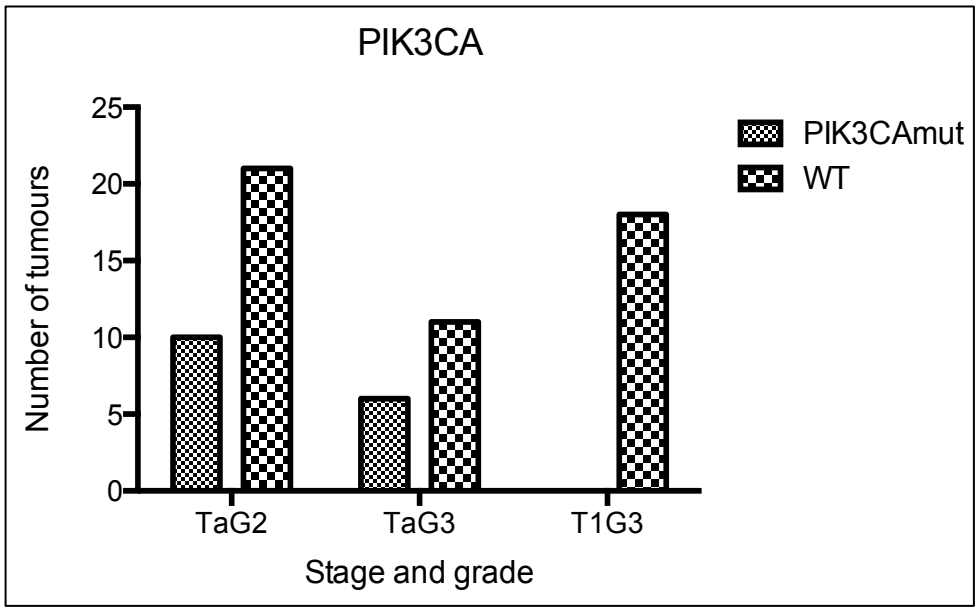

Figure 3.20: *PIK3CA* mutations in all 66 tumours according to stage and grade. The y-axis corresponds to the number of tumours and the x-axis corresponds to tumour stage and grade.

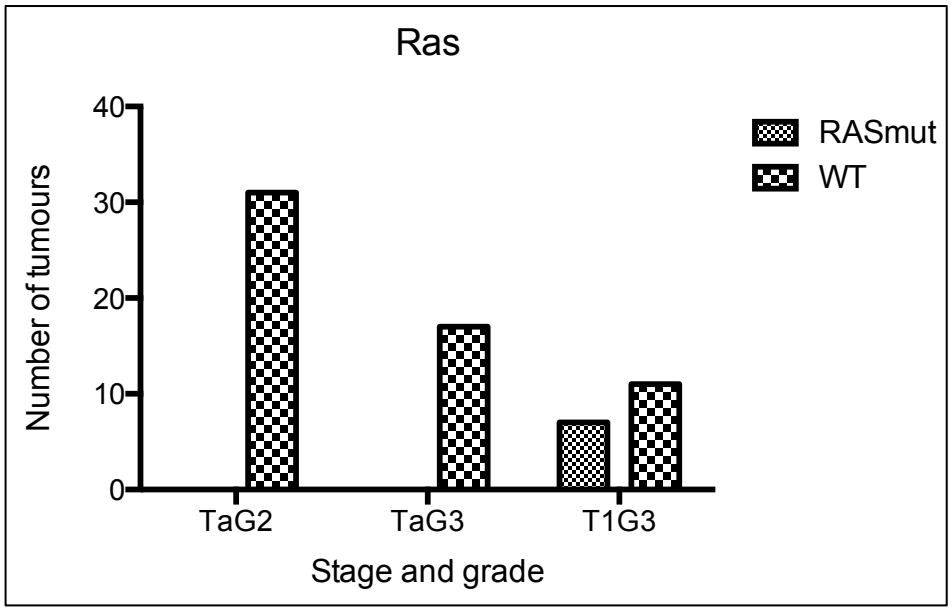

Figure 3.21: *RAS* gene mutations in all 66 tumours according to stage and grade. The y-axis corresponds to the number of tumours and the x-axis corresponds to tumour stage and grade.

When the same comparisons were made per patient, only *FGFR3* mutation analysis reached statistical significance (p=0.002) due to the low number of patients. This analysis revealed that *FGFR3* mutations were more prevalent in TaG2 patients. Figure 3.22 and Table 3.10 shows the distribution of mutations according to stage and grade for the 22 patients.

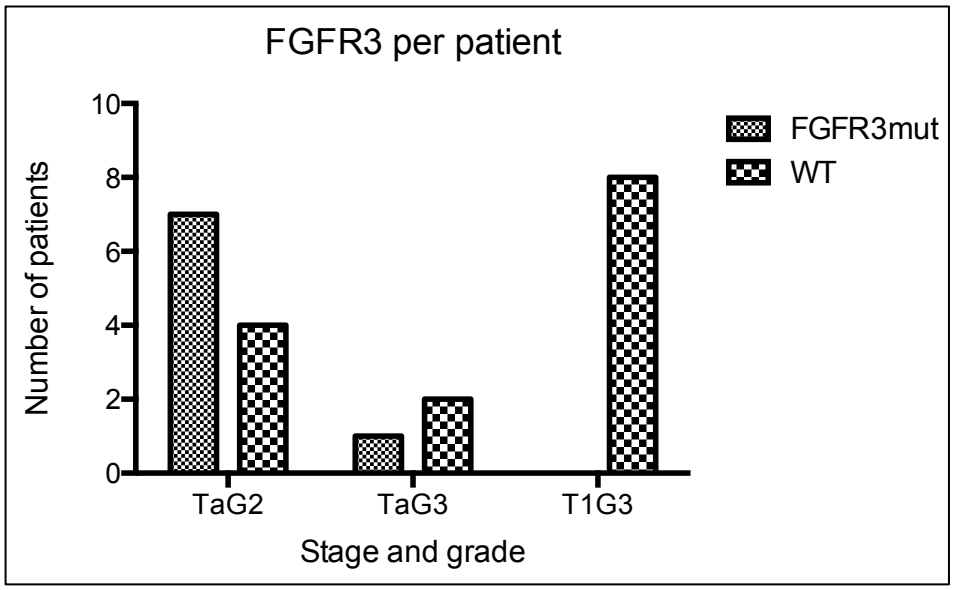

Figure 3.22: *FGFR3* mutations in 22 patients according to stage and grade. The y-axis corresponds to the number of patients and the x-axis corresponds to tumour stage and grade.

Stage \ Mutation	FGFR3	PIK3CA	Ras	No mutations
TaG2	2 (3/3) 5 (2/2) 8 (3/3) 15 (2/2) 17 (3/3) 19 (2/3) 21 (2/2)	1 (2/3) 8 (3/3) 15 (2/2) 17 (3/3)		7 (2) 22 (2)
TaG3	4 (6/6)	4 (6/6)		6 (3) 10 (2) 12 (4) 13 (4) 14 (4)
T1G3			3 (3/3) 16 (4/4)	9 (2) 11 (2) 18 (4) 20 (3)

Table 3.10 Mutations in 22 patients according to stage and grade. In brackets: number of tumours with mutation/total number of tumours in the patient.

3.2.2 Relationships between FGA, mutation status, copy number alterations and risk factor data

A comparison of mutation status and FGA (%) revealed a lower median FGA in tumours with an *FGFR3* mutation (7.9%) as compared to wildtype tumours

(39.6%) (Figure 3.23). The distribution pattern of WT tumours was an interesting one. These tumours tended to group into two separate groups (one with lower and second with higher FGA status). In the first group 9 out of 13 tumours were stage Ta and 6 were of grade 2.

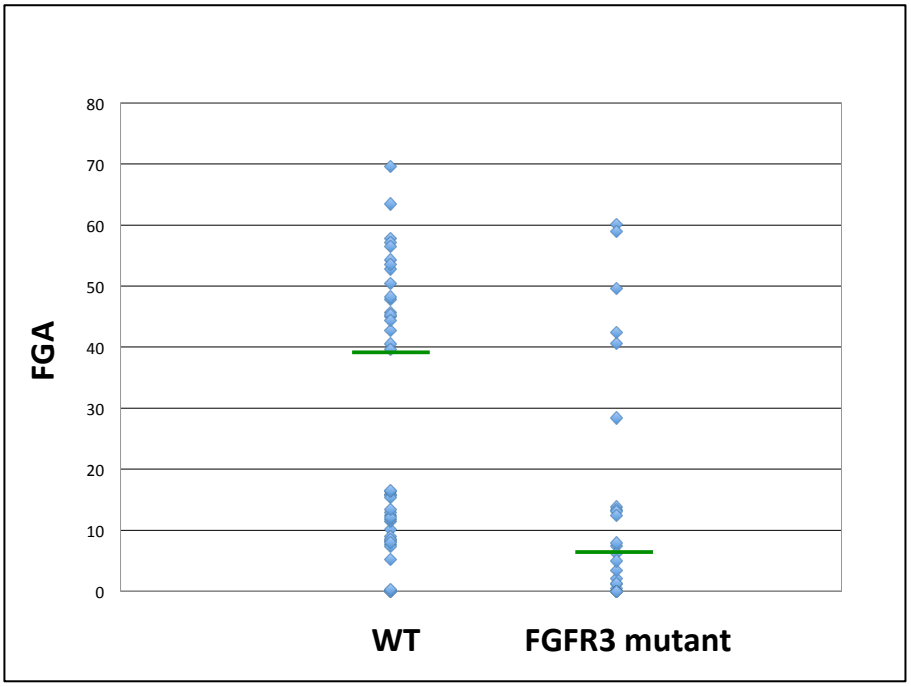

Figure 3.23: FGA (%) in 66 multifocal tumours according to *FGFR3* mutation status. The y–axis corresponds to the percentage of FGA and the x–axis corresponds to *FGFR3* mutation status. Green lines indicate median FGA values (%) for WT tumours (39.6%) and tumours with *FGFR3* mutation (7.9%).

Figure 3.24 shows the distribution of FGA (%) across different stages and grades of tumours according to *FGFR3* mutation status. The majority of tumours with *FGFR3* mutations had <15% of FGA and these were mainly TaG2 tumours. Only one *FGFR3* mutant tumour (tumour 2 from patient 5) exhibited a significant number of copy number alterations and this was reflected in the high FGA value (60.1%) obtained for this tumour.

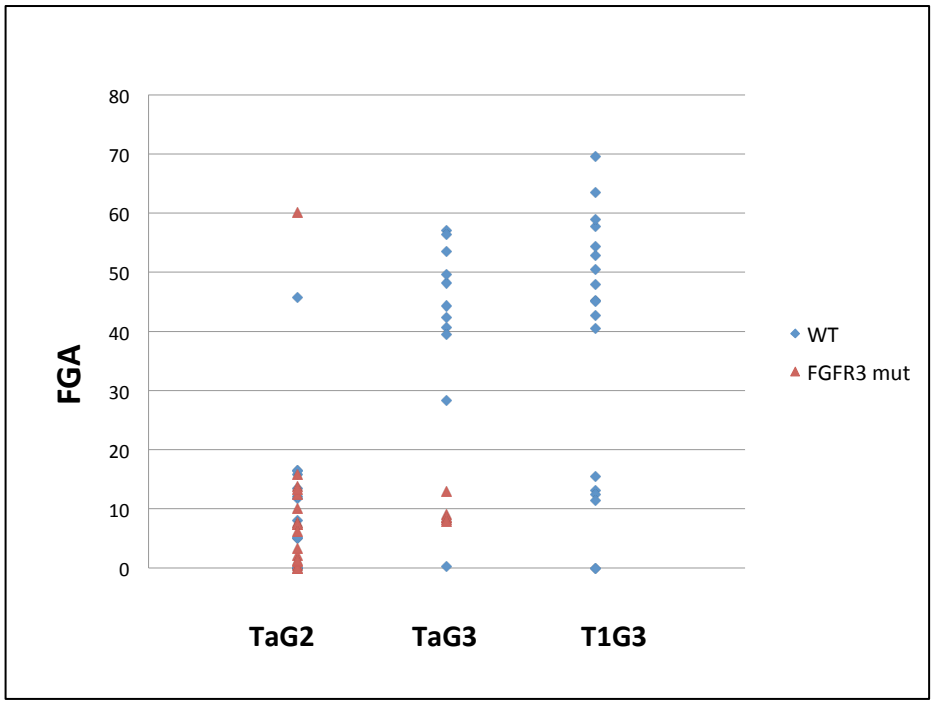

Figure 3.24: FGA (%) and *FGFR3* mutation status in 66 multifocal tumours according to stage and grade. The y–axis corresponds to the percentage of FGA and the x–axis corresponds to stage and grade. Red triangles *FGFR3* mutant; blue diamond, wildtype for *FGFR3*

A comparison of mutation status and FGA (%) revealed a lower median FGA in tumours with an *PIK3CA* mutation (7.7%) as compared to wild-type tumours (16.5%) Figure 3.25. Similarly to *FGFR3* WT tumours, the distribution pattern of *PIK3CA* WT tumours was an interesting one. These tumours tended to group into two separate groups (one with lower and second with higher FGA status).

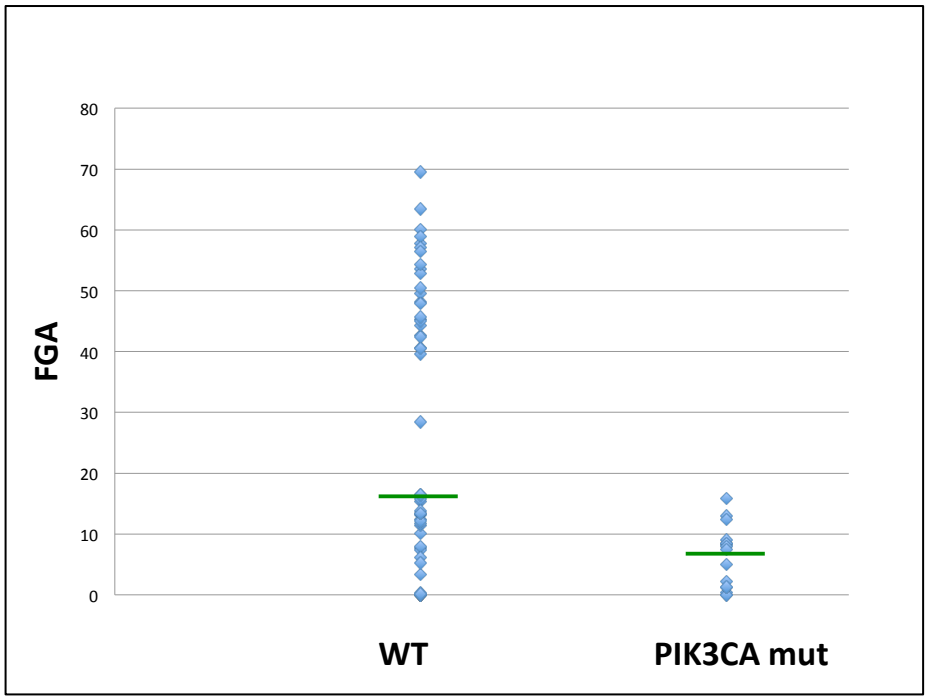

Figure 3.25: FGA (%) in 66 multifocal tumours according to *PIK3CA* mutation status. The y–axis corresponds to the percentage of FGA and the x–axis corresponds to *PIK3CA* mutation status. Green lines indicate median FGA values (%) for WT tumours (16.5%) and tumours with *PIK3CA* mutation (7.7%).

Figure 3.26 shows the distribution of FGA (%) across different stages and grades of tumours according to *PIK3CA* mutation status. The majority of tumours with *PIK3CA* mutations had <10% of FGA and these were mainly TaG2 tumours. Only one patient (patient 4) had *PIK3CA* mutations in all tumours and these were all stage TaG3. All tumours with T1G3 disease were wildtype for *PIK3CA.*

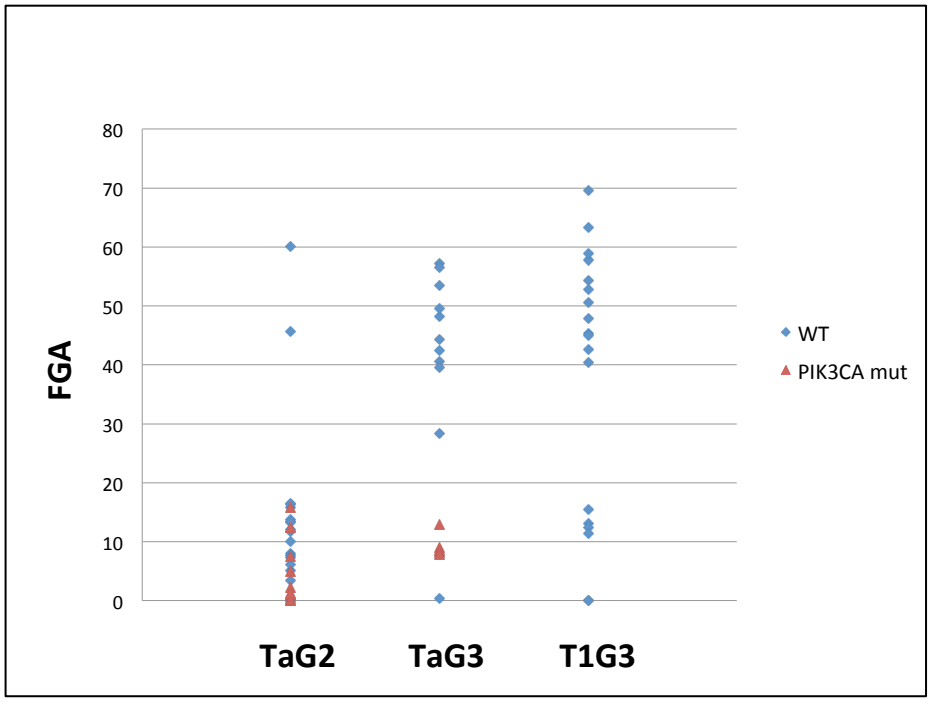

Figure 3.26: FGA (%) and *PIK3CA* mutation status in 66 multifocal tumours according to stage and grade. The y–axis corresponds to the percentage of FGA and the x–axis corresponds to stage and grade. Red triangles *PIK3CA* mutant; blue diamond, wildtype for *PIK3CA.*

Due to low number of tumours with RAS gene mutations similar comparisons were not performed.

3.3 Mutation status and copy number alterations

Using the Comparisons function of the Nexus software package, a Fishers Exact test (0.05 p-value cut off; 25% differential threshold) was used to compare the frequencies of copy number alterations in patients according to *FGFR3* mutation status (Appendix 3.5, Figure 3.27). *FGFR3* wildtype tumours commonly showed gains of 2 regions on the long arm of chromosome 7 (7q21.11 - 7q21.3 and 7q22.1 - 7q36.3, p=0.017). Gain of discrete regions on the long arm of chromosome 8 (8q24.22 and q24.3) was also more frequent in *FGFR3* wildtype tumours (p=0.003 and p=0.02)

(Figure 3.27). These minimal regions on chromosome 8, contained 5 (EFR3A, HHLA1, KCNQ3, LOC100420215, OC90) and 7 genes (COMMD5, LOC101929051, RPL8, ZNF7, ZNF34, ZNF250, ZNF517), respectively. Gain of a region on 20q (20q11.21) was also associated with *FGFR3* wild-type tumours (p=0.03).

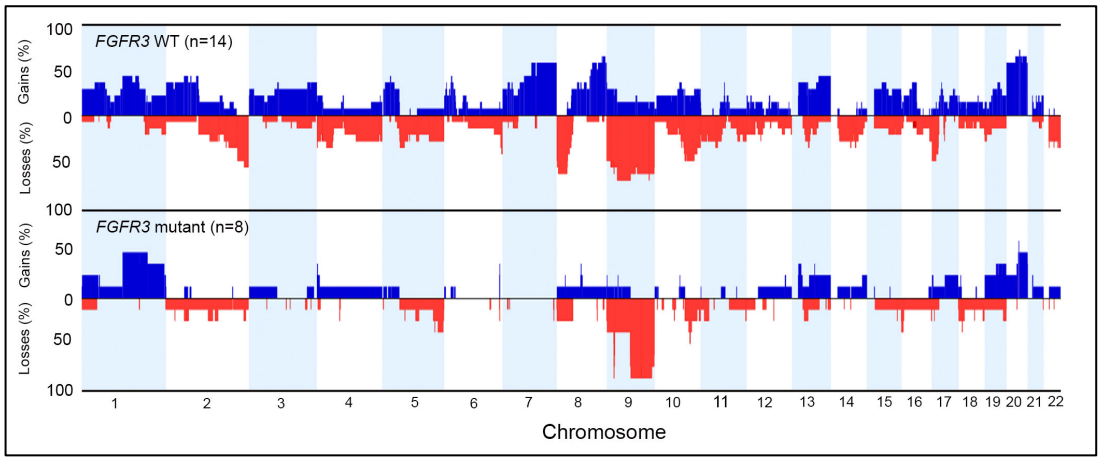

Figure 3.27: *FGFR3* mutation status and copy number alterations in 22 patients. Genome-wide frequency plots of copy number alterations in *FGFR3* wildtype (n=14) and *FGFR3* mutant (n=8) tumours. The x-axis corresponds to chromosomes 1 to 22 and the y-axis corresponds to the percentage of copy number gains (blue) and losses (red).

3.3.1 FGA and smoking status

When comparing FGA with patient smoking status, the majority of smokers (17 patients) were classified into FGA groups C and D (Table 3.11). However due to low patients' numbers included the comparisons did not reach statistical significance, Chi-square test (p=0.2). Due to small number of patients with occupational risk exposure (n=4) no statistically significant conclusions could be drawn from a comparison of occupational risk exposure and FGA.

Smoking status \ FGA	**A** (<1%)	**B** (1-<10%)	**C** (10-<30%)	**D** (≥30%)
Smokers (≥20 packs year)	0	1	6	2
Smokers (< 20 packs year)	0	0	3	5
Non smokers	1	1	2	1

Table 3.11 Distribution of FGA group among smokers (≥20 packs a year and <20 packs a year) and non-smokers.

When smokers were divided into two groups (group one consisting of patients (n=8) who smoked <20 packs a year and group two consisting of patients (n=9) who smoked ≥20 packs a year) significant differences in the frequencies of copy number alterations in these two groups were observed (Figure 3.28). Patients who smoked <20 packs per year had a higher level of chromosomal instability. Patients in first group had tumours which commonly showed gains of one region on chromosome 20 (p11.1 - q11.21, p=0.05) and two regions on the short arm of chromosome 2 (p16.2 - p14 and p13.3 - p13.1, p=0.002). Gain of a discrete region on the long arm of chromosome 19 (q13.12) was also more frequent in these patients (p=0.015). Deletions on chromosome 5 (q34 - q35.3), chromosome 8 (p23.3 - q11.1) and chromosome 9 (p21.3) were more frequent in first group of patients (p=0.015). Similar comparisons with non-smokers were not performed due to small number of non-smokers (n=5).

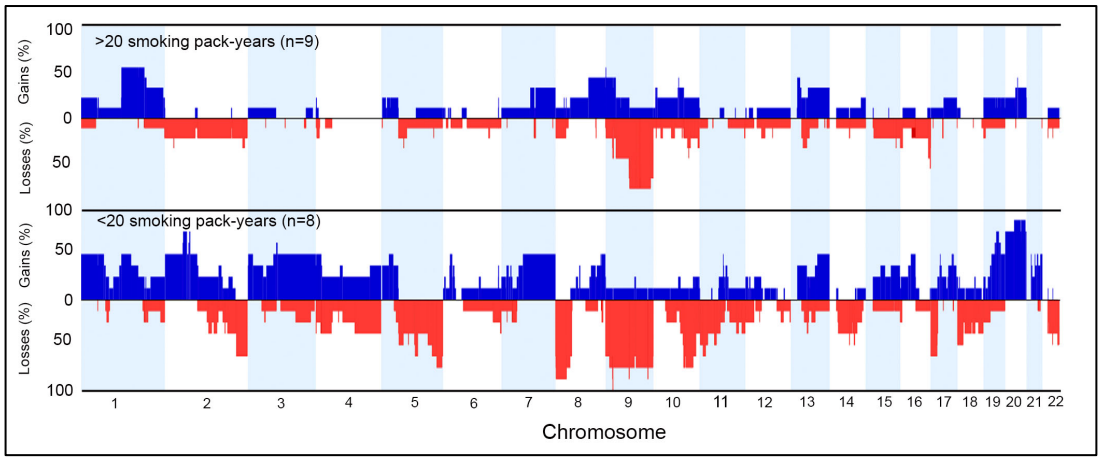

Figure 3.28: Smoking status and copy number alterations in 22 patients. Genome-wide frequency plots of copy number alterations in patients with <20 packs a year (n=8) and with ≥20 packs a year (n=9). The x-axis corresponds to chromosomes 1 to 22 and the y-axis corresponds to the percentage of copy number gains (blue) and losses (red).

Chapter 4
Hierarchical clustering and phylogenetic analysis of copy number data from multifocal tumours

By combing copy number and mutation data and creating the phylogenic trees we aimed to assess whether multifocal tumours from the same patient are monoclonal or oligoclonal in origin. Copy number data for the individual tumours from each patient was used to reconstruct the probable sequence of events, which gave rise to each tumour. This further confirmed the monoclonal origin of tumour samples from the same patient. Our data has also shown a significant intra-patient heterogeneity which could have important prognostic and therapeutic implications. Application of copy number data into risk stratification tables might further enhance the accuracy of calculating the risk for progression and/or recurrence.

In this chapter, one-way unsupervised hierarchical analysis on copy number data is used to assess the relationships between individual multifocal tumours from the same patient and to assess the heterogeneity of copy number alterations in different patients with multifocal disease. Copy number data for the individual tumours from each patient is also used in phylogenetic analysis to reconstruct the probable sequence of events which gave rise to each tumour.

4.1 Hierarchical cluster analysis of 66 individual multifocal tumours

One-way unsupervised hierarchical cluster analysis of copy number data from all 66 tumours was performed to assess the relationships between the individual multifocal tumours of each patient.

Tumours separated into 3 main clusters which varied in chromosomal complexity in the order Cluster 1 < Cluster 2 < Cluster 3 (Appendix 4.1, Figure 4.1). All tumours from the same patient tended to group together

within the same cluster except in 4 cases (Patients 5, 8, 13 and 16). In patient 5, tumours 1 and 2 separated into Clusters 1 and 3 respectively, reflecting the minimal copy number alterations exhibited by tumour 1. A similar situation was observed for patient 13 in which the chromosomally stable tumour 4 was found in Cluster 1 whilst the 3 other tumours from this patient were in Cluster 3. In patient 8, two tumours with minimal copy number alterations (8_1 and 8_3) separated into Cluster 1 whilst tumour 2 which exhibited additional copy number alterations including loss of two regions on chromosome 9 was found in Cluster 2. A similar situation was seen for patient 16 in which tumours 3 and 4 separated into Cluster 1 whilst tumours 1 and 2, which both exhibited several copy number alterations including losses on chromosome 9, were found in Cluster 2. For 3 patients (5, 8, 13) evidence of possible non-clonality was seen based on cluster analysis of copy number events. In patient 5, two tumours had no shared copy number events and grouped in two separate Clusters (1 and 3). However, all tumours from patient 5 shared *FGFR3* mutation. In patient 13 tumour 4 did not share any copy number events with the other 3 synchronous tumours and separated into Cluster 1. Tumours from patient 13 were all wildtype for *FGFR3*, *PIK3CA* and the RAS genes. Tumour 2 from patient 8 remained separated into Cluster 2 while other tumours grouped in Cluster 1. All tumours in this patient shared mutations in *PIK3CA* and *FGFR3*.

The distribution of tumours amongst the clusters was examined in relation to stage, grade, FGA and mutation status. The 31 TaG2 tumours were found mainly in Clusters 1 (n=11) and 2 (n=18) with only two TaG2 tumours separating into Cluster 3 (5_2 and 20_1). T1G3 tumours were predominantly found in Cluster 3 (n=12) with only two and four T1G3 tumours being found in Clusters 1 and 2, respectively. TaG3 tumours were mainly in Clusters 2 (n=6) and 3 (n=10), with only one TaG3 tumour (13_4) separating into Cluster 1.

Cluster 1 contained 14 tumours exhibiting minimal copy number alterations (Figure 4.1). These tumours were mainly FGA group A (n=10) with the remaining 4 tumours (1_1, 17_1, 17_2, 17_3) being FGA group B. Most tumours in this cluster had at least one mutation in *PIK3CA*, *FGFR3* or the

RAS genes, with only 4 out of 14 tumours being wildtype for all of the genes. Ten tumours in Cluster 1 were from patients with recurrent disease and four were from patients with primary disease.

Cluster 2 contained 28 tumours, which were either FGA group B (n=12) or C (n=16) (Figure 4.1). Most tumours from this cluster displayed a characteristic loss of 9q. Apart from this characteristic feature, there was a prevalence of gains over losses in this cluster. Six tumours (all from patient 4) exhibited concomitant gain of 1p and 9p and loss of 9q. As observed for Cluster 1, most tumours in Cluster 2 had at least one mutation in *PIK3CA*, *FGFR3* or RAS. Only seven out of 28 tumours were wildtype for all genes. There was also a prevalence of tumours in this cluster from patients with recurrent (n=21) as compared to primary (n=7) disease.

Cluster 3 contained tumours (n=23) with the highest number of copy number alterations (Figure 4.1). Twenty-two tumours in this cluster were FGA group D, with the remaining tumour (10_1) being FGA group C. Tumours in this cluster were wildtype for all genes apart from tumour 2 from patient 5 which carried an *FGFR3* mutation. Closer inspection revealed that some tumours formed separate sub-clusters based on characteristic copy number alterations. In one sub-cluster, all tumours (8 tumours: 12_1-4, 14_1-4) displayed characteristic losses on chromosome arms 2q, 4q and gain in 20q. Similar losses on chromosome arm 2q but limited to smaller region (214.9-242.1 Mb) were observed in 10 tumours (5_2, 6_2-3, 18_1-4, 10_1-2, 20_2) from another sub cluster. Tumours in Cluster 3 exhibited multiple copy number alterations. Loss of 2q was a common event in all except 1 tumour (6_1), with loss being limited to a small region extending from 2q24-2q37.3 (214.9-242.1 Mb) in 10 tumours (5_2, 6_2-3, 18_1-4, 10_1-2, 20_2). The region contains 77 genes including *CUL3*, *DNER*, *XRCC5*, and the UGT1A gene cluster. A full list of genes in the region is shown in Appendix 4.1B. Losses on chromosome 9 and gains on chromosome 20 were also frequent events in tumours from this cluster. All of the tumours in Cluster 3 were from patients with primary disease.

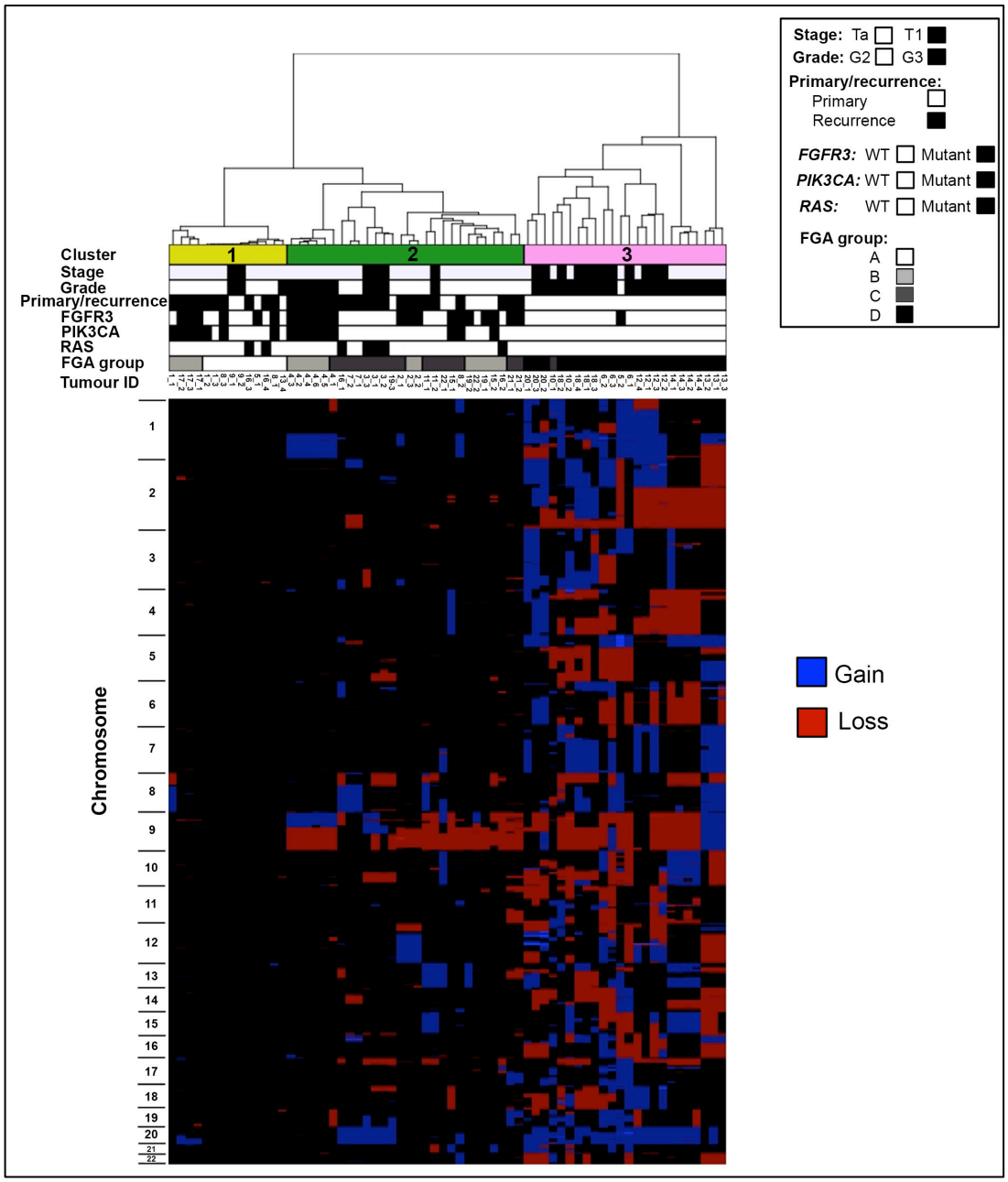

Figure 4.1: Unsupervised hierarchical cluster analysis of aCGH data from 66 individual multifocal tumours. Each column of the heat map represents 1 sample and each row represents the genomic position of individual clones on the array. Blue, copy number gain; red, copy number loss. Chromosome number is shown on the left-hand side of the heat map. Three main clusters of tumours were identified and these are indicated by the colour bars on the top of panel: cluster 1, yellow; cluster 2, green; cluster 3, pink. The grade and stage of each tumour is shown at the top of the figure (black box, T1 or G3; white box, Ta or G2). The *FGFR3, PIK3CA and* RAS gene mutation status is also shown at the top of the figure (black box, mutant; white box, wild type), along with FGA group (A–D) and whether the multifocal tumour was from a patient with primary or recurrent disease (black box, recurrence; white box, primary).

4.2 Hierarchical cluster analysis of merged copy number data from 22 patients

To assess the heterogeneity of copy number alterations in multifocal disease, the same one-way hierarchical clustering approach was applied to the merged copy number data for the 22 patients. Patients separated into 2 main clusters, primarily according to stage and grade (Table 4.1, Figure 4.2). The majority of patients withTaG2 samples (n=10) were found in Cluster 1, with only the TaG2 patient 5 separating into Cluster 2. T1G3 patients were predominantly found in Cluster 2 (n=5) with only 3 patients (3, 9 and 11) being found in Cluster 1. TaG3 patients 10 and 14 were in Cluster 2 and the TaG3 patient 4 was in Cluster 1.

Paitents in Cluster 1 (n=14) exhibited fewer copy number alterations than those in Cluster 2 (n=8). This cluster was characterized by a high frequency of chromosome 9 loss which was observed in 12 patients. Eleven patients in Cluster 1 were FGA group C, 2 were FGA group B and 1 was FGA group A. All except 4 patients (7, 9, 11 and 22) in Cluster 1 carried at least one mutation in *FGFR3*, *PIK3CA* or the three RAS genes. Ten patients in Cluster 1 were patients with recurrent disease and 4 were patients with primary disease.

Cluster 2 contained patients whose samples exhibiting a high level of chromosomal instability with all being FGA group D. All patient samples in Cluster 2, except the sample from patient 5, were wildtype for *FGFR3*, *PIK3CA* and the three RAS genes. The patients in Cluster 2 were all patients with primary disease.

Using the Comparisons function of the Nexus software package, a Fishers Exact test (0.05 p-value cut off; 25% differential threshold) was used to

compare the frequencies of copy number alterations in Clusters 1 and 2 (Figure 4.3 and Appendix 4.2). Loss on 10q was a frequent event in Cluster 2. The majority of patients (87.5%) in Cluster 2 exhibited loss of a region at 10q23.32 containing *PTEN* (Appendix 4.3). Loss of 2q including the previously discussed region extending from 2q24-2q37.3 also occurred at high frequency (>75% difference) in tumours from Cluster 2 (Appendix 4.3). Patients in Cluster 2 also exhibited a high frequency (>75%) of gains on chromosomes 1, 2, 5, 7 and 20 (Appendix 4.4).

Tumours in Cluster 2 exhibited higher frequencies of chromosomal alterations than those in Cluster 1 indicating high inter-patient heterogeneity between patients from the two clusters.

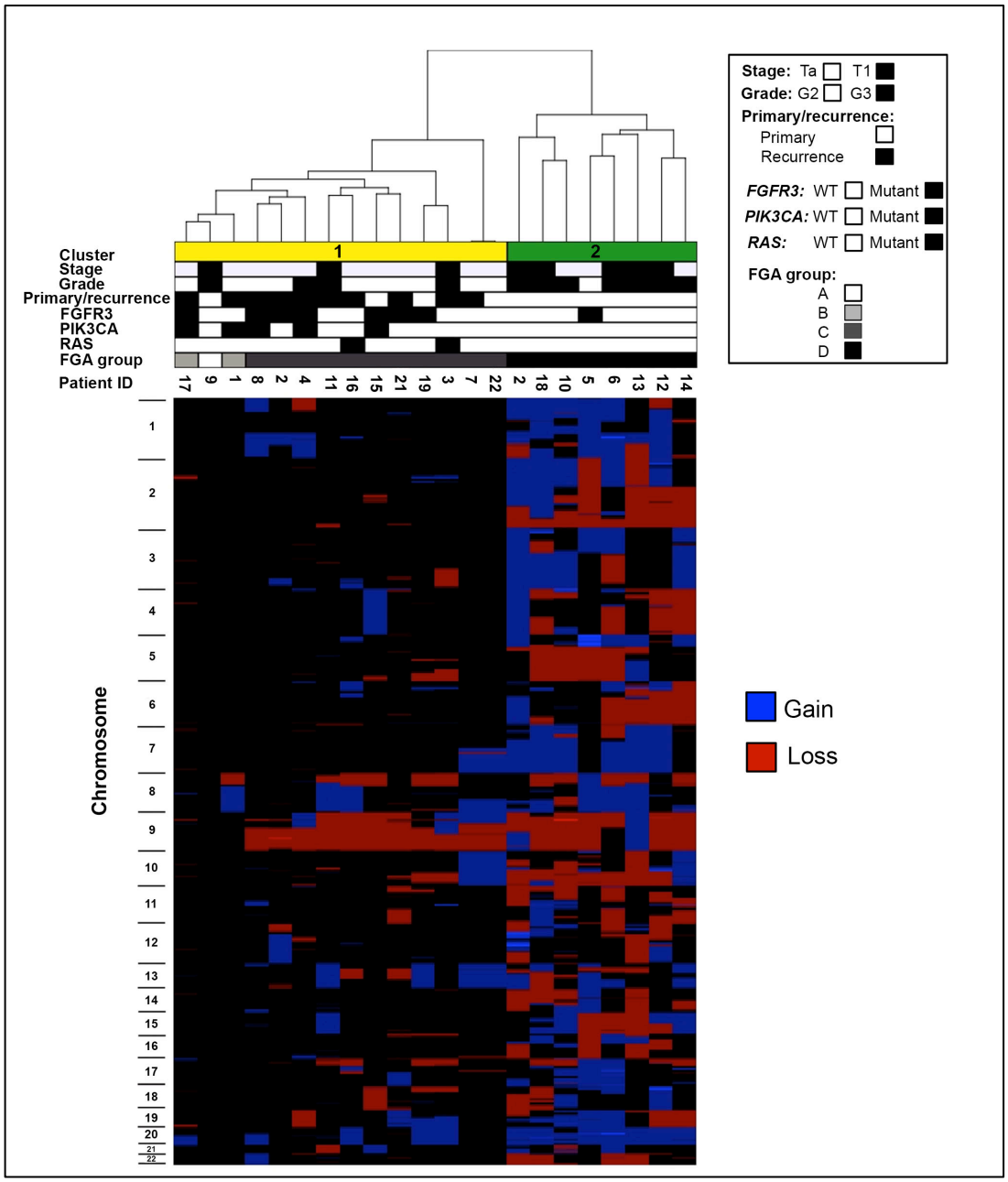

Figure 4.2: Unsupervised hierarchical cluster analysis of aCGH data from 22 patients. Each column of the heat map represents 1 patient and each row represents the genomic position of individual clones on the array. Blue, copy number gain; red, copy number loss. Chromosome number is shown on the left-hand side of the heat map. Two main clusters of patients were identified and these are indicated by the colour bars on the top of panel: cluster 1, yellow; cluster 2, green. The grade and stage of each tumour is shown at the top of the figure (black box, T1 or G3; white box, Ta or G2). The *FGFR3*, *PIK3CA* and RAS gene mutation status is also shown at the top of the figure. (black box, mutant; white box, wild type), along with FGA group (A–D) and whether multifocal tumours were from patients with primary or recurrent disease (black box, recurrence; white box, primary).

Patient	Stage	Grade	FGA group	Primary/recurrent	FGFR3	PIK3CA	RAS	Cluster
1	Ta	G2	B	Recurrence	WT	Mutant	WT	1
2	Ta	G2	C	Recurrence	Mutant	WT	WT	1
3	T1	G3	C	Recurrence	WT	WT	Mutant	1
4	Ta	G3	C	Recurrence	Mutant	Mutant	WT	1
7	Ta	G2	C	Recurrence	WT	WT	WT	1
8	Ta	G2	C	Recurrence	Mutant	Mutant	WT	1
9	T1	G3	A	Primary	WT	WT	WT	1
11	T1	G3	C	Recurrence	WT	WT	WT	1
15	Ta	G2	C	Primary	Mutant	Mutant	WT	1
16	Ta	G2	C	Recurrence	WT	WT	Mutant	1
17	Ta	G2	B	Recurrence	Mutant	Mutant	WT	1
19	Ta	G2	C	Primary	Mutant	WT	WT	1
21	Ta	G2	C	Recurrence	Mutant	WT	WT	1
22	Ta	G2	C	Primary	WT	WT	WT	1
5	Ta	G2	D	Primary	Mutant	WT	WT	2
6	T1	G3	D	Primary	WT	WT	WT	2
10	Ta	G3	D	Primary	WT	WT	WT	2
12	T1	G3	D	Primary	WT	WT	WT	2
13	T1	G3	D	Primary	WT	WT	WT	2
14	Ta	G3	D	Primary	WT	WT	WT	2
18	T1	G3	D	Primary	WT	WT	WT	2
20	T1	G3	D	Primary	WT	WT	WT	2

Table 4.1. Details of samples in the two main clusters obtained by hierarchical cluster analysis of merged copy number data from 22 patients. Grade and stage is the highest reported for tumours form each patient

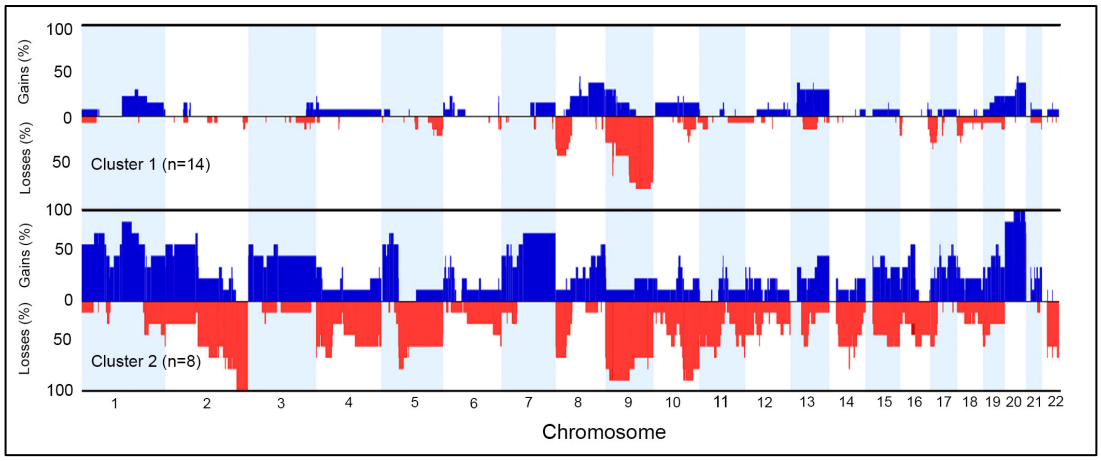

Figure 4.3: Genome-wide frequency plots of copy number alterations in the 2 main clusters obtained by hierarchical cluster analysis of merged copy number data from 22 patients. The *x*-axis corresponds to chromosomes 1 to 22 and the y-axis corresponds to the percentage of copy number gains and losses. Copy number gains are shown in blue and losses in red. Frequencies of copy number alterations are shown for cluster 1 (top panel) and cluster 2 (bottom panel).

4.3 Phylogenetic tree analysis

The relationships between tumours from the same patient were also assessed using phylogenetic analysis. The probable sequence of events that gave rise to each tumour was reconstructed based upon similarities and differences in breakpoint regions and copy number events using the TuMult computational method (see section 2.5.8, Materials and Methods). A phylogenetic tree was constructed for each patient where all tumours are shown as descendants of common hypothetical ancestors. Mutation status was also added to the graphical output of each phylogenetic tree in order to give a full picture of events in each patient. All phylogenetic trees not illustrated in this chapter can be viewed in Appendix 4.5.

For 16 patients (2, 3, 4, 6, 7, 10, 11, 12, 14, 15, 17, 18, 19, 20, 21, 22) evidence for a monoclonal origin of all tumours in a given patient was obtained based on phylogenetic analysis of copy number events. In all patients except patient 4, tumours were linked via a ‘common precursor’ that

had a set of copy number events present in all tumours. Each tumour then acquired it's own set of characteristic copy number events.

Tree reconstruction revealed differences in the level of diversity of copy number alterations in different patients. In some cases trees were relatively simple and involved minimal copy number differences between tumours. A representative example of this is shown for patient 2 (Figure 4.4).

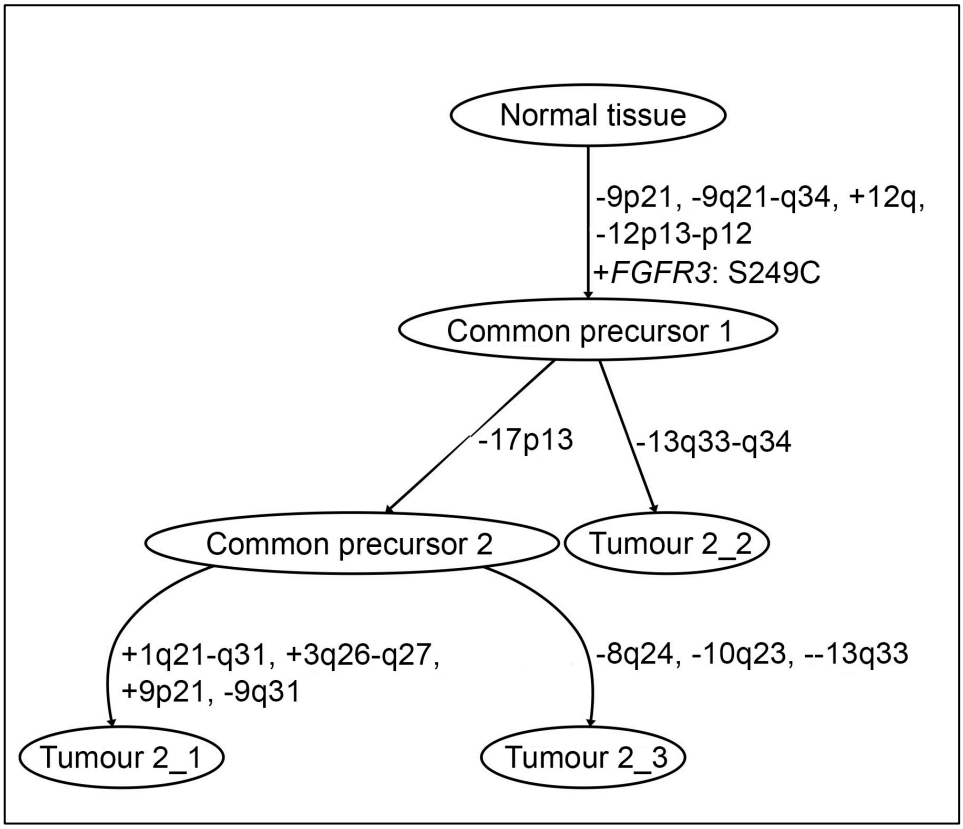

Figure 4.4. Phylogenetic tree showing the relationships between all tumours from patient 2.

In some patients many copy number alterations were acquired following divergence from a common precursor. A representative example of this is shown for patient 6 (Figure 4.5).

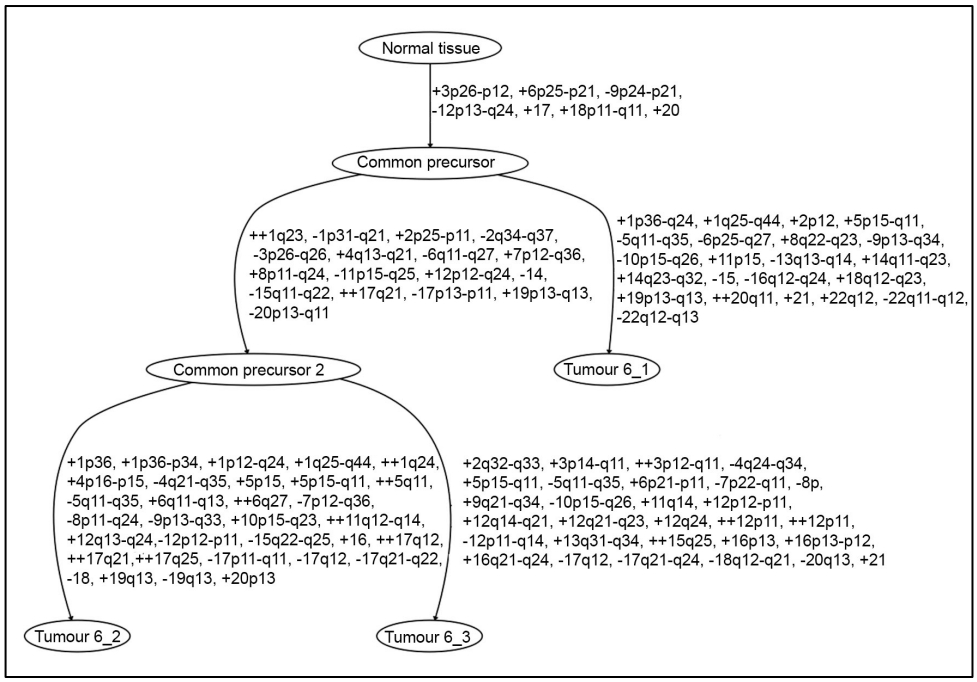

Figure 4.5. Phylogenetic tree showing the relationships between all tumours from patient 6.

In patient 4, tumour 4 appeared to be the common precursor for all other tumours (Figure 4.6).

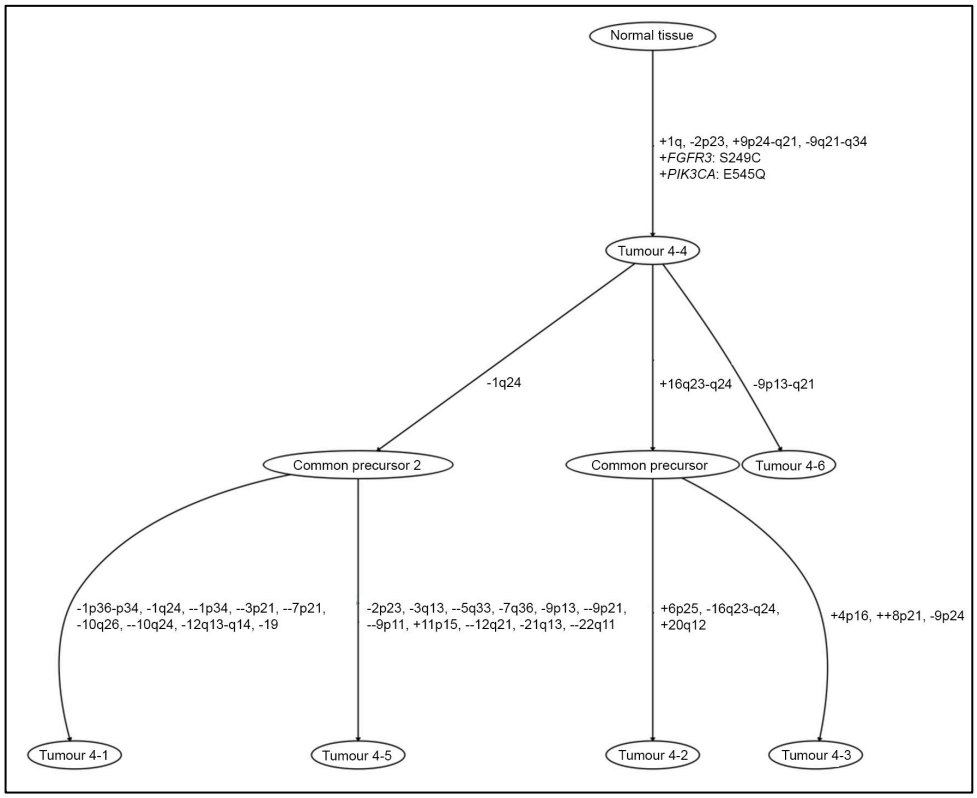

Figure 4.6. Phylogenetic tree showing the relationships between all tumours in patient 4.

Patient 19 represented an interesting case. All 3 tumours from this patient shared a common precursor based on copy number losses on 4q and 9p. Tumour 3 then appeared to diverge away from the other two tumours and accumulated it's own set of characteristic copy number alterations. It also lacked an *FGFR3* Y375C mutation detected in the other two tumours (Figure 4.7).

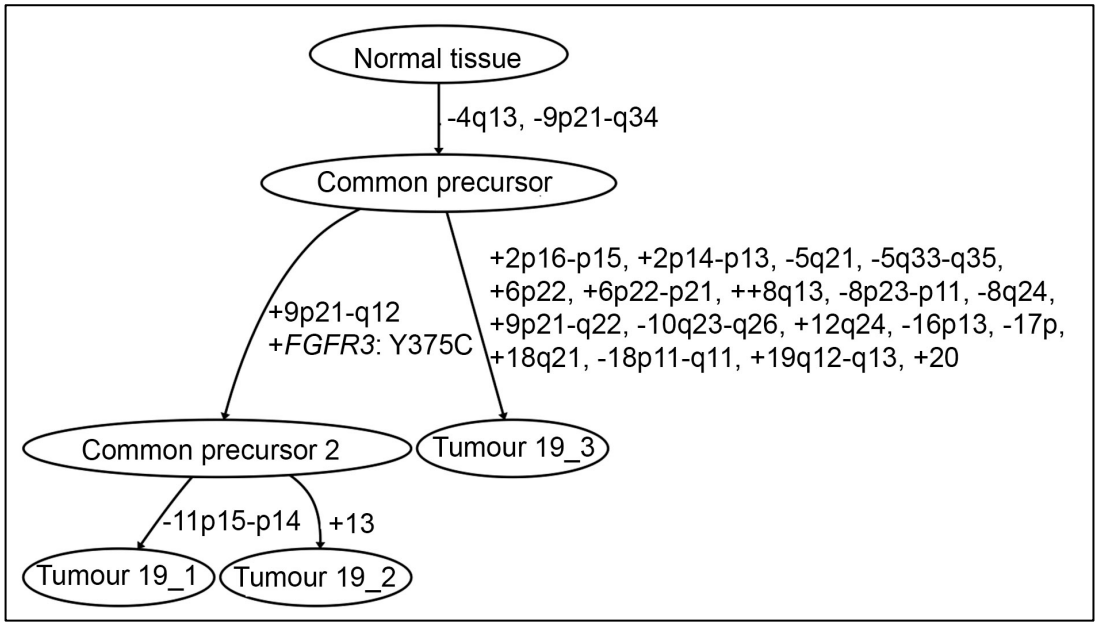

Figure 4.7. Phylogenetic tree showing the relationships between tumours from patient 19.

In 6 cases (patients 1, 5, 8, 9, 13 and 16) a monoclonal origin for all tumours in a given patient could not clearly be confirmed. Each of these cases is discussed below.

A monoclonal origin of tumours from patient 1 could not be determined based on copy number data as two of the three tumours (1_2 and 1_3) exhibited no copy number alterations (Figure 4.8). Evidence of a monoclonal origin could perhaps be inferred for tumours 1_1 and 1_2 as both carried *PIK3CA* E545K mutations. Also it could be hypothesised that tumours 1_2 and 1_3 were predecessors of tumour 1_1.

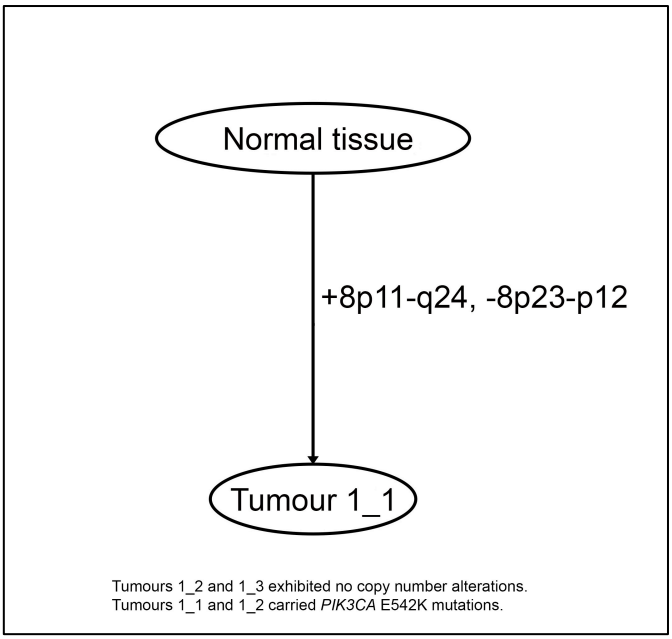

Figure 4.8. Phylogenetic tree for Patient 1.

Two tumours from patient 5 did not share copy number events (Figure 4.9). Circumstantial evidence for a monoclonal origin of these tumours could be inferred from the fact that both tumours carried an *FGFR3* S249C mutation. However, this should be viewed with caution as this mutation is frequent in superficial bladder cancer.

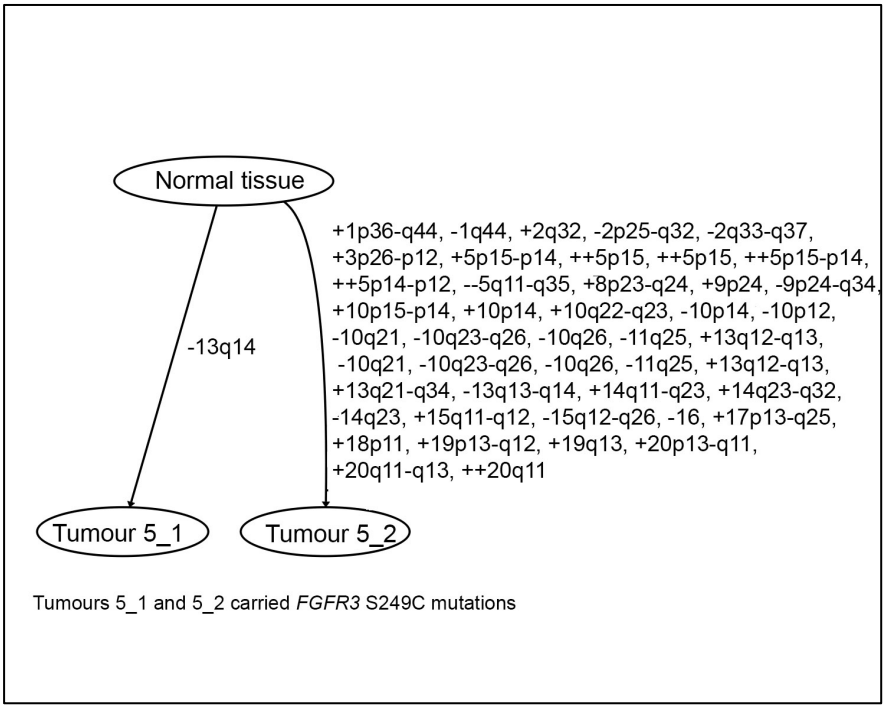

Figure 4.9. Phylogenetic tree showing the relationship between 2 tumours from Patient 5

Two tumours (8_1) and (8_2) from patient 8 shared a common copy number gain on 22q, and both carried *FGFR3* S249C and *PIK3CA* H1047R mutations, confirming a monoclonal origin for these tumours. Tumour 3 from this patient exhibited no copy number alterations and therefore the relatedness of this tumour to the other two tumours could not be assessed based on copy number. This tumour did, however, carry both mutations seen in tumours 1 and 2 making it more likely that all 3 tumours are related and tumour 8_3 represents the precursor for the other 2 tumours (Figure 4.10).

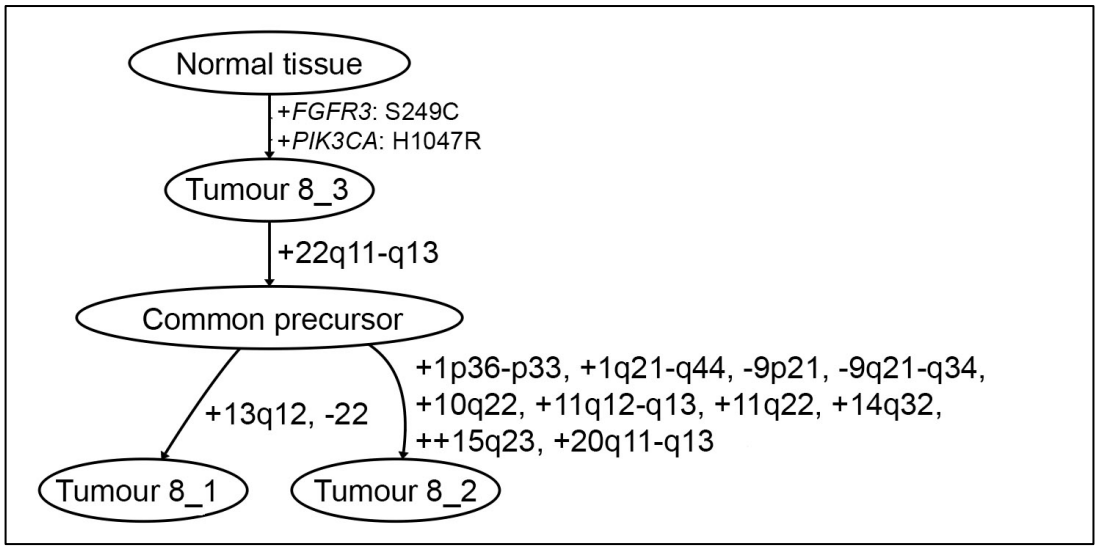

Figure 4.10. Phylogenetic tree showing the relationships between 3 tumours from patient 8.

Tumours from patient 9 exhibited no copy number alterations and did not carry mutations in *FGFR3*, *PIK3CA* or the 3 RAS genes. Therefore, based on this evidence a monoclonal origin of tumours from this patient cannot be confirmed.

A monoclonal origin for three tumours (13_1, 13_2 and 13_3) from patient 13 was confirmed based on copy number events, however tumour 13_4 did not share any of the copy number events in the other 3 tumours and exhibited characteristic losses on 10q and 19p (Figure 4.11). A common

origin for all tumours in this patient cannot therefore be confirmed based on copy number alterations. All tumours from this patient were wildtype for *FGFR3*, *PIK3CA* and the 3 RAS genes therefore no further assessment of relatedness between tumour 13_4 and the other tumours could be made based on this data.

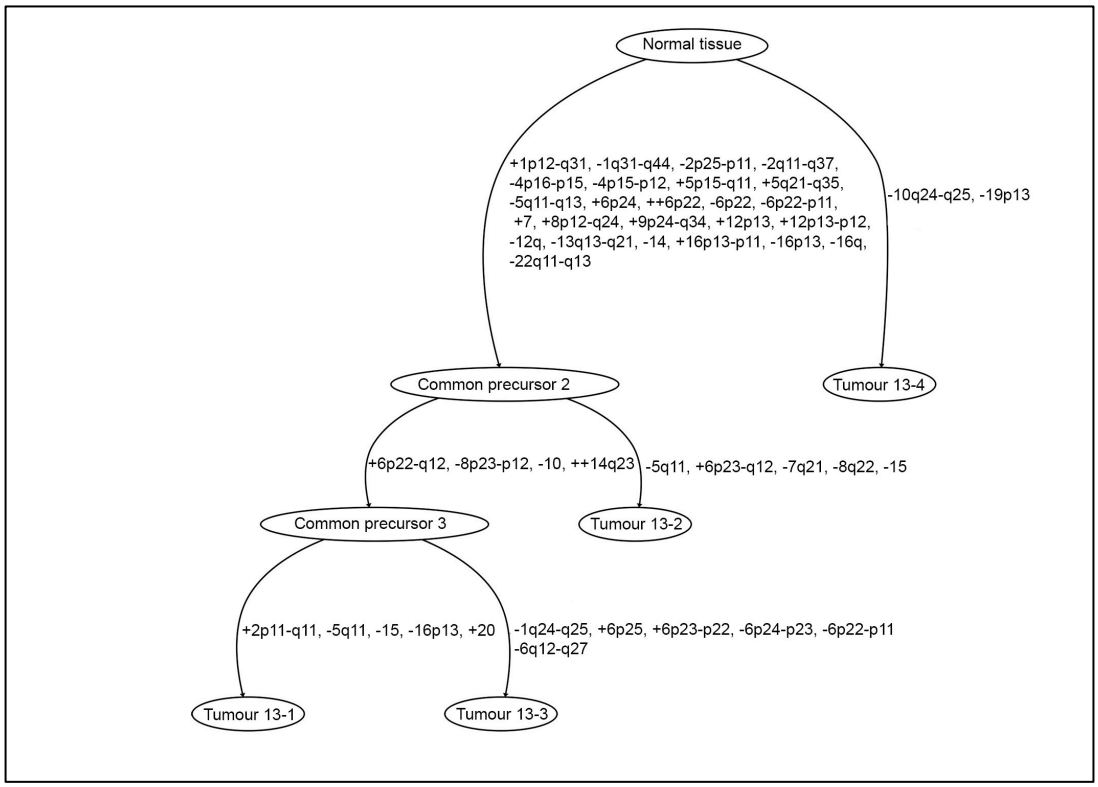

Figure 4.11. Phylogenetic tree showing the relationships between 4 tumours from patient 13.

A monoclonal origin could not be inferred for 4 tumours from patient 16 based on copy number data. Tumour 16_3 carried no copy number alterations and the other 3 tumours carried but did not share copy number events. The only evidence for a monoclonal origin of tumours in this patient was that they all carried the same *HRAS* G12C mutation.

The copy number events and mutations occurring at the top of each tree were analysed to find the most frequently occurring events in all trees.

These were loss and gain of 9p, 9q, 2p, 2q, 4p, 4q, 6p, 6q, 8p, 8q, 10q, 11q, 11p, 12p, 12q, 13q, 14q, 16p, 16q, 19p, 22q. As these events are at the top of the tree it may be that they represent early events in tumorigenesis.

Chapter 5
Comparison of multifocal and solitary tumours

This chapter describes the comparison of the merged copy number dataset for the 22 multifocal patients with an existing dataset of copy number alterations in 103 solitary tumours (data from Hurst *et al*. 2012) comprising 28 TaG1/G2, 10 TaG3, 7 T1G2, 29 T1G3 and 29 ≥ T2 tumours. One-way hierarchical cluster analysis was performed to assess the relationships between multifocal and solitary tumours. Frequency plot comparisons were made to assess differences in copy number alterations in multifocal versus solitary disease. Frequency plots were constructed of copy number events in stage and grade matched tumours from the two datasets. Multifocal tumours exhibited higher frequencies of chromosomal alterations than solitary tumours.

5.1 Hierarchical cluster analysis of copy number data from multifocal and solitary tumours excluding stage ≥ T2 tumours

One-way unsupervised hierarchical cluster analysis of copy number data was initially performed to assess the relationships between multifocal tumours and solitary tumours from patients with superficial disease only. The solitary tumour dataset consisted of 28 TaG1/G2, 10 TaG3, 7 T1G2, and 29 T1G3 tumours.

Tumours separated into 4 main clusters which varied in chromosomal complexity in the order Cluster 1 < Cluster 2 < Cluster 3 < Cluster 4 (Figure 5.1). The distribution and features of multifocal and single tumours in each of

the clusters is summarised in Appendix 5.1. Figure 5.2 shows genome-wide frequency plots of copy number events in each of the clusters.

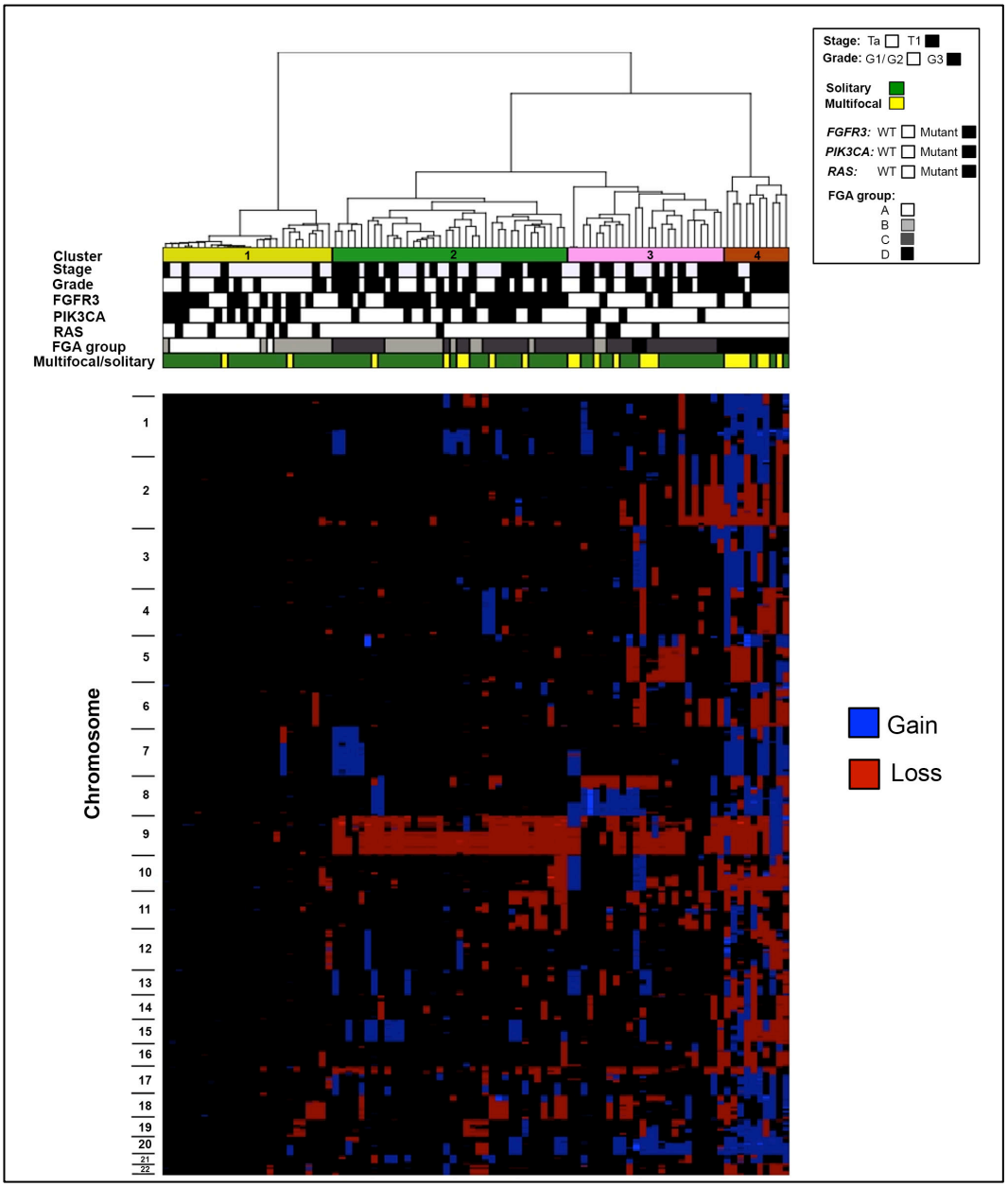

Figure 5.1. Unsupervised hierarchical cluster analysis of aCGH data from 22 patients with multifocal disease and 96 patients with solitary superficial bladder tumours. Each column of the heat map represents 1 patient and each row represents the genomic position of individual clones on the array. Blue, copy number gain; red, copy number loss. Chromosome number is shown on the left-hand side of the heat map. Multifocal tumours are highlighted in yellow and solitary tumours in green. Four main clusters of patients were identified and these are indicated by the colour bars at the top of the panel: cluster 1, yellow; cluster 2, green; cluster 3, pink; cluster 4, brown. The grade and stage of each tumour is shown at the top of the figure (black box, T1 or G3; white box, Ta or G1/G2). The *FGFR3, PIK3CA* and

RAS gene mutation status is also shown at the top of the figure (black box, mutant; white box, wildtype), along with FGA group (A–D) and whether the tumour was from a patient with primary or recurrent disease (black box, recurrence; white box, primary).

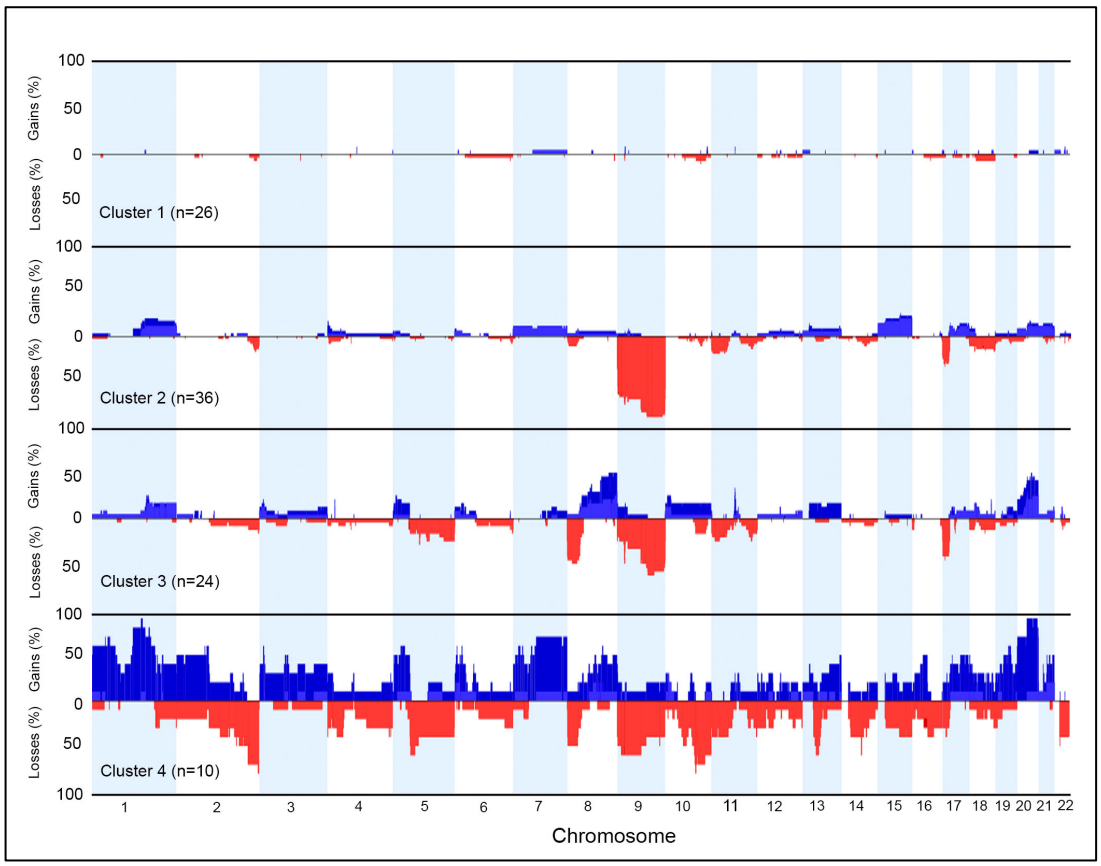

Figure 5.2. Genome-wide frequency plots of copy number alterations in the 4 main clusters obtained by hierarchical cluster analysis of copy number data from multifocal and solitary superficial bladder tumours. The x-axis corresponds to chromosomes 1 to 22 and the y-axis corresponds to the percentage of copy number gains and losses. Copy number gains are shown in blue and losses in red.

Cluster 1 contained 26 tumours that exhibited minimal copy number alterations with all tumours being either FGA groups A or B (Figure 5.2). Most of the tumours in Cluster 1 were solitary. Only tumours from 2 multifocal patients (9 and 17) separated into this cluster (Appendix 5.1). Tumour 9 was a T1G3 tumour exhibiting no copy number alterations and tumour 17 was a TaG2 tumour that exhibited minimal copy number alterations (<5% FGA). TaG1/2 tumours predominated in Cluster 1 (n=18), with only 1 T1G2, 4 TaG3 and 3 T1G3 tumours being found in this cluster. Most tumours in this cluster carried at least one mutation in *FGFR3, PIK3CA*

or the RAS genes, with only 4 tumours (including multifocal patient 9) being wildtype for all genes.

Cluster 2 contained 36 tumours that also exhibited a limited number of copy number alterations but were more chromosomally unstable than those from Cluster 1. T1G3 (n=15) and TaG1/G2 (n=12) tumours predominated in Cluster 2. The other samples in the cluster were 5 T1G2s and 4 TaG3s. Six tumours in Cluster 2 were from multifocal patients (2, 4, 8, 11, 15, 21) and four of these were TaG2 tumours. All tumours were FGA groups B or C. A characteristic feature of this cluster was loss of chromosome 9 with a region from 71.1 to 128.3Mb (9q21.11-q33.3) containing *PTCH1* and *DBC1* being lost in all but one tumour (from the solitary sample set). The other most frequent events in this cluster were gains of 1q (observed in 7 tumours) and 15q (in 9 tumours). Thirty-one of the tumours in this cluster carried at least one mutation in *FGFR3, PIK3CA* or the RAS genes, with only 5 tumours (including multifocal patient 11) being wildtype for all genes.

Tumours in Cluster 3 (n=24) exhibited a higher frequency of copy number alterations than those from Cluster 2. Cluster 3 contained 8 TaG2, 4 TaG3, 1 T1G2 and 11 T1G3 tumours. Nineteen tumours were FGA group C, 2 were FGA group B and 3 were FGA group D. Tumours from seven multifocal patients (1, 3, 7, 14, 16, 19, 22) separated into this cluster. Five of these multifocal tumours were TaG2s (patients 1, 7, 16, 19, 22) and the other 2 were T1G3 (patient 3) and TaG3 (patient 14) tumours. Losses of 8p, 9q and 17p, and gains of 8q, 11q and chromosome 20 were most frequent in this cluster. The region of gain on 11q13.2-q13.3 (68.7-69.3 Mb) was found in 33% of samples (8 samples). It included 4 genes: *MYEOV, CCND1, ORAOV1* and *FGF19*. Twelve tumours carried at least one mutation in *FGFR3, PIK3CA* or the RAS genes, with the other 12 tumours (including multifocal patients 7, 14 and 22) being wildtype for all genes.

Cluster 4 samples (n=10) exhibited the highest level of chromosomal instability with all tumours being FGA group D. T1G3 tumours predominated in this cluster (n=8), with the stages and grades of the other two samples

being TaG2 and TaG3. Seven out of the ten tumours were multifocal and 5 of these were T1G3s. Only one tumour from multifocal patient 5 carried a mutation (*FGFR3* S249C) with all the remaining tumours being wildtype for *FGFR3, PIK3CA* and the RAS genes. Copy number gains and losses were frequent across most chromosomes in tumours from this cluster with the most frequent losses involving 2q, 5p, 8p, 9p, 10q and 13q, and the most frequent gains involving 1q, 5p, 6p, 7q 8q and 20q.

Overall, hierarchical cluster analysis revealed that TaG2 multifocal tumours tended to cluster with solitary tumours of higher stage and grade. T1G3 multifocal tumours clustered with different subsets of T1G3 solitary tumours and interestingly formed the majority in a highly chromosomally unstable subset of tumours.

5.2 Comparisons of copy number alterations in multifocal and solitary superficial bladder tumours

In order to identify specific features related to multifocality, a Fishers Exact test (0.05 p-value cut off; 25% differential threshold) was used to compare the frequencies of copy number alterations in multifocal and solitary superficial bladder tumours matched for stage, grade and *FGFR3* mutation status.

5.2.1 Comparisons of copy number events in multifocal and solitary superficial tumours according to stage and grade

Comparisons were initially made between multifocal and solitary superficial tumours matched for stage or grade.

Using the Comparisons function of the Nexus software package, a Fishers Exact test (0.05 p-value cut off; 25% differential threshold) was used to compare the frequencies of copy number alterations in patients with multifocal or solitary stage Ta tumours. (Figure 5.3, Appendix 5.2). Overall,

multifocal stage Ta tumours were more chromosomally unstable than stage Ta solitary tumours. A difference of >40% in the frequency of copy number events was identified for several regions including gains of 8q24.13 (*ANXA13, FBXO32, KLHL38)*, 13q12.11 - q12.3 and 20q11.23 - q12, and losses of 8p21.2 - p12 (including *NRG1*), 9p21.3 (*CDKN2A, CDKN2A-AS1, CDKN2B, CDKN2B-AS1, DMRTA1, ERVFRD-3, MTAP, TUBB8P1, UBA52P6)* and 9q12 - q34.3 (including *PTCH*, *DBC1* and *TSC1*) which were more common in multifocal patients.

A similar comparison was made in patients with multifocal or solitary stage T1 tumours (Figure 5.4, Appendix 5.3). A difference of >40% in the frequency of copy number events was identified for several regions. This comparison revealed that tumours from multifocal patients had a higher prevalence of gains on 1p12 - q24.3 (*TAGLN2*), 2p25.3 - q11.1, 6p22.3 - p22.1 (*E2F3, CDKAL1, SOX4, PRL*), 7p11.2 - q36.3, 16p12.1 - q11.2, 19q13.11 - q13.2, 20p13 - q13.33, (including *PHACTR3, SYCP2, PPP1R3D, CDH26, C20orf197, miR-646,CDH4*) and losses on 2q33.3 - q37.3 (*SGC2, AP1S3, WDFY1, MRPL44, SERPINE2, FAM124B, CUL3, DOCK10, KIAA1486*), 5q11.2 - q12.3, 6q27, 8p23.2 - p12, chromosome 10 (q22.3 and q23.1 - q26.3), 3q14.2 - q14.3, 14q23.1 and 22q11.1 - q13.33. Overall, stage T1 multifocal tumours exhibited more copy number events than their solitary counterparts.

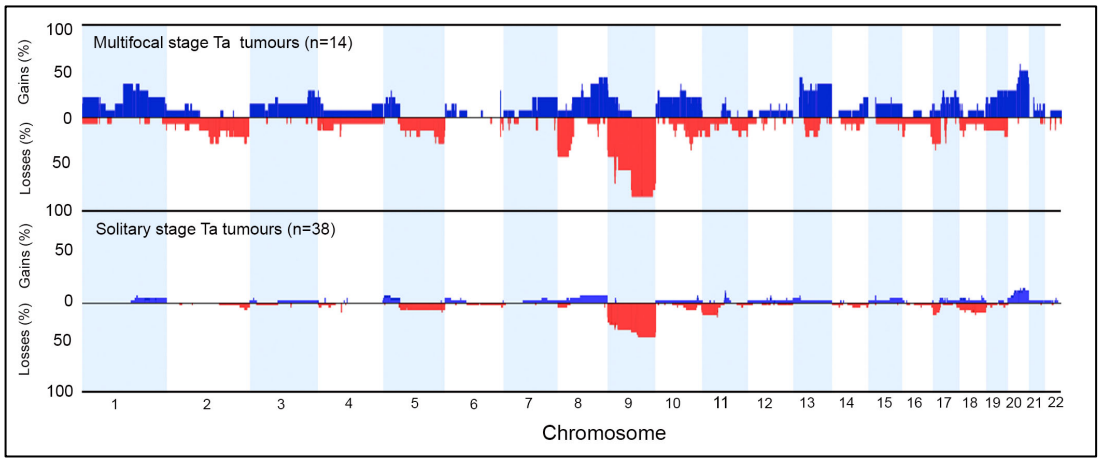

Figure 5.3: Comparison of genome-wide copy number alterations in stage Ta tumours from patients with multifocal and solitary disease. The frequencies of copy number events are shown for multifocal tumours (top panel; n=14) and solitary tumours (bottom panel; n=38). The x-axis

corresponds to chromosomes 1 to 22 and the y-axis corresponds to the percentage of copy number gains and losses. Copy number gains are shown in blue and losses in red.

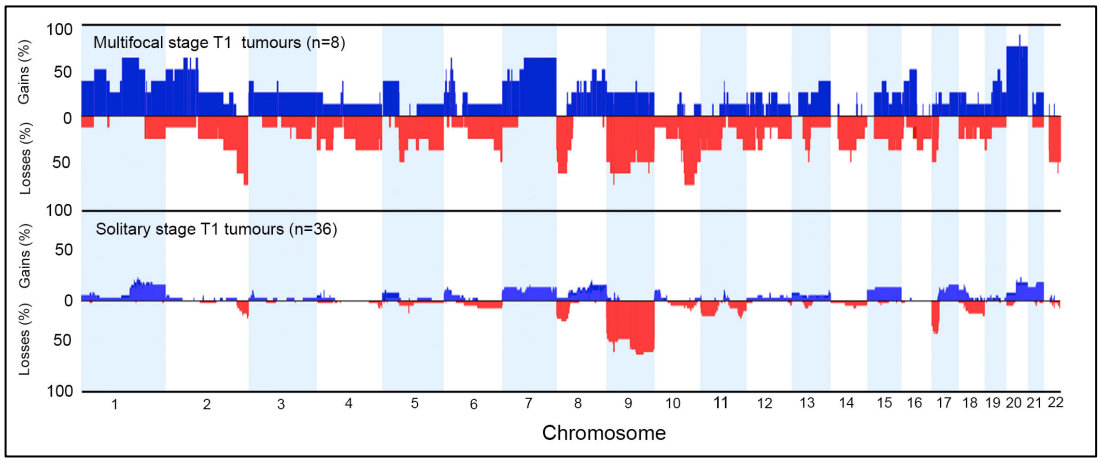

Figure 5.4. Comparison of genome-wide copy number alterations in stage T1 tumours from patients with multifocal and solitary disease. The frequencies of copy number events are shown for multifocal tumours (top panel; n=8) and solitary tumours (bottom panel; n=36). The x-axis corresponds to chromosomes 1 to 22 and the y-axis corresponds to the percentage of copy number gains and losses. Copy number gains are shown in blue and losses in red.

A comparison of copy number events in tumours from patients with multifocal or solitary grade 1/2 disease, was also made.(Figure 5.5, Appendix 5.4). Grade 1/2 multifocal tumours exhibited more copy number events than their solitary counterparts. A difference of >40% in the frequency of copy number events was identified for several regions including gains on 8 q13.2 - q13.3 , 8q22.1 – 24.3, 13q12.11 - q12.3, 13q21.32 - q21.33, and losses on 9q13.3 – 9q 21.33, 9q31.2. - q34.12 (*DBC1*) and 9p21.3 (*MTAP*, *CDKN2AS*) with these events being more common in multifocal tumours.

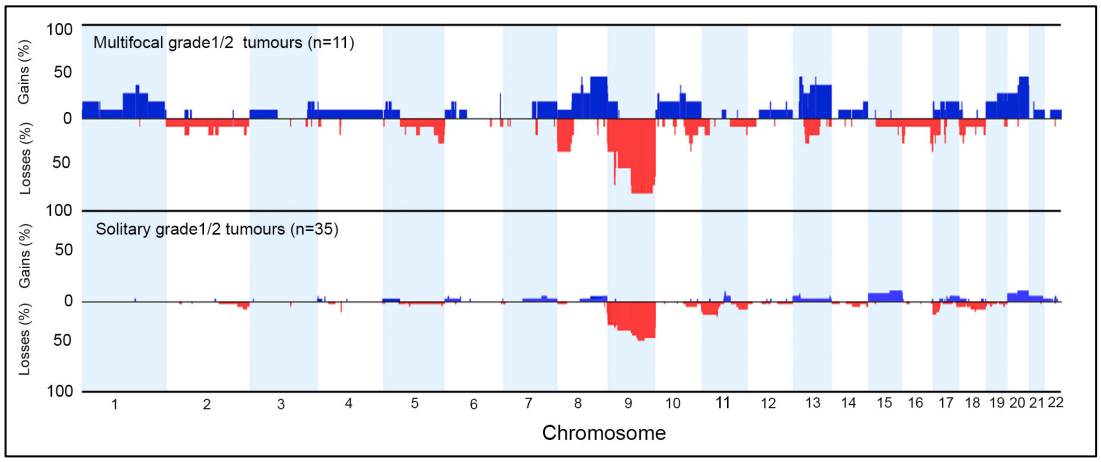

Figure 5.5. Comparison of genome-wide copy number alterations in grade 1/2 tumours from patients with multifocal and solitary disease.

The frequencies of copy number events are shown for multifocal tumours (top panel; n=11) and solitary tumours (bottom panel; n=35).

In a comparison of the frequencies of copy number alterations in patients with multifocal or solitary grade 3 tumours, significant differences were identified for several regions (Figure 5.6, Appendix 5.5). Alterations exhibiting a difference of >50% were gains on chromosome 1 (p12 - q21.1), chromosome 2 (p11.2 - q11.1, p13.3 - p13.1 and p16.3 - p14), and chromosome 20 (p13 - q11.1, q11.21 - q12 and q13.2 -13.33) and losses on chromosome 2 (q33.3 - q37.3), chromosome 8 (q23.2 – q23.32, q23.33 – q25.3, q26.11, q26.13 and q26.2 - q26.3) and chromosome 22 (q11.1 - q11.21). These alterations were more frequent in multifocal tumours (Appendix 5.5).

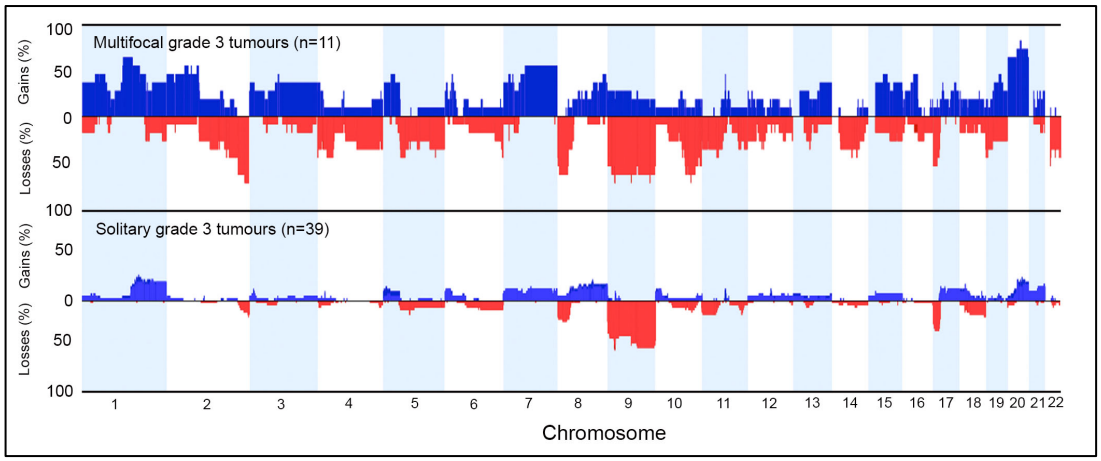

Figure 5.6. Comparison of genome-wide copy number alterations in grade 3 tumours from patients with multifocal and solitary disease. The frequencies of copy number events are shown for multifocal tumours (top panel; n=11) and solitary tumours (bottom panel; n=39). The x-axis corresponds to chromosomes 1 to 22 and the y-axis corresponds to the percentage of copy number gains and losses. Copy number gains are shown in blue and losses in red.

Comparisons of the frequencies of copy number alterations were next made between multifocal and solitary superficial tumours matched for stage and grade (i.e. TaG1/G2, TaG3, T1G3).

A comparison of copy number events in multifocal and solitary tumours from patients with TaG1/G2 disease was performed (Figure 5.7, Appendix 5.6).

Gains of large regions on chromosome 1 (p12 - q22and q23.1 - q31.3), chromosome 8 (p11.21 - q12.3, q13.2 - q21.11, q22.1 - q24.3), chromosome 10 (p15.1 - p14, q22.1 - q23.2), chromosome 13 (q12.11 - q13.1 and q14.3 - q34), chromosome 19 (q12 - q13.43) and chromosome 20 (q11.23 - q13.33) were more common in multifocal patients. Other smaller regions which reached statistical significance included gains on chromosome 6 (q26) and chromosome 9 (p24.3). Losses of large regions on chromosomes 8 (p23.3 - p11.21) and 9 (p21.3, q12 - q34.12 and q34.3) and losses of discrete regions on chromosome 10 (q24.32), chromosome 13 (q13.3 - q14.2), chromosome 16 (p13.3, q23.3 - q24.1 and q24.3) and chromosome 17 (q12 - q21.2) were also more prevalent in multifocal tumours.

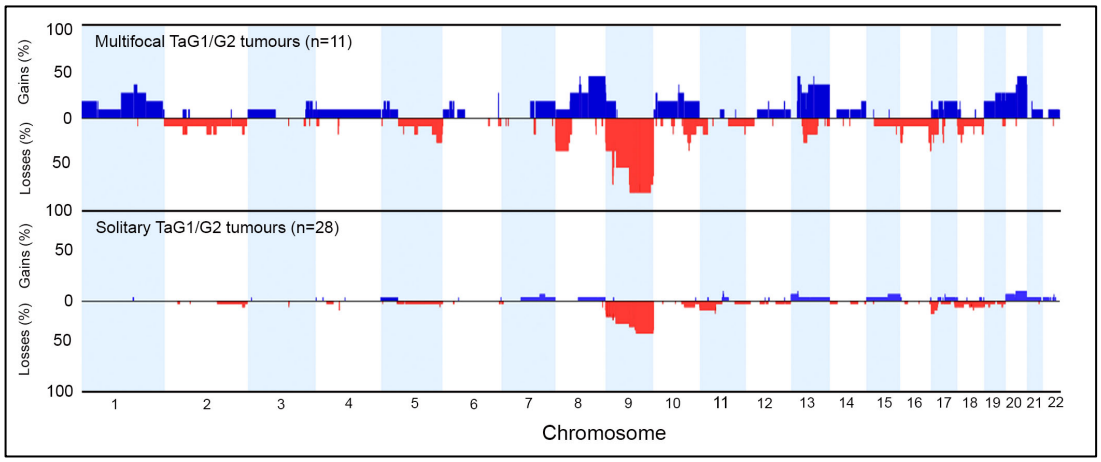

Figure 5.7. Comparison of genome-wide copy number alterations in low stage and low grade (TaG1/2) tumours from patients with multifocal and solitary disease. The frequencies of copy number events are shown for multifocal tumours (top panel; n=11) and solitary tumours (bottom panel; n=28). The x-axis corresponds to chromosomes 1 to 22 and the y-axis corresponds to the percentage of copy number gains and losses. Copy number gains are shown in blue and losses in red.

A comparison of copy number events in tumours from patients with multifocal or solitary T1G3 disease, was also made (Figure 5.8, Appendix 5.7). Large regions of gain on chromosome 1 (p12 - q12 and q23.3), chromosome 2 (p11.2 - q12.3, q13 - q24.1 and q24.3), chromosome 3 (p12.1 - q13.13 and q22.1 - q25.32), chromosome 4 (q13.2 - q21.1 and q35.1), chromosome 7 (p11.2 - q36.3), chromosome 9 (p13.1 - q34.3), chromosome 16 (p11.2 - q11.2), chromosome 19 (p12 - q12, q13.11 -

q13.41, q13.42 and q13.43), and chromosome 20 (p11.1 - q13.33) were more commonly seen in multifocal tumours. Discrete regions of gain on chromosome 5 (p15.33), chromosome 6 (p22.3 - p21.32, p25.1 - p24.3 and q11.1 - q12), chromosome 10 (q22.1 - q22.3), chromosome 11 (q13.5 - q14.1), chromosome 14 (q24.3) and chromosome 17 (p12) were significantly more prevalent in multifocal patients. Regions of deletion more common in multifocal patients included deletions on chromosome 1 (q31.1 - q31.2 and q31.3 - q44), chromosome 2 (q11.1 - q11.2, q22.3 - q37.3), chromosome 3 (q13.33 - q21.1 and q23 - q26.33), chromosome 4 (p15.2 - p12, p16.3 - p15.33 and q21.21 - q34.3), chromosome 5 (q11.2 - q12.3, q21.1 - q21.3 and q31.2 - q35.3), chromosome 6 (q27), chromosome 8 (p11.22 - p11.1 and p23.2 - p22), chromosome 9 (q34.3), chromosome 10 (p11.21 - p11.1, q22.3, q23.1 - q26.3), chromosome 11 (p11.12 - q12.2), chromosome 12 (p11.1 - q13.13, q15 - q21.1 and q22 - q24.31), chromosome 13 (q14.2 - q14.3), chromosome 14 (q12 - q24.2), chromosome 15 (q11.2 - q14 and q22.31 - q26.3), chromosome 16 (p13.3 and p11.2 - q24.3), chromosome 19 (p13.3 - p12) and chromosome 22 (q11.1 - q13.33). Overall, multifocal T1G3 tumours were more chromosomally unstable than their solitary counterparts.

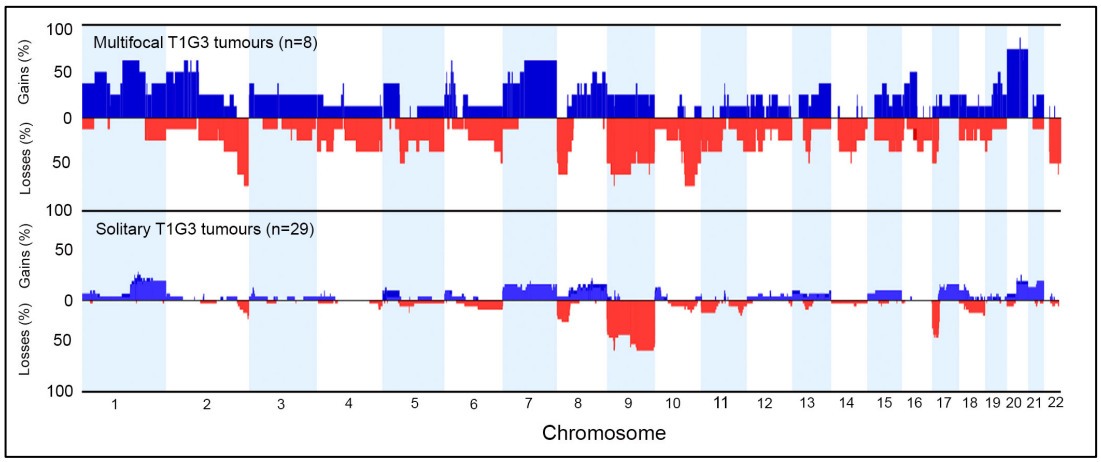

Figure 5.8. Comparison of genome-wide copy number alterations in stage T1 and grade 3 (T1G3) tumours from patients with multifocal and solitary disease. The frequencies of copy number events are shown for multifocal tumours (top panel; n=8) and solitary tumours (bottom panel; n=29). The x-axis corresponds to chromosomes 1 to 22 and the y-axis corresponds to the percentage of copy number gains and losses. Copy number gains are shown in blue and losses in red.

Comparisons of copy number events in TaG3 patients could not be made due to low number of patients in the multifocal dataset (n=3).

5.2.2 Comparisons of copy number events in multifocal and solitary superficial tumours according to *FGFR3* mutation status

The relationship of *FGFR3* mutation status to copy number events in stage and grade matched multifocal and solitary tumours was examined.

A comparison of copy number events in *FGFR3* mutant TaG1/G2 multifocal and solitary tumours was made (Figure 5.9, Appendix 5.8). Deletions on chromosome 5 (q34 - q35.3), chromosome 9 (p21.3 and q21.33), chromosome 10 (q24.2 - q25.1) and chromosome 16 (p13.3), and gains on chromosome 1 (p12 - q31.3), chromosome 6 (q26), chromosome 8 (q13.2 - q13.3), chromosome 13 (q12.11 - q12.3 and q21.32 - q21.33), chromosome 19 (q12 - q13.43) and chromosome 20 (q11.23 - q13.33) were more frequent in mutant *FGFR3*, TaG2, multifocal tumours.

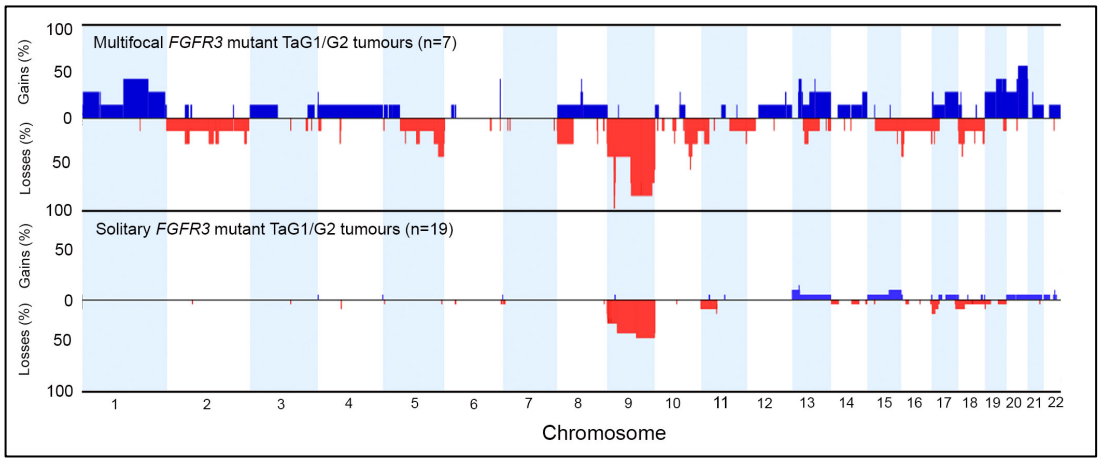

Figure 5.9. Comparison of genome-wide copy number alterations in *FGFR3* mutant TaG1/2 tumours from patients with multifocal and solitary disease. The frequencies of copy number events are shown for multifocal tumours (top panel; n=7) and solitary tumours (bottom panel; n=19). The x-axis corresponds to chromosomes 1 to 22 and the y-axis corresponds to the percentage of copy number gains and losses. Copy number gains are shown in blue and losses in red.

In *FGFR3* wildtype TaG1/G2 tumours gain on chromosome 8 (q22.1 - q24.3) and deletions on chromosome 9 (p21.1 - q12) and chromosome 17 (q12 -

q21.2) were more frequent (p=0.024) in multifocal tumours (Figure 5.10, Appendix 5.9). However, the number of patients in each group was too low to make any further statistically significant conclusions.

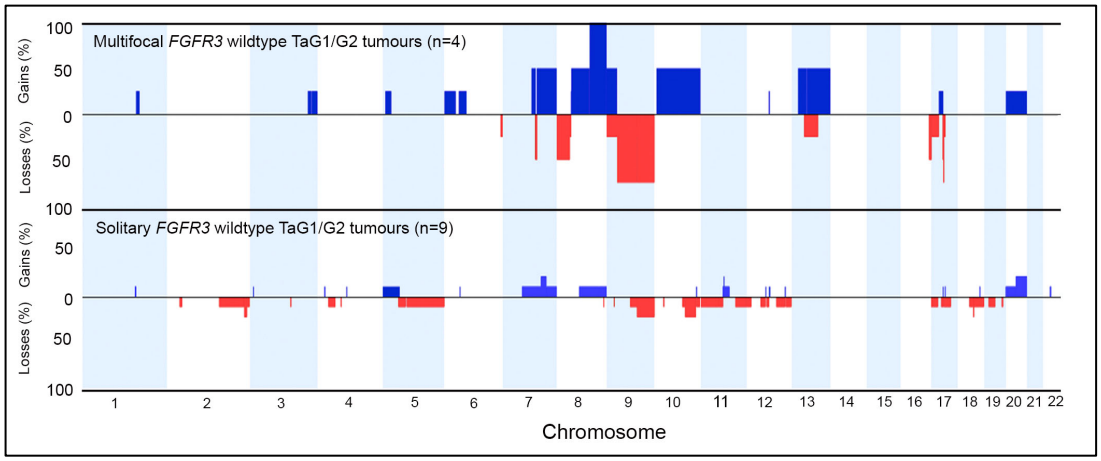

Figure 5.10. Comparison of genome-wide copy number alterations in *FGFR3* wildtype TaG1/2 tumours from patients with multifocal and solitary disease. The frequencies of copy number events are shown for multifocal tumours (top panel; n=4) and solitary tumours (bottom panel; n=9). The x-axis corresponds to chromosomes 1 to 22 and the y-axis corresponds to the percentage of copy number gains and losses. Copy number gains are shown in blue and losses in red.

A comparison of the frequencies of copy number alterations in *FGFR3* wildtype T1G3 tumours from patients with multifocal and solitary disease was performed (Figure 5.11, Appendix 5.10). Gains on chromosome 1 (p34.1, p32.3 - p31.1 and p12 - q12), chromosome 2 (p14 - q11.1, p23.3 - p16.3, p25.3 - p24.1), 3p (p12.1), 4q (q13.3 - q21.1), 6p (p22.3 - p22.1), 7q (q11.21 - q11.22 and q35), chromosome 9 (q21.32 - q21.33 and p24.3), chromosome 16 (p13.2 - q11.2), 19q (q12 and q13.11 - q13.32) and chromosome 20 (p13 - q13.33) and losses on 2q (q24.3 - q37.3), chromosome 4 (p15.2 - p12, p16.3 - p15.33 and q25 - q34.3), 5q (q11.2 - q12.3), 6q (q27), 10q (q23.1 - q26.3), chromosome 11 (p11.2 - q12.1), chromosome 12 (p11.1 - q13.11), 13q (q14.2 - q14.3), 14q (q13.1 and q23.1), 15q (q22.31 - q25.2, q25.3 and q26.1 - q26.3), 16q (q11.2 - q21), 19p (p13.3) and 22q (q11.1 - q11.23 and q12.2 - q13.2) were more frequent in multifocal tumours.

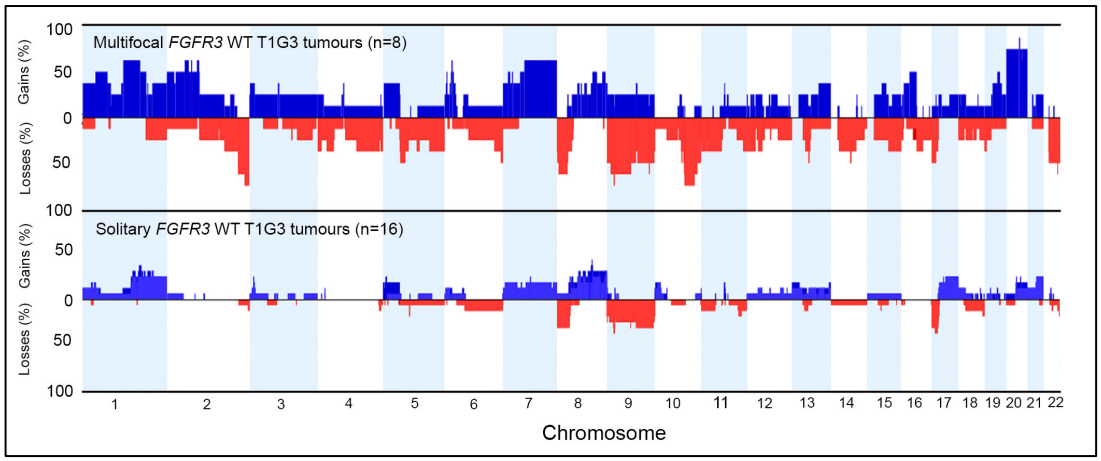

Figure 5.11. Comparison of genome-wide copy number alterations in *FGFR3* wildtype T1G3 tumours from patients with multifocal and solitary disease. The frequencies of copy number events are shown for multifocal tumours (top panel; n=8) and solitary tumours (bottom panel; n=16). The x-axis corresponds to chromosomes 1 to 22 and the y-axis corresponds to the percentage of copy number gains and losses. Copy number gains are shown in blue and losses in red.

5.3 Hierarchical cluster analysis of copy number data from multifocal and solitary tumours including stage ≥ T2 tumours

In all comparisons with superficial solitary tumours, multifocal tumours were more chromosomally unstable. Also, in cluster analysis, multifocal tumours constituted the majority of highly chromosomally unstable tumours present in Cluster 4. With this in mind we performed one-way unsupervised hierarchical cluster analysis again and included 29 ≥ T2 tumours to assess whether the multifocal tumours in Cluster 4 exhibited characteristics of ≥ T2 tumours.

As previously observed, tumours separated into 4 main clusters which varied in chromosomal complexity in the order Cluster 1 < Cluster 2 < Cluster 3 < Cluster 4 (Figure 5.12). The distribution and features of multifocal and single tumours in each of the clusters is summarised in Appendix 5.11. Figure 5.13 shows genome-wide frequency plots of copy number events in each of the clusters. The features of each of the clusters was essentially as described in Section 5.1.

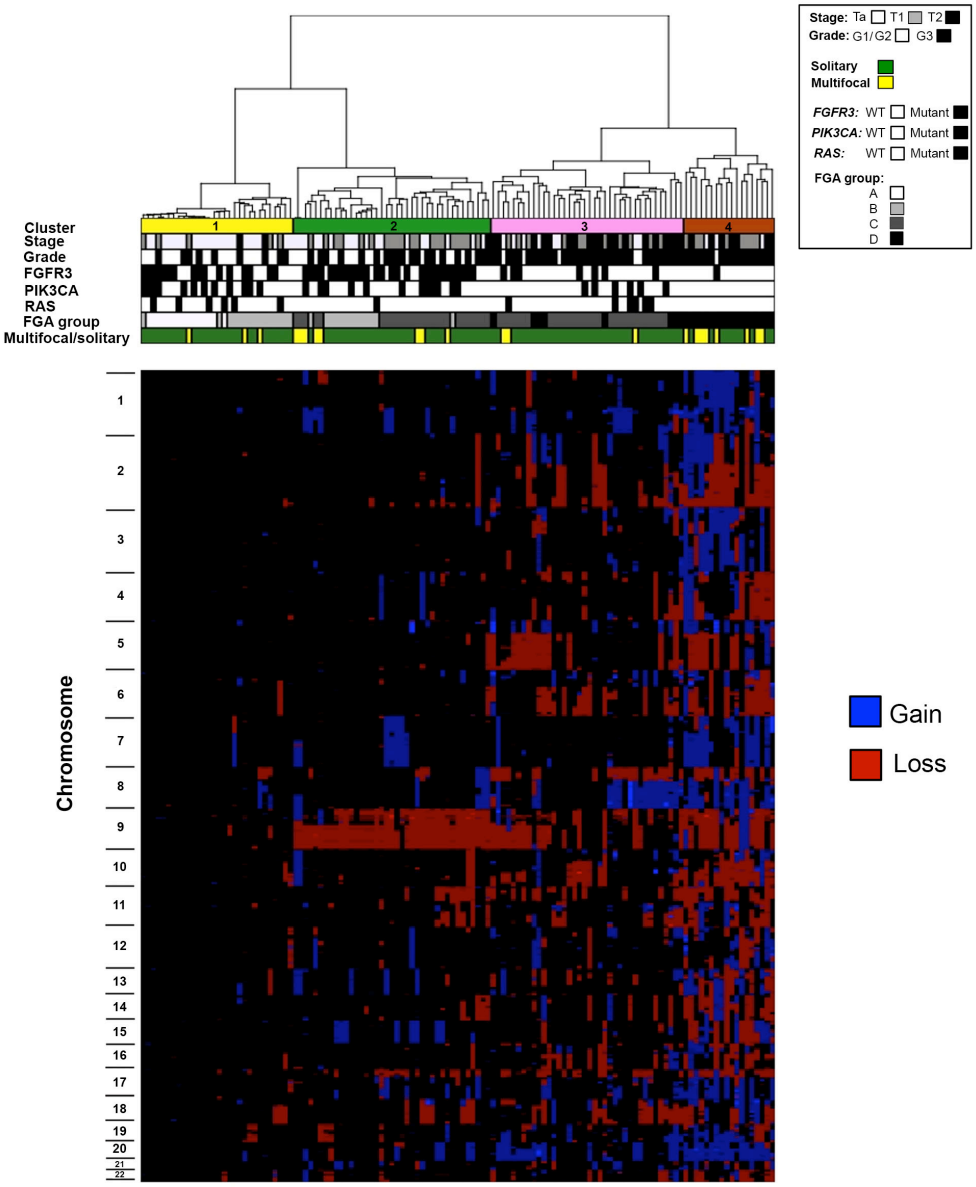

Figure 5.12. Unsupervised hierarchical cluster analysis of aCGH data from 22 patients of multifocal data set and 103 patients with solitary disease including 29 stage ≥ T2 tumours. Each column of the heat map represents 1 patient (labelled on the top) and each row represents the genomic position of individual clones on the array. Blue, copy number gain; red, copy number loss. Chromosome number is shown on the left-hand side of the heat map. Multifocal tumours are highlighted in yellow and solitary tumours in green. Four main clusters of patients were identified and these are indicated by the colour bars on the top of panel: cluster 1, yellow; cluster 2, green; cluster 3, pink; cluster 4, brown. The grade and stage of each tumour is shown at the top of the figure (grey box, T1; black box T2, or G3; white box, Ta or G2). The *FGFR3* PIK3CA and RAS gene mutation status is also shown at the top of the figure (black box, mutant; white box, wildtype), along with FGA group (A–D) and whether the tumour was from a patient with primary or recurrent disease (black box, recurrence; white box, primary).

Cluster 1 tumours were chromosomally stable with low stage and low grade tumours constituting the majority of tumours in this cluster. Tumours were FGA groups A or B and exhibited a high frequency of *FGFR3, PIK3CA* and RAS gene mutations. Only 2 ≥ T2 tumours separated into Cluster 1. As previously observed, multifocal tumours 9 and 17 separated into this cluster. Tumour 1, which previously separated into Cluster 3, was now part of Cluster 1.

Cluster 2 contained tumours that also exhibited a limited number of copy number alterations but were more chromosomally unstable than those from Cluster 1. TaG2 and T1G3 tumours predominated in Cluster 2 with all tumours being FGA groups B or C. A characteristic feature of this cluster was loss of chromosome 9 with other frequent events in this cluster being gains of 1p and 15q. *FGFR3, PIK3CA* and RAS gene mutation was also frequent in Cluster 2. Only 1 ≥ T2 tumour separated into this cluster. Multifocal tumours 2, 4, 8, 11, 15 and 21 separated into this cluster as previously observed. Two other multifocal tumours (7, 22) that had previously been in Cluster 3, also separated into Cluster 2 following inclusion of the ≥ T2 tumours.

Tumours in Cluster 3 exhibited a higher frequency of copy number alterations than those from Cluster 2. Cluster 3 contained 5 TaG2, 3 TaG3 and 11 T1G3 tumours. Nineteen of the ≥ T2 tumours separated into this cluster. Thirty tumours were FGA group C and 8 were FGA group D. Losses of 8p, 9p, 9q and 17p, and gains of 1q, 6p, 8q and chromosome 20 were most frequent in this cluster. Sixteen tumours carried at least one mutation in *FGFR3, PIK3CA* or the RAS genes, with the other 22 tumours being wildtype for all genes. Only 3 of the multifocal tumours (3, 16, 19) that previously separated into this cluster were still present in this cluster.

Cluster 4 samples (n=18) exhibited the highest level of chromosomal instability with all tumours being FGA group D. T1G3 (n=8) and ≥ T2 (n=7)

tumours predominated in this cluster, with the other tumours being 1 TaG2 sample (multifocal tumour 5) and 2 TaG3 samples (multifocal samples 10 and 14). All 8 of the multifocal tumours that had previously separated into this cluster were still present. Apart from the tumour from multifocal patient 5 which carried an S249C mutation in *FGFR3*, all of the tumours in Cluster 4 were wildtype for *FGFR3, PIK3CA* and the RAS genes. Copy number gains and losses were frequent across most chromosomes in tumours from this cluster with the most frequent losses involving 2p, 2q, 5q, 6q, 8p, 9p, 9q, 10q, 13p, 15q, 16q, 17p, and the most frequent gains involving 1p, 1q, 2p, 3p, 3q, 5p, 7p, 7q, 8q, 17q, 19q, 20p and 20q. Analysis of this cluster revealed similarities in the characteristics of a subset of multifocal tumours and a subset of ≥ T2 tumours.

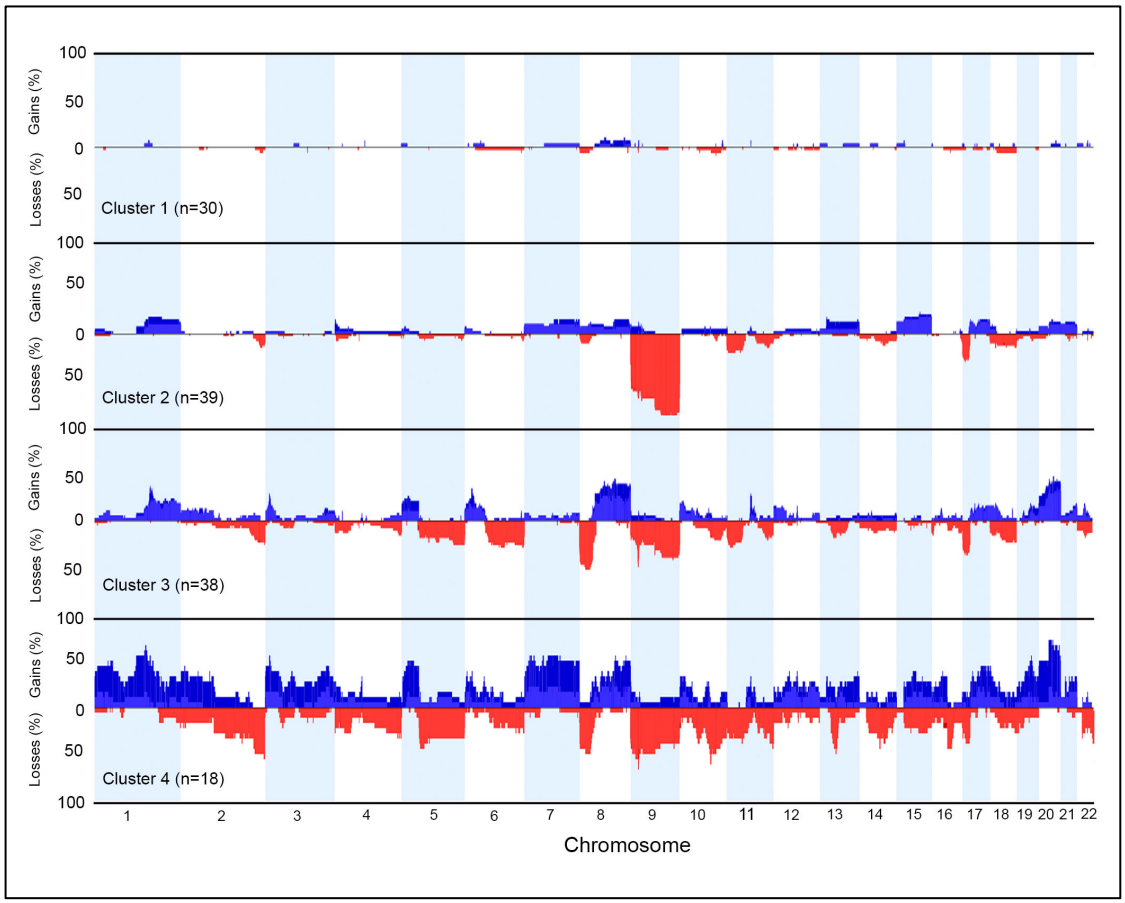

Figure 5.13. Genome-wide frequency plots of copy number alterations in the 4 main clusters obtained by hierarchical cluster analysis of copy number data from multifocal and solitary bladder tumours including 29 ≥ T2 tumours. The x-axis corresponds to chromosomes 1 to 22 and the y-axis corresponds to the percentage of copy number gains and losses. Copy number gains are shown in blue and losses in red.

Chapter 6
Immunohistochemical analysis of FGFR3 expression in matched primary and metastatic bladder cancer samples

FGFR3 is considered a good therapeutic target for bladder cancer. However, to our knowledge it is unknown whether the FGFR3 status of primary tumours is a surrogate for related metastases, which must be targeted by FGFR targeted systemic therapies. We assessed FGFR3 protein expression in primary bladder tumours and matched nodal metastases. FGFR3 expression in matched primary and metastasized bladder cancer specimens showed good but not absolute concordance. Thus, in most patients primary tumour FGFR3 status can guide the selection of FGFR targeted therapy.

This chapter describes the results of experiments in which immunohistochemistry was used to determine the expression of the FGFR3 in primary bladder tumours and matched nodal metastases. This data has now been published [248]. The TMA was constructed with six tissue cores per patient: two each from normal urothelium, primary tumour (centre and invasion front), and a nodal metastasis. Biopsies were placed on slides with 17 columns and 9 rows with one liver biopsy as a control sample. Unstained TMA slides and clinicopathological data for each patient were provided for this study by collaborators in Bern (Drs A Fleischmann, G Thalmann and R Seiler).

6.1 FGFR3 protein expression in primary tumours and metastases

As described in detail in Materials and Methods, the following scoring system was adopted: 0, absent staining; 1, faint but detectable positivity; 2, weak but extensive positivity; 3, strong positivity (Figure 6.1). For the statistical analysis, tumours with the score 0 and 1 were grouped as low (L)

and tumours scored 2 and 3 as high (H). FGFR3 protein was not detected by IHC in the normal urothelial samples.

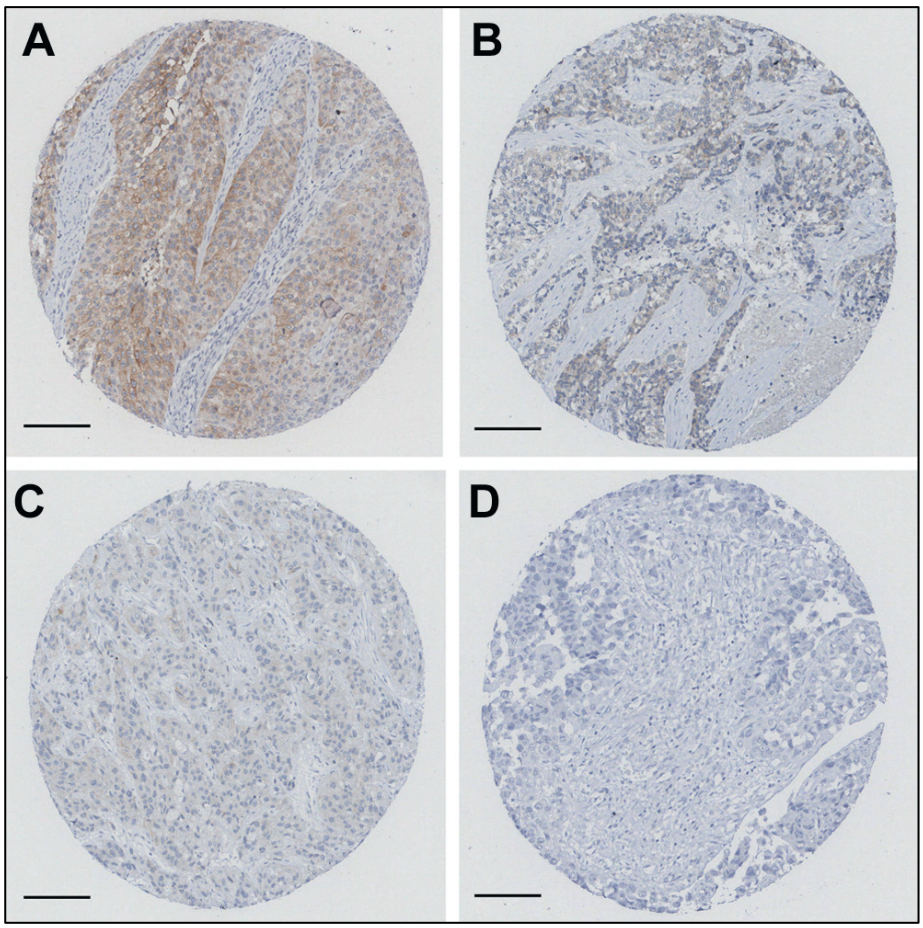

Figure 6.1: Immunohistochemistry detection of FGFR3. A – strong FGFR3 expression (score 3, High), B – weak but extensive positivity (score 2, High), C – faint but detectable positivity (score 1, Low), D – absent staining (score 0, Low). Scale bar indicates 100μm

In 123 primary tumours (centre core), FGFR3 status was determined by IHC: 55 tumours (44.7%) with a score H, 68 tumours (55.3%) with a score L. For the primary tumours with invasion front core, a total of 110 primary samples were available for analysis: 34 tumours (30.9%) with a score H, 76 tumours

(69.1%) with a score L. There were 97 tumours where both primary tumour cores from the same patient were available for analysis. Seventy-three (74.5%) of them were concordant (OR=8.6, p=0.000003, Fisher's exact test) (Table 6.1).

	Number of cores
Primary tumour invasion centre/front:	
Low/low	48
Low/high	9
High/low	15
High/high	25
p Value	0.000003
Metastases core 2/1:	
Low/low	42
Low/high	5
High/low	14
High/high	29
p Value	0.0000002

Table 6.1. FGFR3 expression concordance in samples from the same primary tumours and metastases

Corresponding numbers from the 102 patients with evaluable metastases were 48 (47.1%) score H, 54 (52.9%) score L for the first biopsy, and 104 patients for the second biopsy with 41 (39.4%) score H, and 63 (60.6%) score L. There were 90 patients with both metastases biopsies available. Seventy-one (78.9%) of them were concordant (OR=16.7, p=0.0000002, Fisher's exact test). Table 6.1.

Overall, the levels of FGFR3 protein expression did not differ between primary and metastatic lesions (p=0.78, Mann-Whitney test) (Table 6.2). FGFR3 protein expression was assessable in 106 matched primary tumours and their matched nodal metastases. In the primary tumour, 53 out of 106 patients showed protein overexpression defined as high and 53 out of 106

defined as low. In the metastasis the corresponding numbers were 56 and 50, respectively.

For 79 patients, the concordance between FGFR3 expression levels in primary tumours and matched metastasis was high (OR=8.45, p=0.000007, Fisher's exact test). In 15 patients the primary tumour had low protein expression and the matched nodal metastasis had high expression. The converse was observed for 12 patients (Table 6.2).

	Number of cores
Primary tumour / metastases:	
Low/low	38
Low/high	15
High/low	12
High/high	41
p Value	0.000007

Table 6.2. Comparison of primary tumours and corresponding lymph node metastases. High concordance was found between FGFR3 expression levels in primary tumours and matched lymph node metastases.

6.2 FGFR3 relationship to metastatic phenotype, survival and adjuvant chemotherapy

Patients with FGFR3 overexpressed in their metastases had more metastases (median: 0.21 vs 0.13; p = 0.31, Mann-Whitney test) (Figure 6.2), smaller total diameter of metastases (median: 0.79 cm vs 1.04 cm; p = 0.065) (Figure 6.3), and lower maximum diameter of metastases (median: 5.09 cm vs 5.59 cm; p = 0.065) than patients without such overexpression; however, these differences were not significant. Tumour stage and extracapsular extension of lymph node metastases were not associated with FGFR3 status. In univariate analyses, OS did not differ significantly for patients with FGFR3 overexpression in the primary tumours compared with those patients without overexpression (Figure 6.4). This was also the case

for patients with FGFR3 overexpression in metastases (p = 0.241) (Figure 6.5). FGFR3 IHC did not correlate with RFS (Figure 6.6).

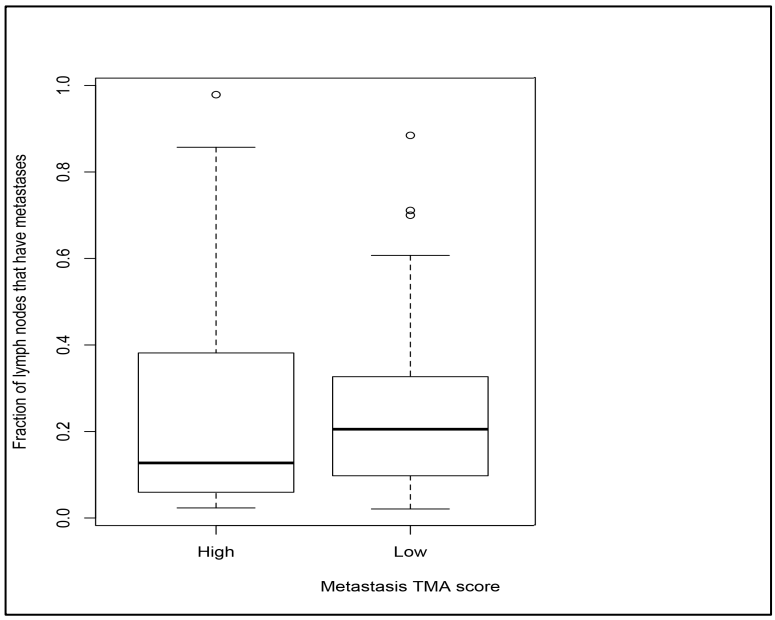

Figure 6.2: Patients with FGFR3 overexpressed in their metastases had more metastases (median: 0.21 vs 0.13; p = 0.31). *Y*- axis: fraction of lymph nodes with metastasis; *X* – axis: metastatic FGFR3 expression (low or high).

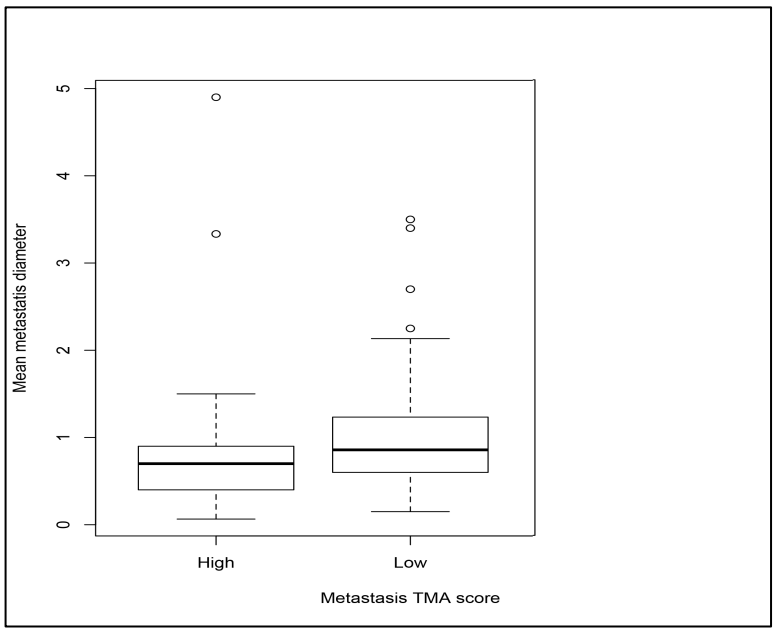

Figure 6.3: Patients with FGFR3 overexpressed in their metastases had smaller total diameter of metastases (median: 0.79 cm vs 1.04 cm; p = 0.065). Y- axis: mean metastasis diameter in cm; X – axis: metastatic FGFR3 expression (low or high).

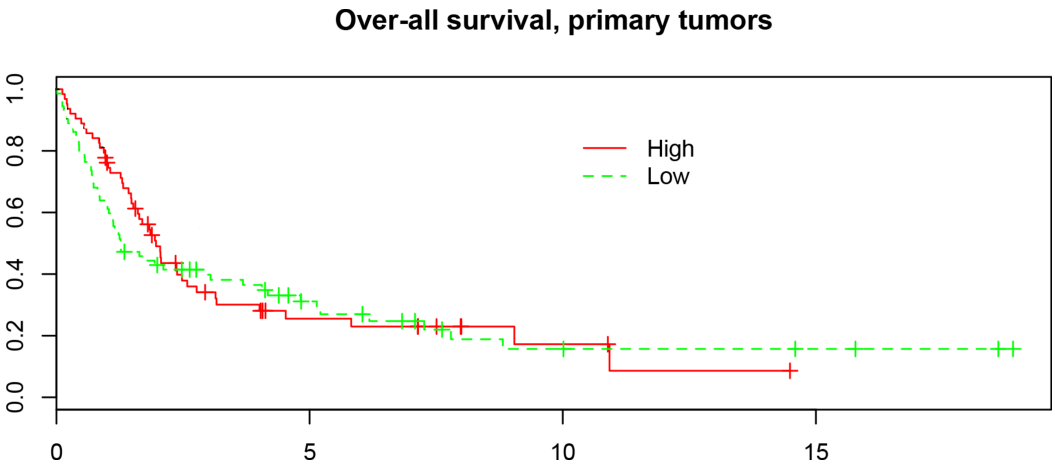

Figure 6.4: Immunohistochemically determined FGFR3 status in primary tumours does not segregate significantly into low- and high-risk patients regarding over-all survival, p=0.70

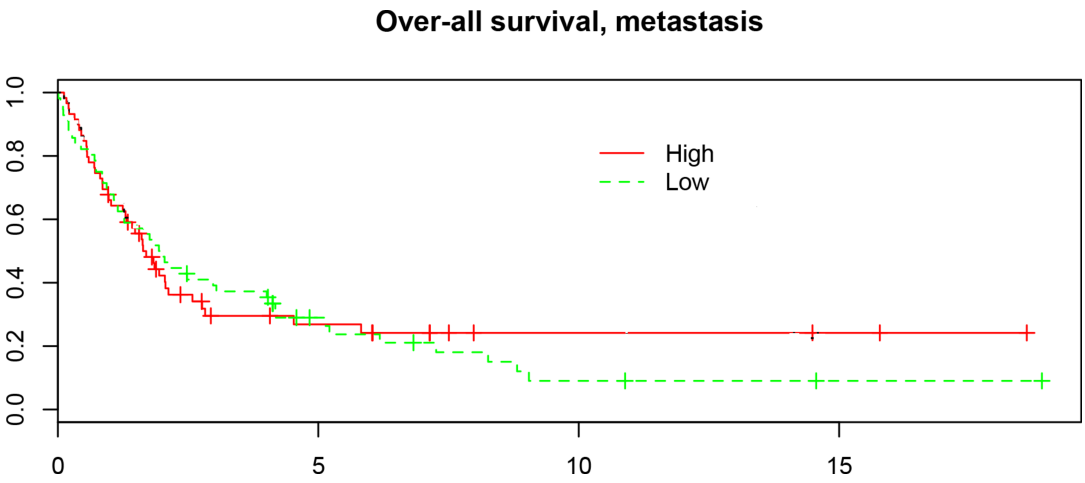

Figure 6.5: Immunohistochemically determined FGFR3 status in metastasis does not segregate significantly into low- and high-risk patients regarding over-all survival, p=0.94

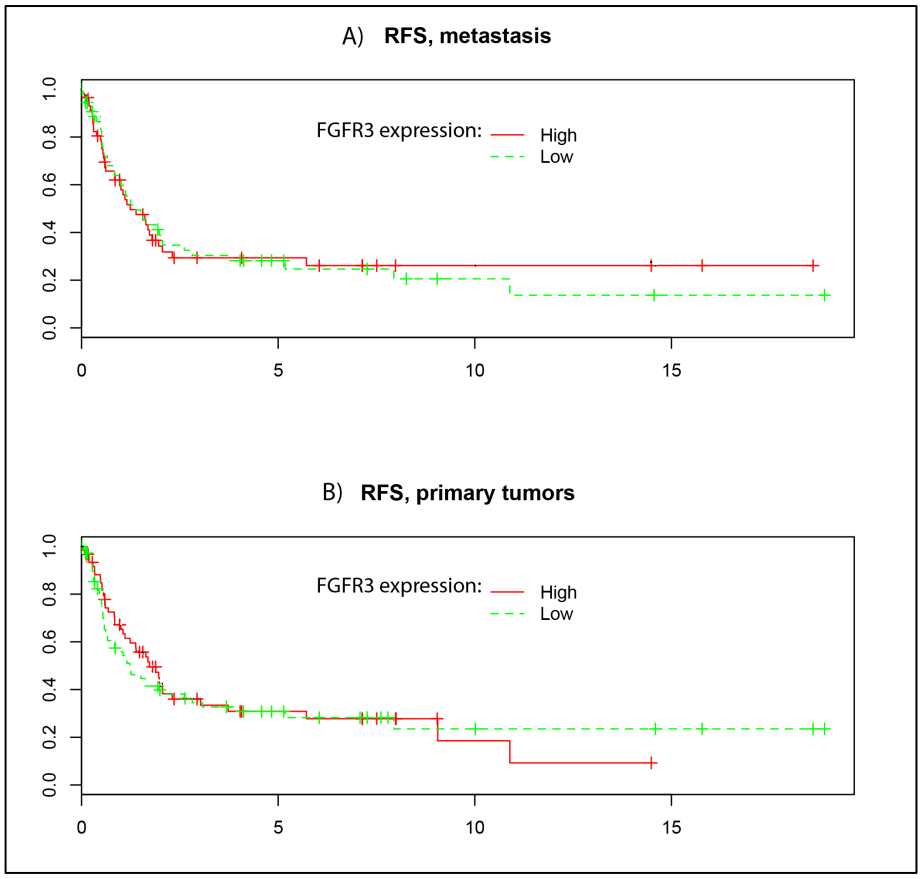

Figure 6.6: Immunohistochemically determined FGFR3 status in metastasis A) and primary tumours B) does not segregate significantly into low- and high-risk patients regarding RFS.

In multivariate analyses, advanced primary tumour stage (pT3/4 vs pT1/2; p = 0.019) and extracapsular extension of lymph node metastases (p = 0.001) were the only independent adverse risk factors for OS. FGFR3 overexpresion in primary tumours (p = 0.66) and metastases (p = 0.88) failed to add independent prognostic information.

In this series 63 patients received adjuvant chemotherapy, which was cisplatin based in 37. We examined the relationship of FGFR3 expression in primary and metastatic tissue, and chemotherapy (none, any and cisplatin based) to OS and RFS. No significant relationship was found.

Chapter 7
Discussion

Multifocal tumours study

Bladder cancer represents a heterogeneous disease and commonly is described by multifocality and high number of recurrences. Detailed molecular characterization and comparison of genetic alterations in clinically and morphologically distinct multifocal tumour cell populations may provide information about the clonal evolution of carcinoma of the urinary bladder. Furthermore, enhanced knowledge of the molecular genetic characteristics of multifocal bladder tumours may offer a combined molecular and histo-pathological approach to classification and thus improve clinical management and the decision-making process of this common cancer.

In most of the published studies on multifocal bladder cancer, conventional CGH, LOH analysis, FISH and mutation scanning of *TP53* and *FGFR3* have been applied to the study of small sets of tumours [184, 242-247]. There have been few studies that have applied array-based CGH (aCGH) to the study of multifocal bladder cancer and the numbers of tumours analysed in these studies have also been low [249-251]. The main advantages of aCGH over conventional CGH are its high resolution and throughput. In this study we have mutation scanned key genes (*FGFR3*, *PIK3CA* and RAS) and used aCGH to screen for genome-wide copy number changes in 66 bladder tumours from 22 patients with superficial disease. To our knowledge, this study is the first to use aCGH to analyse such a large panel of superficial multifocal bladder tumours. We have used the combined copy number and mutation data to assess whether multifocal tumours from the same patient are monoclonal or oligoclonal in origin, to assess the molecular heterogeneity of tumours within and between patients, and to identify

specific features related to multifocality i.e. is multifocal disease different to solitary disease matched for stage and grade.

Sample collection and processing was crucial to the success of this project. We were able to successfully collect such a large panel of multifocal tumours due to several factors. Tissue collection was carried out at the tertiary referring centre that already has a well-established tissue collection program and experienced staff. At St James's University Hospital procedures such as TURBT and cystectomies were performed on a daily basis, offering multiple opportunities for patients recruitment. Every Friday theatre lists were accessed and studied for potential tissue donors. Information on prior cystoscopic examination findings enabled selection of patients with multifocal tumours suitable for inclusion in the study. All staff (clinicians, nurses, theatre staff) involved in the tissue collection process were well informed about the on-going study. Two formal departmental meetings were organized where the study proposals were presented. On the day of operation, the operating surgeon and theatre staff were also informed about participants. At that time tissue collection nuances were re-emphasized. We think that this informal way of direct communication between a researcher and clinician might have had a significant impact on the number of samples collected. It also provided a rare opportunity for clinical staff to receive continuous updates on the results of the study. The SSO and myself were the only people involved in the tissue collection process during the three years of the project. This 'simplicity' allowed the process to run more efficiently and avoided 'mistakes' due to miscommunication.

This study identified numerous copy number alterations many of which involve regions previously implicated in conventional CGH and LOH studies of bladder cancer [252-254]. Copy number gains and losses involving whole chromosomes, chromosome arms or smaller regions were identified in our study. The most common region gained was 20q (68.2%), and the most common region lost was 9q (81.8%). Other common deletions were observed on 9p (77.3%), 10q (63.6%), 5q (54.5%), 8p (50%) and 2q (50%).

Loss of the whole of chromosome 9 or 9p/9q is the most frequently described genetic alteration in TCC of the bladder. Several tumour suppressor genes have been previously identified on both arms of chromosome 9 with regions involving 9p21 (CDKN2A) [1], 9q12–q31 (PTCH) [2], 9q32–q33 (DBC1) [3] and 9q34 (TSC1) [4]. Another commonly identified loss was observed on the long arm of chromosome 5 (54.5%). Loss on 5q was a common event in grade 3 tumours (72.7%). Previously published studies involving conventional CGH of bladder tumours have also found frequent deletion of 5q [243-246, 255-258]. Some studies have reported that loss of 5q is often associated with concomitant gain of 5p [246, 259]. We have detected gains of 5p in 12 patients (54.5%), with associated losses of 5q being observed in seven of these.

Fifty percent of our tumours had deletions of the short arm of chromosome 8 and gains of the long arm were detected in 63.6% of patients. The gains of long arm of chromosome 8 were associated with stage Ta tumours (57.1%) and grade 3 tumours (63.6%). When tumours were assessed by stage and grade together it was found that gains of 8q were detected in 63.4% of patients with TaG2 disease and gains of 8q in 75% of patients with T1G3 tumours. More than 60% of patients with TaG3 and 62.5% with T1G3 tumours exhibit losses of 8p. In the literature, it was reported that the loss of 8p occurs in 25–30% of urothelial carcinomas and is primarily associated with high-grade and stage tumours [260]. Our chromosome 8 alterations findings might indicate that multifocal tumours exhibit chromosome 8 copy number alterations characteristic of muscle invasive tumours rather than superficial tumours.

High-level amplifications involving regions of chromosome 20 and gains of 20q have been widely reported in various cancers including ovarian, colon, breast and bladder [247, 255, 261]. Gain of 20q was the most frequent gain observed in our patients (68.2%). Bruch and colleagues reported an association of gains of 5p and 20q in carcinomas stage ≥pT2 [262]. In the

present study this association has been observed in 7 patients (patient 5, 6, 10, 13, 14, 16 and 20) the majority of which had grade 3 tumours.

Sixty-nine high-level amplifications were detected in 66 tumours. The most frequently amplified regions were 11q13.2 - q13.4 and 6p22.3 - p22.2 present in ten and eight tumours from 4 and 3 patients, respectively. Amplification at 11q13.3 has been previously reported in bladder cancer and candidate genes within this amplicon include cyclin D1 [184, 243, 245, 259]. Studies applying conventional CGH, detected in bladder tumours and in the cell lines amplification at 6p22 [247, 251, 262-265]. Candidate genes within this amplicon were OX4, E2F3, PRL and CDKAL1 as reported by Hurst and colleagues [5]. The CDKAL1 showed amplicon-related expression in tumour cell lines indicating its putative oncogenic role [5].

In multifocal tumours the most frequent recurrent regions of HD included chromosome 3 (p21.2 - p21.1), 7 (p21.1), 10 (q24.32) and chromosome 12 (q21.31). When we have analysed the frequencies of the recurrent regions of HD and recurrent amplicons in our study and in the study of Hurst et al (2012) we found no striking similarities. In the study of Hurst et al (2012) the most frequent recurrent regions of HD were detected on chromosome 1 (1p34.1), 2 (2q36.1-q36.3), chromosome 9 (9p21.3), chromosome 11 (11p11.2), chromosome 18 (18p11.22-p11.21) and chromosome 19 (19q12). The region 9p21.3 on chromosome 9 containing *MTAP, CDKN2A, CDKN2B, ANRIL* was homozygously deleted in 16 (50.9%) tumours in the study of Hurst et al (2012) and only in 1 (4.5%) tumour (10_2) in the multifocal data set.

When chromosomal alterations were assessed according to stage and grade we observed that the distribution of these alterations did not significantly differ between stages or grades, but the frequencies of events increased with stage and grade. Ta and T1 tumours showed alterations on 18% and 30% of chromosome arms respectively. Grade 2 tumours showed a lower

average frequency (10%) than grade 3 tumours (27%). These findings are in accordance with other studies. Low-grade and stage tumours have been reported to show fewer molecular alterations and these generally include deletions on chromosome 9, 11p, 10q and gains of chromosome 17, 1q, 20q 11q [252, 266]. In our study gains on chromosome 17, 1q, 20q, 11q and losses on chromosome 9 and 11p were more frequent in TaG3 patients. Increased chromosomal instability may be partially explained in relation to stage and grade. As higher stage and grade tumours represent more ‘aggressive’ disease one might expect higher level of chromosomal instability in these tumours. However, our study has shown that chromosomal instability of multifocal tumours cannot completely be explained by the higher stage and grade of the disease. When we performed hierarchical clustering of copy number data from all 66 tumours, four tumours, matched for the same stage and grade separated into three different clusters. For example, two tumours from patient 5 (both stage TaG2) were in Clusters 1 and 3. In cluster 3 tumours were mostly of higher stage and/or grade (T1G3s mainly). One tumour from patient 5 belonged to FGA group A and the other to group D.

The knowledge of significant intra-patient heterogeneity could have important prognostic and therapeutic implications. At present, we apply a limited number of factors from histology results (stage and grade, tumour size, number of tumours and presence of CIS) into risk stratification tables (e.g. EORTC tables) to quantify individual risk for progression and recurrence. Based on the example for patient 5 from our study, this patient would be classified as an intermediate-risk patient in conventional risk classification. However our results have shown that based on aCGH data, one tumour from this patient grouped with highly chromosomally unstable tumours in Cluster 3. Therefore from a therapeutic point of view, this patient might benefit more from being classified as a high-risk patient for disease progression and/or recurrence. If we applied this knowledge into clinical practice we could offer this patient closer surveillance or immediate radical treatment. It would also be very interesting to further follow up this patient and determine subsequent disease associated events such as recurrence, progression and mortality.

Another interesting observation made from the clustering of merged copy number data was that Cluster 1 contained mainly more chromosomally stable tumours and that a high proportion of these were from patients with recurrent disease. The fact that recurrent tumours were more chromosomally stable may support the hypothesis that the chronology of tumour presentation is not reflected in the genetic evolution of the tumours. In studies by van Tilborg *et al* and Lindgren *et al* authors compared the chronology of tumour appearance with the chronology of genetic events in patients with multiple recurrences and observed that the genetic progression trees better reflected the tumour evolution than their chronologic order of presentation [214, 251].

A comparison of the merged copy number dataset for the multifocal patients with a subset of solitary tumours from the dataset of Hurst et al 2012 revealed interesting findings that further characterize superficial multifocal bladder cancer and also give new insight into the significant complexity of this disease. The hierarchical cluster analysis revealed that TaG2 multifocal tumours tended to cluster with solitary tumours of higher stage and grade. T1G3 multifocal tumours clustered with different subsets of T1G3 solitary tumours and interestingly formed the majority in a highly chromosomally unstable subset of tumours. Cluster 4, which exhibited the highest level of chromosomal instability with all tumours being FGA group D, contained mostly multifocal tumours (seven out of ten tumours). Next we made comparisons between multifocal and solitary superficial tumours matched for stage or grade. Overall, multifocal stage Ta and T1 tumours were more chromosomally unstable than stage Ta and T1 solitary tumours. Several regions including gains of 8q24.13 (ANXA13, FBXO32, KLHL38), 13q12.11 - q12.3 and 20q11.23 - q12, and losses of 8p21.2 - p12 (including NRG1), 9p21.3 (CDKN2A, CDKN2B) and 9q12 - q34.3 (including PTCH, DBC1 and TSC1) were more common in multifocal stage Ta patients. Stage T1 tumours from multifocal patients had a higher prevalence of gains on 1p12 - q24.3 (TAGLN2), 2p25.3 - q11.1, 6p22.3 - p22.1 (E2F3, CDKAL1, SOX4,

PRL), 7p11.2 - q36.3, 16p12.1 - q11.2, 19q13.11 - q13.2, 20p13 - q13.33 and losses on 2q33.3 - q37.3 (SGC2, AP1S3, WDFY1, MRPL44, SERPINE2, FAM124B, CUL3, DOCK10, KIAA1486), 5q11.2 - q12.3, 6q27, 8p23.2 - p12, chromosome 10 (q22.3 and q23.1 - q26.3), 3q14.2 - q14.3, 14q23.1 and 22q11.1 - q13.33. Our study showed that these regions are strongly associated with tumour 'multifocality'. Therefore we could hypothesise that mutifocality is characterized by unique features at the genomic level which 'drive' the tumours development into more aggressive disease. By studying further these unique regions and the genes they contain targeted therapies for multifocal bladder cancer could be developed.

As multifocal tumours constituted the majority of the highly chromosomally unstable tumours present in Cluster 4, we also included ≥ T2 tumours in the cluster analysis to see whether the multifocal tumours in this cluster exhibited characteristics of muscle invasive disease. As previously observed, the same multifocal tumours separated into cluster 4 along with T1G3 (n=8) and ≥ T2 (n=7) solitary tumours. Analysis of this cluster revealed copy number events characteristic of ≥ T2 tumours. Copy number gains and losses were frequent across most chromosomes in tumours from this cluster with the most frequent losses involving 2p, 2q, 5q, 6q, 8p, 9p, 9q, 10q, 13p, 15q, 16q, 17p, and the most frequent gains involving 1p, 1q, 2p, 3p, 3q, 5p, 7p, 7q, 8q, 17q, 19q, 20p and 20q. One of the interesting features of Cluster 4 was a high frequency of chromosome 7 gains. One of the oncogenes located on chromosome 7 is EGFR. Mutations leading to EGFR upregulation have been associated with a number of cancers (lung, colon cancer). Currently, various therapeutic approaches are aimed at EGFR including afatinib, erlotinib, gefitinib, icotinib in lung cancer and cetuximab in gastro-intestinal cancer. In our study, it would be of high interest to study EGFR expression levels to examine if this correlates with copy number increase as this potentially could be considered as a targeted therapy option for these patients.

One of the most interesting findings of the comparison of the multifocal tumour dataset with that of the solitary dataset involved patients with TaG1/G2 tumours. Multifocal tumours revealed a higher frequency of gains on chromosome 6 (q26), chromosome 9 (p24.3) and losses of regions on chromosomes 8 (p23.3 - p11.21), chromosome 9 (p21.3, q12 - q34.12 and q34.3), chromosome 10 (q24.32), chromosome 13 (q13.3 - q14.2), chromosome 16 (p13.3, q23.3 - q24.1 and q24.3) and chromosome 17 (q12 - q21.2). Theoretically, these tumours despite being classified as low grade and stage might need a different clinical follow up regime and might represent disease with a high risk of progression due to the presence of these chromosomal aberrations.

We next investigated the diversity of copy number alterations in multifocal and solitary disease and compared these to *FGFR3* mutation status. *FGFR3* mutation was still associated with low stage and grade tumours. When the relationship of *FGFR3* mutation status to copy number events in stage and grade matched multifocal and solitary tumours was examined, several regions of gain and loss were more common in multifocal tumours. *FGFR3* mutant, multifocal tumours commonly exhibited losses on chromosome 5, 10, 16 and gains on chromosome 1, 6, 8 and 19 whereas their solitary counterparts have shown no such events. In a comparison of copy number events in *FGFR3* mutant TaG1/G2 multifocal and solitary tumours deletions on chromosome 5 (q34 - q35.3), chromosome 9 (p21.3 and q21.33), chromosome 10 (q24.2 - q25.1) and chromosome 16 (p13.3), and gains on chromosome 1 (p12 - q31.3), chromosome 6 (q26), chromosome 8 (q13.2 - q13.3), chromosome 13 (q12.11 - q12.3 and q21.32 - q21.33), chromosome 19 (q12 - q13.43) and chromosome 20 (q11.23 - q13.33) were more frequent in mutant *FGFR3*, TaG2, multifocal tumours.

Most patients presenting with bladder cancer have more than one tumour during the course of their treatment. Determination of whether tumours are monoclonal or oligoclonal is of paramount importance due to therapeutic implications. If tumours are monoclonal in origin, with all tumours (multifocal

and recurrent) arising from a single progenitor cell, then application of adjuvant treatment post TURBT is more likely to benefit the patient. This treatment, in the form of intravesical, topical chemotherapy will potentially eradicate all micrometastatic deposits following primary resection. However, if bladder tumours arise as a consequence of a ‘field effect’ post global exposure to carcinogens present in the urine then tumours are genetically unrelated and chemotherapeutic bladder installations could potentially increase mutagenic pressures and cause healthy urothelium to develop further tumours. Understanding the mechanisms behind tumour multifocality and the origin of bladder cancer is important also from a personalized-medicine and targeted therapies point of view. If we could identify common genetic or epigenetic changes in synchronous or metachronous development of multifocal tumours then we could ‘’target’ these alterations and establish new strategies in bladder cancer treatment and prevention.

In the literature there has been much debate about bladder tumour clonality with the majority of these studies favouring the hypothesis of the monoclonal origin of multifocal bladder tumours [203, 205, 207, 214, 218, 267, 268]. One objective of the current study was to use our copy number and mutation status data to determine the relationships between tumours from the same patient and to assess tumour clonality. Visualisation of whole genome profiles revealed that some patients had tumours that shared all or the majority of copy number events (patients 2, 3, 4, 7, 11, 13, 14, 17, 20, 21), whilst others had tumours that shared some common copy number events but were otherwise highly divergent (patients 6, 10, 12, 15, 18, 19, 22) thus suggesting a monoclonal origin for tumours in these patients. However, we also identified a group of patients where the evidence for monoclonality of at least one tumour could not be determined (patient 1, 5, 8, 9, 13, 16).

We performed one-way unsupervised hierarchical cluster analysis of copy number data from all 66 tumours in order to further assess the relationships between the individual multifocal tumours of each patient. In the majority of cases tumours from the same patient tended to group together. In 3 patients

(5, 8, 13) evidence of possible non-clonality was obtained from the observation that not all tumours clustered together. In patient 5, two tumours had no shared copy number events and grouped in two separate Clusters (1 and 3). In patient 13 tumour 4 did not share any copy number events with the other 3 synchronous tumours and separated into Cluster 1. Tumour 2 from patient 8 separated into Cluster 2 while other tumours grouped in Cluster 1.

The relationships between tumours from the same patient were also assessed using phylogenetic analysis. When we reconstructed the probable sequence of events that gave rise to each tumour based upon similarities and differences in breakpoint regions and copy number events a phylogenetic tree was produced for each patient. This phylogenetic tree analysis shows all tumours as descendants of common hypothetical ancestors.

Common initiating events revealed by phylogenetic tree analysis were deletions of chromosome 9 and mutations of *FGFR3*. Most of the evidence currently recorded shows that chromosome 9 genes might participate early in tumorigenesis [121-123]. In this study, abnormalities involving partial or complete loss of 9q and/or 9p (including small regions of homozygous deletion) were detected in majority of tumours and were among the most frequent copy number changes detected. Interestingly, it has been shown that the reduplication of a single parental homologue of chromosome 9 appears to be common in more aggressive tumours [5]. Chromosome 9 deletions have been widely studied in bladder cancer because they are present during the earliest stages of urothelial tumorigenesis [269]. Loss of heterozygosity studies performed by Spruck *et al* showed that deletions of 9q are more prevalent in the low grade non muscle invasive papillary tumours than in CIS and muscle invasive tumours [94]. Other studies also confirmed association of low stage and grade tumours with chromosome 9 deletions [270, 271]. Interestingly, these alterations were also observed in the normal-appearing urothelium that is adjacent to the tumour lesion [217].

In 16 patients (2, 3, 4, 6, 7, 10, 11, 12, 14, 15, 17, 18, 19, 20, 21, 22) we were able to confirm a monoclonal origin for all tumours. The majority of these patients had tumours that were descendants of a 'common precursor'. Tumours also underwent substantive clonal evolution, often diverging significantly from the other synchronous tumours. This could be illustrated in patient 19 where all tumours from the patient shared a common precursor based on copy number losses on 4q and 9p. Tumour 3 appears to have acquired unique characteristics and diverged away from the remaining tumours and also lacked an *FGFR3* Y375C mutation detected in the other two tumours.

In patients 1, 5, 8, 9, 13, 16 we could not determine a clonal origin for all tumours based on phylogenetic analysis of the available copy number and mutation data. For two tumours (8_1) and (8_2) from patient 8 we have confirmed a monoclonal origin based on shared common copy number gain on 22q, and shared *FGFR3* (S249C) and *PIK3CA* (H1047R) mutations. Tumour 3 from this patient exhibited no copy number alterations and therefore the relatedness of this tumour to the other two tumours could not be assessed based on copy number. This tumour did, however, carry both mutations seen in tumours 1 and 2 making it more likely that all 3 tumours are related and tumour 8_3 represents the precursor for the other 2 tumours. In patient 1, two out of three tumours exhibited no copy number alterations. Potentially, these tumours were resected at the 'early' time of tumorigenesis and have not yet acquired any chromosomal changes. When we have analysed the mutation status of these tumours, two carried the same *PIK3CA* E545K mutation, which could imply common origin. Mutation status data for a limited number of genes should be interpreted with caution when analysing clonality. Tumours sharing the same mutations are not necessary related as they could acquire common mutations independently. Some of the mutations detected in the current study occur frequently in bladder cancer (e.g. *FGFR3* S249C). In patient 5, none of the tumours shared copy number events but all carried *FGFR3* S249C mutations. This could be taken as

evidence for a monoclonal origin of tumours in this patient but should be viewed with caution. None of the tumours in patient 9 carried copy number alterations or mutations hence the clonal origin of these tumours could not be determined. In patient 13 tumour 4, seemed to be unrelated to the other tumours based on copy number data and exhibited characteristic losses on 10q and 19p. Mutational data could not shed further light on the relatedness of tumour 4 to the tumours, as all were wildtype for *FGFR3*, *PIK3CA* and the 3 RAS genes. In patient 16 we have observed the situation where all tumours where 'related' when mutational data was analysed (all shared *HRAS* G12C mutation) but the same tumours were 'unrelated' when copy number data was analysed (three tumours did not share copy number events and one tumour carried no copy number events). As *HRAS* mutations are relatively infrequent (~12%, unlike FGFR3), this provides a better suggestion that they are related than *FGFR3* or PIK3Ca mutations do. Whole exome sequencing could possibly be applied on these tumours to further assess the clonality in these particular cases. This approach could potentially provide additional variants that could be used to assess clonal relatedness.

In the majority of tumours, the hypothesis of a monoclonal origin was supported by the sharing of chromosome aberrations. Interestingly, in all but one case, there was no 'pure' linear evolution observed, where one tumour could be indicated as the direct descendant of another tumour. Each tumour exhibited a sub-set of specific alterations, which occurred after the divergence of the tumours. However, in patient 4 tumour 4 appeared to be the common precursor. Evidence of significant sub-clonal divergence within patients with monoclonal disease may prove that development of targeted therapies for these patients might be difficult.

Matched primary and metastatic bladder cancer samples

FGFR3 plays an important role in bladder tumour pathogenesis. Recently there has been increased interest in analysing the association between mutation status of *FGFR3* and bladder TCC. It has been revealed that these mutations are significantly more frequent in low stage and grade tumours. However, our understanding of the role of FGFR3 remains incomplete. There have been several studies assessing FGFR3 expression but most of these examined only primary tumours of various stages and grades. The aim of this study was to examine the relationship of FGFR3 expression between primary and matched metastasis from the same patient. One of the earlier studies performed by Matsumoto *et al.* reported at least moderate expression in nearly half of the primary tumours [272]. Later, two independent investigators reported correlation between protein expression levels and lower tumour stage and grade [273, 274].

It has been proposed that FGFR3 could be a valuable therapeutic target in bladder cancer. However, in order to evaluate FGFR3 usefulness in targeted therapy its expression status needs to be studied in relation to metastasis. As a potential therapy would act at the protein level, this study aimed to investigate FGFR3 protein status by performing IHC. The most important finding of this research is the good correlation between FGFR3 expression in primary tumour and its corresponding metastasis. While FGFR3 was highly expressed in 44.7% of the primary tumours, this was present in matched metastases of 47.1% patients. By analysing expression status of the primary tumour it was relatively easy to predict the status of the corresponding metastasis. Overall 74.5% of patients had high levels of concordance between primary tumours and matched metastasis. Thirty-six percentage of patients who had low FGFR3 expression in primary had corresponding low expression in matched metastasis and similarly the figure was 38.7% for high level of expression. This might indicate high similarity for expression of the protein after occurrence in the primary. Also, one might hypothesise that the clone of cells with metastatic potential dominates the primary tumour and

later spreads to distant lymph nodes. Therefore, tumour cells of the primary and metastasis are genetically identical or closely related. This might have useful clinical applicability in targeted therapies. The findings of discordant cases may also have clinical applicability. This study showed that 14% of samples expressed FGFR3 in the metastasis but not in the primary tumour. In this scenario the relevant treatment might be withheld in a clinical trial setting. Conversely, patients who reveal expression in the primary tumour but not in the metastasis might be over-treated.

When planning targeted therapies it is important to have consistent expression results in the sampled tissue with little variability depending on tumour site. In this study two biopsies were obtained from the metastatic site and two from the primary. Seventy-five percent of patients showed concordance at both primary sites with 50% of patients showing low expression levels and 25% showing high levels at both sites. Corresponding numbers between metastatic samples were 46.7% for low expression and 32.2% for high expression and overall 79% concordance. These high concordance rates between sites of sampled tissue are quite reassuring. It might indicate that the specific site of biopsy is less relevant when planning treatment options.

In breast cancer, the HER2 status works as a predictor for treatment response [275]. However, the choice of assay for HER2 determination remains a subject of dispute [275-277]. Some authors consider IHC as a method of choice others consider cytogenetic studies (FISH etc.) more appropriate. The arguments for using IHC are multiple: the targeted therapy works at the protein level, protein expression might not be just the result of gene amplification [276] and there is high concordance between IHC and cytogenetic testing [276]. In our study we have observed high concordance rates between matched primary tumour and metastasis despite the fact that samples were paraffin-embedded and thus subject to tissue processing artefacts.

One of the limitations of IHC is its variability in reporting. It often reflects differences in antibodies and kits used, protocols and methods of interpretation. In this study the scoring criteria have been simplified by grouping samples into only two groups (low and high). If applied in clinical practice this might potentially enhance the interpretation of results for response to therapy. However, the group of patients with only few cells stained, who were labelled as ‘low’, would need to be further examined. It is not known if such a small percentage of protein expression could indicate positive response to the therapy. Also it is recognised that assessment of a therapeutic target has different requirements than assessment of a prognostic indicator. Therefore the scoring used in this study based on the worst feature or presence of minor cell population in a tumour may be inappropriate for application in clinical practice and new scoring criteria may be required.

Another interesting analysis would be to determine *FGFR3* mutation status. As it has been previously shown on primary tumour samples, high FGFR3 expression, and its relationship to the mutation status, was significantly more frequent in non-invasive (pTa) compared to invasive (pT2) tumours and more frequent in low grade compared with high grade tumours [62]. Additional characteristics of mutation status may contribute to a predictive value for progression and overall survival. A recently published study examining FGFR3 expression levels and mutation status in primary and metastatic urethral carcinoma found high levels of FGFR3 expression in both primary tumours and metastasis (29% and 49%, respectively) with low *FGFR3* mutation rate (2% in primary tumours and 9% in metastases) [278]. Similarly to our study, FGFR3 immunohistochemistry staining did not impact overall survival ($p = 0.89$, primary tumours; $p = 0.78$, metastases).

The role of FGFR3 inhibitors in advanced bladder cancer has not yet been fully characterized and awaits results of ongoing clinical trials. Interestingly, in this study the survival of the immunohistochemically FGFR3-positive and -negative subgroups was not significantly different (Figures 6.4 and 6.5). This

finding was in contrast to the results of a recently published study on the relationship of *FGFR3* mutation and expression status to outcome in muscle-invasive bladder cancer treated by cystectomy with or without adjuvant cisplatin-gemcitabine chemotherapy [279]. In this paper researchers reported FGFR3 over-expression to be an independent predictor of reduced OS and RFS.

An interesting finding of this study is the relationship between FGFR3 expression and metastatic deposit characteristics. Metastases, which were scored low were associated with a higher number of metastasis (lower ratio of lymph node positive to total lymph nodes dissected). Also, the diameter of metastasis correlated with the level of FGFR3 expression, with metastatic deposits of larger diameter scoring low on IHC staining. However, both findings were not statistically significant.

This study has some limitations. Despite including large number of matched samples it might be still underpowered to show statistical significance between different parameters (tumour characteristics etc.). Hence, these features merit investigation in a larger sample series.

Suggestions for future work

This work has produced the data that has further added to the evidence of the vast complexity of molecular events associated with evolution of multifocal and metastatic urothelial cancer. There are many opportunities to further work on this subject. Future work should include:

- LOH analysis could be performed to further assess clonal relatedness. Patterns of LOH were used as genetic fingerprints in a study by Takahashi *et al* [209] where he confirmed the clonal origin of multifocal bladder cancer. The ploidy profiling technique developed by

Navin *et al* [280] could also be used to assess relatedness based the ploidy of different multifocal tumours from the same patient. X chromosome inactivation analysis of the multifocal tumours used in this study could also be used to see if tumours carry the same inactivation patterns. By applying this technique, Sidransky *et al* [203] confirmed a monoclonal origin for bladder tumours from four patients. However one of the disadvantages of this method is that it can only be performed on female patients thus we would only be able to use this approach for samples from six of the patients used in the current study.

- State-of-the-art next generation sequencing (NGS) approaches such as whole exome sequencing could also be used to further analyse tumours used in this study. Whole exome-sequencing could be performed using DNA samples from the multifocal bladder tumours in which a monoclonal origin of all tumours could not definitively be defined. This approach provides sequence information for all exons in the genome and is likely to provide a wealth of variants that could be used to assess clonal relatedness.

  Sample validation by NGS. NGS platforms are able to perform parallel sequencing, during which millions of fragments of DNA from a single sample are sequenced in unison. This technology facilitates high-throughput sequencing, which allows an entire genome to be sequenced in less than one day. Recently several NGS platforms have been developed that provide high-throughput sequencing at low cost. It has been also confirmed that this technique can be used to interrogate DNA from fresh frozen material, cell lines, and FFPE samples, providing highly reproducible results [281].

- Continued collection of mutifocal bladder cancer samples. Despite the fact that we have collected one of the largest multifocal bladder tumours panels that have been reported, it is still a relatively small number of tumours to enable detection of small differences in copy number data.

- Analysis of copy number changes of the tumours and comparison to those in the urothelium adjacent to the tumour or ‘normal’ urothelium, distant from the tumour. This could further shed the light on clonal relationship or ‘field effect’ changes. In the study performed by Steidl et al. authors revealed the occurrence of similar patterns of chromosomal aberrations in the tumours and their associated urothelium by FISH analysis [216].

In conclusion, our study suggests that based on mutation and copy number data the majority of multifocal tumours are monoclonal in origin but there is significant intra-patient sub-clonal divergence, and also inter-patient diversity in the extent of chromosomal instability exists in multifocal disease. Multifocal tumours are more chromosomally unstable than stage and grade matched solitary tumours. These findings may have implications with respect to the differential response to treatment of multifocal disease.

Appendix 2.1
Bladder cancer questionnaire

QUESTIONNAIRE: EPIDEMIOLOGY OF DNA REPAIR AND BLADDER TUMOURS (PROJECT 02/192)

Name
DOB
Sex
Hospital number

Date .....

1. Smoking history

Have you ever smoked as much as one cigarette a day for as long as a year? Yes ☐ No ☐

If Yes, how old were you when you started smoking cigarettes regularly? ☐☐ years old

Did you smoke at the following ages? If so, how many cigarettes did you smoke and were they usually filter cigarettes?

Age 20	☐☐☐ cigs per day	Filter ☐	No filter ☐	Non smoker ☐
Age 30	☐☐☐ cigs per day	Filter ☐	No filter ☐	Non smoker ☐
Age 40	☐☐☐ cigs per day	Filter ☐	No filter ☐	Non smoker ☐
Age 50	☐☐☐ cigs per day	Filter ☐	No filter ☐	Non smoker ☐

Did you smoke cigarettes one year ago? Yes ☐ No ☐

If Yes, how many cigarettes did you smoke each day? ☐☐☐ cigarettes

Did you usually smoke filter cigarettes? ☐ Yes ☐ No ☐

Did you usually smoke low tar cigarettes? ☐ Yes ☐ No ☐

Which brand did you normally smoke? _____

How deeply did you inhale? Deeply into lungs ☐ A little ☐ Not at all ☐

If you have stopped smoking, how old were you when you last smoked? ☐☐ years old

Did you smoke cigars one year ago? Yes ☐ no ☐

Did you smoke a pipe one year ago? Yes ☐ no ☐

2. **Occupational exposure**
Have you ever worked in the following:

Rubber industry	Yes ☐	No ☐
Plastics industry	Yes ☐	No ☐
Laboratories	Yes ☐	No ☐
Printing	Yes ☐	No ☐
Dyes and paints	Yes ☐	No ☐
With diesel fumes	Yes ☐	No ☐

Please turn over

Name:

What jobs have you done? _____
_____
_____

Please would you give us a contact telephone number for us to ask about your jobs in more detail?

Tel: _____ (optional)

3. Family history

Have any members of your family (*blood relatives NOT relatives by marriage*) had bladder cancer?

	Yes	No	Don't know		Yes	No	Don't know	Not applicable
Mother	☐	☐	☐	Son(s)	☐	☐	☐	☐
Father	☐	☐	☐	Daughter(s)	☐	☐	☐	☐
Mother's mother	☐	☐	☐	Sister(s)	☐	☐	☐	☐
Mother's father	☐	☐	☐	Brother(s)	☐	☐	☐	☐
Father's mother	☐	☐	☐	Aunt/uncles	☐	☐	☐	☐
Father's father	☐	☐	☐	If **Yes**, numbers of aunts/uncles			☐	

4. Ethnic group

Do you consider yourself Caucasian (white skinned)? Yes ☐ No ☐

Do you consider yourself from another ethnic group? Yes ☐ No ☐

Please state _____

What was your place of birth? Town _____ Country _____

What was your mother's place of birth? Town _____ Country _____

What was your father's place of birth? Town _____ Country _____

Patients were asked to complete this questionnaire prior TURBT.

Appendix 3.1 Whole genome plots of array CGH data for 3 tumours from patient 1

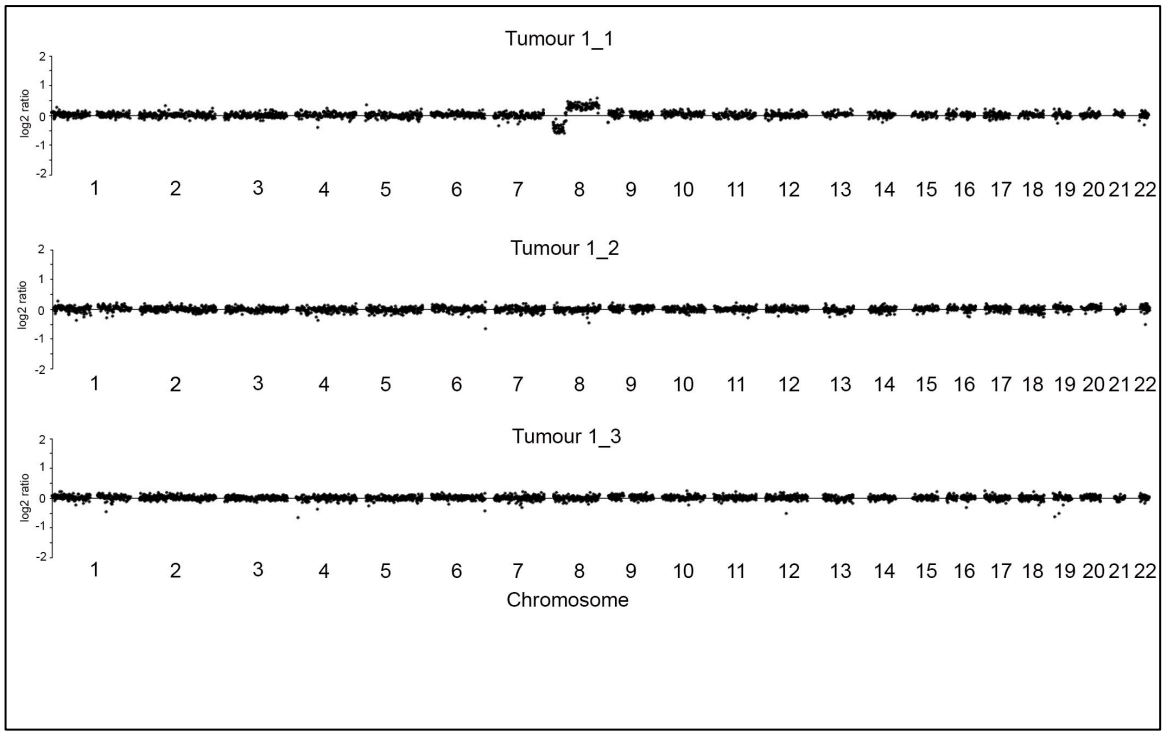

Whole genome plots of array CGH data for 3 tumours from patient 2

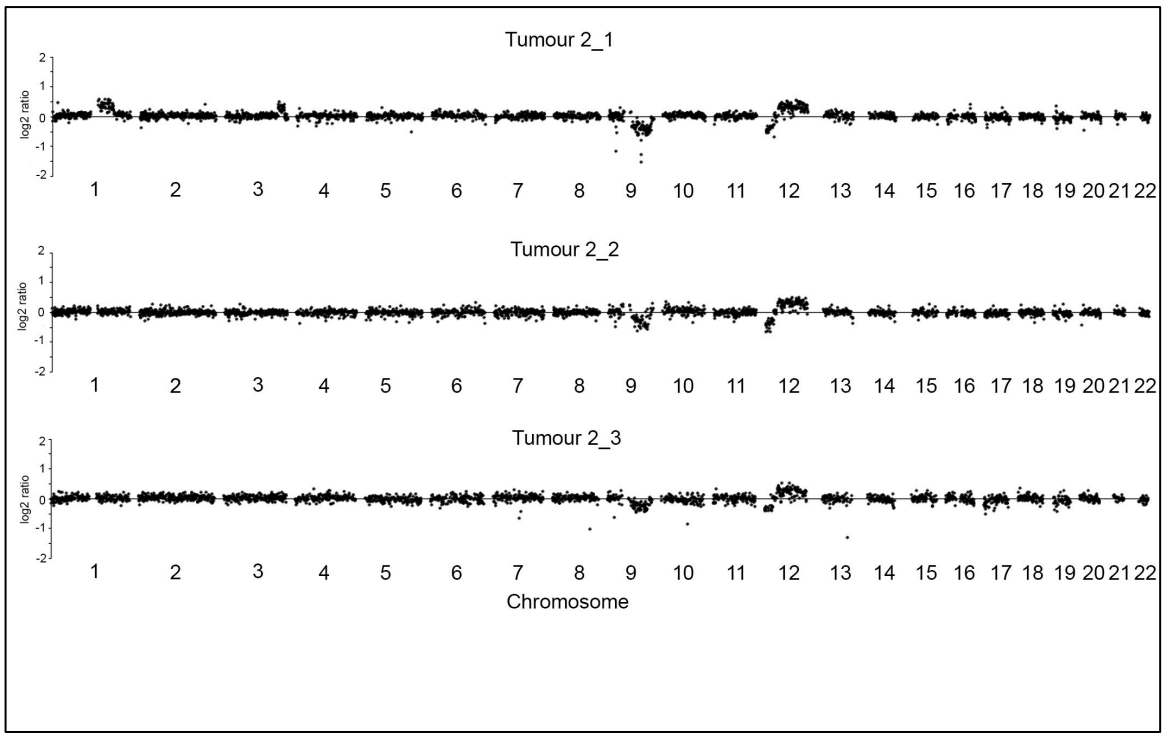

Whole genome plots of array CGH data for 3 tumours from patient 3

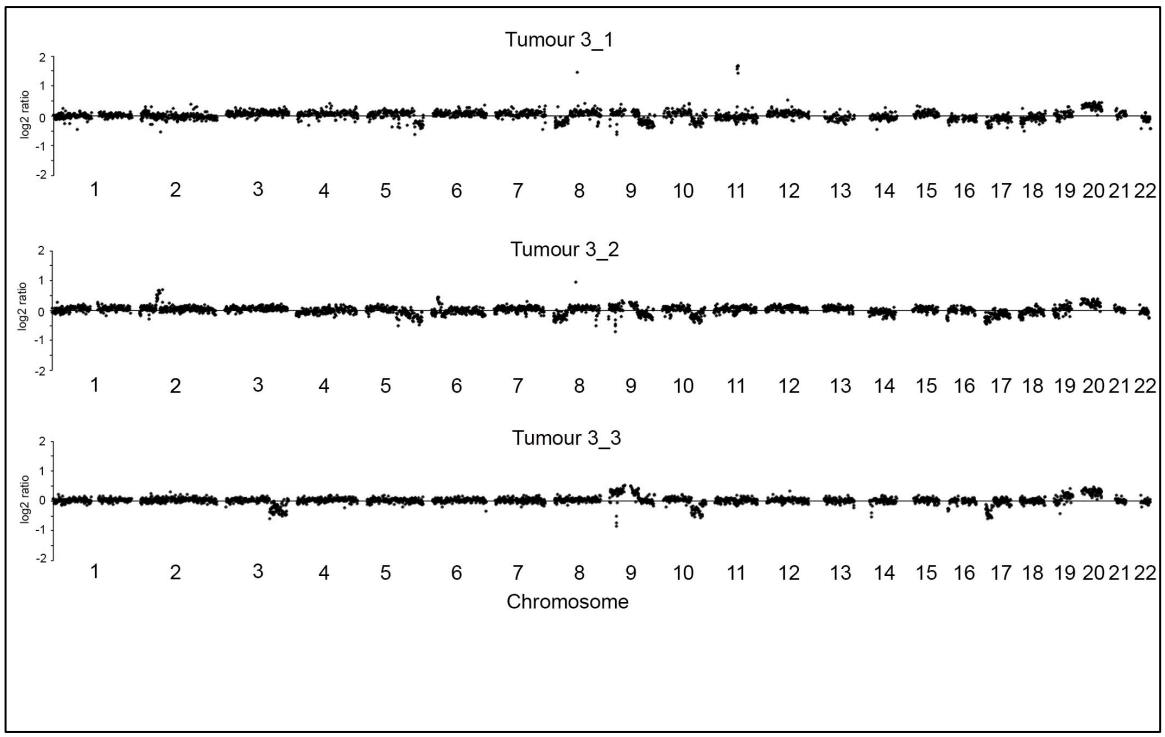

Whole genome plots of array CGH data for 6 tumours from patient 4

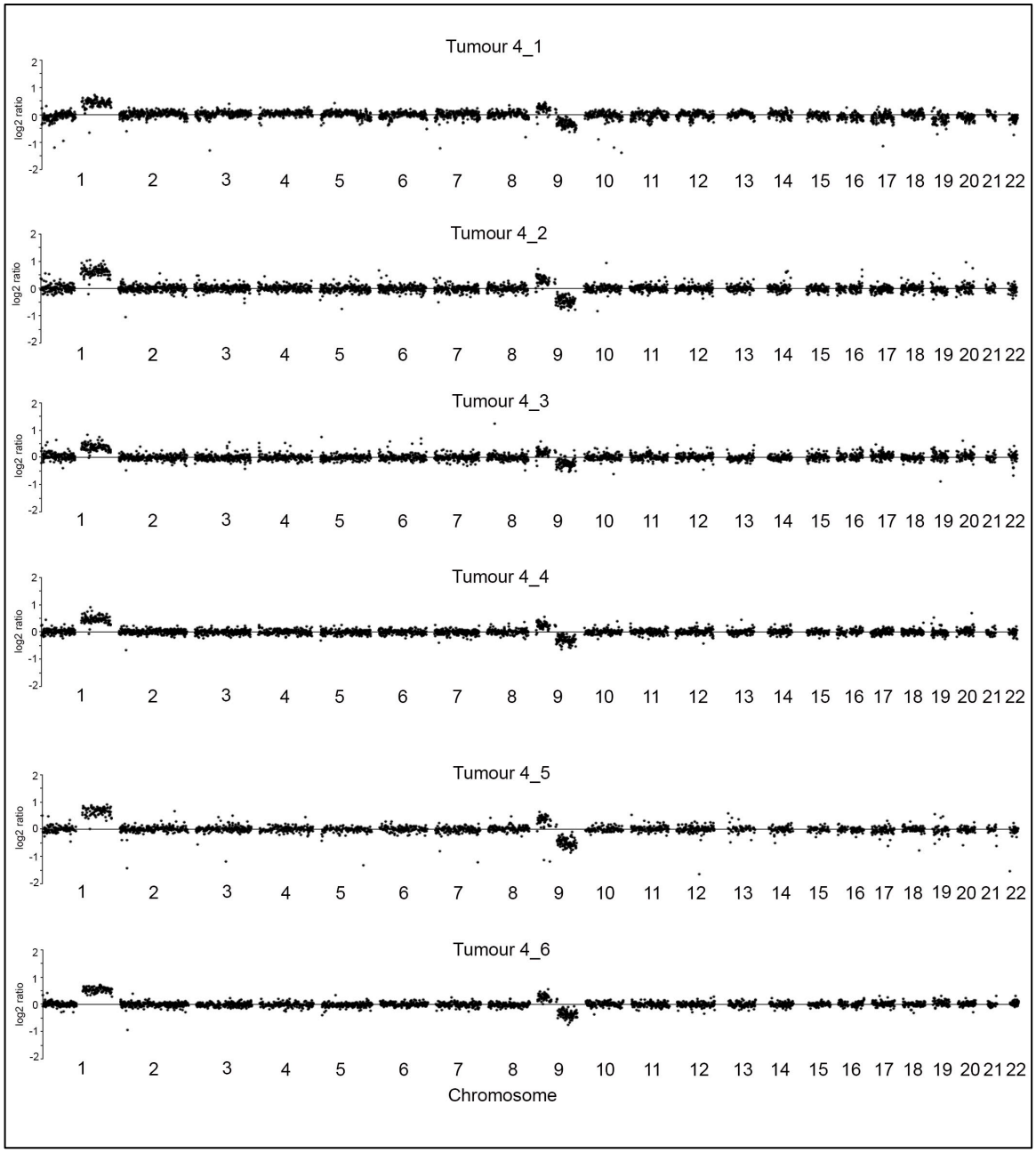

Whole genome plots of array CGH data for 2 tumours from patient 5

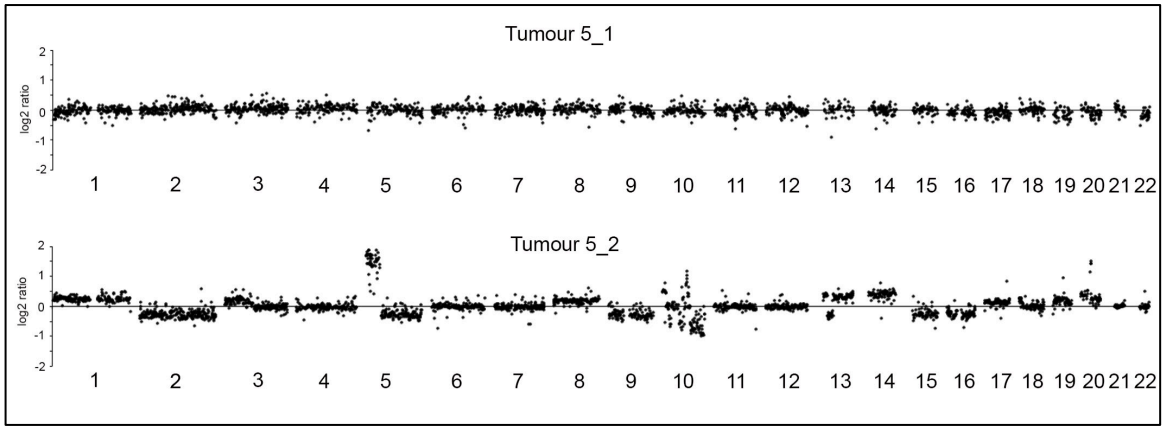

Whole genome plots of array CGH data for 3 tumours from patient 6

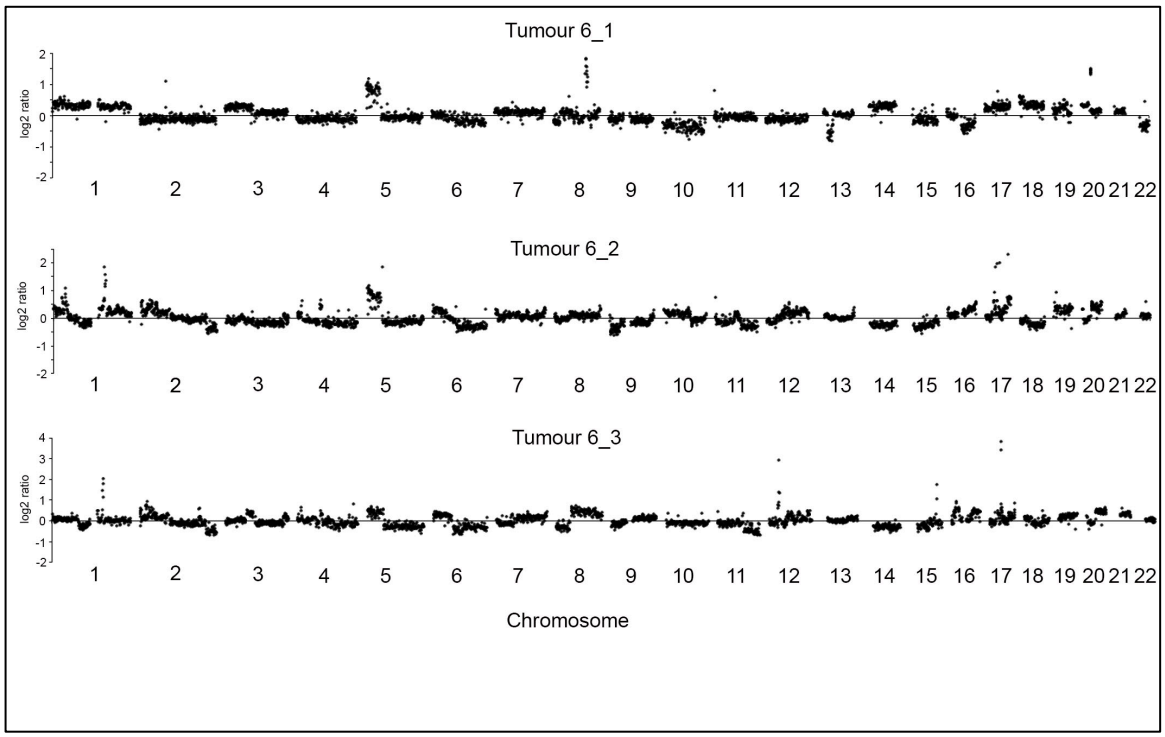

Whole genome plots of array CGH data for 2 tumours from patient 7

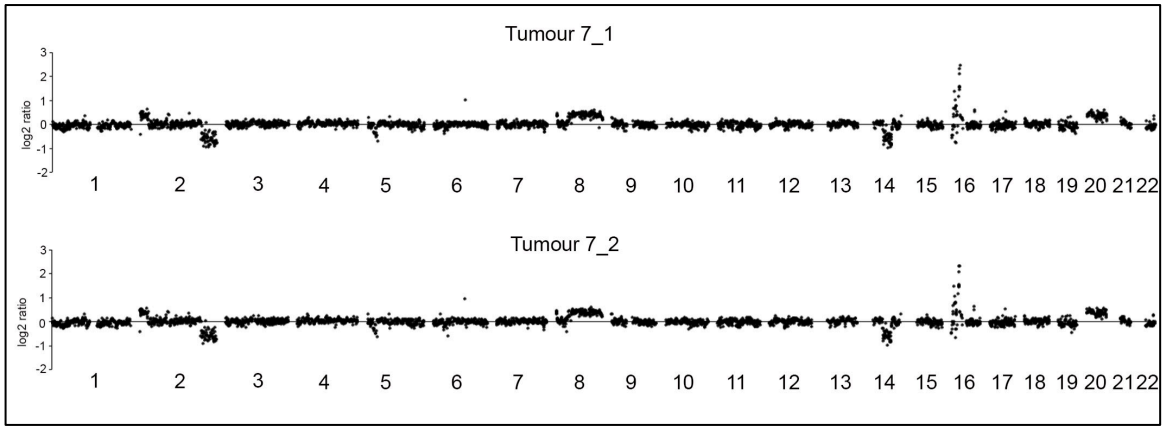

Whole genome plots of array CGH data for 3 tumours from patient 8

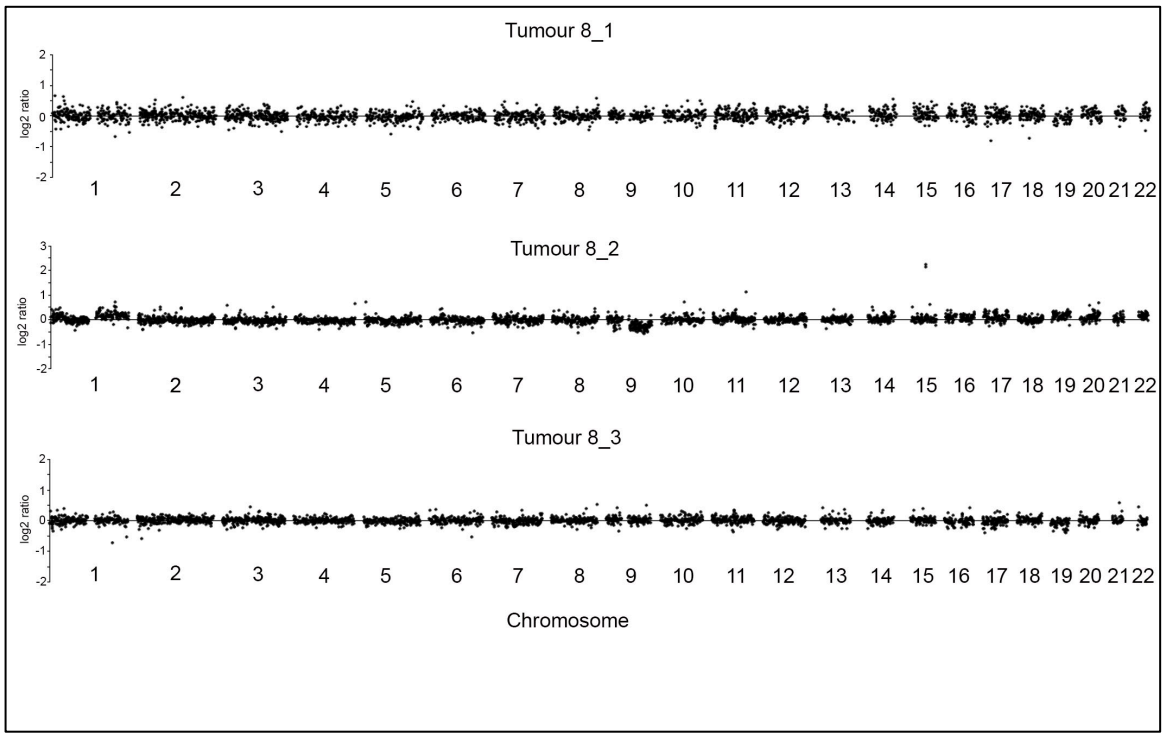

Whole genome plots of array CGH data for 2 tumours from patient 9

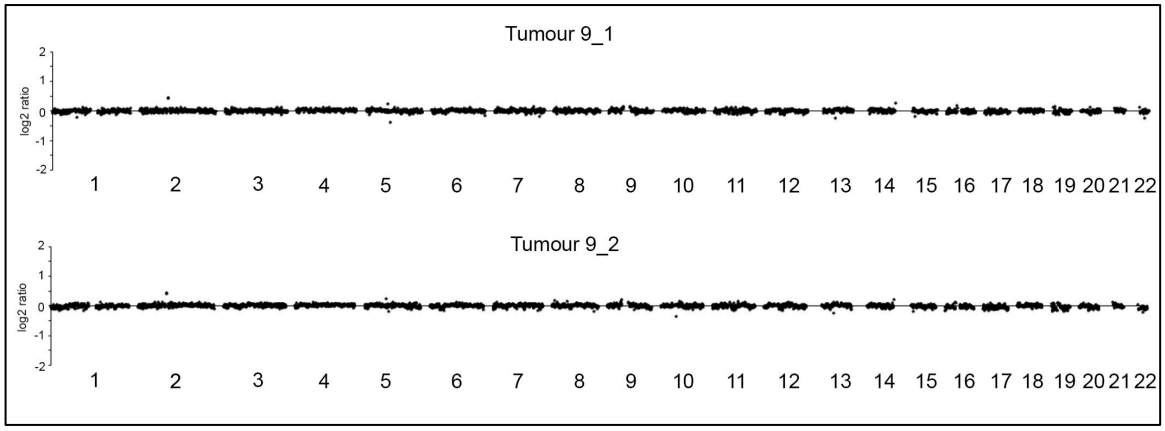

Whole genome plots of array CGH data for 2 tumours from patient 10

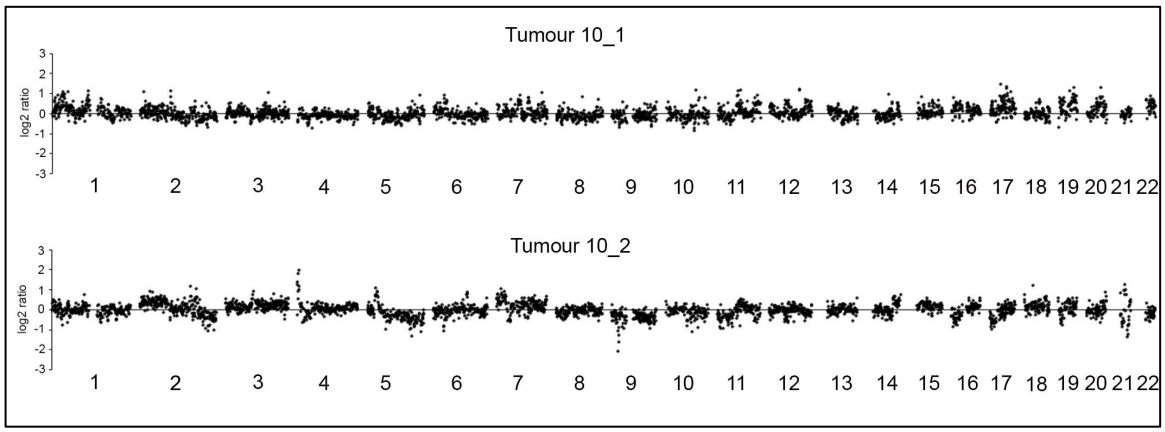

Whole genome plots of array CGH data for 2 tumours from patient 11

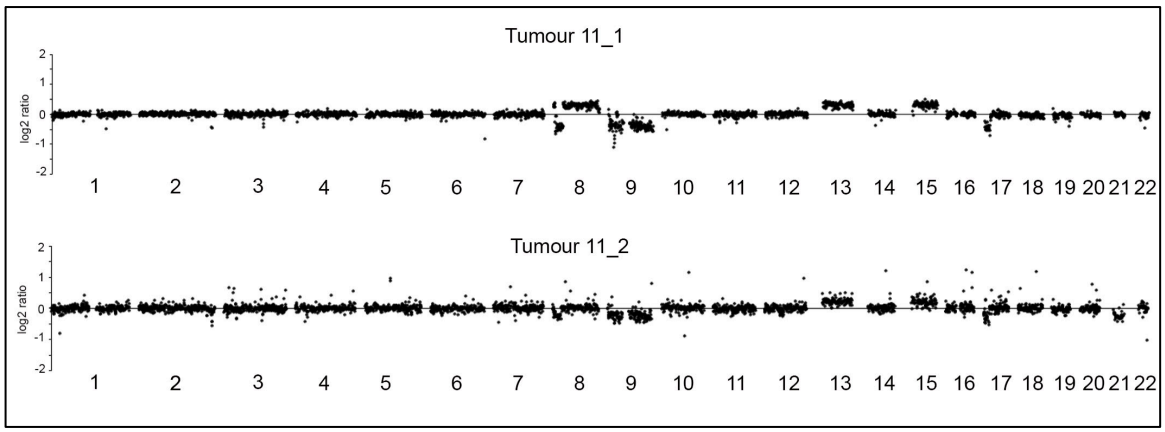

Whole genome plots of array CGH data for 4 tumours from patient 12

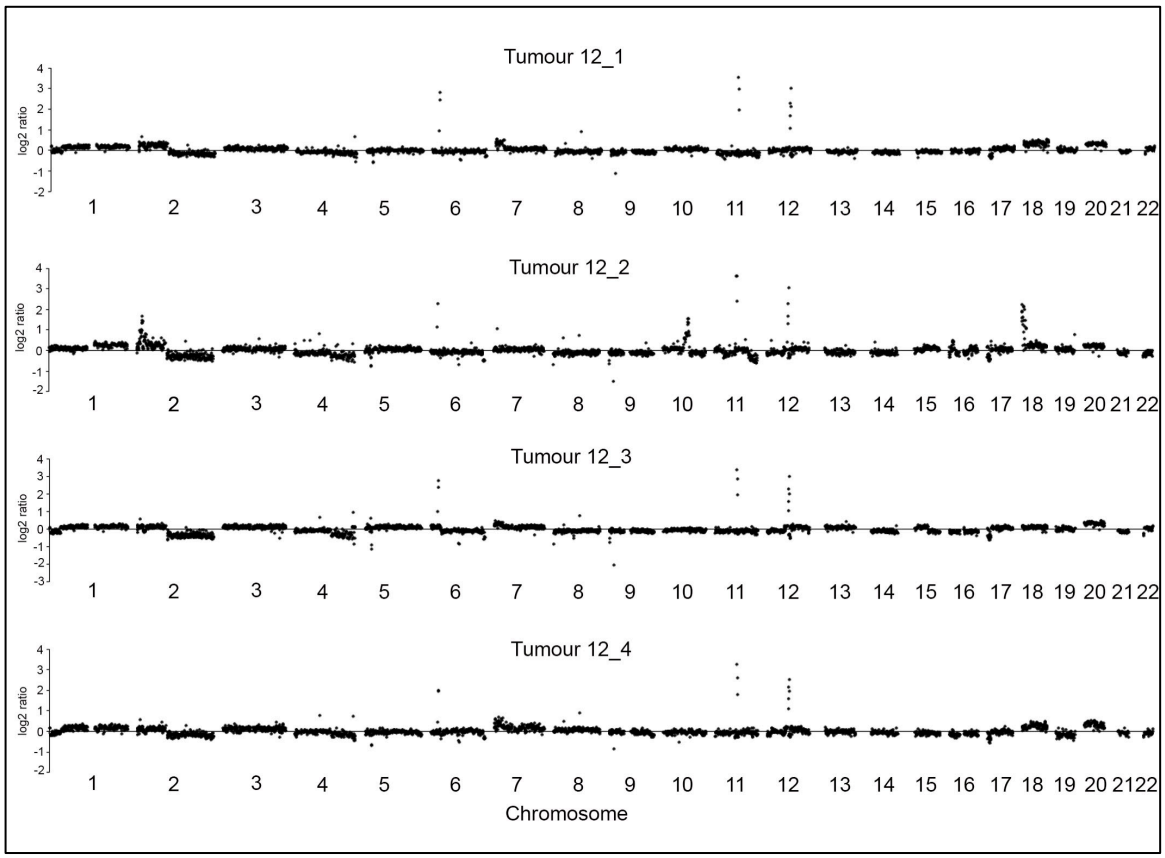

Whole genome plots of array CGH data for 4 tumours from patient 13

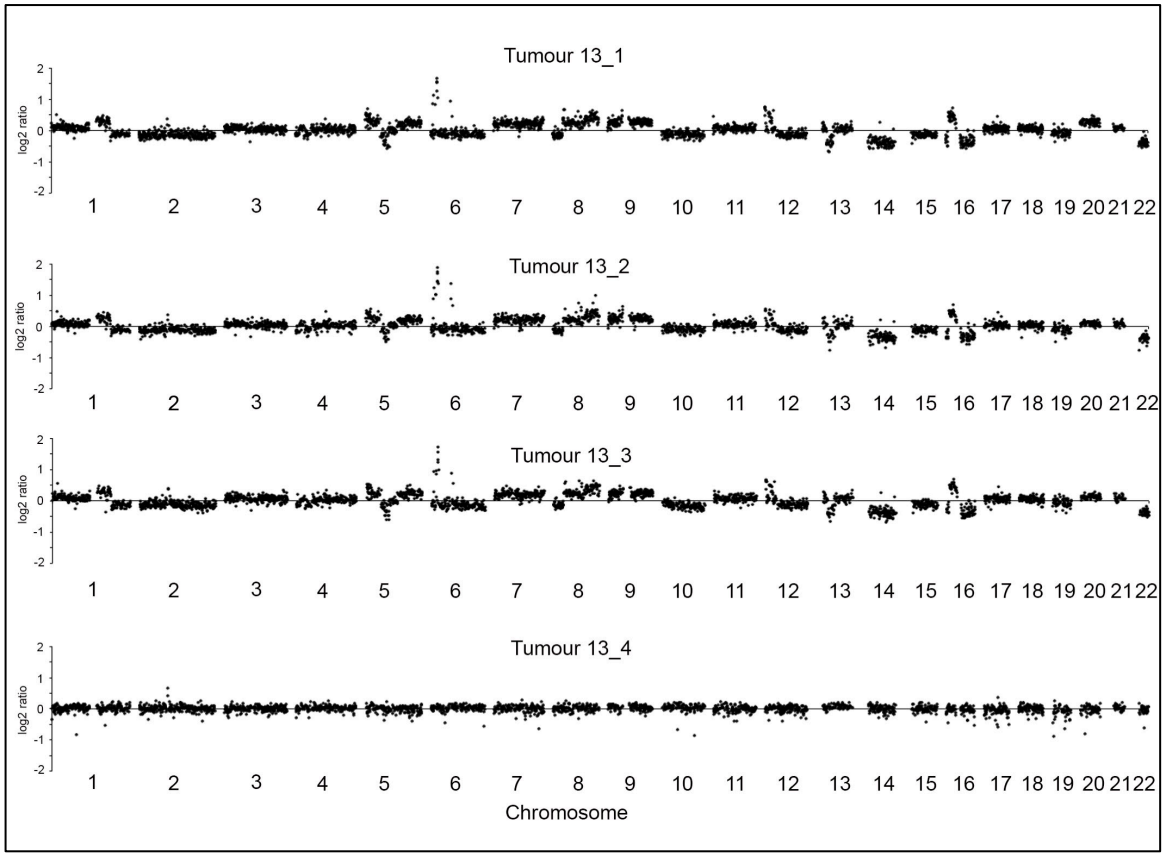

Whole genome plots of array CGH data for 4 tumours from patient 14

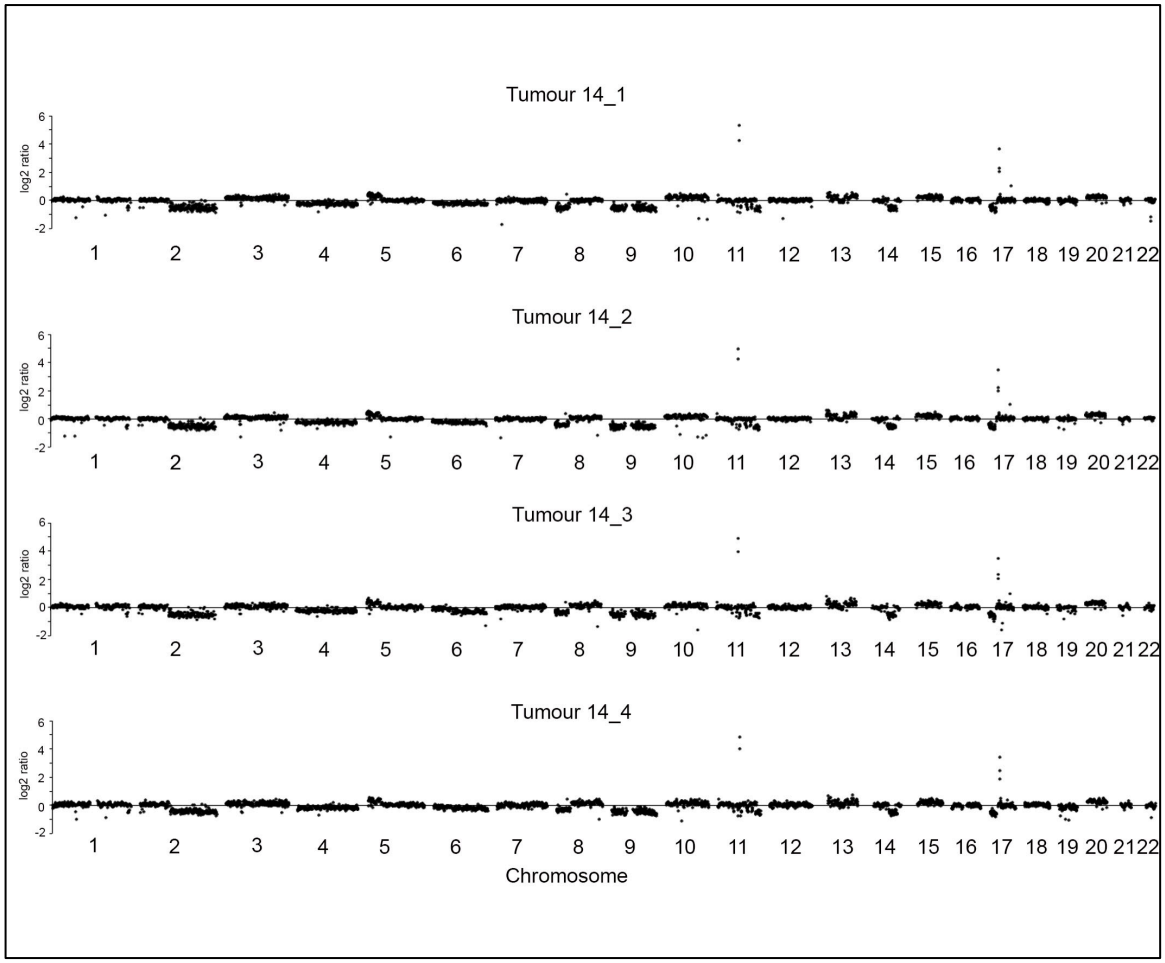

Whole genome plots of array CGH data for 2 tumours from patient 15

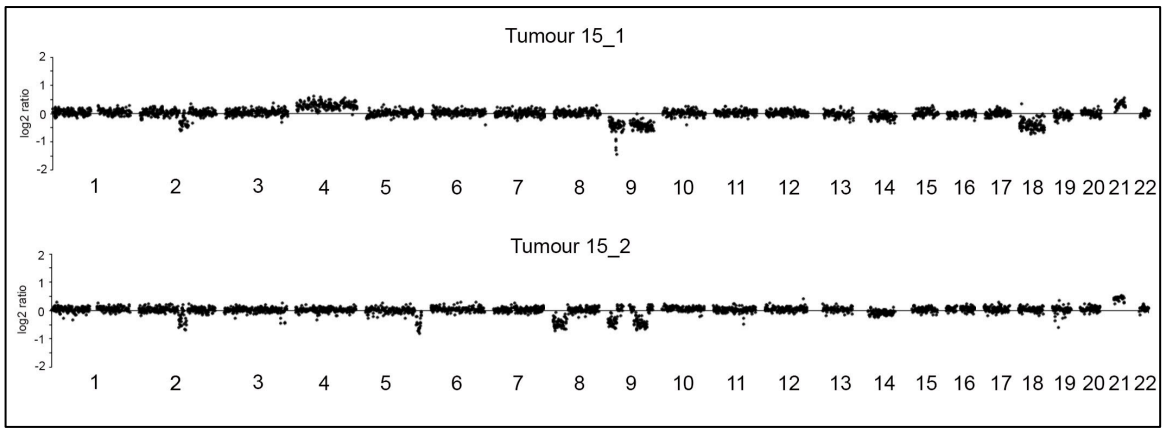

Whole genome plots of array CGH data for 4 tumours from patient 16

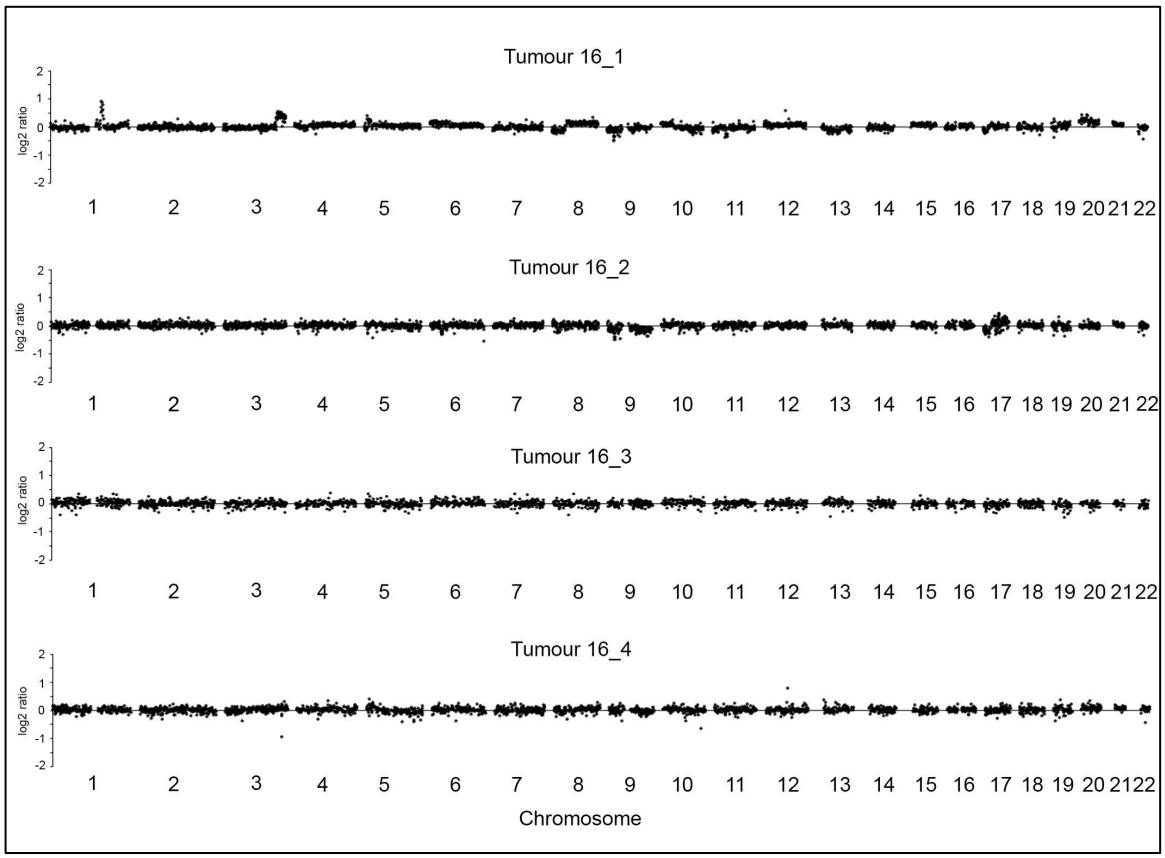

Whole genome plots of array CGH data for 3 tumours from patient 17

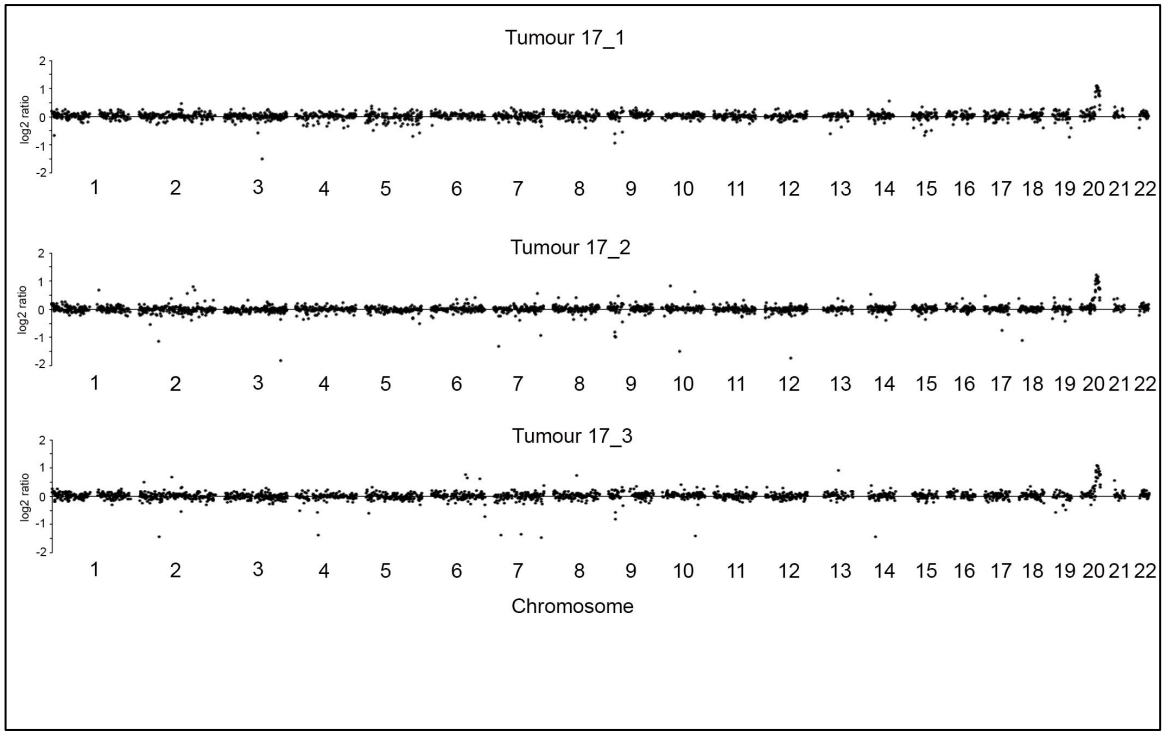

Whole genome plots of array CGH data for 4 tumours from patient 18

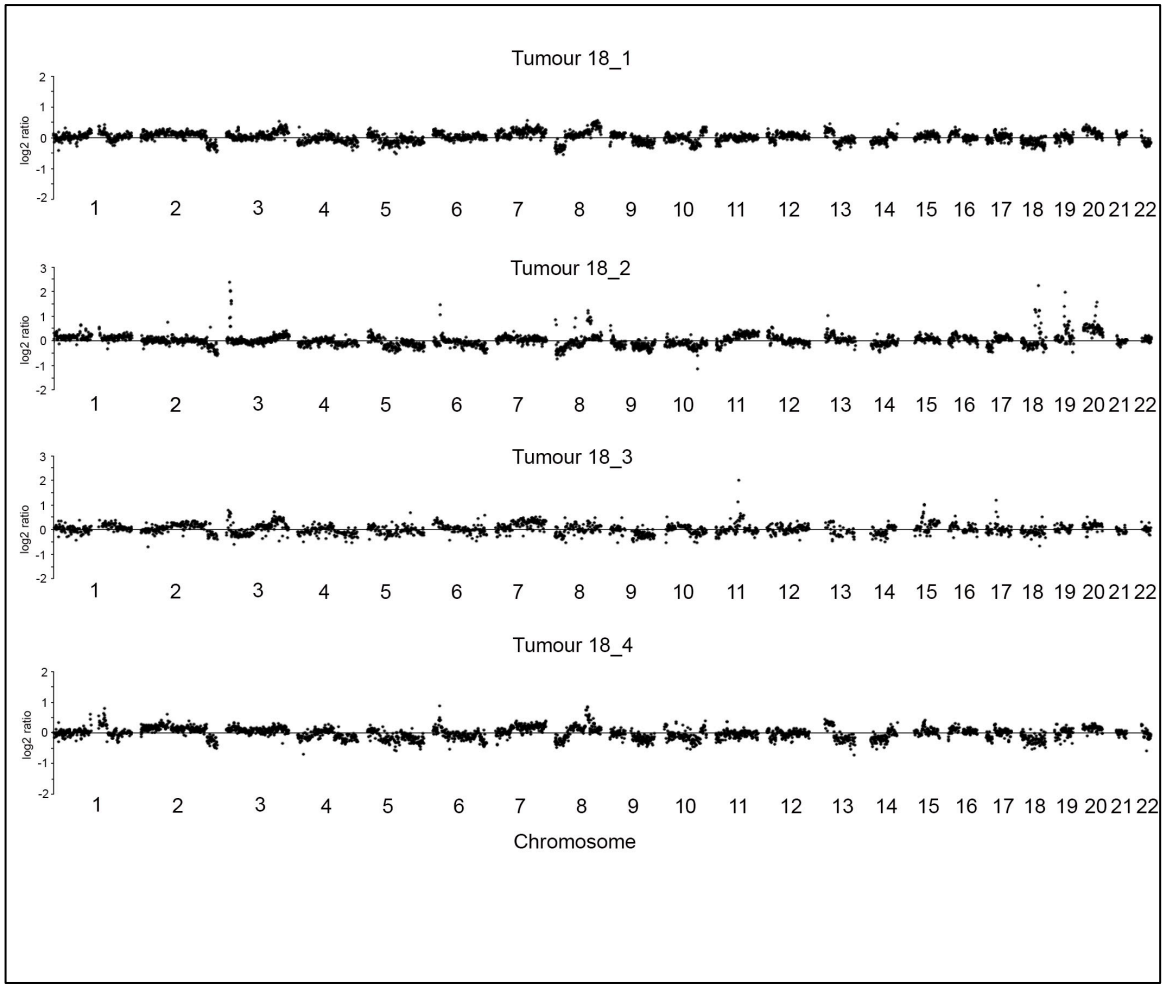

Whole genome plots of array CGH data for 3 tumours from patient 19

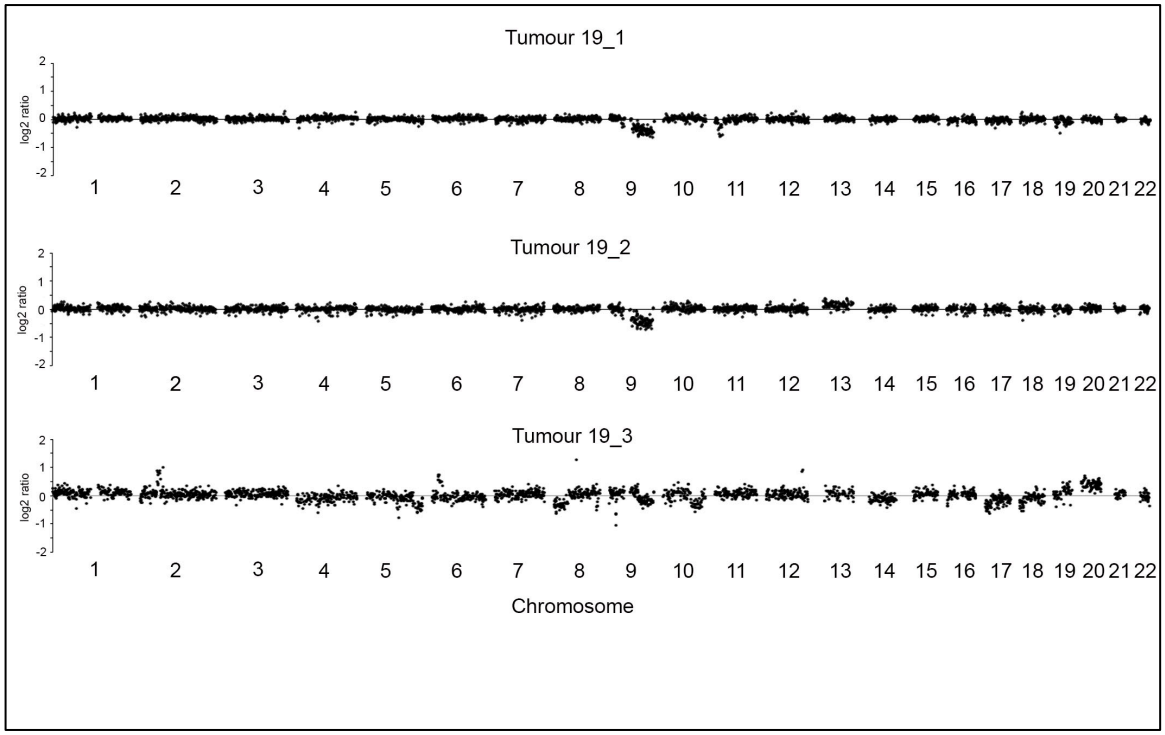

Whole genome plots of array CGH data for 3 tumours from patient 20

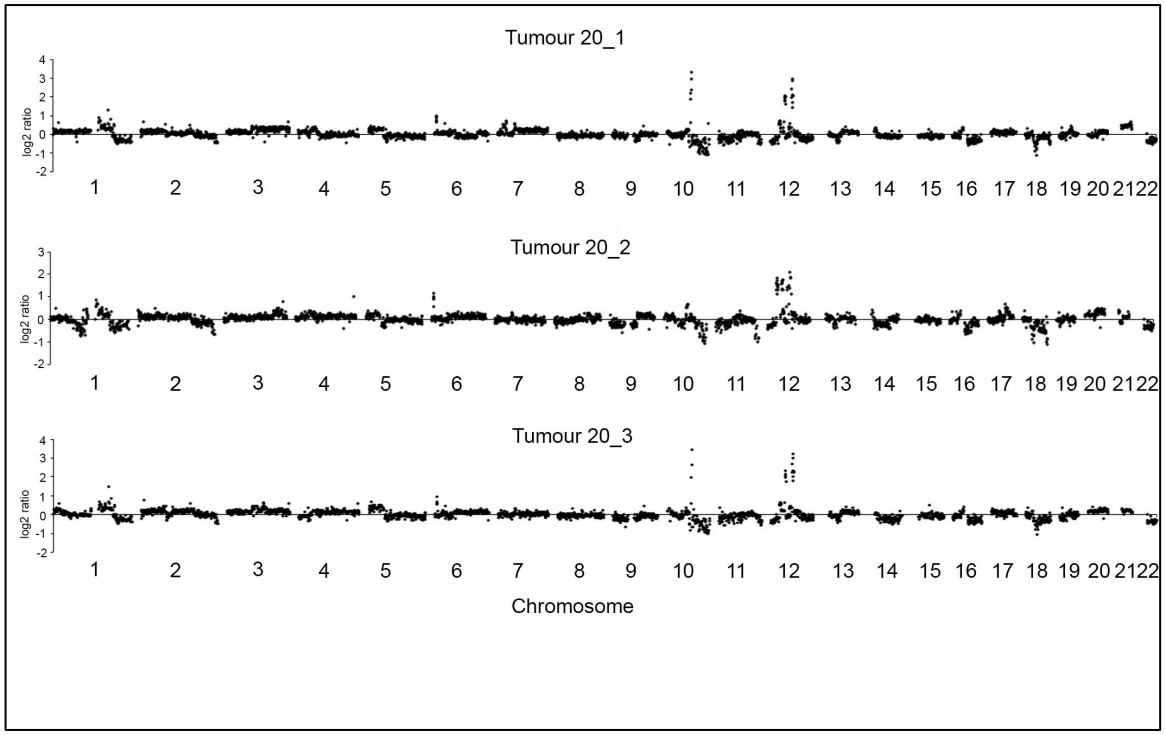

Whole genome plots of array CGH data for 2 tumours from patient 21

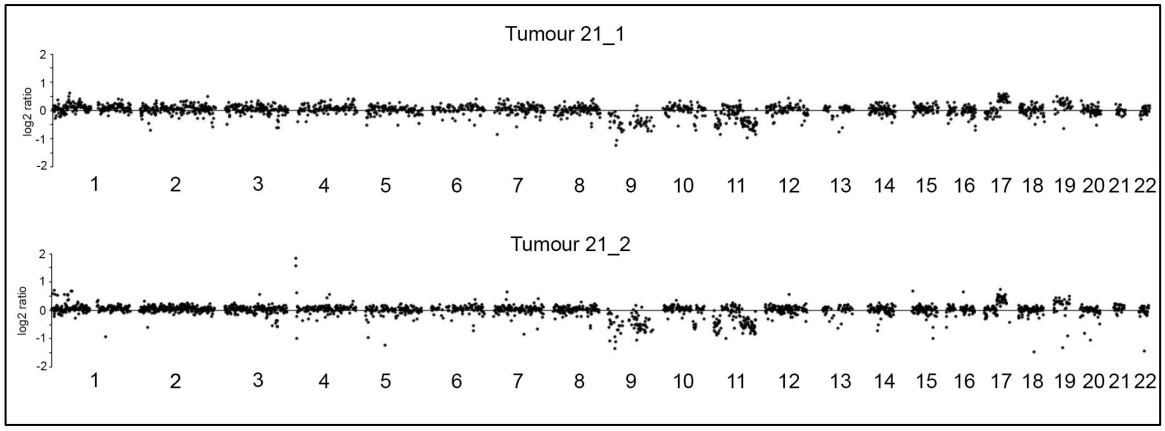

Whole genome plots of array CGH data for 2 tumours from patient 22

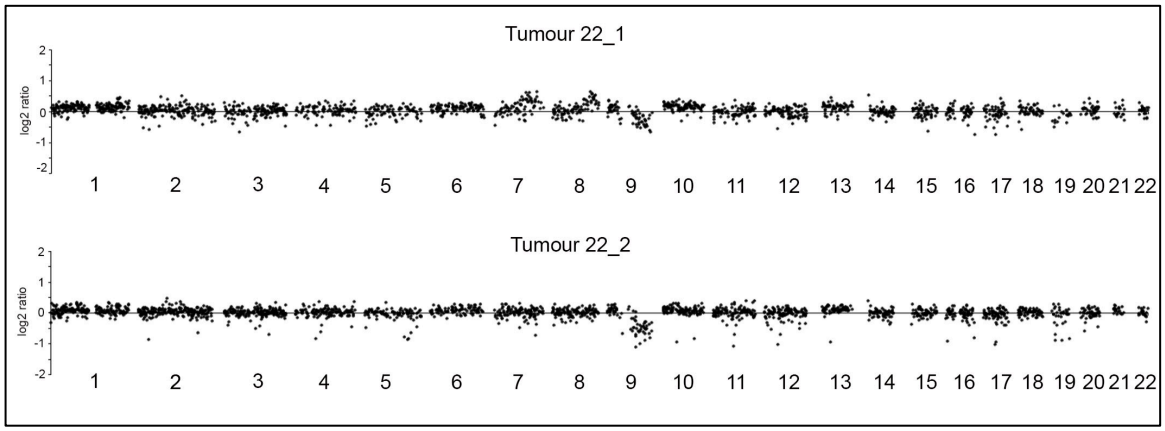

Appendix 3.2: Regions showing significant copy number differences in multifocal stage Ta (n=14) versus T1 (n=8) tumours.

Region[1]	Cytoband Location	Event	Region Length	Freq. in T1 (%)	Freq. in Ta (%)	Difference	p-value
chr1:50,594,589-50,823,305	p33	Gain	228716	50	7.14	42.86	0.04
chr1:68,609,865-73,625,895	p31.3 - p31.1	Gain	5016030	50	7.14	42.86	0.04
chr2:20,215,537-21,280,646	p24.1	Gain	1065109	50	7.14	42.86	0.04
chr2:224,263-20,037,859	p25.3 - p24.1	Gain	19813596	50	7.14	42.86	0.04
chr2:232,368,564-232,541,867	q37.1	Loss	173303	75	21.43	53.57	0.03
chr2:232,987,278-241,796,109	q37.1 - q37.3	Loss	8808831	75	21.43	53.57	0.03
chr2:25,870,821-52,373,212	p23.3 - p16.3	Gain	26502391	50	7.14	42.86	0.04
chr2:52,373,212-53,101,240	p16.3 - p16.2	Gain	728028	62.5	7.14	55.36	0.01
chr2:64,478,283-69,024,185	p14	Gain	4545902	50	7.14	42.86	0.04
chr2:74,335,462-88,214,979	p13.1 - p11.2	Gain	13879517	50	7.14	42.86	0.04
chr2:88,214,979-94,782,159	p11.2 - q11.1	Gain	6567180	62.5	7.14	55.36	0.01
chr2:94,782,159-95,675,764	q11.1	Gain	893605	50	0.00	50.00	0.01
chr6:146,266,178-162,794,027	q24.3 - q26	Loss	16527849	37.5	0.00	37.50	0.04
chr6:163,005,402-165,244,688	q26 - q27	Loss	2239286	37.5	0.00	37.50	0.04
chr6:165,244,688-168,121,846	q27	Loss	2877158	50	7.14	42.86	0.04
chr6:6,382,300-7,427,280	p25.1 - p24.3	Gain	1044980	50	7.14	42.86	0.04
chr7:12,919,070-13,079,613	p21.3	Gain	160543	37.5	0.00	37.50	0.04
chr7:15,056,488-21,588,275	p21.2 - p15.3	Gain	6531787	50	7.14	42.86	0.04
chr7:26,749,335-29,450,068	p15.2 - p15.1	Gain	2700733	50	7.14	42.86	0.04
chr7:32,275,005-45,048,865	p14.3 - p13	Gain	12773860	37.5	0.00	37.50	0.04
chr7:50,617,642-63,102,874	p12.2 - q11.21	Gain	12485232	50	7.14	42.86	0.04

chr7:63,102,874-84,591,194	q11.21 - q21.11	Gain	21488320	62.5	7.14	55.36	0.01
chr7:97,101,588-100,038,722	q21.3 - q22.1	Gain	2937134	62.5	7.14	55.36	0.01
chr9:84,783,002-89,446,315	q21.32 - q21.33	Gain	4663313	37.5	0.00	37.50	0.04
chr10:109,290,751-116,774,295	q25.1 - q25.3	Loss	7483544	75	21.43	53.57	0.03
chr10:78,996,385-80,472,830	q22.3	Loss	1476445	50	7.14	42.86	0.04
chr10:85,567,652-86,390,131	q23.1	Loss	822479	50	7.14	42.86	0.04
chr10:86,390,131-88,222,653	q23.1 - q23.2	Loss	1832522	62.5	7.14	55.36	0.01
chr10:88,222,653-89,694,469	q23.2 - q23.31	Loss	1471816	75	21.43	53.57	0.03
chr10:89,694,975-93,738,544	q23.31 - q23.32	Loss	4043569	75	21.43	53.57	0.03
chr10:93,738,544-94,907,303	q23.32 - q23.33	Loss	1168759	75	14.29	60.71	0.01
chr10:94,907,303-99,781,492	q23.33 - q24.2	Loss	4874189	75	21.43	53.57	0.03
chr12:33,333,489-40,716,974	p11.1 - q12	Loss	7383485	37.5	0.00	37.50	0.04
chr12:42,413,160-46,156,911	q12 - q13.11	Loss	3743751	37.5	0.00	37.50	0.04
chr14:23,749,068-25,757,198	q12	Loss	2008130	37.5	0.00	37.50	0.04
chr14:65,655,482-66,870,415	q23.3	Loss	1214933	37.5	0.00	37.50	0.04
chr16:23,756,350-31,190,651	p12.1 - p11.2	Gain	7434301	50	0.00	50.00	0.01
chr16:31,190,651-45,067,244	p11.2 - q11.2	Gain	13876593	50	7.14	42.86	0.04
chr16:7,019,846-23,756,350	p13.2 - p12.1	Gain	16736504	37.5	0.00	37.50	0.04
chr22:16,347,244-16,899,186	q11.21	Loss	551942	50	7.14	42.86	0.04
chr22:16,899,186-18,151,355	q11.21	Loss	1252169	50	0.00	50.00	0.01
chr22:18,151,355-18,151,891	q11.21	Loss	536	37.5	0.00	37.50	0.04
chr22:18,151,891-30,032,831	q11.21 - q12.2	Loss	11880940	50	0.00	50.00	0.01
chr22:30,032,831-30,535,980	q12.2 - q12.3	Loss	503149	50	7.14	42.86	0.04
chr22:30,535,980-30,623,768	q12.3	Loss	87788	50	0.00	50.00	0.01
chr22:30,623,768-30,623,867	q12.3	Loss	99	37.5	0.00	37.50	0.04
chr22:30,646,302-30,646,401	q12.3	Loss	99	37.5	0.00	37.50	0.04
chr22:30,646,401-40,803,595	q12.3 - q13.2	Loss	10157194	50	0.00	50.00	0.01

chr22:40,803,595-42,473,589	q13.2	Loss	1669994	62.5	0.00	62.50	0.00
chr22:42,473,589-44,175,906	q13.2 - q13.31	Loss	1702317	50	0.00	50.00	0.01
chr22:44,175,906-49,453,810	q13.31 - q13.33	Loss	5277904	50	7.14	42.86	0.04

[1]Physical position is according to hg19/NCBI build 37

Appendix 3.3: Regions showing significant copy number differences in multifocal grade 2 (n=11) versus grade 3 (n=11) tumours.

Region[1]	Cytoband Location	Event	Region Length	Freq. in G3 (%)	Freq. in G2 (%)	Difference	p-value
chr2:195,231,804-196,753,496	q32.3	Loss	1521692	45.45	0.00	45.45	0.04
chr2:20,215,537-21,280,646	p24.1	Gain	1065109	45.45	0.00	45.45	0.04
chr2:208,876,525-227,205,229	q33.3 - q36.3	Loss	18328704	63.64	9.09	54.55	0.02
chr2:224,263-20,037,859	p25.3 - p24.1	Gain	19813596	45.45	0.00	45.45	0.04
chr2:228,542,036-232,368,564	q36.3 - q37.1	Loss	3826528	72.73	18.18	54.55	0.03
chr2:232,368,564-232,541,867	q37.1	Loss	173303	72.73	9.09	63.64	0.01
chr2:232,541,867-232,987,278	q37.1	Loss	445411	72.73	18.18	54.55	0.03
chr2:232,987,278-241,796,109	q37.1 - q37.3	Loss	8808831	72.73	9.09	63.64	0.01
chr2:25,870,821-52,373,212	p23.3 - p16.3	Gain	26502391	45.45	0.00	45.45	0.04
chr2:52,373,212-53,101,240	p16.3 - p16.2	Gain	728028	54.55	0.00	54.55	0.01
chr2:64,478,283-69,024,185	p14	Gain	4545902	45.45	0.00	45.45	0.04
chr2:74,335,462-88,214,979	p13.1 - p11.2	Gain	13879517	45.45	0.00	45.45	0.04
chr2:88,214,979-94,782,159	p11.2 - q11.1	Gain	6567180	54.55	0.00	54.55	0.01
chr3:82,799,401-87,044,540	p12.2 - p12.1	Gain	4245139	45.45	0.00	45.45	0.04
chr4:26,747,433-45,608,190	p15.2 - p12	Loss	18860757	45.45	0.00	45.45	0.04
chr4:55,628-1,065,598	p16.3	Loss	1009970	45.45	0.00	45.45	0.04
chr5:26,353,486-26,539,834	p14.1	Gain	186348	45.45	0.00	45.45	0.04
chr7:15,056,488-21,588,275	p21.2 - p15.3	Gain	6531787	45.45	0.00	45.45	0.04
chr7:26,749,335-29,450,068	p15.2 - p15.1	Gain	2700733	45.45	0.00	45.45	0.04
chr7:50,617,642-63,102,874	p12.2 - q11.21	Gain	12485232	45.45	0.00	45.45	0.04
chr7:63,102,874-84,591,194	q11.21 - q21.11	Gain	21488320	54.55	0.00	54.55	0.01
chr7:97,101,588-100,038,722	q21.3 - q22.1	Gain	2937134	54.55	0.00	54.55	0.01
chr10:78,996,385-80,472,830	q22.3	Loss	1476445	45.45	0.00	45.45	0.04
chr10:85,567,652-86,390,131	q23.1	Loss	822479	45.45	0.00	45.45	0.04
chr10:86,390,131-88,222,653	q23.1 - q23.2	Loss	1832522	54.55	0.00	54.55	0.01
chr11:43,020,941-50,013,069	p12 - p11.12	Loss	6992128	45.45	0.00	45.45	0.04
chr14:71,308,003-74,588,657	q24.2 - q24.3	Loss	3280654	45.45	0.00	45.45	0.04

chr15:42,756,125-56,535,071	q21.1 - q22.1	Gain	13778946	45.45	0.00	45.45	0.04
chr16:31,190,651-45,067,244	p11.2 - q11.2	Gain	13876593	45.45	0.00	45.45	0.04
chr19:211,322-6,523,485	p13.3	Loss	6312163	45.45	0.00	45.45	0.04
chr20:29,503,014-29,779,350	q11.21	Gain	276336	72.73	18.18	54.55	0.03
chr22:15,745,966-16,347,244	q11.1 - q11.21	Loss	601278	54.55	0.00	54.55	0.01
chr22:16,347,244-16,899,186	q11.21	Loss	551942	45.45	0.00	45.45	0.04
chr22:30,032,831-30,535,980	q12.2 - q12.3	Loss	503149	45.45	0.00	45.45	0.04
chr22:40,803,595-42,473,589	q13.2	Loss	1669994	45.45	0.00	45.45	0.04
chr22:44,175,906-49,453,810	q13.31 - q13.33	Loss	5277904	45.45	0.00	45.45	0.04

[1]Physical position is according to hg19/NCBI build 37

Chromosome	Cytoband	Position[1] (Mb)	No of genes	Candidate genes	Tumours[2]	Gain frequency of patients (%)[3]	Number of tumours with amplification
4	p16.3 - p16.1	0.21-7.94	151	ABCA11P, ADD1, ADRA2C, AFAP1, AFAP1-AS1, ALG1L7P, ATP5I, BLOC1S4, C4orf6, C4orf48, C4orf50, CCDC96, CFAP99, COX6B1P5, CPLX1, CRIPAK, CRMP1, CTBP1, CTBP1-AS2, CYTL1, DGKQ, DOK7, ENPP7P9, EVC, EVC2, FAM53A, FAM86EP, FAM193A, FGFR3, FGFRL1, FLJ36777, GAK, GRK4, GRPEL1, HAUS3, HGFAC, HTT, HTT-AS, IDUA, JAKMIP1, KIAA0232, LDHAP1, LETM1, LINC00955, MIR571, MIR943, MIR4274, MIR4798, MIR4800, MRFAP1, MRFAP1L1, MSANTD1, MSX1, MXD4, MYL5, NAT8L, NELFA, NOP14, NOP14-AS1, NSG1, OR4D12P, OR7E43P, OR7E99P, OR7E162P, OTOP1, PCGF3, PDE6B, PIGG, POLN, PPP2R2C, PSAPL1, RGS12, RNF4, RNF212, RPL7AP29, RPS3AP16, RPS7P15, S100P, SCARNA22, SH3BP2, SLBP, SLC26A1, SORCS2, SPON2, STK32B, STX18, STX18-AS1, TACC3, TADA2B, TBC1D14, TMED11P, TMEM128, TMEM129, TMEM175, TNIP2, TRSUP-TTA3-1, UNC93B4, UVSSA, WFS1, WHSC1, ZBTB49, ZFYVE28, ZNF141, ZNF721, ZNF732, ZNF876P	10_2, 21_2	4.55	2

5	p14.1 - q11.1	26.54 - 49.91	172	ADAMTS12, AGXT2, AMACR, ANXA2R, BRIX1, C1QTNF3, C1QTNF3-AMACR, C5orf22, C5orf28, C5orf34, C5orf42, C5orf51, C6, C7, C9, CAPSL, CARD6, CCDC11P1, CCDC152, CCL28, CCNB3P1, CDH6, CDH9, CTD-2118P12.1, DAB2, DNAJC21, DROSHA, EEF1A1P19, EGFLAM, EGFLAM-AS2, EGFLAM-AS4, EMB, FBXO4, FGF10, FGF10-AS1, FYB, GDNF, GDNF-AS1, GHR, GOLGA5P1, GOLPH3, HCN1, HMGCS1, HPRTP2, IL7R, INTS6P1, KCTD9P5, KRT18P31, LIFR, LIFR-AS1, MIR579, MIR580, MIR3650, MIR4279, MROH2B, MRPS30, MTHFD2P6, MTMR12, NADK2, NIM1K, NIPBL, NIPBL-AS1, NNT, NNT-AS1, NPR3, NUP155, OFD1P17, OSMR, OSMR-AS1, OXCT1, PAIP1, PDZD2, PGBD3P2, PLCXD3, PRDX4P2, PRKAA1, PRLR, PSMC6P3, PTGER4, RAD1, RAI14, RANBP3L, RICTOR, RNA5SP181, RNU7-75P, RPL5P14, RPL9P17, RPL19P11, RPL21P54, RPL21P56, RPL27P10, RPL29P12, RPL37, RPL39P22, RPS2P22, RPS4XP6, RPS8P8, RPSAP38, RXFP3, SEPP1, SERBP1P6, SKP2, SLC1A3, SLC45A2, SNORD72, SPEF2, ST3GAL5P1, SUB1, SUCLG2P4, TARS, TCP1P2, TPT1P5, TTC23L, TTC33, UBL5P1, UGT3A1, UGT3A2, WDR70, ZFR, ZNF131	5_2, 6_2	4.55	2

6	p22.3 - p22.2	19.13 - 24.25	27	CASC14, CASC15, CDKAL1, DCDC2, E2F3, HDGFL1, HNRNPA1P58, ID4, KRT18P38, LINC00581, MBOAT1, NRSN1, PRL, RNA5SP205, RPL5P20, RPL6P18, RPL21P61, RPL29P17, RPL36AP25, SOX4, SPTLC1P2, UQCRFS1P3	12_1, 12_2, 12_3, 12_4, 13_1, 13_2, 13_3, 18_2	4.55	8
8	q13.2 - q13.3	69.61 - 72.6	27	BTF3P12, C8orf34, EYA1, H2AFZP2, LACTB2, NCOA2, PRDM14, RPL13P11, RPS18P11, SDCBPP2, SLCO5A1, SULF1, SUMO2P20, TRAM1, TRAPPC2P2, TRE-CTC14-1, XKR9	3_1, 19_3	9.1	2

10	q22.2 - q23.1	74.95 - 83.64	140	ADK, AGAP5, ANXA7, ANXA11, AP3M1, ATP5G1P8, BEND3P3, BMS1P4, C1DP2, C1DP3, C1DP4, C10orf11, C10orf55, CAMK2G, CFAP70, CHCHD1, COMTD1, CTSLP6, DLG5, DLG5-AS1, DNAJC9, DNAJC9-AS1, DUPD1, DUSP13, DYDC1, DYDC2, EIF4A2P2, EIF5AL1, EIF5AP4, FAM32C, FAM149B1, FAM213A, FARSBP1, FUT11, GLUD1P3, GNAI2P2, H2AFZP5, HMGA1P5, IMPDH1P5, KAT6B, KCNMA1, KCNMA1-AS1, KCNMA1-AS2, KCNMA1-AS3, LINC00595, LINC00856, LINC00857, MAT1A, MBL1P, MBL3P, MIR606, MRPL35P3, MRPS16, MSS51, MYOZ1, NDST2, NPAP1P2, NRG3, NUTM2B, NUTM2B-AS1, NUTM2E, PGGT1BP2, PLAC9, PLAU, POLR3A, POLR3DP1, PPIAP13, PPIF, PPP3CB, PPP3CB-AS1, RAB5CP1, RBBP6P1, RNA5SP320, RNA5SP321, RPA2P2, RPL22P18, RPL26P6, RPL39P25, RPS7P9, RPS12P2, RPS12P18, RPS24, RPS26P41, RPS26P42, RPSAP6, SAMD8, SEC24C, SFTPA1, SFTPA2, SFTPA3P, SFTPD, SH2D4B, SPA17P1, SYNPO2L, TIMM9P1, TMEM254, TMEM254-AS1, TPRX1P1, TSPAN14, USP54, VCL, VDAC2, WARS2P1, ZCCHC24, ZMIZ1, ZMIZ1-AS1, ZNF503, ZNF503-AS1, ZNF503-AS2, ZNF519P1, ZNRF2P3, ZSWIM8, ZSWIM8-AS1	12_2, 20_1, 20_3	4.55	3

11	q13.2 - q13.4	68.28 - 72.38	98	ALG1L9P, ANAPC15, ANO1, ANO1-AS2, ART2P, CCND1, CLPB, CPT1A, CTTN, DEFB108B, DHCR7, ENPP7P8, FADD, FAM86C1, FGF3, FGF4, FGF19, FLJ42102, FOLR1, FOLR1P1, FOLR2, FOLR3, FOLR3P1, GAL, H2AFZP4, IFITM9P, IGHMBP2, IL18BP, INPPL1, KRTAP5-7, KRTAP5-8, KRTAP5-9, KRTAP5-10, KRTAP5-11, KRTAP5-13P, KRTAP5-14P, LAMTOR1, LINC01488, LINC01537, LRTOMT, MIR139, MIR548K, MIR3164, MIR3165, MIR3664, MRGPRD, MRGPRF, MRGPRF-AS1, MRPL21, MTL5, MYEOV, NADSYN1, NUMA1, OR7E4P, OR7E87P, OR7E126P, OR7E128P, ORAOV1, PDE2A, PHOX2A, PPFIA1, PPP6R3, RNF121, RPEP6, RPS3AP41, S100A11P3, SHANK2, SHANK2-AS1, SHANK2-AS3, SNRPCP14, TPCN2, UNC93B6, ZNF705E	3_1, 12_1, 12_2, 12_3, 12_4, 14_1, 14_2, 14_3, 14_4, 18_3	4.55	10

12	p12.1 - p11.21	25.56 - 33.17	96	AK4P3, AMN1, ARNTL2, ARNTL2-AS1, ASS1P14, ASUN, BHLHE41, BICD1, C12orf71, CAPRIN2, CCDC91, DDX11, DDX11-AS1, DENND5B, DENND5B-AS1, DNM1L, DSPA2D, ERGIC2, FAM60A, FAR2, FGD4, FGFR1OP2, FLJ13224, H3F3C, HMGB1P49, IPO8, ITPR2, KIAA1551, KLHL42, LINC00941, LMNTD1,, MANSC4, MED21, METTL20, MIR4302, MRPL30P2, MRPS35, OVCH1, OVCH1-AS1, OVOS2, PKP2, PPFIBP1, PTHLH, RARSP1, RASSF8, RASSF8-AS1, REP15, RNA5SP354, RNA5SP356, RNU5F-4P, RPL12P32, RPL13AP22, RPL21P99, RPL29P27, RPL31P50, RPL35AP27, RPL39P27, RPLP2P4, SMCO2, SSPN, STK38L, STMN1P1, TDGP1, TM7SF3, TMTC1, TSPAN11, YARS2	6_3, 20_2	4.55	2

12	q14.3 - q21.1	64.71 - 73.07	107	APOOP3, ATP5HP4, ATP6V1E1P3, BEST3, C12orf56, CAND1, CCT2, CHCHD3P2, CNOT2, CPM, CPSF6, DYRK2, FAHD2P1, FLJ41278, FRS2, GGTA2P, GNS, GRIP1, HELB, HMGA2, HNRNPA1P70, IFNG, IFNG-AS1, IL22, IL26, IRAK3, KCNMB4, KRT8P39, KRT18P60, LEMD3, LGR5, LINC01479, LINC01481, LLPH, LRRC10, LYZ, MDM1, MDM2, MIR548C, MIR548Z, MIR1279, MIR3913-1, MIR3913-2, MRPL40P1, MRS2P2, MSRB3, MYRFL, NTAN1P3, NUP107, OSBPL9P4, PCNPP3, PDCL3P7, PSMC6P2, PTPRB, PTPRR, RAB3IP, RAB21, RAP1B, RASSF3, RBMS1P1, RNA5SP362, RPL7P39, RPL7P42, RPL10P12, RPL21P18, RPL39P28, RPS11P6, RPS26P45, RPSAP12, RPSAP52, SLC35E3, SNORA70G, TBC1D15, TBC1D30, TBK1, THAP2, TMBIM4, TMEM19, TPH2, TRHDE, TRHDE-AS1, TSPAN8, WIF1, XPOT, YEATS4, ZFC3H1	12_1, 12_2, 12_3, 12_4, 20_1, 20_2, 20_3	4.55	7

17	q11.2 - q12	26.58 - 29.51	104	ABHD15, ADAP2, ALDOC, ALOX12P1, ANKRD13B, ATAD5, BLMH, CORO6, CPD, CRLF3, CRYBA1, DHRS13, DPRXP4, EFCAB5, ERAL1, FAM222B, FLOT2, FOXN1, GIT1, GOSR1, H3F3BP2, IFT20, KIAA0100, KRT17P3, KRT18P55, MIR144, MIR423, MIR451A, MIR451B, MIR3184, MIR4523, MIR4723, MIR4732, MIR4733, MYO18A, NARR, NDUFS5P7, NEK8, NF1, NSRP1, NUFIP2, PHF12, PIGS, PIPOX, POLDIP2, PPY2, PROCA1, RAB34, RNF135, RNY4P13, RPL9P30, RPL21P123, RPL23A, RPL31P58, RPL35AP35, RPS7P1, RPS12P28, RPS17P3, SARM1, SDF2, SEBOX, SEZ6, SGK494, SH3GL1P2, SLC6A4, SLC13A2, SLC46A1, SNORD4A, SNORD4B, SNORD42A, SNORD42B, SPAG5, SPAG5-AS1, SSH2, STX18P1, SUPT6H, SUZ12P1, TAOK1, TBC1D29, TEFM, TIAF1, TLCD1, TMEM97, TMEM199, TMIGD1, TNFAIP1, TP53I13, TRAF4, TWF1P1, UNC119, VTN	6_2, 14_1, 14_2, 14_3, 14_4	4.55	5

20	q11.1 - q11.22	28.27 - 32.56	94	ACTL10, ASXL1, BAK1P1, BCL2L1, BPIFA1, BPIFA2, BPIFA3, BPIFA4P, BPIFB1, BPIFB2, BPIFB3, BPIFB4, BPIFB5P, BPIFB6, BPIFB9P, C20orf144, C20orf203, CBFA2T2, CCM2L, CD24P3, CDK5RAP1, CHMP4B, COMMD7, COX4I2, DEFB115, DEFB116, DEFB117, DEFB118, DEFB119, DEFB121, DEFB122, DEFB123, DEFB124, DKKL1P1, DNMT3B, DUSP15, E2F1, EFCAB8, FOXS1, FRG1B, HAUS6P2, HCK, HDHD1P3, HM13, HM13-AS1, ID1, KIF3B, LINC00028, MAPRE1, MCTS2P, MIR1825, MIR3193, MLLT10P1, MYLK2, NECAB3, NOL4L, PDRG1, PIGPP3, PLAGL2, POFUT1, PXMP4, REM1, RNA5SP480, RNA5SP481, RPL12P3, RPL31P2, RPL31P3, RSL24D1P6, SNTA1, SOCS2P1, SUN5, TM9SF4, TPM3P2, TPX2, TRS-AGA7-1, TSPY26P, TTLL9, XKR7, ZNF341, ZNF341-AS1	5_2, 6_1	4.55	2

Appendix 3.4: Recurrent regions of high-level amplification detected in all 66 tumours.

[1]Physical position is according to hg19/NCBI build 37.

[2]Amplifications were classified as those regions where the normalized $\log_2$ ratio was ≥1.2 detected in 2 or more tumours are listed.

[3]The frequency of gain across candidate regions was estimated as the percentage of samples with $\log_2$ratio ≥0.15

Appendix 3.5: Regions showing significant copy number differences in multifocal *FGFR3* wildtype (n=14) versus *FGFR3* mutant (n=8) tumours.

Region	Cytoband Location	Event	Region Length	Freq. in WT (%)	Freq. in Mutant (%)	Difference	p-value
chr7:84,591,194-97,101,588	q21.11 - q21.3	Gain	12510394	57.14	0	57.14	0.02
chr7:100,038,722-158,625,992	q22.1 - q36.3	Gain	58587270	57.14	0	57.14	0.02
chr8:132,638,132-133,156,783	q24.22	Gain	518651	64.29	12.5	51.79	0.03
chr8:134,255,043-142,612,553	q24.22 - q24.3	Gain	8357510	64.29	12.5	51.79	0.03
chr8:146,003,740-146,133,884	q24.3	Gain	130144	57.14	0	57.14	0.02
chr20:29,503,014-29,779,350	q11.21	Gain	276336	64.29	12.5	51.79	0.03

[1]Physical position is according to hg19/NCBI build 37

Appendix 4.1: Details of samples in the three main clusters obtained by hierarchical cluster analysis of copy number data from 66 tumours.

Tumour Number	Stage & grade	Primary/ Recurrent	FGA group	*FGFR3* Mutation Status	*PIK3CA* Mutation Status	RAS gene Mutation Status	Cluster
1_1	Ta G2	Recurrence	B	WT	MUTANT	WT	1
1_2	Ta G2	Recurrence	A	WT	MUTANT	WT	1
1_3	Ta G2	Recurrence	A	WT	WT	WT	1
5_1	Ta G2	Primary	A	MUTANT	WT	WT	1
8_1	Ta G2	Recurrence	A	MUTANT	MUTANT	WT	1
8_3	Ta G2	Recurrence	A	MUTANT	MUTANT	WT	1
9_1	T1 G3	Primary	A	WT	WT	WT	1
9_2	T1 G3	Primary	A	WT	WT	WT	1
13_4	Ta G3	Primary	A	WT	WT	WT	1
16_3	Ta G2	Recurrence	A	WT	WT	MUTANT	1

Tumour Number	**Stage & grade**	**Primary/ Recurrent**	**FGA group**	***FGFR3* Mutation Status**	***PIK3CA* Mutation Status**	***Ras* Mutation Status**	**Cluster**
16_4	Ta G2	Recurrence	A	WT	WT	MUTANT	1
17_1	Ta G2	Recurrence	B	MUTANT	MUTANT	WT	1
17_2	Ta G2	Recurrence	B	MUTANT	MUTANT	WT	1
17_3	Ta G2	Recurrence	B	MUTANT	MUTANT	WT	1
2_1	Ta G2	Recurrence	C	MUTANT	WT	WT	2
2_2	Ta G2	Recurrence	B	MUTANT	WT	WT	2
2_3	Ta G2	Recurrence	B	MUTANT	WT	WT	2
3_1	T1 G3	Recurrence	C	WT	WT	MUTANT	2
3_2	T1 G3	Recurrence	C	WT	WT	MUTANT	2
3_3	T1 G3	Recurrence	C	WT	WT	MUTANT	2
4_1	Ta G3	Recurrence	C	MUTANT	MUTANT	WT	2
4_2	Ta G3	Recurrence	B	MUTANT	MUTANT	WT	2
4_3	Ta G3	Recurrence	B	MUTANT	MUTANT	WT	2
4_4	Ta G3	Recurrence	B	MUTANT	MUTANT	WT	2

Tumour Number	**Stage & grade**	**Primary/ Recurrent**	**FGA group**	***FGFR3* Mutation Status**	***PIK3CA* Mutation Status**	***Ras* Mutation Status**	**Cluster**
4_5	Ta G3	Recurrence	B	MUTANT	MUTANT	WT	2
4_6	Ta G3	Recurrence	B	MUTANT	MUTANT	WT	2
7_1	Ta G2	Recurrence	C	WT	WT	WT	2
7_2	Ta G2	Recurrence	C	WT	WT	WT	2
8_2	Ta G2	Recurrence	C	MUTANT	MUTANT	WT	2
11_1	Ta G2	Recurrence	C	WT	WT	WT	2
11_2	T1 G3	Recurrence	C	WT	WT	WT	2
15_1	Ta G2	Primary	C	MUTANT	MUTANT	WT	2
15_2	Ta G2	Primary	B	MUTANT	MUTANT	WT	2
16_1	Ta G2	Recurrence	C	WT	WT	MUTANT	2
16_2	Ta G2	Recurrence	B	WT	WT	MUTANT	2
19_1	Ta G2	Primary	B	MUTANT	WT	WT	2
19_2	Ta G2	Primary	B	MUTANT	WT	WT	2
19_3	Ta G2	Primary	C	WT	WT	WT	2

Tumour Number	**Stage & grade**	**Primary/ Recurrent**	**FGA group**	***FGFR3* Mutation Status**	***PIK3CA* Mutation Status**	***Ras* Mutation Status**	**Cluster**
21_1	Ta G2	Recurrence	C	MUTANT	WT	WT	2
21_2	Ta G2	Recurrence	C	MUTANT	WT	WT	2
22_1	Ta G2	Primary	C	WT	WT	WT	2
22_2	Ta G2	Primary	B	WT	WT	WT	2
5_2	Ta G2	Primary	D	MUTANT	WT	WT	3
6_1	T1 G3	Primary	D	WT	WT	WT	3
6_2	T1 G3	Primary	D	WT	WT	WT	3
6_3	T1 G3	Primary	D	WT	WT	WT	3
10_1	Ta G3	Primary	C	WT	WT	WT	3
10_2	Ta G3	Primary	D	WT	WT	WT	3
12_1	T1 G3	Primary	D	WT	WT	WT	3
12_2	T1 G3	Primary	D	WT	WT	WT	3
12_3	T1 G3	Primary	D	WT	WT	WT	3

Tumour Number	**Stage & grade**	**Primary/ Recurrent**	**FGA group**	***FGFR3* Mutation Status**	***PIK3CA* Mutation Status**	***Ras* Mutation Status**	**Cluster**
12_4	Ta G3	Primary	D	WT	WT	WT	3
13_1	Ta G3	Primary	D	WT	WT	WT	3
13_2	Ta G3	Primary	D	WT	WT	WT	3
13_3	Ta G3	Primary	D	WT	WT	WT	3
14_1	Ta G3	Primary	D	WT	WT	WT	3
14_2	Ta G3	Primary	D	WT	WT	WT	3
14_3	Ta G3	Primary	D	WT	WT	WT	3
14_4	Ta G3	Primary	D	WT	WT	WT	3
18_1	T1 G3	Primary	D	WT	WT	WT	3
18_2	T1 G3	Primary	D	WT	WT	WT	3
18_3	T1 G3	Primary	D	WT	WT	WT	3
18_4	T1 G3	Primary	D	WT	WT	WT	3
20_1	Ta G2	Primary	D	WT	WT	WT	3
20_2	T1 G3	Primary	D	WT	WT	WT	3

Tumour Number	**Stage & grade**	**Primary/ Recurrent**	**FGA group**	***FGFR3*** **Mutation Status**	***PIK3CA*** **Mutation Status**	***Ras*** **Mutation Status**	**Cluster**
20_3	T1 G3	Primary	D	WT	WT	WT	3

Appendix 4.1B: Candidate genes in a minimal region of copy number loss extending from 2q24-2q27.3 (214.9-242.1 Mb) in multifocal tumours from Cluster 3.

AAMP, ABCA12, ABCB6, ACKR3, ACSL3, AGAP1, AGAP1-IT1, AGFG1, AGXT, ALPI, ALPP, ALPPL2, ANKMY1, ANKZF1, AP1S3, AQP12A, AQP12B, ARL4C, ARMC9, ARPC2, ASB1, ASB18, ASIC4, ATG9A, ATG12P2, ATG16L1, ATIC, B3GNT7, BANF1P3, BARD1, BCS1L, C2orf54, C2orf57, C2orf72, C2orf82, C2orf83, CAB39, CAPN10, CAPN10-AS1, CATIP, CATIP-AS1, CCDC108, CCDC140, CCL20, CDK5R2, CHPF, CHRND, CHRNG, CNPPD1, COL4A3, COL4A4, COL6A3, COPS7B, COPS8, COX20P2, CRYBA2, CTDSP1, CUL3, CXCR1, CXCR2, CXCR2P1, CYP27A1, DAW1, DES, DGKD, DIRC3, DIS3L2, DIS3L2P1, DNAJB2, DNAJB3, DNER, DNPEP, DOCK10, DUSP28, ECEL1, ECEL1P2, ECEL1P3, EFHD1, EIF4E2, ENSAP3, EPHA4, ESPNL, FABP5P14, FAM124B, FAM132B, FAM134A, FARSB, FBXO36, FEV, FLJ43879, FN1, GAMTP1, GAPDHP49, GBX2, GIGYF2, GLB1L, GMPPA, GPBAR1, GPC1, GPR35, GPR55, HDAC4, HES6, HIGD1AP4, HJURP, HMGB1P3, HMGB1P9, HSPA8P10, HSPA9P1, HTR2B, IGFBP2, IGFBP5, IHH, ILKAP, INHA, INPP5D, IQCA1, IRS1, ITM2C, KCNE4, KCNJ13, KIF1A, KLHL30, KRT8P30, LINC00471, LINC00607, LINC00608, LINC01107, LINC01280, LINC01494, LRRFIP1, MARCH4, MFF, MGC16025, MIR26B, MIR149, MIR153-1, MIR375, MIR562, MIR1244-1, MIR1471, MIR2467, MIR3131, MIR3132, MIR4268, MIR4269, MIR4439, MIR4440, MIR4441, MIR4777, MIR4786, MIR5001, MIR5702, MIR5703, MLPH, MOGAT1, MREG, MROH2A, MRPL44, MSL3P1, MTERF4, MYEOV2, NANOGP2, NCL, NDUFA10, NEU2, NGEF, NHEJ1, NMUR1, NPPC, NYAP2, OBSL1, OR5S1P, OR6B2, OR6B3, OR9S24P, OTOS, PASK, PAX3, PDE6D, PECR, PER2, PID1, PKI55, PLCD4, PNKD, PP14571, PPP1R7, PRKAG3, PRLH, PRR21, PRSS56, PSMB3P2, PSMD1, PTMA, PTPRN, RAB17, RAMP1, RBM44, RESP18, RHBDD1, RNA5SP120, RNA5SP121, RNF25, RNPEPL1, RNY4P19, RPL3P5, RPL5P8, RPL7L1P9, RPL10P6, RPL17P11, RPL17P14, RPL19P5, RPL21P35, RPL23AP26, RPL23AP28, RPL23AP31, RPL23P4, RPL23P5, RPL28P2, RPL31P14, RPL31P17, RPL37A, RPS20P12, RPS28P4, RQCD1, RUFY4, SAG, SCARNA5, SCARNA6, SCG2, SCLY, SERPINE2, SGPP2, SH3BP4, SLC4A3, SLC11A1, SLC16A14, SLC19A3, SLC23A3, SMARCAL1, SNED1, SNORA75, SNORD20, SNORD82, SNRPGP8, SP100, SP110, SP140, SP140L, SPAG16, SPATA3, SPATA3-AS1, SPEG, SPHKAP, SPP2, STIP1P2, STK11IP, STK16, STK36, TDGF1P2, TIGD1, TM4SF20, TMBIM1, TMEM169, TMEM198, TMSB10P1, TNP1, TNS1, TPM3P8, TRAF3IP1, TRIP12, TRK-TTT15-1, TRPM8, TRQ-CTG16-1, TRY-ATA1-1, TTLL4, TUBA4A, TUBA4B, TWIST2, UBE2F, UBE2F-SCLY, UGT1A, UGT1A1, UGT1A2P, UGT1A3, UGT1A4, UGT1A5, UGT1A6, UGT1A7, UGT1A8, UGT1A9, UGT1A10, UGT1A11P, UGT1A12P, UGT1A13P, USP37, USP40, VIL1, VWC2L, VWC2L-IT1, WDFY1, WNT6, WNT10A, XRCC5, ZBTB8OSP2, ZFAND2B, ZNF142

Appendix 4.2 Regions showing significant copy number differences in multifocal tumours from cluster 1 (n=14) versus cluster 2 (n=8).

Region[1]	Cytoband Location	Event	Region Length	Freq. in Cluster 2 (%)	Freq. in Cluster 1 (%)	Difference	p-value
chr1:1,144,379-38,051,746	p36.33 - p34.3	Gain	36907367	62.5	7.14	55.36	0.0109
chr1:113,473,675-119,480,610	p13.2 - p12	Gain	6006935	62.5	0.00	62.50	0.0021
chr1:119,480,610-119,708,536	p12	Gain	227926	87.5	0.00	87.50	0.0000
chr1:119,708,536-148,424,834	p12 - q21.2	Gain	28716298	87.5	21.43	66.07	0.0062
chr1:148,424,834-157,241,521	q21.2 - q23.1	Gain	8816687	75.0	21.43	53.57	0.0260
chr1:167,621,290-169,324,707	q24.2 - q24.3	Gain	1703417	75.0	21.43	53.57	0.0260
chr1:185,614,023-191,477,703	q31.1 - q31.2	Loss	5863680	37.5	0.00	37.50	0.0364
chr1:192,424,789-197,774,987	q31.3 - q32.1	Loss	5350198	37.5	0.00	37.50	0.0364
chr1:234,285,489-246,181,016	q42.3 - q44	Loss	11895527	37.5	0.00	37.50	0.0364
chr1:242,491,517-247,029,735	q44	Gain	4538218	50.0	7.14	42.86	0.0393
chr1:246,181,016-247,164,041	q44	Loss	983025	50.0	0.00	50.00	0.0096
chr1:38,051,746-48,917,318	p34.3 - p33	Gain	10865572	75.0	7.14	67.86	0.0023
chr1:48,917,318-50,594,589	p33	Gain	1677271	75.0	0.00	75.00	0.0004
chr1:50,594,589-50,823,305	p33	Gain	228716	62.5	0.00	62.50	0.0021
chr1:50,823,305-53,509,194	p33 - p32.3	Gain	2685889	75.0	7.14	67.86	0.0023
chr1:53,509,194-68,609,865	p32.3 - p31.3	Gain	15100671	75.0	0.00	75.00	0.0004
chr1:68,609,865-73,625,895	p31.3 - p31.1	Gain	5016030	62.5	0.00	62.50	0.0021
chr1:73,625,895-83,494,525	p31.1	Gain	9868630	50.0	0.00	50.00	0.0096
chr1:83,678,458-95,929,212	p31.1 - p21.3	Gain	12250754	37.5	0.00	37.50	0.0364
chr1:918,164-1,144,379	p36.33	Gain	226215	50.0	7.14	42.86	0.0393
chr1:95,929,212-113,473,675	p21.3 - p13.2	Gain	17544463	50.0	0.00	50.00	0.0096
chr10:103,282,021-104,340,398	q24.32	Loss	1058377	87.5	28.57	58.93	0.0237
chr10:104,340,398-104,342,397	q24.32	Loss	1999	87.5	21.43	66.07	0.0062
chr10:104,342,397-104,652,460	q24.32	Loss	310063	87.5	28.57	58.93	0.0237
chr10:104,652,460-109,290,751	q24.32 - q25.1	Loss	4638291	87.5	21.43	66.07	0.0062
chr10:109,290,751-116,774,295	q25.1 - q25.3	Loss	7483544	87.5	14.29	73.21	0.0015
chr10:116,774,295-122,467,467	q25.3 - q26.12	Loss	5693172	75.0	14.29	60.71	0.0083

chr10:122,467,970-125,057,698	q26.12 - q26.13	Loss	2589728	75.0	14.29	60.71	0.0083
chr10:125,057,698-130,095,088	q26.13 - q26.2	Loss	5037390	75.0	0.00	75.00	0.0004
chr10:130,095,088-131,816,154	q26.2 - q26.3	Loss	1721066	75.0	7.14	67.86	0.0023
chr10:131,816,154-131,982,049	q26.3	Loss	165895	62.5	7.14	55.36	0.0109
chr10:131,982,049-135,247,831	q26.3	Loss	3265782	75.0	7.14	67.86	0.0023
chr10:38,812,575-52,328,336	p11.1 - q11.23	Loss	13515761	37.5	0.00	37.50	0.0364
chr10:52,328,336-56,882,157	q11.23 - q21.1	Loss	4553821	50.0	0.00	50.00	0.0096
chr10:56,882,157-59,005,947	q21.1	Loss	2123790	50.0	7.14	42.86	0.0393
chr10:59,005,947-62,853,055	q21.1 - q21.2	Loss	3847108	50.0	0.00	50.00	0.0096
chr10:62,853,055-68,138,624	q21.2 - q21.3	Loss	5285569	37.5	0.00	37.50	0.0364
chr10:78,996,385-80,472,830	q22.3	Loss	1476445	50.0	7.14	42.86	0.0393
chr10:80,472,830-83,637,155	q22.3 - q23.1	Loss	3164325	50.0	0.00	50.00	0.0096
chr10:83,637,155-84,577,760	q23.1	Loss	940605	50.0	7.14	42.86	0.0393
chr10:84,577,760-85,567,652	q23.1	Loss	989892	62.5	7.14	55.36	0.0109
chr10:85,567,652-86,390,131	q23.1	Loss	822479	62.5	0.00	62.50	0.0021
chr10:86,390,131-88,222,653	q23.1 - q23.2	Loss	1832522	75.0	0.00	75.00	0.0004
chr10:88,222,653-89,694,469	q23.2 - q23.31	Loss	1471816	87.5	14.29	73.21	0.0015
chr10:89,694,469-89,694,975	q23.31	Loss	506	87.5	0.00	87.50	0.00005
chr10:89,694,975-93,738,544	q23.31 - q23.32	Loss	4043569	87.5	14.29	73.21	0.0015
chr10:93,738,544-94,907,303	q23.32 - q23.33	Loss	1168759	75.0	14.29	60.71	0.0083
chr10:94,907,303-99,781,492	q23.33 - q24.2	Loss	4874189	87.5	14.29	73.21	0.0015
chr10:99,781,492-103,282,021	q24.2 - q24.32	Loss	3500529	87.5	21.43	66.07	0.0062
chr11:1,785,273-9,667,022	p15.5 - p15.4	Loss	7881749	50.0	7.14	42.86	0.0393
chr11:107,722,054-115,161,463	q22.3 - q23.2	Loss	7439409	50.0	7.14	42.86	0.0393
chr11:123,449,312-131,065,134	q24.1 - q25	Loss	7615822	50.0	7.14	42.86	0.0393
chr11:131,065,134-133,984,028	q25	Loss	2918894	62.5	7.14	55.36	0.0109
chr11:133,984,028-134,156,487	q25	Loss	172459	62.5	0.00	62.50	0.0021
chr11:178,227-267,210	p15.5	Loss	88983	37.5	0.00	37.50	0.0364
chr11:24,362,912-37,838,885	p14.3 - p12	Loss	13475973	50.0	0.00	50.00	0.0096
chr11:37,838,885-40,185,000	p12	Loss	2346115	50.0	7.14	42.86	0.0393
chr11:40,185,000-43,020,941	p12	Loss	2835941	50.0	0.00	50.00	0.0096
chr11:43,020,941-50,013,069	p12 - p11.12	Loss	6992128	62.5	0.00	62.50	0.0021
chr11:50,013,069-60,851,894	p11.12 - q12.2	Loss	10838825	50.0	0.00	50.00	0.0096
chr11:60,851,894-63,843,056	q12.2 - q13.1	Loss	2991162	37.5	0.00	37.50	0.0364

chr11:76,232,396-81,301,979	q13.5 - q14.1	Gain	5069583	37.5	0.00	37.50	0.0364
chr12:103,714,143-111,697,547	q23.3 - q24.13	Loss	7983404	37.5	0.00	37.50	0.0364
chr12:11,018,640-14,521,944	p13.2 - p13.1	Gain	3503304	37.5	0.00	37.50	0.0364
chr12:129,839,417-132,272,931	q24.33	Loss	2433514	37.5	0.00	37.50	0.0364
chr12:152,534-3,099,629	p13.33	Gain	2947095	37.5	0.00	37.50	0.0364
chr12:33,333,489-40,716,974	p11.1 - q12	Loss	7383485	37.5	0.00	37.50	0.0364
chr12:40,716,974-42,413,160	q12	Loss	1696186	50.0	0.00	50.00	0.0096
chr12:42,413,160-46,156,911	q12 - q13.11	Loss	3743751	37.5	0.00	37.50	0.0364
chr13:31,870,598-36,083,776	q13.1 - q13.3	Loss	4213178	37.5	0.00	37.50	0.0364
chr14:26,561,378-26,744,993	q12	Loss	183615	37.5	0.00	37.50	0.0364
chr14:26,744,993-38,933,843	q12 - q21.1	Loss	12188850	50.0	0.00	50.00	0.0096
chr14:38,933,843-40,363,695	q21.1	Loss	1429852	50.0	7.14	42.86	0.0393
chr14:40,363,695-57,420,120	q21.1 - q23.1	Loss	17056425	50.0	0.00	50.00	0.0096
chr14:57,420,120-58,323,469	q23.1	Loss	903349	75.0	0.00	75.00	0.0004
chr14:58,323,469-58,470,270	q23.1	Loss	146801	62.5	0.00	62.50	0.0021
chr14:58,470,270-59,336,011	q23.1	Loss	865741	75.0	0.00	75.00	0.0004
chr14:59,336,011-65,655,482	q23.1 - q23.3	Loss	6319471	50.0	0.00	50.00	0.0096
chr14:65,655,482-66,870,415	q23.3	Loss	1214933	37.5	0.00	37.50	0.0364
chr14:66,870,415-71,308,003	q23.3 - q24.2	Loss	4437588	50.0	0.00	50.00	0.0096
chr14:71,308,003-74,588,657	q24.2 - q24.3	Loss	3280654	62.5	0.00	62.50	0.0021
chr14:74,588,657-81,191,238	q24.3 - q31.1	Loss	6602581	50.0	0.00	50.00	0.0096
chr14:81,191,238-94,901,754	q31.1 - q32.13	Loss	13710516	37.5	0.00	37.50	0.0364
chr15:20,363,717-22,736,034	q11.2	Gain	2372317	50.0	7.14	42.86	0.0393
chr15:22,894,833-62,510,397	q11.2 - q22.31	Loss	39615564	37.5	0.00	37.50	0.0364
chr15:42,756,125-56,535,071	q21.1 - q22.1	Gain	13778946	50.0	7.14	42.86	0.0393
chr15:62,510,397-82,907,017	q22.31 - q25.2	Loss	20396620	50.0	0.00	50.00	0.0096
chr15:82,907,017-83,883,618	q25.2 - q25.3	Loss	976601	37.5	0.00	37.50	0.0364
chr15:83,883,618-87,527,174	q25.3 - q26.1	Loss	3643556	50.0	0.00	50.00	0.0096
chr15:87,527,174-89,307,983	q26.1	Loss	1780809	50.0	7.14	42.86	0.0393
chr15:89,307,983-100,022,043	q26.1 - q26.3	Loss	10714060	50.0	0.00	50.00	0.0096
chr16:23,756,350-31,190,651	p12.1 - p11.2	Gain	7434301	50.0	0.00	50.00	0.0096
chr16:31,190,651-45,067,244	p11.2 - q11.2	Gain	13876593	62.5	0.00	62.50	0.0021
chr16:33,715,230-45,231,075	p11.2 - q11.2	Loss	11515845	37.5	0.00	37.50	0.0364
chr16:45,231,075-63,462,907	q11.2 - q21	Loss	18231832	50.0	0.00	50.00	0.0096

chr16:63,462,907-82,569,517	q21 - q23.3	Loss	19106610	37.5	0.00	37.50	0.0364
chr16:7,019,846-23,756,350	p13.2 - p12.1	Gain	16736504	37.5	0.00	37.50	0.0364
chr16:88,421,159-88,552,007	q24.3	Loss	130848	37.5	0.00	37.50	0.0364
chr17:12,108,967-14,364,543	p12	Gain	2255576	37.5	0.00	37.50	0.0364
chr17:20,230,301-22,465,647	p11.2 - q11.1	Gain	2235346	37.5	0.00	37.50	0.0364
chr17:26,575,095-28,423,748	q11.2	Gain	1848653	50.0	7.14	42.86	0.0393
chr17:28,423,748-29,512,898	q11.2 - q12	Gain	1089150	62.5	7.14	55.36	0.0109
chr17:29,512,898-33,099,942	q12	Gain	3587044	50.0	7.14	42.86	0.0393
chr17:35,682,018-38,327,610	q21.2 - q21.31	Gain	2645592	37.5	0.00	37.50	0.0364
chr17:52,172,780-62,246,742	q22 - q24.2	Gain	10073962	50.0	7.14	42.86	0.0393
chr17:62,246,742-66,194,639	q24.2 - q24.3	Gain	3947897	62.5	7.14	55.36	0.0109
chr17:66,194,639-67,327,134	q24.3	Gain	1132495	50.0	7.14	42.86	0.0393
chr17:67,327,134-68,199,396	q24.3	Gain	872262	62.5	7.14	55.36	0.0109
chr17:68,199,396-76,183,573	q24.3 - q25.3	Gain	7984177	50.0	7.14	42.86	0.0393
chr17:77,729,550-78,374,103	q25.3	Gain	644553	37.5	0.00	37.50	0.0364
chr18:130,336-2,479,744	p11.32	Gain	2349408	50.0	0.00	50.00	0.0096
chr18:2,479,744-6,213,636	p11.32 - p11.31	Gain	3733892	37.5	0.00	37.50	0.0364
chr18:6,933,612-9,449,205	p11.31 - p11.22	Gain	2515593	37.5	0.00	37.50	0.0364
chr19:211,322-6,523,485	p13.3	Loss	6312163	50.0	7.14	42.86	0.0393
chr2:123,095,058-127,253,875	q14.3	Loss	4158817	50.0	7.14	42.86	0.0393
chr2:127,253,875-136,875,479	q14.3 - q22.1	Loss	9621604	62.5	7.14	55.36	0.0109
chr2:136,875,479-142,876,374	q22.1 - q22.2	Loss	6000895	62.5	0.00	62.50	0.0021
chr2:142,876,374-151,825,968	q22.2 - q23.3	Loss	8949594	62.5	7.14	55.36	0.0109
chr2:151,825,968-152,428,325	q23.3	Loss	602357	50.0	7.14	42.86	0.0393
chr2:152,428,325-153,751,686	q23.3	Loss	1323361	50.0	0.00	50.00	0.0096
chr2:153,751,686-156,410,442	q23.3 - q24.1	Loss	2658756	62.5	0.00	62.50	0.0021
chr2:156,410,442-169,397,061	q24.1 - q24.3	Loss	12986619	50.0	0.00	50.00	0.0096
chr2:157,250,015-165,687,734	q24.1 - q24.3	Gain	8437719	37.5	0.00	37.50	0.0364
chr2:169,397,061-175,231,393	q24.3 - q31.1	Loss	5834332	62.5	0.00	62.50	0.0021
chr2:175,231,393-176,870,358	q31.1	Loss	1638965	75.0	0.00	75.00	0.0004
chr2:176,870,358-183,311,858	q31.1 - q32.1	Loss	6441500	62.5	0.00	62.50	0.0021
chr2:183,311,858-195,231,804	q32.1 - q32.3	Loss	11919946	75.0	0.00	75.00	0.0004
chr2:193,940,783-196,538,333	q32.3	Gain	2597550	37.5	0.00	37.50	0.0364
chr2:195,231,804-196,753,496	q32.3	Loss	1521692	62.5	0.00	62.50	0.0021

chr2:196,753,496-208,876,525	q32.3 - q33.3	Loss	12123029	75.0	0.00	75.00	0.0004
chr2:20,037,859-20,215,537	p24.1	Gain	177678	50.0	0.00	50.00	0.0096
chr2:20,215,537-21,280,646	p24.1	Gain	1065109	62.5	0.00	62.50	0.0021
chr2:208,876,525-227,205,229	q33.3 - q36.3	Loss	18328704	100.0	0.00	100.00	0.000003
chr2:21,280,646-25,870,821	p24.1 - p23.3	Gain	4590175	50.0	0.00	50.00	0.0096
chr2:224,263-20,037,859	p25.3 - p24.1	Gain	19813596	62.5	0.00	62.50	0.0021
chr2:227,205,229-228,542,036	q36.3	Loss	1336807	100.0	7.14	92.86	0.00003
chr2:228,542,036-232,368,564	q36.3 - q37.1	Loss	3826528	100.0	14.29	85.71	0.0001
chr2:232,368,564-232,541,867	q37.1	Loss	173303	100.0	7.14	92.86	0.00003
chr2:232,541,867-232,987,278	q37.1	Loss	445411	100.0	14.29	85.71	0.0001
chr2:232,987,278-241,796,109	q37.1 - q37.3	Loss	8808831	100.0	7.14	92.86	0.00003
chr2:25,870,821-52,373,212	p23.3 - p16.3	Gain	26502391	62.5	0.00	62.50	0.0021
chr2:52,373,212-53,101,240	p16.3 - p16.2	Gain	728028	62.5	7.14	55.36	0.0109
chr2:64,478,283-69,024,185	p14	Gain	4545902	62.5	0.00	62.50	0.0021
chr2:69,024,185-71,285,149	p14 - p13.3	Gain	2260964	62.5	7.14	55.36	0.0109
chr2:74,335,462-88,214,979	p13.1 - p11.2	Gain	13879517	62.5	0.00	62.50	0.0021
chr2:88,214,979-94,782,159	p11.2 - q11.1	Gain	6567180	75.0	0.00	75.00	0.0004
chr2:94,782,159-95,675,764	q11.1	Gain	893605	50.0	0.00	50.00	0.0096
chr2:94,983,765-123,095,058	q11.1 - q14.3	Loss	28111293	50.0	0.00	50.00	0.0096
chr2:96,200,121-97,472,556	q11.2	Gain	1272435	37.5	0.00	37.50	0.0364
chr20:26,220,344-29,503,014	p11.1 - q11.21	Gain	3282670	100.0	21.43	78.57	0.0010
chr20:275,014-26,220,344	p13 - p11.1	Gain	25945330	87.5	21.43	66.07	0.0062
chr20:29,503,014-29,779,350	q11.21	Gain	276336	87.5	21.43	66.07	0.0062
chr20:29,779,350-30,102,016	q11.21	Gain	322666	100.0	21.43	78.57	0.0010
chr20:30,102,016-34,346,661	q11.21 - q11.23	Gain	4244645	100.0	28.57	71.43	0.0017
chr20:34,346,661-35,931,146	q11.23	Gain	1584485	100.0	35.71	64.29	0.0055
chr20:35,931,146-37,522,311	q11.23 - q12	Gain	1591165	100.0	42.86	57.14	0.0177
chr20:37,522,311-37,666,045	q12	Gain	143734	100.0	35.71	64.29	0.0055
chr20:37,666,045-40,680,814	q12	Gain	3014769	100.0	42.86	57.14	0.0177
chr20:40,680,814-45,646,214	q12 - q13.12	Gain	4965400	100.0	35.71	64.29	0.0055
chr20:45,646,214-47,243,628	q13.12 - q13.13	Gain	1597414	87.5	35.71	51.79	0.0310
chr20:47,243,628-47,383,084	q13.13	Gain	139456	100.0	35.71	64.29	0.0055
chr20:47,538,301-59,894,661	q13.13 - q13.33	Gain	12356360	100.0	35.71	64.29	0.0055
chr20:59,894,661-62,392,510	q13.33	Gain	2497849	87.5	35.71	51.79	0.0310

chr22:15,621,248-15,745,966	q11.1	Loss	124718	50.0	0.00	50.00	0.0096
chr22:15,745,966-16,347,244	q11.1 - q11.21	Loss	601278	62.5	7.14	55.36	0.0109
chr22:16,347,244-16,899,186	q11.21	Loss	551942	50.0	7.14	42.86	0.0393
chr22:16,899,186-18,151,355	q11.21	Loss	1252169	50.0	0.00	50.00	0.0096
chr22:18,151,355-18,151,891	q11.21	Loss	536	37.5	0.00	37.50	0.0364
chr22:18,151,891-30,032,831	q11.21 - q12.2	Loss	11880940	50.0	0.00	50.00	0.0096
chr22:30,032,831-30,535,980	q12.2 - q12.3	Loss	503149	62.5	0.00	62.50	0.0021
chr22:30,535,980-30,623,768	q12.3	Loss	87788	50.0	0.00	50.00	0.0096
chr22:30,623,768-30,623,867	q12.3	Loss	99	37.5	0.00	37.50	0.0364
chr22:30,623,867-30,646,302	q12.3	Loss	22435	50.0	7.14	42.86	0.0393
chr22:30,646,302-30,646,401	q12.3	Loss	99	37.5	0.00	37.50	0.0364
chr22:30,646,401-40,803,595	q12.3 - q13.2	Loss	10157194	50.0	0.00	50.00	0.0096
chr22:40,803,595-42,473,589	q13.2	Loss	1669994	50.0	7.14	42.86	0.0393
chr22:42,473,589-44,175,906	q13.2 - q13.31	Loss	1702317	50.0	0.00	50.00	0.0096
chr22:44,175,906-49,453,810	q13.31 - q13.33	Loss	5277904	62.5	0.00	62.50	0.0021
chr3:14,886,339-44,567,516	p24.3 - p21.32	Gain	29681177	50.0	0.00	50.00	0.0096
chr3:169,732,146-170,729,895	q26.2	Gain	997749	50.0	7.14	42.86	0.0393
chr3:179,511,139-179,653,380	q26.32	Gain	142241	50.0	7.14	42.86	0.0393
chr3:180,293,412-181,647,155	q26.32 - q26.33	Gain	1353743	50.0	7.14	42.86	0.0393
chr3:186,817-958,261	p26.3	Gain	771444	50.0	0.00	50.00	0.0096
chr3:190,563,330-199,160,165	q28 - q29	Gain	8596835	50.0	7.14	42.86	0.0393
chr3:44,567,516-54,188,434	p21.32 - p21.1	Gain	9620918	37.5	0.00	37.50	0.0364
chr3:54,188,434-74,391,234	p21.1 - p12.3	Gain	20202800	50.0	0.00	50.00	0.0096
chr3:74,391,234-82,655,862	p12.3 - p12.2	Gain	8264628	62.5	0.00	62.50	0.0021
chr3:82,655,862-82,799,401	p12.2	Gain	143539	50.0	0.00	50.00	0.0096
chr3:82,799,401-87,044,540	p12.2 - p12.1	Gain	4245139	62.5	0.00	62.50	0.0021
chr3:87,044,540-169,732,146	p12.1 - q26.2	Gain	82687606	50.0	0.00	50.00	0.0096
chr3:958,261-14,886,339	p26.3 - p24.3	Gain	13928078	62.5	0.00	62.50	0.0021
chr4:1,065,598-1,784,503	p16.3	Loss	718905	50.0	0.00	50.00	0.0096
chr4:1,784,503-10,207,878	p16.3 - p16.1	Loss	8423375	50.0	7.14	42.86	0.0393
chr4:10,207,878-11,429,778	p16.1 - p15.33	Loss	1221900	50.0	0.00	50.00	0.0096
chr4:11,429,778-13,655,289	p15.33	Loss	2225511	37.5	0.00	37.50	0.0364
chr4:113,578,539-182,025,739	q25 - q34.3	Loss	68447200	50.0	0.00	50.00	0.0096
chr4:13,655,289-26,747,433	p15.33 - p15.2	Loss	13092144	50.0	0.00	50.00	0.0096

chr4:182,025,739-184,561,840	q34.3 - q35.1	Loss	2536101	37.5	0.00	37.50	0.0364
chr4:184,561,840-191,020,215	q35.1 - q35.2	Loss	6458375	50.0	0.00	50.00	0.0096
chr4:26,747,433-45,608,190	p15.2 - p12	Loss	18860757	62.5	0.00	62.50	0.0021
chr4:45,608,190-47,677,803	p12	Loss	2069613	50.0	0.00	50.00	0.0096
chr4:47,677,803-48,524,316	p12	Loss	846513	37.5	0.00	37.50	0.0364
chr4:55,628-1,065,598	p16.3	Loss	1009970	62.5	0.00	62.50	0.0021
chr4:80,547,099-113,578,539	q21.21 - q25	Loss	33031440	37.5	0.00	37.50	0.0364
chr5:107,339,380-136,366,234	q21.3 - q31.2	Loss	29026854	50.0	0.00	50.00	0.0096
chr5:12,216,435-12,262,939	p15.2	Gain	46504	50.0	7.14	42.86	0.0393
chr5:12,262,939-13,218,128	p15.2	Gain	955189	62.5	7.14	55.36	0.0109
chr5:13,218,128-16,546,966	p15.2 - p15.1	Gain	3328838	50.0	7.14	42.86	0.0393
chr5:136,366,234-148,846,264	q31.2 - q33.1	Loss	12480030	50.0	7.14	42.86	0.0393
chr5:16,546,966-22,468,834	p15.1 - p14.3	Gain	5921868	62.5	7.14	55.36	0.0109
chr5:2,570,762-7,530,112	p15.33 - p15.31	Gain	4959350	62.5	0.00	62.50	0.0021
chr5:22,468,834-25,187,412	p14.3 - p14.1	Gain	2718578	75.0	7.14	67.86	0.0023
chr5:25,187,412-26,353,486	p14.1	Gain	1166074	75.0	0.00	75.00	0.0004
chr5:26,353,486-26,539,834	p14.1	Gain	186348	62.5	0.00	62.50	0.0021
chr5:26,539,834-35,388,213	p14.1 - p13.2	Gain	8848379	75.0	0.00	75.00	0.0004
chr5:35,388,213-49,907,782	p13.2 - q11.1	Gain	14519569	62.5	0.00	62.50	0.0021
chr5:50,093,906-50,168,170	q11.1	Loss	74264	50.0	0.00	50.00	0.0096
chr5:50,168,170-51,232,444	q11.1 - q11.2	Loss	1064274	62.5	0.00	62.50	0.0021
chr5:51,232,444-65,239,073	q11.2 - q12.3	Loss	14006629	75.0	0.00	75.00	0.0004
chr5:65,239,073-65,352,862	q12.3	Loss	113789	75.0	7.14	67.86	0.0023
chr5:65,352,862-66,695,993	q12.3 - q13.1	Loss	1343131	62.5	7.14	55.36	0.0109
chr5:66,695,993-75,600,638	q13.1 - q13.3	Loss	8904645	62.5	0.00	62.50	0.0021
chr5:7,530,112-12,216,435	p15.31 - p15.2	Gain	4686323	62.5	7.14	55.36	0.0109
chr5:75,600,638-79,219,538	q13.3 - q14.1	Loss	3618900	50.0	0.00	50.00	0.0096
chr5:79,219,538-79,936,331	q14.1	Loss	716793	62.5	0.00	62.50	0.0021
chr5:79,936,331-97,113,079	q14.1 - q15	Loss	17176748	50.0	0.00	50.00	0.0096
chr5:97,113,079-99,111,442	q15 - q21.1	Loss	1998363	50.0	7.14	42.86	0.0393
chr6:146,266,178-162,794,027	q24.3 - q26	Loss	16527849	37.5	0.00	37.50	0.0364
chr6:163,005,402-165,244,688	q26 - q27	Loss	2239286	37.5	0.00	37.50	0.0364
chr6:6,382,300-7,427,280	p25.1 - p24.3	Gain	1044980	50.0	7.14	42.86	0.0393
chr7:100,038,722-158,625,992	q22.1 - q36.3	Gain	58587270	75.0	14.29	60.71	0.0083

chr7:12,919,070-13,079,613	p21.3	Gain	160543	37.5	0.00	37.50	0.0364
chr7:13,079,613-15,056,488	p21.3 - p21.2	Gain	1976875	50.0	0.00	50.00	0.0096
chr7:15,056,488-21,588,275	p21.2 - p15.3	Gain	6531787	62.5	0.00	62.50	0.0021
chr7:188,219-12,919,070	p22.3 - p21.3	Gain	12730851	50.0	0.00	50.00	0.0096
chr7:21,588,275-26,749,335	p15.3 - p15.2	Gain	5161060	50.0	0.00	50.00	0.0096
chr7:26,749,335-29,450,068	p15.2 - p15.1	Gain	2700733	62.5	0.00	62.50	0.0021
chr7:29,450,068-32,275,005	p15.1 - p14.3	Gain	2824937	50.0	0.00	50.00	0.0096
chr7:32,275,005-45,048,865	p14.3 - p13	Gain	12773860	37.5	0.00	37.50	0.0364
chr7:45,048,865-50,617,642	p13 - p12.2	Gain	5568777	50.0	0.00	50.00	0.0096
chr7:50,617,642-63,102,874	p12.2 - q11.21	Gain	12485232	62.5	0.00	62.50	0.0021
chr7:63,102,874-84,591,194	q11.21 - q21.11	Gain	21488320	75.0	0.00	75.00	0.0004
chr7:84,591,194-97,101,588	q21.11 - q21.3	Gain	12510394	75.0	14.29	60.71	0.0083
chr7:97,101,588-100,038,722	q21.3 - q22.1	Gain	2937134	75.0	0.00	75.00	0.0004
chr9:11,341,967-20,172,465	p23 - p21.3	Loss	8830498	87.5	28.57	58.93	0.0237
chr9:20,172,465-20,351,121	p21.3	Loss	178656	87.5	21.43	66.07	0.0062
chr9:20,351,121-21,158,452	p21.3	Loss	807331	87.5	28.57	58.93	0.0237
chr9:24,090,721-25,069,382	p21.3	Loss	978661	87.5	21.43	66.07	0.0062
chr9:25,069,382-30,699,255	p21.3 - p21.1	Loss	5629873	87.5	28.57	58.93	0.0237

[1]Physical position is according to hg19/NCBI build 37

Chromosome	Cytoband	Position (Mb)[1]	Region length	Freq. in cluster 2 (%)	Freq. in cluster 1 (%)	Difference	Number of Genes	Candidate genes
2	208.88 - 227.21	q33.3 - q36.3	18328704	100	0	100	122	MARCH4, AAMP, ABCA12, ABCB6, ACADL, ACSL3, ANKZF1, AP1S3, ARPC2, ASIC4, ATG9A, ATG12P2, ATIC, BARD1, BCS1L, C2orf80, CATIP, CATIP-AS1, CCDC108, CCDC140, CDK5R2, CHPF, CNPPD1, CPS1, CPS1-IT1, CRYBA2, CRYGA, CRYGB, CRYGC, CRYGD, CRYGEP, CRYGFP, CTDSP1, CUL3, CXCR1, CXCR2, CXCR2P1, CYP27A1, DES, DIRC3, DNAJB2, DNPEP, DOCK10, ENSAP3, EPHA4, ERBB4, FABP5P14, FAM124B, FAM134A, FARSB, FEV, FN1, GAPDHP49, GLB1L, GMPPA, GPBAR1, HIGD1AP4, HMGB1P9, HSPA8P6, HSPA9P1, IDH1, IDH1-AS1, IGFBP2, IGFBP5, IHH, IKZF2, INHA, KANSL1L, KCNE4, KRT8P30, LANCL1, LINC00607, LINC00608, LINC01280, LINC01494, MAP2, MEAF6P1, MIR26B, MIR153-1, MIR375, MIR548F2, MIR3131, MIR3132, MIR4268, MIR4438, MIR4439, MIR4776-1, MIR4776-2, MOGAT1, MREG, MRPL44, MTND2P23, MYL1, NANOGP2, NHEJ1, NYAP2, OBSL1, PAX3, PCED1CP, PECR, PIKFYVE, PKI55, PKP4P1, PLCD4, PLEKHM3, PNKD, PRKAG3, PSMB3P2, PTH2R, PTPRN, RESP18, RNA5SP116, RNA5SP117, RNA5SP118, RNA5SP119, RNA5SP120, RNF25, RPE, RPL5P8, RPL6P6, RPL7L1P9, RPL9P14, RPL10P6, RPL12P17, RPL19P5, RPL23AP28, RPL23AP31, RPL23P4, RPL23P5, RPL31P14, RPL31P17, RPL37A, RPS27P10, RPSAP27, RQCD1, RUFY4, SCG2, SERPINE2, SGPP2, SLC4A3, SLC11A1, SLC23A3, SMARCAL1, SNAI1P1, SPAG16, SPEG, STK11IP, STK16, STK36, TMBIM1, TMEM169, TMEM198, TNP1, TNS1, TPT1P2, TRK-TTT15-1, TRQ-CTG16-1, TRY-ATA1-1, TTLL4, TUBA4A, TUBA4B, UNC80, USP37, VIL1, VWC2L, VWC2L-IT1, WDFY1, WNT6, WNT10A, XRCC5, ZFAND2B, ZNF142
2	227.21 - 228.54	q36.3	1336807	100	7.1	92.9	13	AGFG1, C2orf83, COL4A3, COL4A4, IRS1, LOC654841, LOC100420667, MFF, MIR5702, MIR5703, RHBDD1, STIP1P2, TM4SF20
2	228.54 - 232.368.564	q36.3 - q37.1	3826528	100	14.3	85.7	36	ARMC9, B3GNT7, BANF1P3, C2orf72, CAB39, CCL20, COX20P2, DAW1, DNER, FBXO36, GPR55, HMGB1P3, HTR2B, ITM2C, MIR4777, NCL, PID1, PSMD1, RNA5SP121, RNY4P19, RPL17P14, RPS28P4, SLC16A14, SLC19A3, SNORA75, SNORD20, SNORD82, SNRPGP8, SP100, SP110, SP140, SP140L, SPATA3, SPATA3-AS1, SPHKAP, TDGF1P2, TPM3P8, TRIP12, ZBTB8OSP2
2	232.37 - 232.54	q37.1	173303	100	7.1	92.9	4	C2orf57, LINC00471, NMUR1, RPL21P35, RPL23AP26
2	232.54 - 232.99	q37.1	445411	100	14.3	85.7	4	COPS7B, DIS3L2, GAMTP1, MIR1244-1, MIR1471, NPPC, PDE6D, PTMA, RPL28P2
2	232.99 -241.8	q37.1 - q37.3	8808831	100	7.1	92.9	99	ACKR3, AGAP1, AGAP1-IT1, ALPI, ALPP, ALPPL2, ANKMY1, AQP12A, AQP12B, ARL4C, ASB1, ASB18, ATG16L1, C2orf82, CAPN10, CAPN10-AS1, CHRND, CHRNG, COL6A3, COPS8, DGKD, DIS3L2, DIS3L2P1, DNAJB3, DUSP28, ECEL1, ECEL1P2, ECEL1P3, EFHD1, EIF4E2, ESPNL, FAM132B, FLJ43879, GBX2, GIGYF2, GPC1, GPR35, HDAC4, HES6, HJURP, HSPA8P10, ILKAP, INPP5D, IQCA1, KCNJ13, KIF1A, KLHL30, LINC01107, LRRFIP1, MGC16025, MIR149, MIR562, MIR2467, MIR4269, MIR4440, MIR4441, MIR4786, MIR5001, MLPH, MROH2A, MSL3P1, MYEOV2, NDUFA10, NEU2, NGEF, OR5S1P, OR6B2, OR6B3, OR9S24P, OTOS, PER2, PP14571, PRLH, PRR21,

								PRSS56, RAB17, RAMP1, RBM44, RNPEPL1, RPL3P5, RPL17P11, RPS20P12, SAG, SCARNA5, SCARNA6, SCLY, SH3BP4, SPP2, TIGD1, TMSB10P1, TRAF3IP1, TRPM8, TWIST2, UBE2F, UBE2F-SCLY, UGT1A, UGT1A1, UGT1A2P, UGT1A3, UGT1A4, UGT1A5, UGT1A6, UGT1A7, UGT1A8, UGT1A9, UGT1A10, UGT1A11P, UGT1A12P, UGT1A13P, USP40
10	89.69-89.69	q23.31	506	87.5	0	87.5	1	PTEN

Appendix 4.3: Regions showing significant differences in copy number loss (>75% difference) in multifocal tumours from cluster 1 (n=14) versus cluster 2 (n=8).

[1]Physical position is according to hg18/NCBI build 37

Chromosome	Cytoband	Position (Mb)[1]	Region length	Freq. in cluster 2 (%)	Freq. in cluster 1 (%)	Difference	Number of Genes	Candidate genes
1	p12	119.48 -119.7	227926	87.5	0	87.5	5	LOC101929147, RBMX2P3, RPS3AP12, TBX15, WARS2
1	p32.3 - p31.3	53.51-68.61	15100671	75	0	75	96	ACOT11, AK2P1, AK4, ALG6, ANGPTL3, ATG4C, BSND, C1orf87, C1orf123, C1orf141, C1orf168, C1orf177, C8A, C8B, CACHD1, CDCP2, CFL1P3, CPT2, CPT2P1, CYB5RL, CYP2J2, DAB1, DAB1-AS1, DHCR24, DIO1, DIRAS3, DLEU2L, DMRTB1, DNAJC6, DOCK7, EFCAB7, FAM151A, FGGY, FOXD3, FOXD3-AS1, GADD45A, GLIS1, GNG12, GNG12-AS1, GOT2P1, GYG1P3, HIGD1AP11, HNRNPA1P6, HNRNPA1P63, HNRNPA3P12, HNRNPCP9, HOOK1, HSD52, HSPB11, IL12RB2, IL23R, INADL, INSL5, ITGB3BP, JAK1, JUN, KANK4, L1TD1, LDLRAD1, LEPR, LEPROT, LINC00466, LINC01135, LINC01358, LINC01359,, LRP8, LRRC42, MAGOH, MGC34796, MIER1, MIR101-1, MIR3116-1, MIR3116-2, MIR3117, MIR3671, MIR4422, MIR4711, MIR4781, MIR4794, MROH7, MROH7-TTC4, MRPL37, MRPS21P1, MYSM1, NDC1, NFIA, NFIA-AS1, NFIA-AS2, OMA1, PARS2, PCSK9, PDE4B, PGBD4P8, PGM1, PHBP3, PODN, PPAP2B, PRKAA2, RAVER2, RNA5SP49, RNU7-80P, ROR1, ROR1-AS1, RPL13AP9, RPL19P3, RPL21P23, RPL37P7, RPS15AP7, RPS20P5, RPS26P15, RPS29P7, RPSAP20, SCP2, SERBP1, SGIP1, SLC1A7, SLC2A3P2, SLC25A3P1, SLC35D1, SSBP3, SSBP3-AS1, TACSTD2, TALDO1P1, TCEANC2, TCTEX1D1, TM2D1, TMEM59, TMEM61, TRNAK-CUU, TTC4, TTC22, UBE2U, USP1, USP24, VKORC1P2, WDR78, WLS, YIPF1
1	p33	48.92-50.59	1677271	75	0	75	7	AGBL4, BEND5, ELAVL4, LOC101929721, MTND2P29, RPL21P25, SPATA6, ZNF859P
2	p11.2 - q11.1	88.21-94.78	6567180	75	0	75	10	ABCD1P5, ACTR3BP2, ANKRD36BP2, CHEK2P3, DRD5P1, EIF2AK3, FABP1, FOXI3, GGT8P, IGK, IGKC, IGKJ1, IGKJ2, IGKJ3, IGKJ4, IGKJ5, IGKV1-5, IGKV1-6, IGKV1-8, IGKV1-9, IGKV1-12, IGKV1-13, IGKV1-16, IGKV1-17, IGKV1-22, IGKV1-27, IGKV1-32, IGKV1-33, IGKV1-35, IGKV1-37, IGKV1-39, IGKV1D-8, IGKV1D-12, IGKV1D-13, IGKV1D-16, IGKV1D-17, IGKV1D-22, IGKV1D-27, IGKV1D-32, IGKV1D-33, IGKV1D-35, IGKV1D-37, IGKV1D-39, IGKV1D-42, IGKV1D-43, IGKV1OR2-118, IGKV2-4, IGKV2-10, IGKV2-14, IGKV2-18, IGKV2-19, IGKV2-23, IGKV2-24, IGKV2-26, IGKV2-28, IGKV2-29, IGKV2-30, IGKV2-36, IGKV2-38, IGKV2-40, IGKV2D-10, IGKV2D-14, IGKV2D-18, IGKV2D-19, IGKV2D-23, IGKV2D-24, IGKV2D-26, IGKV2D-28, IGKV2D-29, IGKV2D-30, IGKV2D-36, IGKV2D-38, IGKV2D-40, IGKV3-7, IGKV3-11, IGKV3-15, IGKV3-20, IGKV3-25, IGKV3-31, IGKV3-34, IGKV3D-7, IGKV3D-11, IGKV3D-15, IGKV3D-20, IGKV3D-25, IGKV3D-31, IGKV3D-34, IGKV4-1, IGKV5-2, IGKV6-21, IGKV6D-21, IGKV6D-41, IGKV7-3, KRCC1, MIR4436A, MIR4780, MRPL45P1, PABPC1P6, PGBD4P5, RPIA, SLC9B1P2, SMYD1, TEX37, THNSL2
5	p14.1	25.19-26.35	1166074	75	0	75	0	No genes in region.
5	p14.1 - p13.2	26.54-35.39	8848379	75	0	75	28	ADAMTS12, AGXT2, AMACR, BRIX1, C1QTNF3, C1QTNF3-AMACR, C5orf22, CCNB3P1, CDH6, CDH9, CTD-2118P12.1, DNAJC21, DROSHA, GOLPH3, HPRTP2, LINC01021,LSP1P3, MIR579, MIR4279, MTMR12, NPR3, PDZD2, PGBD3P2, PRLR, PSMC6P3, RAD1, RAI14, RPL5P14, RPL9P17, RPL19P11, RPL21P54, RPL21P56, RPL27P10, RPS8P8, RXFP3, SLC45A2, ST3GAL5P1, SUB1, SUCLG2P4, TARS, TPT1P5, TTC23L, UBL5P1, ZFR
7	q11.21 -	63.1-84.59	21488320	75	0	75	150	ABCF2P2, ABHD11, ABHD11-AS1, APTR, ARAFP1, ASL, AUTS2, BAZ1B, BCL7B, CACNA2D1, CALN1,

	q21.11							CCDC146, CCL24, CCL26, CCT6P1, CCT6P3, CD36, CLDN3, CLDN4, CLIP2, CRCP, DNAJC30, DTX2, DTX2P1-UPK3BP1-PMS2P11, EEF1DP4, EIF4H, ELN, ERV3-1, FAM185BP, FDPSP2, FDPSP7, FGL2, FKBP6, FZD9, GABPAP, GATSL1, GATSL2, GCNT1P5, GNAI1, GNAT3, GSAP, GTF2I, GTF2IP1, GTF2IRD1, GTF2IRD1P1, GTF2IRD2, GTF2IRD2B, GTF2IRD2P1, GUSB, HGF, HIP1, HMGN2P11, HNRNPCP7, HSPB1, INTS4P1, INTS4P2, KCTD7, LAT2, LIMK1, LINC00174, LINC01005, LINC01372, MAGI2, MAGI2-AS2, MAGI2-AS3, MDH2, MIR590, MIR3914-1, MIR3914-2, MIR4284, MIR4650-1, MIR4650-2, MIR4651, MLXIPL, MTHFD2P5, MTND1P2, MTND2P4, MTND3P2, MTND4P2, MTND4P3, NCF1, NCF1B, NCF1C, NMD3P1, NSUN5, NSUN5P1, NSUN5P2, PCLO, PHBP15, PHTF2, PMS2L2, PMS2P3, PMS2P4, PMS2P5, PMS2P6, PMS2P7, PMS2P8, PMS2P9, PMS2P10, POM121, POM121B, POM121C, POMZP3, POR, PTPN12, RABGEF1, RAD23BP2, RFC2, RHBDD2, RNA5SP231, RNA5SP233, RNA5SP234, RNA5SP235, RPL6P20, RPL7AP43, RPL7L1P3, RPL7P30, RPL10P11, RPL13AP17, RPL31P38, RPL35P5, RPS28P6, RSBN1L, RSL24D1P3, SAPCD2P1, SAPCD2P3, SBDS, SBDSP1, SEMA3A, SEMA3C, SEMA3E, SEPHS1P1, SKP1P1, SLC25A1P3, SNORA14A, SNORA22, SNRPBP1, SPDYE5, SPDYE7P, SPDYE8P, SPDYE9P, SRRM3, SSC4D, STAG3L1, STAG3L2, STAG3L3, STAG3L4, STX1A, STYXL1, TBL2, TMEM60, TMEM120A, TMEM248, TPST1, TRIM50, TRIM60P17, TRIM60P18, TRIM73, TRIM74, TYW1, TYW1B, UPK3B, VKORC1L1, VN1R34P, VN1R35P, VN1R36P, VN1R37P, VN1R38P, VN1R39P, VN1R40P, VN1R41P, VN1R42P, VN1R43P, VPS37D, WBSCR16, WBSCR17, WBSCR22, WBSCR27, WBSCR28, YWHAEP1, YWHAG, ZNF92, ZNF107, ZNF117, ZNF138, ZNF273, ZNF679, ZNF680, ZNF680P1, ZNF727P, ZNF735, ZNF736, ZP3
7	q21.3 - q22.1	97.1-100.04	2937134	75	0	75	77	AP4M1, ARPC1A, ARPC1B, ASNS, ATP5J2, ATP5J2-PTCD1, AZGP1, AZGP1P1, BAIAP2L1, BHLHA15, BRI3, BUD31, C7orf43, CNPY4, COPS6, CPSF4, CYP3A4, CYP3A5, CYP3A7, CYP3A7-CYP3AP1, CYP3A43, CYP3AP1, CYP3AP2, FAM200A, GAL3ST4, GATS, GJC3, GPC2, GS1-259H13.2, KPNA7, LAMTOR4, LMTK2, LOC442603, LOC442713, LOC100128334, LOC100131859, LOC100419451, LOC100419643, LOC101927550, LOC101927610, LOC101927632, LOC101929496, MBLAC1, MCM7, MEPCE, MGC72080, MIR25, MIR93, MIR106B, MIR3609, MIR4658, MIR5692A1, MIR5692C2, MYH16, NPTX2, OCM2, OR2AE1, OR7E7P, OR7E38P, PDAP1, PILRA, PILRB, PMS2P1, PPP1R35, PTCD1, PVRIG, PVRIG2P, RPL7P60, RPS3AP26, RPS3AP29, RPS26P33, SMURF1, SNRPCP9, SPDYE3, STAG3, STAG3L5P, STAG3L5P-PVRIG2P-PILRB, TAF6, TECPR1, TMEM130, TRIM4, TRRAP, TRW-CCA5-1, ZCWPW1, ZKSCAN1, ZKSCAN5, ZNF3, ZNF394, ZNF655, ZNF789, ZSCAN21, ZSCAN25
20	q11.21	29.78-30.1	322666	100	21.4	78.6	8	CD24P3, DEFB115, DEFB116, DEFB117, DEFB118, DEFB119, DEFB121, DEFB122, DEFB123, DEFB124, DKKL1P1, HAUS6P2, LINC00028, LOC149935, REM1, RNA5SP480, RPL31P3, TRS-AGA7-1
20	q11.21 - q11.23	30.1-34.35	4244645	100	28.5	71.4	76	ACSS2, ACTL10, AHCY, ASIP, ASXL1, BAK1P1, BCL2L1, BPIFA1, BPIFA2, BPIFA3, BPIFA4P, BPIFB1, BPIFB2, BPIFB3, BPIFB4, BPIFB5P, BPIFB6, BPIFB9P, C20orf144, C20orf173, C20orf203, CBFA2T2, CCM2L, CDC42P1, CDK5RAP1, CEP250, CHMP4B, COMMD7, COX4I2, CPNE1, DNMT3B, DUSP15, DYNLRB1, E2F1, EDEM2, EFCAB8, EIF2S2, EIF6, ERGIC3, FAM83C, FDX1P1, FER1L4, FOXS1, GDF5, GGT7, GSS, HCK, HDHD1P3, HM13, HM13-AS1, HMGB3P1, ID1, ITCH, KIF3B, MAP1LC3A, MAPRE1, MCTS2P, MIR499A, MIR499B, MIR644A, MIR1289-1, MIR1825, MIR3193, MIR4755, MMP24, MMP24-AS1, MT1P3, MYH7B, MYLK2, NCOA6, NECAB3, NFS1, NOL4L, PDRG1, PIGPP3, PIGU, PLAGL2, POFUT1, PROCR, PXMP4,

								RALY, RALY-AS1, RBM12, RBM39, RNA5SP481, RNA5SP483, ROMO1, RPF2P1, RPL12P3, RPL31P2, RPL36P4, RPL37P1, RPS2P1, RSL24D1P6, SNTA1, SOCS2P1, SPAG4, SUN5, TM9SF4, TP53INP2, TPM3P2, TPX2, TRPC4AP, TSPY26P, TTLL9, UQCC1, XKR7, XPOTP1, ZNF341, ZNF341-AS1

Appendix 4.4: Regions showing significant differences in copy number gain (>70% difference) in multifocal tumours from cluster 1 (n=14) versus cluster 2 (n=8).

[1]Physical position is according to hg18/NCBI build 37

Appendix 4.5

Phylogenetic tree showing the relationships between 3 tumours from patient 3

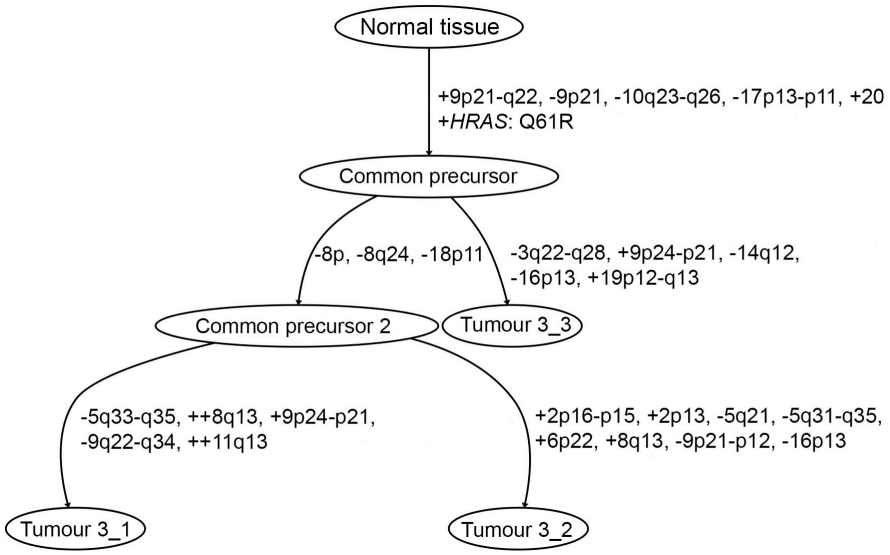

Phylogenetic tree showing the relationships between 2 tumours from patient 7

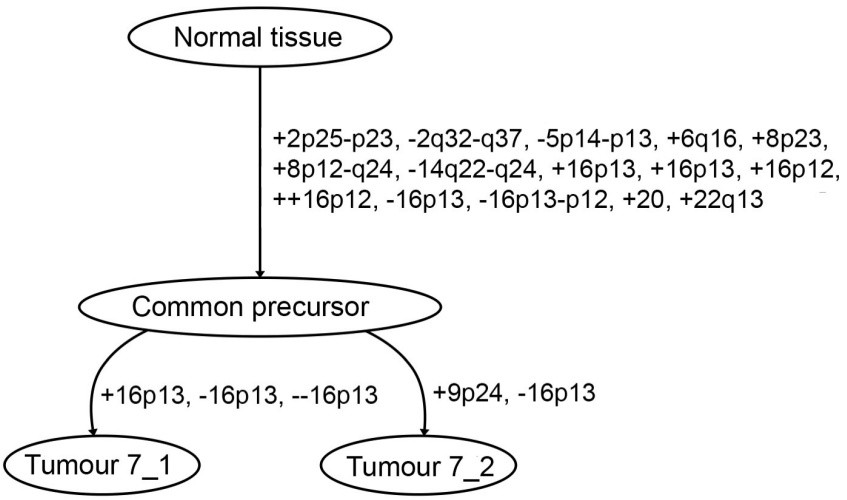

Phylogenetic tree showing the relationships between 2 tumours from patient 10

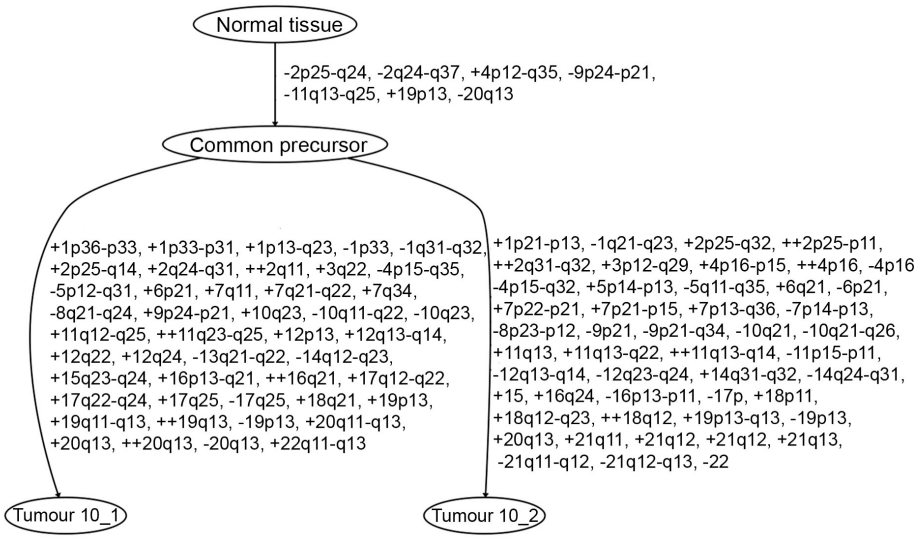

Phylogenetic tree showing the relationships between 2 tumours from patient 11

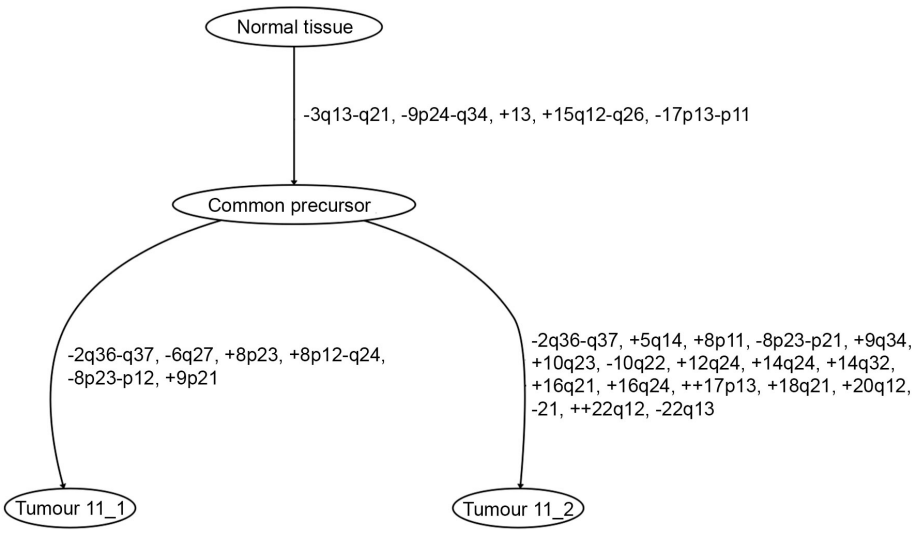

Phylogenetic tree showing the relationships between 4 tumours from patient 12

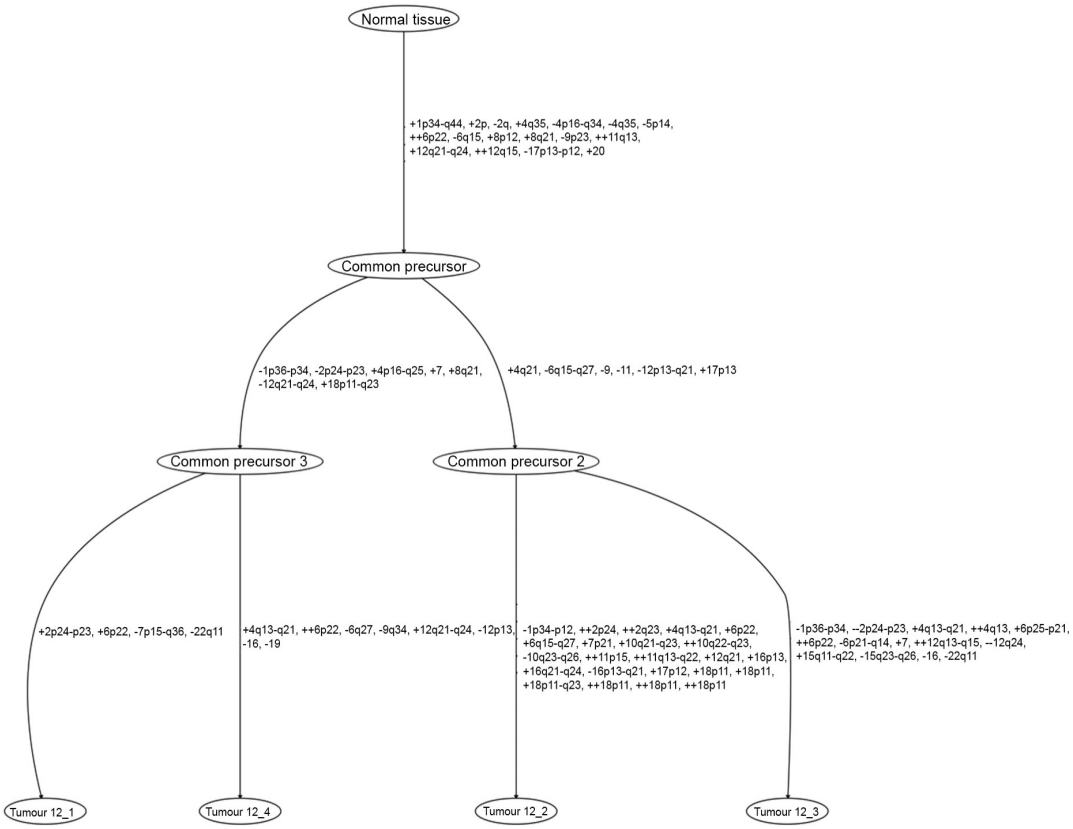

Phylogenetic tree showing the relationships between 4 tumours from patient 14

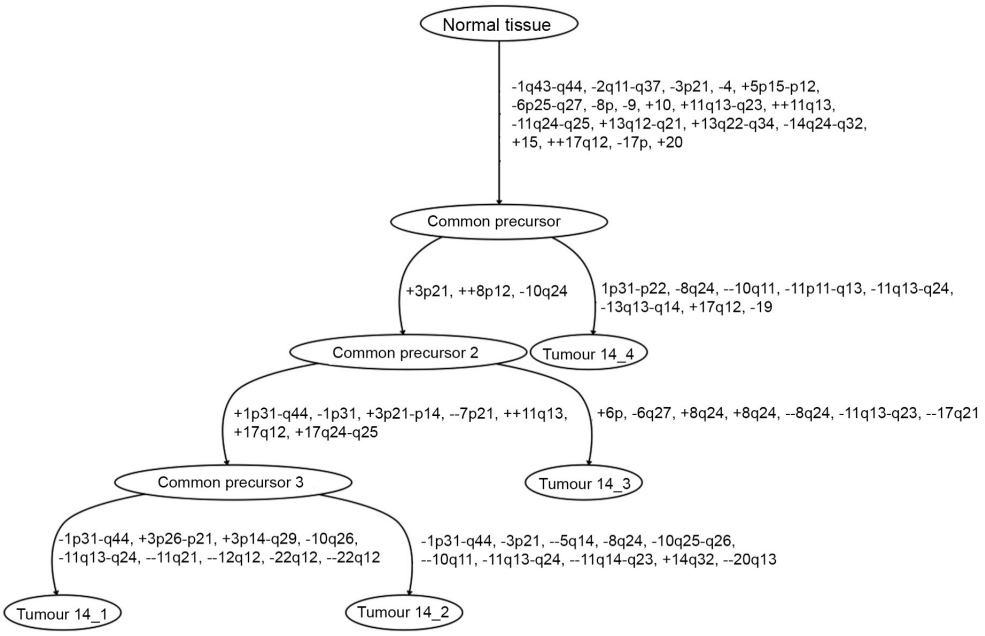

Phylogenetic tree showing the relationships between 2 tumours from patient 15

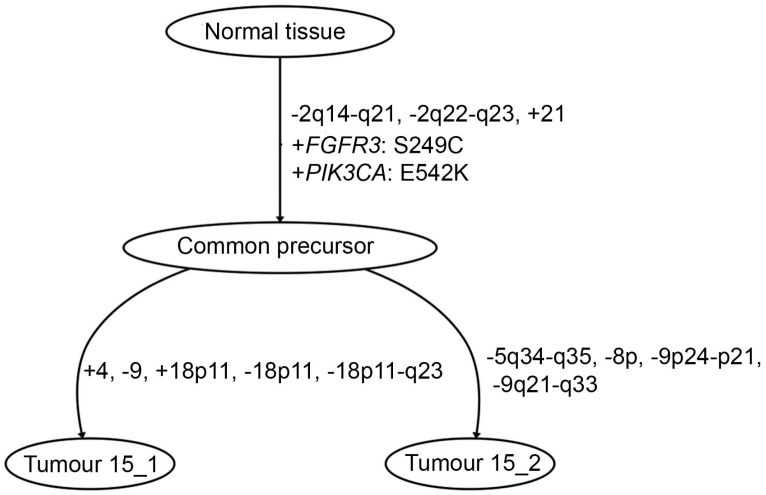

Phylogenetic tree showing the relationships between 3 tumours from patient 17

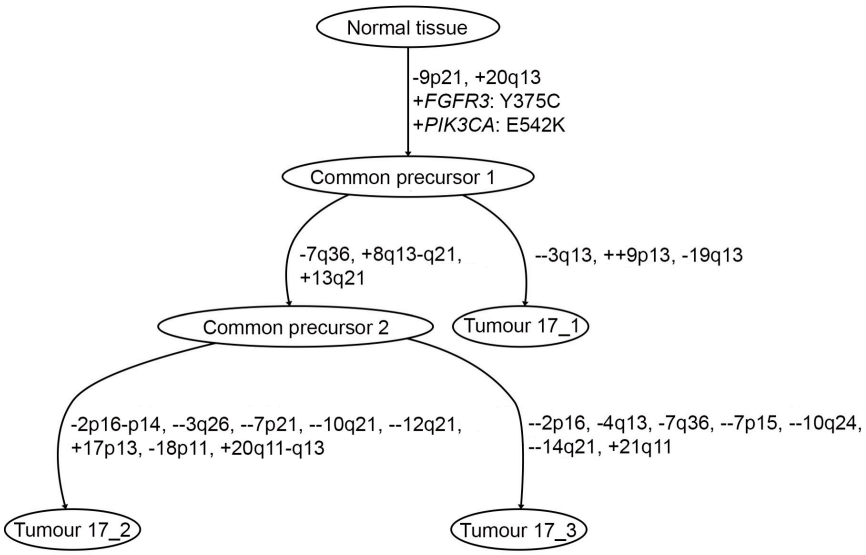

Phylogenetic tree showing the relationships between 4 tumours from patient 18

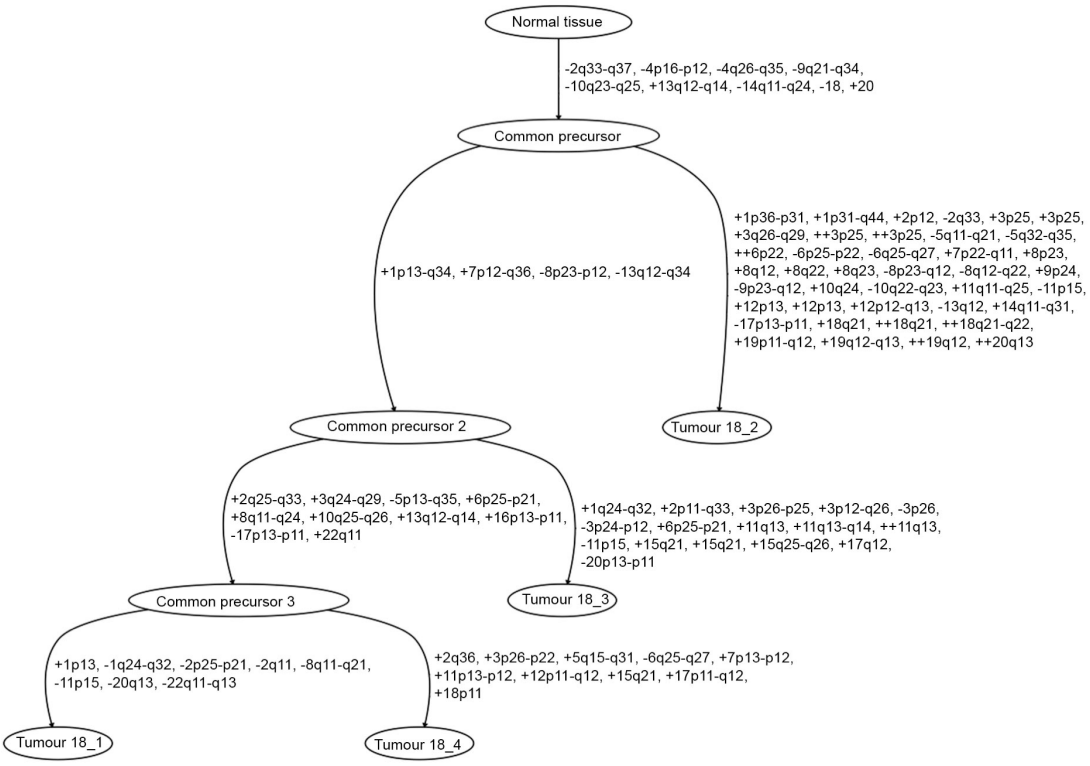

Phylogenetic tree showing the relationships between 3 tumours from patient 20

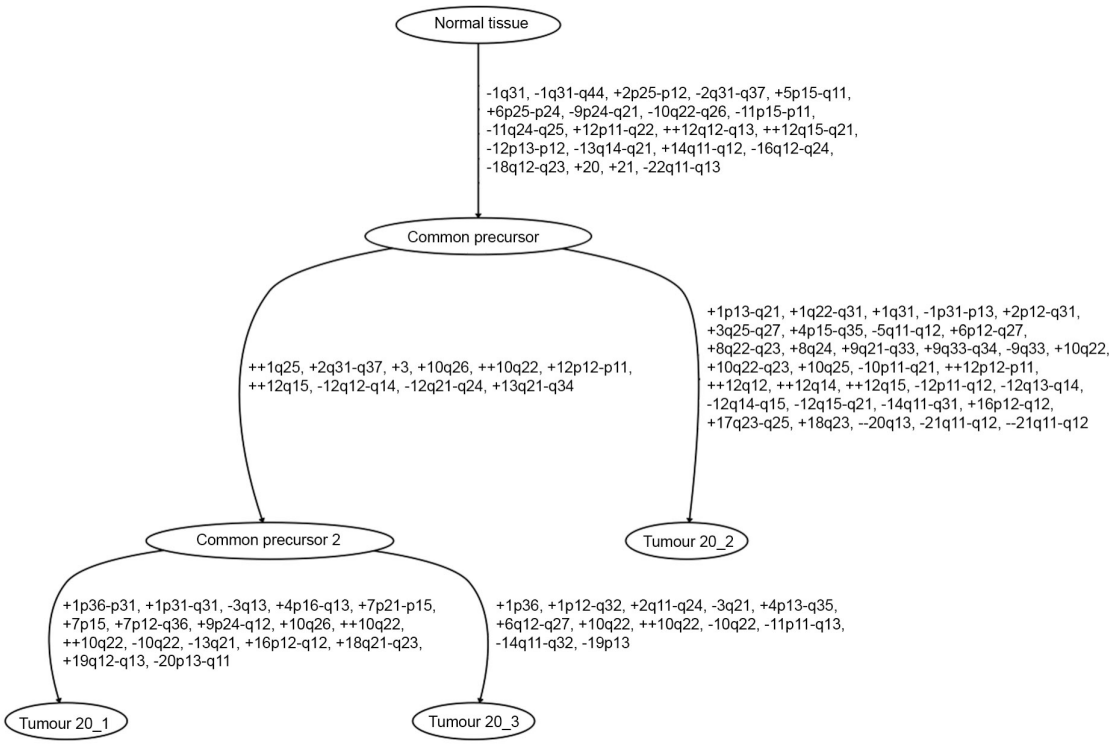

Phylogenetic tree showing the relationships between 2 tumours from patient 21

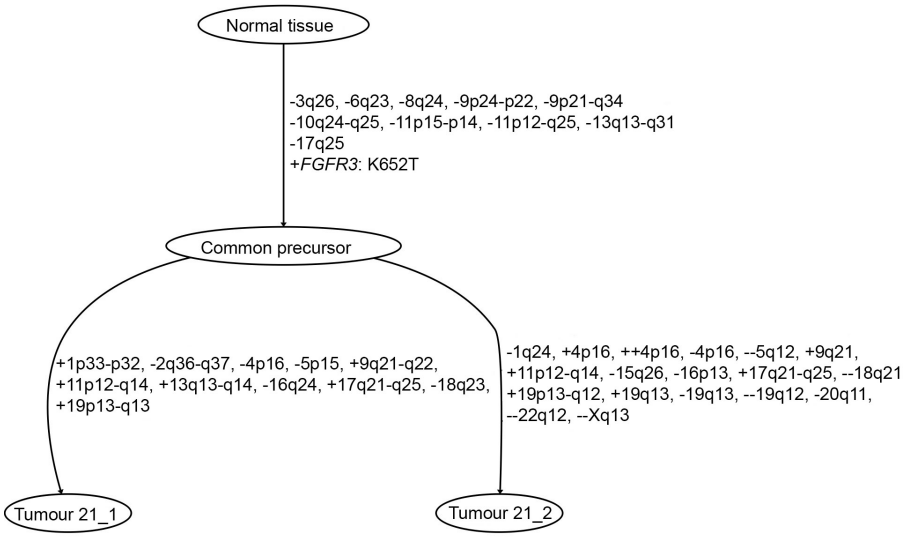

Phylogenetic tree showing the relationships between 2 tumours from patient 22

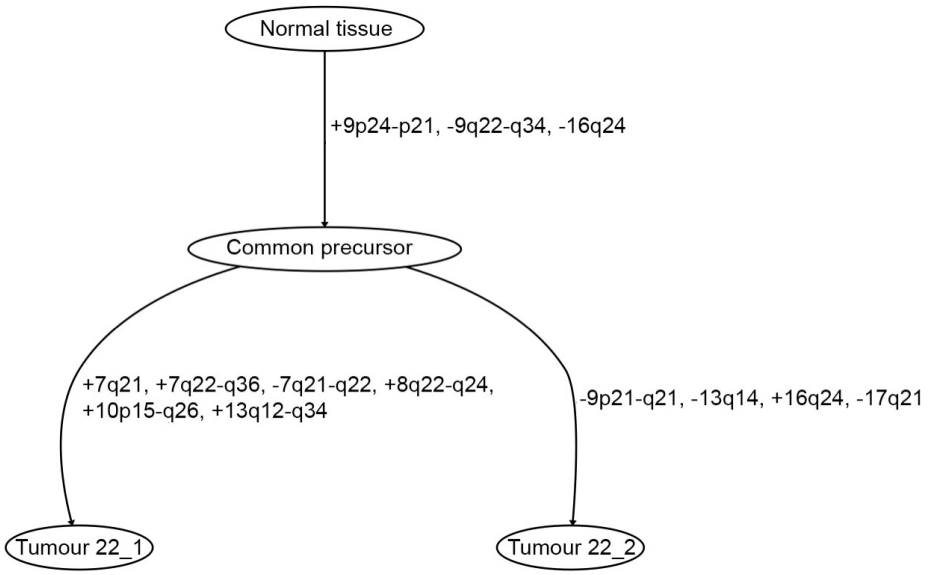

Appendix 5.1: Details of samples in the four main clusters obtained by hierarchical cluster analysis of copy number data from 22 patients with multifocal tumours and 74 solitary tumours excluding stage ≥ T2 tumours.

Tumour	Stage	Grade	Multifocal/Single	FGA group	FGFR3	PIK3CA	RAS	Cluster
9	T1	G3	Multifocal	A	WT	WT	WT	1
17	Ta	G2	Multifocal	B	Mutant	Mutant	WT	1
239	Ta	G1	Single	A	WT	WT	Mutant	1
397	Ta	G2	Single	A	Mutant	Mutant	Mutant	1
406	Ta	G2	Single	B	Mutant	WT	WT	1
489	Ta	G3	Single	A	WT	Mutant	WT	1
494	Ta	G2	Single	A	Mutant	WT	WT	1
518	Ta	G2	Single	A	Mutant	Mutant	WT	1
536	Ta	G2	Single	A	Mutant	Mutant	WT	1
575	Ta	G2	Single	B	Mutant	Mutant	WT	1
578	Ta	G2	Single	B	Mutant	WT	WT	1
584	Ta	G3	Single	A	Mutant	WT	WT	1
672	Ta	G2	Single	A	WT	WT	Mutant	1
695	Ta	G2	Single	B	WT	WT	WT	1
811	Ta	G2	Single	A	Mutant	Mutant	WT	1
868	Ta	G2	Single	A	Mutant	WT	WT	1
894	Ta	G1	Single	A	WT	WT	Mutant	1
924	Ta	G2	Single	B	WT	WT	Mutant	1
933	Ta	G2	Single	B	Mutant	Mutant	WT	1
961	Ta	G2	Single	A	Mutant	WT	WT	1
983	T1	G2	Single	B	Mutant	Mutant	WT	1
989	Ta	G3	Single	B	WT	WT	WT	1
1010	T1	G3	Single	B	WT	WT	Mutant	1
1044	Ta	G2	Single	B	WT	WT	WT	1
1103	Ta	G3	Single	A	WT	Mutant	WT	1
1315	T1	G3	Single	A	Mutant	Mutant	WT	1
2	Ta	G2	Multifocal	C	Mutant	WT	WT	2
4	Ta	G3	Multifocal	C	Mutant	Mutant	WT	2
8	Ta	G2	Multifocal	C	Mutant	Mutant	WT	2
11	T1	G3	Multifocal	C	WT	WT	WT	2
15	Ta	G2	Multifocal	C	Mutant	Mutant	WT	2
21	Ta	G2	Multifocal	C	Mutant	WT	WT	2
94	T1	G3	Single	C	Mutant	WT	WT	2

Tumour	Stage	Grade	Multifocal/Single	FGA group	FGFR3	PIK3CA	RAS	Cluster
140	T1	G3	Single	C	WT	Mutant	WT	2
243	T1	G3	Single	C	WT	WT	WT	2
418	T1	G3	Single	B	WT	Mutant	WT	2
457	T1	G2	Single	C	Mutant	Mutant	WT	2
461	T1	G3	Single	B	Mutant	WT	WT	2
468	T1	G2	Single	B	WT	WT	WT	2
540	Ta	G2	Single	C	Mutant	WT	WT	2
554	T1	G2	Single	B	Mutant	WT	WT	2
572	T1	G3	Single	C	Mutant	WT	WT	2
579	T1	G2	Single	B	Mutant	Mutant	WT	2
675	Ta	G2	Single	B	Mutant	WT	WT	2
718	Ta	G2	Single	C	Mutant	WT	WT	2
736	Ta	G3	Single	B	Mutant	WT	Mutant	2
837	Ta	G1	Single	B	Mutant	WT	WT	2
860	Ta	G2	Single	B	Mutant	Mutant	WT	2
866	T1	G3	Single	B	Mutant	WT	WT	2
934	Ta	G2	Single	B	Mutant	Mutant	WT	2
969	T1	G3	Single	B	Mutant	WT	WT	2
979	T1	G3	Single	C	Mutant	WT	WT	2
1006	Ta	G2	Single	B	Mutant	WT	WT	2
1046	Ta	G2	Single	C	Mutant	WT	WT	2
1079	Ta	G3	Single	C	Mutant	Mutant	WT	2
1082	Ta	G3	Single	C	WT	WT	WT	2
1094	T1	G3	Single	C	Mutant	WT	WT	2
1118	T1	G3	Single	C	Mutant	Mutant	WT	2
1161	T1	G3	Single	C	Mutant	Mutant	WT	2
1210	T1	G3	Single	C	WT	WT	WT	2
1230	T1	G3	Single	C	Mutant	WT	WT	2
1342	T1	G2	Single	C	Mutant	WT	WT	2
1	Ta	G2	Multifocal	B	WT	Mutant	WT	3
3	T1	G3	Multifocal	C	WT	WT	Mutant	3
7	Ta	G2	Multifocal	C	WT	WT	WT	3
14	Ta	G3	Multifocal	D	WT	WT	WT	3
16	Ta	G2	Multifocal	C	WT	WT	Mutant	3
19	Ta	G2	Multifocal	C	Mutant	WT	WT	3
22	Ta	G2	Multifocal	C	WT	WT	WT	3

Tumour	Stage	Grade	Multifocal/Single	FGA group	FGFR3	PIK3CA	RAS	Cluster
358	Ta	G2	Single	C	WT	WT	WT	3
366	Ta	G2	Single	C	WT	WT	WT	3
385	T1	G2	Single	B	Mutant	WT	WT	3
511	Ta	G3	Single	C	Mutant	WT	WT	3
519	T1	G3	Single	D	Mutant	WT	WT	3
561	T1	G3	Single	C	WT	Mutant	Mutant	3
589	T1	G3	Single	C	WT	WT	WT	3
657	Ta	G2	Single	C	WT	Mutant	WT	3
734	Ta	G3	Single	D	WT	WT	WT	3
884	T1	G3	Single	C	WT	WT	WT	3
1021	T1	G3	Single	C	WT	Mutant	WT	3
1072	Ta	G3	Single	C	WT	WT	WT	3
1129	T1	G3	Single	C	WT	WT	Mutant	3
1138	T1	G3	Single	C	WT	WT	WT	3
1145	T1	G3	Single	C	WT	WT	WT	3
1229	T1	G3	Single	C	Mutant	WT	WT	3
1264	T1	G3	Single	C	WT	WT	WT	3
5	Ta	G2	Multifocal	D	Mutant	WT	WT	4
6	T1	G3	Multifocal	D	WT	WT	WT	4
10	Ta	G3	Multifocal	D	WT	WT	WT	4
12	T1	G3	Multifocal	D	WT	WT	WT	4
13	T1	G3	Multifocal	D	WT	WT	WT	4
18	T1	G3	Multifocal	D	WT	WT	WT	4
20	T1	G3	Multifocal	D	WT	WT	WT	4
411	T1	G3	Single	D	WT	WT	WT	4
930	T1	G3	Single	D	WT	WT	WT	4
1320	T1	G3	Single	D	WT	WT	WT	4

Appendix 5.2: Regions showing significant copy number differences in stage Ta multifocal (n=14) versus solitary (n=38) tumours.

Region[1]	Cytoband Location	Event	Region Length	Freq. in Multifocal (%)	Freq. in Solitary (%)	Difference	p-value
chr1:119,708,536-142,787,183	p12 - q21.1	Gain	23078647	35.71	0.00	35.71	0.001
chr1:142,787,183-148,424,834	q21.1 - q21.2	Gain	5637651	35.71	2.63	33.08	0.004
chr1:148,424,834-153,581,460	q21.2 - q22	Gain	5156626	28.57	2.63	25.94	0.015
chr1:157,241,521-157,953,509	q23.1 - q23.2	Gain	711988	35.71	5.26	30.45	0.011
chr1:157,953,509-158,150,295	q23.2	Gain	196786	35.71	2.63	33.08	0.004
chr1:158,150,295-159,891,087	q23.2 - q23.3	Gain	1740792	35.71	5.26	30.45	0.011
chr1:159,891,087-160,195,246	q23.3	Gain	304159	35.71	7.89	27.82	0.025
chr1:160,195,246-160,195,822	q23.3	Gain	576	35.71	5.26	30.45	0.011
chr1:160,195,822-161,212,962	q23.3	Gain	1017140	35.71	7.89	27.82	0.025
chr1:161,212,962-167,621,290	q23.3 - q24.2	Gain	6408328	35.71	5.26	30.45	0.011
chr10:103,282,021-104,340,398	q24.32	Loss	1058377	35.71	7.89	27.82	0.025
chr10:104,342,397-104,652,460	q24.32	Loss	310063	35.71	7.89	27.82	0.025
chr10:5,844,781-8,219,578	p15.1 - p14	Gain	2374797	28.57	2.63	25.94	0.015
chr10:71,487,752-73,834,924	q22.1	Gain	2347172	28.57	2.63	25.94	0.015
chr10:73,834,924-74,954,700	q22.1 - q22.2	Gain	1119776	35.71	2.63	33.08	0.004
chr10:74,954,700-81,634,066	q22.2 - q22.3	Gain	6679366	28.57	2.63	25.94	0.015
chr10:8,346,526-11,805,252	p14	Gain	3458726	28.57	2.63	25.94	0.015
chr10:81,634,066-81,634,692	q22.3	Gain	626	28.57	0.00	28.57	0.004
chr10:81,634,692-89,597,006	q22.3 - q23.2	Gain	7962314	28.57	2.63	25.94	0.015
chr13:19,137,297-19,920,905	q12.11	Gain	783608	42.86	5.26	37.59	0.003
chr13:19,920,905-20,982,693	q12.11	Gain	1061788	42.86	7.89	34.96	0.008
chr13:20,982,693-22,108,664	q12.11	Gain	1125971	42.86	5.26	37.59	0.003
chr13:22,108,664-27,824,701	q12.11 - q12.3	Gain	5716037	42.86	2.63	40.23	0.001
chr13:27,824,701-31,703,968	q12.3 - q13.1	Gain	3879267	35.71	2.63	33.08	0.004
chr13:31,703,968-44,121,309	q13.1 - q14.11	Gain	12417341	28.57	2.63	25.94	0.015
chr13:44,301,217-50,471,832	q14.12 - q14.3	Gain	6170615	28.57	2.63	25.94	0.015
chr13:50,471,832-55,372,320	q14.3 - q21.1	Gain	4900488	35.71	2.63	33.08	0.004

chr13:55,372,320-56,523,630	q21.1	Gain	1151310	28.57	2.63	25.94	0.015
chr13:56,523,630-56,717,407	q21.1	Gain	193777	28.57	0.00	28.57	0.004
chr13:56,717,407-66,421,707	q21.1 - q21.32	Gain	9704300	28.57	2.63	25.94	0.015
chr13:66,421,707-67,895,141	q21.32 - q21.33	Gain	1473434	35.71	2.63	33.08	0.004
chr13:67,895,141-71,256,801	q21.33	Gain	3361660	28.57	2.63	25.94	0.015
chr13:71,256,801-113,927,980	q21.33 - q34	Gain	42671179	35.71	2.63	33.08	0.004
chr16:88,552,007-88,552,722	q24.3	Loss	715	28.57	2.63	25.94	0.015
chr17:30,523,581-33,099,942	q12	Gain	2576361	28.57	2.63	25.94	0.015
chr17:37,370,848-38,137,289	q21.2 - q21.31	Loss	766441	28.57	2.63	25.94	0.015
chr17:5,098,018-5,293,177	p13.2	Loss	195159	28.57	0.00	28.57	0.004
chr17:62,246,742-66,194,639	q24.2 - q24.3	Gain	3947897	28.57	2.63	25.94	0.015
chr17:67,327,134-68,199,396	q24.3	Gain	872262	28.57	2.63	25.94	0.015
chr19:33,399,234-36,171,164	q12	Gain	2771930	28.57	0.00	28.57	0.004
chr19:36,322,238-37,664,852	q12 - q13.11	Gain	1342614	28.57	0.00	28.57	0.004
chr19:37,664,852-38,091,356	q13.11	Gain	426504	28.57	2.63	25.94	0.015
chr19:38,091,356-38,091,878	q13.11	Gain	522	28.57	0.00	28.57	0.004
chr19:38,091,878-40,876,527	q13.11 - q13.12	Gain	2784649	28.57	2.63	25.94	0.015
chr19:41,059,171-51,988,000	q13.12 - q13.32	Gain	10928829	28.57	2.63	25.94	0.015
chr19:52,342,137-63,602,791	q13.32 - q13.43	Gain	11260654	28.57	0.00	28.57	0.004
chr2:127,253,875-136,875,479	q14.3 - q22.1	Loss	9621604	28.57	0.00	28.57	0.004
chr2:142,876,374-152,428,325	q22.2 - q23.3	Loss	9551951	28.57	0.00	28.57	0.004
chr20:26,220,344-28,267,569	p11.1 - q11.1	Gain	2047225	35.71	10.53	25.19	0.048
chr20:30,102,016-34,346,661	q11.21 - q11.23	Gain	4244645	42.86	13.16	29.70	0.050
chr20:34,346,661-35,931,146	q11.23	Gain	1584485	50.00	13.16	36.84	0.010
chr20:35,931,146-36,843,266	q11.23	Gain	912120	57.14	13.16	43.98	0.003
chr20:36,843,266-37,522,311	q11.23 - q12	Gain	679045	57.14	15.79	41.35	0.005
chr20:37,522,311-39,296,098	q12	Gain	1773787	50.00	15.79	34.21	0.026
chr20:39,296,098-44,398,282	q12 - q13.12	Gain	5102184	50.00	13.16	36.84	0.010
chr20:44,398,282-45,646,214	q13.12	Gain	1247932	50.00	15.79	34.21	0.026
chr20:47,243,628-47,383,084	q13.13	Gain	139456	50.00	15.79	34.21	0.026
chr20:47,538,301-51,561,551	q13.13 - q13.2	Gain	4023250	50.00	15.79	34.21	0.026
chr20:51,561,551-59,894,661	q13.2 - q13.33	Gain	8333110	50.00	13.16	36.84	0.010
chr20:59,894,661-62,392,510	q13.33	Gain	2497849	42.86	13.16	29.70	0.050
chr3:170,729,895-179,511,139	q26.2 - q26.32	Gain	8781244	28.57	2.63	25.94	0.015

chr3:179,653,380-180,293,412	q26.32	Gain	640032	28.57	2.63	25.94	0.015
chr3:181,647,155-187,914,171	q26.33 - q27.3	Gain	6267016	28.57	2.63	25.94	0.015
chr3:187,914,171-187,914,682	q27.3	Gain	511	28.57	0.00	28.57	0.004
chr3:187,914,682-190,563,330	q27.3 - q28	Gain	2648648	28.57	2.63	25.94	0.015
chr4:2,656,057-2,718,557	p16.3	Gain	62500	28.57	0.00	28.57	0.004
chr4:207,197-2,656,057	p16.3	Gain	2448860	28.57	2.63	25.94	0.015
chr6:162,865,542-162,954,569	q26	Gain	89027	28.57	0.00	28.57	0.004
chr8:120,863,829-124,550,528	q24.12 - q24.13	Gain	3686699	42.86	7.89	34.96	0.008
chr8:124,550,528-124,718,428	q24.13	Gain	167900	42.86	2.63	40.23	0.001
chr8:124,718,428-133,156,783	q24.13 - q24.22	Gain	8438355	42.86	7.89	34.96	0.008
chr8:133,156,783-134,255,043	q24.22	Gain	1098260	35.71	7.89	27.82	0.025
chr8:134,255,043-146,003,740	q24.22 - q24.3	Gain	11748697	42.86	7.89	34.96	0.008
chr8:146,003,740-146,133,884	q24.3	Gain	130144	35.71	7.89	27.82	0.025
chr8:27,277,284-32,530,048	p21.2 - p12	Loss	5252764	42.86	2.63	40.23	0.001
chr8:32,530,048-32,715,279	p12	Loss	185231	28.57	2.63	25.94	0.015
chr8:32,715,279-37,204,481	p12	Loss	4489202	35.71	2.63	33.08	0.004
chr8:37,204,481-38,289,058	p12	Loss	1084577	35.71	0.00	35.71	0.001
chr8:38,289,058-42,487,636	p12 - p11.21	Loss	4198578	28.57	0.00	28.57	0.004
chr8:477,653-658,324	p23.3	Loss	180671	35.71	5.26	30.45	0.011
chr8:658,324-27,277,284	p23.3 - p21.2	Loss	26618960	42.86	5.26	37.59	0.003
chr8:70,378,901-72,600,219	q13.2 - q13.3	Gain	2221318	35.71	7.89	27.82	0.025
chr8:96,177,980-120,863,829	q22.1 - q24.12	Gain	24685849	35.71	7.89	27.82	0.025
chr9:1,101,150-1,340,595	p24.3	Gain	239445	28.57	0.00	28.57	0.004
chr9:132,631,265-139,523,184	q34.12 - q34.3	Loss	6891919	78.57	36.84	41.73	0.012
chr9:139,523,184-140,012,327	q34.3	Loss	489143	71.43	36.84	34.59	0.033
chr9:140,012,327-140,118,015	q34.3	Loss	105688	71.43	31.58	39.85	0.013
chr9:140,118,015-140,273,252	q34.3	Loss	155237	0.00	31.58	-31.58	0.023
chr9:21,734,602-21,851,433	p21.3	Loss	116831	71.43	28.95	42.48	0.010
chr9:21,851,433-21,998,414	p21.3	Loss	146981	64.29	26.32	37.97	0.021
chr9:21,998,414-22,046,818	p21.3	Loss	48404	57.14	23.68	33.46	0.043
chr9:22,046,818-22,155,847	p21.3	Loss	109029	71.43	23.68	47.74	0.003
chr9:22,155,847-22,155,946	p21.3	Loss	99	64.29	23.68	40.60	0.010
chr9:22,155,946-22,309,530	p21.3	Loss	153584	64.29	26.32	37.97	0.021
chr9:22,309,530-22,479,595	p21.3	Loss	170065	64.29	23.68	40.60	0.010

chr9:22,479,595-23,376,562	p21.3	Loss	896967	64.29	26.32	37.97	0.021
chr9:23,376,562-24,090,721	p21.3	Loss	714159	57.14	23.68	33.46	0.043
chr9:68,858,635-70,488,655	q12 - q13	Loss	1630020	78.57	31.58	46.99	0.004
chr9:70,488,655-82,003,000	q13 - q21.31	Loss	11514345	85.71	31.58	54.14	0.001
chr9:82,003,000-82,148,095	q21.31	Loss	145095	85.71	13.16	72.56	0.000
chr9:82,148,095-85,485,840	q21.31 - q21.32	Loss	3337745	85.71	31.58	54.14	0.001
chr9:85,485,840-87,920,679	q21.32 - q21.33	Loss	2434839	85.71	34.21	51.50	0.001
chr9:87,920,679-88,054,773	q21.33	Loss	134094	85.71	31.58	54.14	0.001
chr9:88,054,773-88,787,420	q21.33	Loss	732647	85.71	34.21	51.50	0.001
chr9:88,787,420-88,883,454	q21.33	Loss	96034	71.43	34.21	37.22	0.027
chr9:88,883,454-88,940,656	q21.33	Loss	57202	71.43	28.95	42.48	0.010
chr9:88,940,656-89,058,511	q21.33	Loss	117855	85.71	34.21	51.50	0.001
chr9:89,058,511-132,631,265	q21.33 - q34.12	Loss	43572754	85.71	36.84	48.87	0.004

[1]Physical position is according to hg18/NCBI build 36

Appendix 5.3: Regions showing significant copy number differences in stage T1 multifocal (n=8) versus solitary (n=36) tumours.

Region[1]	Cytoband Location	Event	Region Length	Freq. in Multifocal (%)	Freq. in Solitary (%)	Difference	p-value
chr1:113,473,675-117,407,078	p13.2 - p13.1	Gain	3933403	37.5	2.78	34.72	0.0154
chr1:117,407,078-119,480,610	p13.1 - p12	Gain	2073532	37.5	5.56	31.94	0.0349
chr1:119,480,610-141,672,545	p12 - q12	Gain	22191935	62.5	5.56	56.94	0.0009
chr1:141,672,545-142,787,183	q12 - q21.1	Gain	1114638	62.5	8.33	54.17	0.0024
chr1:142,787,183-143,613,581	q21.1	Gain	826398	62.5	13.89	48.61	0.0092
chr1:143,613,581-143,614,341	q21.1	Gain	760	62.5	11.11	51.39	0.0049
chr1:143,614,341-146,342,686	q21.1	Gain	2728345	62.5	13.89	48.61	0.0092
chr1:146,342,686-154,399,117	q21.1 - q22	Gain	8056431	62.5	16.67	45.83	0.0157
chr1:154,399,117-156,056,126	q22 - q23.1	Gain	1657009	62.5	22.22	40.28	0.0375
chr1:156,056,126-160,195,246	q23.1 - q23.3	Gain	4139120	62.5	19.44	43.06	0.0249
chr1:160,195,246-160,195,822	q23.3	Gain	576	62.5	16.67	45.83	0.0157
chr1:160,195,822-162,629,394	q23.3	Gain	2433572	62.5	19.44	43.06	0.0249
chr1:162,629,394-165,523,632	q23.3 - q24.2	Gain	2894238	62.5	22.22	40.28	0.0375
chr1:166,251,815-169,324,707	q24.2 - q24.3	Gain	3072892	62.5	22.22	40.28	0.0375
chr1:185,614,023-191,477,703	q31.1 - q31.2	Loss	5863680	25	0.00	25.00	0.0296
chr1:192,424,789-237,780,877	q31.3 - q43	Loss	45356088	25	0.00	25.00	0.0296
chr1:241,339,986-247,164,041	q43 - q44	Loss	5824055	25	0.00	25.00	0.0296
chr1:29,481,197-33,046,828	p35.3 - p35.1	Gain	3565631	37.5	5.56	31.94	0.0349
chr1:38,051,746-39,307,926	p34.3	Gain	1256180	50	8.33	41.67	0.0140
chr1:39,307,926-44,062,032	p34.3 - p34.1	Gain	4754106	50	5.56	44.44	0.0065
chr1:44,062,032-45,524,938	p34.1	Gain	1462906	50	2.78	47.22	0.0024
chr1:45,524,938-53,077,428	p34.1 - p32.3	Gain	7552490	50	5.56	44.44	0.0065
chr1:53,077,428-73,625,895	p32.3 - p31.1	Gain	20548467	50	2.78	47.22	0.0024
chr1:73,625,895-83,494,525	p31.1	Gain	9868630	37.5	2.78	34.72	0.0154
chr1:918,164-25,159,219	p36.33 - p36.11	Gain	24241055	37.5	5.56	31.94	0.0349
chr10:104,813,472-108,400,155	q24.32 - q25.1	Loss	3586683	75	11.11	63.89	0.0007
chr10:108,400,155-114,874,404	q25.1 - q25.2	Loss	6474249	75	8.33	66.67	0.0003

chr10:114,874,404-116,774,295	q25.2 - q25.3	Loss	1899891	75	5.56	69.44	0.0001
chr10:116,774,295-119,495,422	q25.3 - q26.11	Loss	2721127	62.5	5.56	56.94	0.0009
chr10:119,495,422-120,558,865	q26.11	Loss	1063443	62.5	2.78	59.72	0.0003
chr10:120,558,865-123,214,100	q26.11 - q26.13	Loss	2655235	62.5	5.56	56.94	0.0009
chr10:123,214,100-125,057,698	q26.13	Loss	1843598	62.5	2.78	59.72	0.0003
chr10:125,057,698-126,007,431	q26.13	Loss	949733	50	2.78	47.22	0.0024
chr10:126,007,431-131,816,154	q26.13 - q26.3	Loss	5808723	50	0.00	50.00	0.0005
chr10:131,816,154-131,982,049	q26.3	Loss	165895	37.5	0.00	37.50	0.0042
chr10:131,982,049-135,247,831	q26.3	Loss	3265782	50	0.00	50.00	0.0005
chr10:34,638,996-38,812,575	p11.21 - p11.1	Loss	4173579	25	0.00	25.00	0.0296
chr10:72,803,738-79,687,959	q22.1 - q22.3	Gain	6884221	25	0.00	25.00	0.0296
chr10:76,882,526-78,996,385	q22.2 - q22.3	Loss	2113859	37.5	5.56	31.94	0.0349
chr10:78,996,385-80,472,830	q22.3	Loss	1476445	50	5.56	44.44	0.0065
chr10:80,472,830-83,636,464	q22.3 - q23.1	Loss	3163634	37.5	5.56	31.94	0.0349
chr10:83,636,464-83,637,155	q23.1	Loss	691	37.5	2.78	34.72	0.0154
chr10:83,637,155-84,577,760	q23.1	Loss	940605	37.5	5.56	31.94	0.0349
chr10:84,577,760-86,390,131	q23.1	Loss	1812371	50	5.56	44.44	0.0065
chr10:86,390,131-87,373,214	q23.1	Loss	983083	62.5	5.56	56.94	0.0009
chr10:87,373,214-88,222,653	q23.1 - q23.2	Loss	849439	62.5	8.33	54.17	0.0024
chr10:88,222,653-89,694,469	q23.2 - q23.31	Loss	1471816	75	8.33	66.67	0.0003
chr10:89,694,469-89,694,975	q23.31	Loss	506	62.5	8.33	54.17	0.0024
chr10:89,694,975-90,596,444	q23.31	Loss	901469	75	8.33	66.67	0.0003
chr10:90,596,444-95,924,122	q23.31 - q23.33	Loss	5327678	75	5.56	69.44	0.0001
chr10:95,924,122-104,813,472	q23.33 - q24.32	Loss	8889350	75	8.33	66.67	0.0003
chr11:50,013,045-54,839,338	p11.12 - q11	Loss	4826293	37.5	5.56	31.94	0.0349
chr11:54,839,338-59,697,061	q11 - q12.1	Loss	4857723	37.5	0.00	37.50	0.0042
chr11:59,697,061-60,851,894	q12.1 - q12.2	Loss	1154833	37.5	2.78	34.72	0.0154
chr12:152,534-152,582	p13.33	Loss	48	37.5	2.78	34.72	0.0154
chr12:152,582-153,169	p13.33	Loss	587	37.5	0.00	37.50	0.0042
chr12:153,169-16,742,828	p13.33 - p12.3	Loss	16589659	37.5	2.78	34.72	0.0154
chr12:16,742,828-25,552,960	p12.3 - p12.1	Loss	8810132	37.5	0.00	37.50	0.0042
chr12:29,733,366-30,740,646	p11.22 - p11.21	Loss	1007280	25	0.00	25.00	0.0296
chr12:30,939,600-33,333,489	p11.21 - p11.1	Loss	2393889	25	0.00	25.00	0.0296
chr12:33,333,489-46,156,911	p11.1 - q13.11	Loss	12823422	37.5	0.00	37.50	0.0042

chr12:46,156,911-52,417,126	q13.11 - q13.13	Loss	6260215	25	0.00	25.00	0.0296
chr12:68,627,676-71,742,532	q15 - q21.1	Loss	3114856	25	0.00	25.00	0.0296
chr12:91,367,961-121,982,522	q22 - q24.31	Loss	30614561	25	0.00	25.00	0.0296
chr13:47,794,572-47,964,053	q14.2	Loss	169481	37.5	5.56	31.94	0.0349
chr13:47,964,053-51,243,111	q14.2 - q14.3	Loss	3279058	50	5.56	44.44	0.0065
chr13:51,243,111-53,669,880	q14.3 - q21.1	Loss	2426769	37.5	5.56	31.94	0.0349
chr13:78,112,209-107,482,925	q31.1 - q33.3	Gain	29370716	37.5	5.56	31.94	0.0349
chr14:23,749,068-26,561,378	q12	Loss	2812310	37.5	2.78	34.72	0.0154
chr14:26,744,993-33,897,190	q12 - q13.1	Loss	7152197	37.5	2.78	34.72	0.0154
chr14:33,897,190-34,061,283	q13.1	Loss	164093	37.5	0.00	37.50	0.0042
chr14:34,061,283-41,500,259	q13.1 - q21.2	Loss	7438976	37.5	2.78	34.72	0.0154
chr14:41,500,259-57,420,120	q21.2 - q23.1	Loss	15919861	37.5	5.56	31.94	0.0349
chr14:57,420,120-58,323,469	q23.1	Loss	903349	50	5.56	44.44	0.0065
chr14:58,323,469-58,470,270	q23.1	Loss	146801	37.5	2.78	34.72	0.0154
chr14:58,470,270-59,336,011	q23.1	Loss	865741	50	5.56	44.44	0.0065
chr14:59,336,011-66,870,415	q23.1 - q23.3	Loss	7534404	37.5	5.56	31.94	0.0349
chr14:73,931,005-74,588,657	q24.3	Loss	657652	37.5	5.56	31.94	0.0349
chr14:75,833,225-77,328,585	q24.3	Gain	1495360	25	0.00	25.00	0.0296
chr15:20,363,717-31,975,417	q11.2 - q14	Loss	11611700	25	0.00	25.00	0.0296
chr15:62,510,397-63,070,265	q22.31	Loss	559868	37.5	2.78	34.72	0.0154
chr15:63,070,265-82,907,017	q22.31 - q25.2	Loss	19836752	37.5	0.00	37.50	0.0042
chr15:82,907,017-83,883,618	q25.2 - q25.3	Loss	976601	25	0.00	25.00	0.0296
chr15:83,883,618-85,362,775	q25.3	Loss	1479157	37.5	0.00	37.50	0.0042
chr15:85,362,775-87,338,954	q25.3 - q26.1	Loss	1976179	37.5	2.78	34.72	0.0154
chr15:87,338,954-100,022,043	q26.1 - q26.3	Loss	12683089	37.5	0.00	37.50	0.0042
chr16:2,267,343-7,019,846	p13.3 - p13.2	Gain	4752503	25	0.00	25.00	0.0296
chr16:23,756,350-24,856,451	p12.1	Gain	1100101	50	0.00	50.00	0.0005
chr16:24,856,451-29,550,785	p12.1 - p11.2	Gain	4694334	50	2.78	47.22	0.0024
chr16:29,550,785-45,067,244	p11.2 - q11.2	Gain	15516459	50	0.00	50.00	0.0005
chr16:3,918,289-4,131,849	p13.3	Loss	213560	25	0.00	25.00	0.0296
chr16:33,715,230-45,231,075	p11.2 - q11.2	Loss	11515845	25	0.00	25.00	0.0296
chr16:45,231,075-63,462,907	q11.2 - q21	Loss	18231832	37.5	0.00	37.50	0.0042
chr16:63,462,907-88,552,722	q21 - q24.3	Loss	25089815	25	0.00	25.00	0.0296
chr16:7,019,846-23,756,350	p13.2 - p12.1	Gain	16736504	37.5	0.00	37.50	0.0042

chr17:12,108,967-14,364,543	p12	Gain	2255576	25	0.00	25.00	0.0296
chr19:183,116-211,322	p13.3	Loss	28206	25	0.00	25.00	0.0296
chr19:21,345,165-22,729,077	p12	Gain	1383912	25	0.00	25.00	0.0296
chr19:211,322-5,009,897	p13.3	Loss	4798575	37.5	0.00	37.50	0.0042
chr19:23,732,302-32,891,236	p12 - q12	Gain	9158934	37.5	2.78	34.72	0.0154
chr19:32,891,236-33,399,234	q12	Gain	507998	37.5	0.00	37.50	0.0042
chr19:33,399,234-35,629,568	q12	Gain	2230334	37.5	5.56	31.94	0.0349
chr19:35,629,568-36,171,164	q12	Gain	541596	37.5	2.78	34.72	0.0154
chr19:36,322,238-36,979,850	q12	Gain	657612	37.5	2.78	34.72	0.0154
chr19:36,979,850-37,664,852	q12 - q13.11	Gain	685002	37.5	5.56	31.94	0.0349
chr19:37,664,852-38,091,322	q13.11	Gain	426470	50	5.56	44.44	0.0065
chr19:38,091,322-38,282,890	q13.11	Gain	191568	50	2.78	47.22	0.0024
chr19:38,282,890-39,226,664	q13.11	Gain	943774	50	5.56	44.44	0.0065
chr19:39,226,664-45,806,715	q13.11 - q13.2	Gain	6580051	50	2.78	47.22	0.0024
chr19:45,806,715-46,479,845	q13.2	Gain	673130	37.5	2.78	34.72	0.0154
chr19:46,479,845-51,023,195	q13.2 - q13.32	Gain	4543350	37.5	0.00	37.50	0.0042
chr19:5,009,897-5,549,421	p13.3	Loss	539524	37.5	2.78	34.72	0.0154
chr19:5,549,421-6,523,485	p13.3	Loss	974064	37.5	0.00	37.50	0.0042
chr19:51,023,195-58,336,597	q13.32 - q13.41	Gain	7313402	25	0.00	25.00	0.0296
chr19:59,359,392-59,464,022	q13.42	Gain	104630	25	0.00	25.00	0.0296
chr19:6,523,485-20,458,451	p13.3 - p12	Loss	13934966	25	0.00	25.00	0.0296
chr19:63,602,791-63,771,717	q13.43	Gain	168926	25	0.00	25.00	0.0296
chr2:1,785,220-11,122,011	p25.3 - p25.1	Gain	9336791	50	5.56	44.44	0.0065
chr2:109,111,217-109,319,695	q13	Gain	208478	25	0.00	25.00	0.0296
chr2:11,122,011-20,037,859	p25.1 - p24.1	Gain	8915848	50	2.78	47.22	0.0024
chr2:111,491,810-141,564,023	q13 - q22.1	Gain	30072213	25	0.00	25.00	0.0296
chr2:143,499,679-143,667,001	q22.2	Gain	167322	25	0.00	25.00	0.0296
chr2:144,588,986-159,300,999	q22.2 - q24.1	Gain	14712013	25	0.00	25.00	0.0296
chr2:148,009,604-151,825,968	q22.3 - q23.3	Loss	3816364	25	0.00	25.00	0.0296
chr2:153,751,686-169,397,061	q23.3 - q24.3	Loss	15645375	25	0.00	25.00	0.0296
chr2:167,445,852-169,206,769	q24.3	Gain	1760917	25	0.00	25.00	0.0296
chr2:169,397,061-207,861,345	q24.3 - q33.3	Loss	38464284	37.5	0.00	37.50	0.0042
chr2:20,037,859-20,215,537	p24.1	Gain	177678	37.5	2.78	34.72	0.0154
chr2:20,215,537-21,280,646	p24.1	Gain	1065109	50	2.78	47.22	0.0024

chr2:207,861,345-208,876,525	q33.3	Loss	1015180	37.5	5.56	31.94	0.0349
chr2:208,876,525-210,331,732	q33.3 - q34	Loss	1455207	62.5	5.56	56.94	0.0009
chr2:21,280,646-25,870,821	p24.1 - p23.3	Gain	4590175	37.5	2.78	34.72	0.0154
chr2:210,331,732-216,402,525	q34 - q35	Loss	6070793	62.5	8.33	54.17	0.0024
chr2:216,402,525-224,018,802	q35 - q36.1	Loss	7616277	62.5	11.11	51.39	0.0049
chr2:224,018,802-225,739,791	q36.1 - q36.2	Loss	1720989	62.5	13.89	48.61	0.0092
chr2:224,263-1,785,220	p25.3	Gain	1560957	50	2.78	47.22	0.0024
chr2:225,739,791-227,039,805	q36.2 - q36.3	Loss	1300014	62.5	16.67	45.83	0.0157
chr2:227,039,805-228,542,036	q36.3	Loss	1502231	62.5	13.89	48.61	0.0092
chr2:228,542,036-230,386,971	q36.3	Loss	1844935	75	13.89	61.11	0.0014
chr2:230,386,971-230,387,771	q36.3	Loss	800	75	11.11	63.89	0.0007
chr2:230,387,771-238,252,220	q36.3 - q37.3	Loss	7864449	75	13.89	61.11	0.0014
chr2:238,252,220-239,091,229	q37.3	Loss	839009	75	16.67	58.33	0.0027
chr2:239,091,229-241,620,162	q37.3	Loss	2528933	75	19.44	55.56	0.0048
chr2:241,620,162-241,796,109	q37.3	Loss	175947	75	16.67	58.33	0.0027
chr2:25,870,821-48,938,583	p23.3 - p16.3	Gain	23067762	50	2.78	47.22	0.0024
chr2:48,938,583-52,373,212	p16.3	Gain	3434629	50	0.00	50.00	0.0005
chr2:52,373,212-64,478,283	p16.3 - p14	Gain	12105071	62.5	0.00	62.50	0.0001
chr2:64,478,283-71,285,149	p14 - p13.3	Gain	6806866	50	0.00	50.00	0.0005
chr2:71,285,149-74,335,462	p13.3 - p13.1	Gain	3050313	62.5	0.00	62.50	0.0001
chr2:74,335,462-82,716,433	p13.1 - p12	Gain	8380971	50	0.00	50.00	0.0005
chr2:82,716,433-83,447,850	p12	Gain	731417	50	2.78	47.22	0.0024
chr2:83,447,850-88,214,979	p12 - p11.2	Gain	4767129	50	0.00	50.00	0.0005
chr2:88,214,979-94,782,159	p11.2 - q11.1	Gain	6567180	62.5	0.00	62.50	0.0001
chr2:94,782,159-95,675,764	q11.1	Gain	893605	50	0.00	50.00	0.0005
chr2:94,983,765-100,292,273	q11.1 - q11.2	Loss	5308508	25	0.00	25.00	0.0296
chr2:95,675,764-108,345,037	q11.1 - q12.3	Gain	12669273	25	0.00	25.00	0.0296
chr20:26,006,126-26,220,344	p11.1	Gain	214218	75	5.56	69.44	0.0001
chr20:26,220,344-28,267,569	p11.1 - q11.1	Gain	2047225	75	8.33	66.67	0.0003
chr20:275,014-424,783	p13	Gain	149769	75	5.56	69.44	0.0001
chr20:28,267,569-29,779,350	q11.1 - q11.21	Gain	1511781	75	19.44	55.56	0.0048
chr20:29,779,350-30,526,698	q11.21	Gain	747348	75	22.22	52.78	0.0080
chr20:30,526,698-37,666,045	q11.21 - q12	Gain	7139347	75	19.44	55.56	0.0048
chr20:37,666,045-40,680,814	q12	Gain	3014769	87.5	19.44	68.06	0.0006

chr20:40,680,814-40,792,351	q12	Gain	111537	75	19.44	55.56	0.0048
chr20:40,792,351-43,889,716	q12 - q13.12	Gain	3097365	75	25.00	50.00	0.0126
chr20:424,783-26,006,126	p13 - p11.1	Gain	25581343	75	8.33	66.67	0.0003
chr20:43,889,716-47,383,084	q13.12 - q13.13	Gain	3493368	75	19.44	55.56	0.0048
chr20:47,383,084-47,538,301	q13.13	Gain	155217	62.5	19.44	43.06	0.0249
chr20:47,538,301-62,393,015	q13.13 - q13.33	Gain	14854714	75	19.44	55.56	0.0048
chr22:15,621,248-15,745,966	q11.1	Loss	124718	37.5	0.00	37.50	0.0042
chr22:15,745,966-18,151,355	q11.1 - q11.21	Loss	2405389	50	0.00	50.00	0.0005
chr22:18,151,355-18,151,891	q11.21	Loss	536	37.5	0.00	37.50	0.0042
chr22:18,151,891-24,286,893	q11.21 - q11.23	Loss	6135002	50	2.78	47.22	0.0024
chr22:24,286,893-28,379,404	q11.23 - q12.2	Loss	4092511	50	5.56	44.44	0.0065
chr22:28,379,404-30,623,768	q12.2 - q12.3	Loss	2244364	50	2.78	47.22	0.0024
chr22:30,623,768-30,623,867	q12.3	Loss	99	37.5	2.78	34.72	0.0154
chr22:30,646,302-30,646,401	q12.3	Loss	99	37.5	2.78	34.72	0.0154
chr22:30,646,401-40,803,595	q12.3 - q13.2	Loss	10157194	50	2.78	47.22	0.0024
chr22:40,803,595-42,473,589	q13.2	Loss	1669994	62.5	5.56	56.94	0.0009
chr22:42,473,589-45,618,622	q13.2 - q13.31	Loss	3145033	50	5.56	44.44	0.0065
chr22:45,618,622-49,453,810	q13.31 - q13.33	Loss	3835188	50	8.33	41.67	0.0140
chr3:122,541,183-125,236,945	q13.33 - q21.1	Loss	2695762	25	0.00	25.00	0.0296
chr3:133,822,599-158,979,197	q22.1 - q25.32	Gain	25156598	25	0.00	25.00	0.0296
chr3:140,451,428-140,626,759	q23	Loss	175331	25	0.00	25.00	0.0296
chr3:140,627,376-184,141,428	q23 - q26.33	Loss	43514052	25	0.00	25.00	0.0296
chr3:54,612,454-71,816,463	p14.3 - p13	Gain	17204009	25	0.00	25.00	0.0296
chr3:6,636,703-10,788,431	p26.1 - p25.3	Gain	4151728	37.5	5.56	31.94	0.0349
chr3:77,584,830-79,097,077	p12.3	Gain	1512247	25	0.00	25.00	0.0296
chr3:82,799,401-83,768,022	p12.2 - p12.1	Gain	968621	37.5	2.78	34.72	0.0154
chr3:83,768,022-87,044,540	p12.1	Gain	3276518	37.5	0.00	37.50	0.0042
chr3:87,044,540-111,740,734	p12.1 - q13.13	Gain	24696194	25	0.00	25.00	0.0296
chr3:958,261-6,636,703	p26.3 - p26.1	Gain	5678442	37.5	2.78	34.72	0.0154
chr4:113,578,539-152,907,961	q25 - q31.3	Loss	39329422	37.5	0.00	37.50	0.0042
chr4:152,907,961-179,587,711	q31.3 - q34.3	Loss	26679750	37.5	2.78	34.72	0.0154
chr4:179,587,711-180,006,495	q34.3	Loss	418784	37.5	5.56	31.94	0.0349
chr4:184,404,421-185,872,338	q35.1	Gain	1467917	25	0.00	25.00	0.0296
chr4:185,872,338-190,151,886	q35.1 - q35.2	Loss	4279548	37.5	5.56	31.94	0.0349

chr4:2,865,088-11,429,778	p16.3 - p15.33	Loss	8564690	37.5	2.78	34.72	0.0154
chr4:26,747,433-47,264,023	p15.2 - p12	Loss	20516590	37.5	2.78	34.72	0.0154
chr4:47,264,023-47,677,803	p12	Loss	413780	37.5	0.00	37.50	0.0042
chr4:47,677,803-48,524,316	p12	Loss	846513	25	0.00	25.00	0.0296
chr4:55,628-2,865,088	p16.3	Loss	2809460	37.5	0.00	37.50	0.0042
chr4:69,912,758-74,866,776	q13.2 - q13.3	Gain	4954018	25	0.00	25.00	0.0296
chr4:74,866,776-78,196,278	q13.3 - q21.1	Gain	3329502	37.5	0.00	37.50	0.0042
chr4:80,547,099-113,578,539	q21.21 - q25	Loss	33031440	25	0.00	25.00	0.0296
chr5:136,366,234-180,626,608	q31.2 - q35.3	Loss	44260374	37.5	2.78	34.72	0.0154
chr5:3,426,805-3,559,003	p15.33	Gain	132198	37.5	2.78	34.72	0.0154
chr5:3,559,003-4,533,614	p15.33 - p15.32	Gain	974611	37.5	5.56	31.94	0.0349
chr5:5,500,139-6,708,632	p15.32 - p15.31	Gain	1208493	37.5	5.56	31.94	0.0349
chr5:50,168,170-51,232,444	q11.1 - q11.2	Loss	1064274	37.5	5.56	31.94	0.0349
chr5:51,232,444-65,352,862	q11.2 - q12.3	Loss	14120418	50	5.56	44.44	0.0065
chr5:65,352,862-75,600,638	q12.3 - q13.3	Loss	10247776	37.5	5.56	31.94	0.0349
chr5:99,111,442-107,339,380	q21.1 - q21.3	Loss	8227938	37.5	2.78	34.72	0.0154
chr6:165,244,688-169,488,215	q27	Loss	4243527	50	8.33	41.67	0.0140
chr6:169,576,118-170,622,773	q27	Loss	1046655	50	8.33	41.67	0.0140
chr6:170,622,773-170,728,000	q27	Loss	105227	50	5.56	44.44	0.0065
chr6:19,131,847-20,272,069	p22.3	Gain	1140222	50	11.11	38.89	0.0256
chr6:20,272,069-22,580,422	p22.3	Gain	2308353	62.5	11.11	51.39	0.0049
chr6:22,580,422-23,499,391	p22.3	Gain	918969	62.5	5.56	56.94	0.0009
chr6:23,499,391-27,152,460	p22.3 - p22.1	Gain	3653069	50	5.56	44.44	0.0065
chr6:27,152,460-32,404,070	p22.1 - p21.32	Gain	5251610	37.5	5.56	31.94	0.0349
chr6:6,382,300-7,427,280	p25.1 - p24.3	Gain	1044980	50	11.11	38.89	0.0256
chr6:62,586,405-69,438,735	q11.1 - q12	Gain	6852330	25	0.00	25.00	0.0296
chr7:142,857,956-144,143,399	q35	Gain	1285443	62.5	11.11	51.39	0.0049
chr7:144,143,399-147,259,180	q35	Gain	3115781	62.5	8.33	54.17	0.0024
chr7:147,259,180-148,089,302	q35 - q36.1	Gain	830122	62.5	11.11	51.39	0.0049
chr7:148,089,302-151,558,264	q36.1	Gain	3468962	62.5	13.89	48.61	0.0092
chr7:15,056,488-21,588,275	p21.2 - p15.3	Gain	6531787	50	13.89	36.11	0.0422
chr7:151,558,264-153,901,560	q36.1 - q36.2	Gain	2343296	62.5	11.11	51.39	0.0049
chr7:153,901,560-158,625,992	q36.2 - q36.3	Gain	4724432	62.5	13.89	48.61	0.0092
chr7:26,749,335-29,450,068	p15.2 - p15.1	Gain	2700733	50	13.89	36.11	0.0422

chr7:50,617,642-52,867,234	p12.2 - p12.1	Gain	2249592	50	11.11	38.89	0.0256
chr7:52,867,234-56,264,968	p12.1 - p11.2	Gain	3397734	50	13.89	36.11	0.0422
chr7:56,264,968-63,102,874	p11.2 - q11.21	Gain	6837906	50	8.33	41.67	0.0140
chr7:63,102,874-67,229,358	q11.21 - q11.22	Gain	4126484	62.5	8.33	54.17	0.0024
chr7:67,229,358-71,274,704	q11.22	Gain	4045346	62.5	11.11	51.39	0.0049
chr7:71,274,704-80,528,144	q11.22 - q21.11	Gain	9253440	62.5	13.89	48.61	0.0092
chr7:80,528,144-81,356,796	q21.11	Gain	828652	62.5	16.67	45.83	0.0157
chr7:81,356,796-142,857,956	q21.11 - q35	Gain	61501160	62.5	13.89	48.61	0.0092
chr8:14,461,142-28,432,298	p22 - p21.1	Loss	13971156	62.5	22.22	40.28	0.0375
chr8:28,432,298-30,816,370	p21.1 - p12	Loss	2384072	62.5	19.44	43.06	0.0249
chr8:38,289,058-39,836,613	p12 - p11.22	Loss	1547555	37.5	5.56	31.94	0.0349
chr8:39,836,613-43,315,811	p11.22 - p11.1	Loss	3479198	37.5	2.78	34.72	0.0154
chr8:4,386,741-14,461,142	p23.2 - p22	Loss	10074401	62.5	19.44	43.06	0.0249
chr9:124,954,691-140,118,015	q33.2 - q34.3	Gain	15163324	25	0.00	25.00	0.0296
chr9:13,729,630-21,157,685	p23 - p21.3	Gain	7428055	25	0.00	25.00	0.0296
chr9:140,118,015-140,273,252	q34.3	Loss	155237	0	41.67	-41.67	0.0368
chr9:190-336,203	p24.3	Gain	336013	37.5	0.00	37.50	0.0042
chr9:27,417,088-29,639,053	p21.2 - p21.1	Gain	2221965	25	0.00	25.00	0.0296
chr9:336,203-991,152	p24.3	Gain	654949	37.5	2.78	34.72	0.0154
chr9:38,427,196-84,783,002	p13.1 - q21.32	Gain	46355806	25	0.00	25.00	0.0296
chr9:84,783,002-89,446,315	q21.32 - q21.33	Gain	4663313	37.5	0.00	37.50	0.0042
chr9:89,446,315-123,651,685	q21.33 - q33.2	Gain	34205370	25	0.00	25.00	0.0296

[1]Physical position is according to hg18/NCBI build 36

Appendix 5.4: Regions showing significant copy number differences in grade 1/2 multifocal (n=11) versus solitary (n=35) tumours.

Region[1]	Cytoband Location	Event	Region Length	Freq. in Multifocal (%)	Freq. in Solitary (%)	Difference	p-value
chr1:119,708,536-153,581,460	p12 - q22	Gain	33872924	27.27	0.00	27.27	0.011
chr1:157,241,521-157,953,509	q23.1 - q23.2	Gain	711988	36.36	2.86	33.51	0.009
chr1:157,953,509-167,621,290	q23.2 - q24.2	Gain	9667781	36.36	0.00	36.36	0.002
chr1:167,621,290-193,197,934	q24.2 - q31.3	Gain	25576644	27.27	0.00	27.27	0.011
chr10:104,342,397-104,652,460	q24.32	Loss	310063	36.36	5.71	30.65	0.023
chr10:5,844,781-8,219,578	p15.1 - p14	Gain	2374797	27.27	0.00	27.27	0.011
chr10:71,487,752-73,834,924	q22.1	Gain	2347172	27.27	0.00	27.27	0.011
chr10:73,834,924-74,954,700	q22.1 - q22.2	Gain	1119776	36.36	0.00	36.36	0.002
chr10:74,954,700-89,597,006	q22.2 - q23.2	Gain	14642306	27.27	0.00	27.27	0.011
chr10:8,346,526-11,805,252	p14	Gain	3458726	27.27	0.00	27.27	0.011
chr13:107,482,925-110,508,381	q33.3 - q34	Gain	3025456	36.36	5.71	30.65	0.023
chr13:110,508,381-113,927,980	q34	Gain	3419599	36.36	2.86	33.51	0.009
chr13:19,137,297-19,920,905	q12.11	Gain	783608	45.45	5.71	39.74	0.005
chr13:19,920,905-20,982,693	q12.11	Gain	1061788	45.45	8.57	36.88	0.013
chr13:20,982,693-22,108,664	q12.11	Gain	1125971	45.45	5.71	39.74	0.005
chr13:22,108,664-27,824,701	q12.11 - q12.3	Gain	5716037	45.45	2.86	42.60	0.002
chr13:27,824,701-31,703,968	q12.3 - q13.1	Gain	3879267	36.36	2.86	33.51	0.009
chr13:37,218,551-47,794,572	q13.3 - q14.2	Loss	10576021	27.27	0.00	27.27	0.011
chr13:50,471,832-56,523,630	q14.3 - q21.1	Gain	6051798	36.36	2.86	33.51	0.009
chr13:56,523,630-56,717,407	q21.1	Gain	193777	36.36	0.00	36.36	0.002
chr13:56,717,407-66,421,707	q21.1 - q21.32	Gain	9704300	36.36	2.86	33.51	0.009
chr13:66,421,707-67,895,141	q21.32 - q21.33	Gain	1473434	45.45	2.86	42.60	0.002
chr13:67,895,141-107,482,925	q21.33 - q33.3	Gain	39587784	36.36	2.86	33.51	0.009
chr16:193,278-6,165,969	p13.3	Loss	5972691	27.27	0.00	27.27	0.011
chr16:82,569,517-84,922,020	q23.3 - q24.1	Loss	2352503	27.27	0.00	27.27	0.011
chr16:87,260,485-88,421,159	q24.3	Loss	1160674	36.36	2.86	33.51	0.009
chr16:88,552,007-88,552,722	q24.3	Loss	715	36.36	0.00	36.36	0.002

chr16:88,552,722-88,643,456	q24.3	Loss	90734	27.27	0.00	27.27	0.011
chr17:35,227,093-35,920,940	q12 - q21.2	Loss	693847	27.27	0.00	27.27	0.011
chr19:33,399,234-36,171,164	q12	Gain	2771930	27.27	0.00	27.27	0.011
chr19:36,322,238-40,876,527	q12 - q13.12	Gain	4554289	27.27	0.00	27.27	0.011
chr19:41,059,171-51,988,000	q13.12 - q13.32	Gain	10928829	27.27	0.00	27.27	0.011
chr19:52,342,137-63,602,791	q13.32 - q13.43	Gain	11260654	27.27	0.00	27.27	0.011
chr20:34,346,661-62,392,510	q11.23 - q13.33	Gain	28045849	45.45	11.43	34.03	0.025
chr6:162,865,542-162,954,569	q26	Gain	89027	27.27	0.00	27.27	0.011
chr8:124,550,528-124,718,428	q24.13	Gain	167900	45.45	0.00	45.45	0.000
chr8:124,718,428-131,641,498	q24.13 - q24.22	Gain	6923070	45.45	5.71	39.74	0.005
chr8:131,641,498-131,795,149	q24.22	Gain	153651	45.45	2.86	42.60	0.002
chr8:131,795,149-146,003,740	q24.22 - q24.3	Gain	14208591	45.45	5.71	39.74	0.005
chr8:146,003,740-146,133,884	q24.3	Gain	130144	36.36	5.71	30.65	0.023
chr8:28,432,298-38,289,058	p21.1 - p12	Loss	9856760	36.36	0.00	36.36	0.002
chr8:38,289,058-42,487,636	p12 - p11.21	Loss	4198578	27.27	0.00	27.27	0.011
chr8:42,674,285-65,551,264	p11.21 - q12.3	Gain	22876979	27.27	0.00	27.27	0.011
chr8:658,324-28,432,298	p23.3 - p21.1	Loss	27773974	36.36	2.86	33.51	0.009
chr8:69,616,969-70,378,901	q13.2	Gain	761932	36.36	2.86	33.51	0.009
chr8:70,378,901-72,600,219	q13.2 - q13.3	Gain	2221318	45.45	2.86	42.60	0.002
chr8:72,600,219-75,850,345	q13.3 - q21.11	Gain	3250126	36.36	2.86	33.51	0.009
chr8:96,177,980-124,550,528	q22.1 - q24.13	Gain	28372548	45.45	5.71	39.74	0.005
chr9:108,208,167-132,631,265	q31.2 - q34.12	Loss	24423098	81.82	40.00	41.82	0.035
chr9:190-1,340,595	p24.3	Gain	1340405	27.27	0.00	27.27	0.011
chr9:21,734,602-21,851,433	p21.3	Loss	116831	72.73	28.57	44.16	0.014
chr9:21,998,414-22,046,818	p21.3	Loss	48404	63.64	25.71	37.92	0.032
chr9:22,046,818-22,155,847	p21.3	Loss	109029	72.73	25.71	47.01	0.010
chr9:22,155,847-22,155,946	p21.3	Loss	99	63.64	25.71	37.92	0.032
chr9:68,858,635-70,488,655	q12 - q13	Loss	1630020	72.73	34.29	38.44	0.038
chr9:70,488,655-72,637,606	q13 - q21.11	Loss	2148951	81.82	34.29	47.53	0.013
chr9:72,637,606-82,003,000	q21.11 - q21.31	Loss	9365394	81.82	37.14	44.68	0.015
chr9:82,003,000-82,148,095	q21.31	Loss	145095	81.82	14.29	67.53	0.001
chr9:82,148,095-85,485,840	q21.31 - q21.32	Loss	3337745	81.82	37.14	44.68	0.015
chr9:85,485,840-87,920,679	q21.32 - q21.33	Loss	2434839	81.82	40.00	41.82	0.035
chr9:87,920,679-88,054,773	q21.33	Loss	134094	81.82	34.29	47.53	0.013

chr9:88,054,773-88,787,420	q21.33	Loss	732647	81.82	40.00	41.82	0.035
chr9:88,940,656-89,058,511	q21.33	Loss	117855	81.82	40.00	41.82	0.035
chr9:89,058,511-108,208,167	q21.33 - q31.2	Loss	19149656	81.82	42.86	38.96	0.038

[1]Physical position is according to hg18/NCBI build 36

Appendix 5.5: Regions showing significant copy number differences in grade 3 multifocal (n=11) versus solitary (n=39) tumours.

Region[1]	Cytoband Location	Event	Region Length	Freq. in Multifocal (%)	Freq. in Solitary (%)	Difference	p-value
chr1:113,473,675-117,407,078	p13.2 - p13.1	Gain	3933403	37.5	2.78	34.72	0.0154
chr1:113,473,675-117,407,078	p13.2 - p13.1	Gain	3933403	36.36	2.56	33.80	0.00629
chr1:117,407,078-119,480,610	p13.1 - p12	Gain	2073532	36.36	5.13	31.24	0.01655
chr1:119,480,610-119,708,536	p12	Gain	227926	54.55	5.13	49.42	0.00066
chr1:119,708,536-141,672,545	p12 - q12	Gain	21964009	63.64	5.13	58.51	0.00010
chr1:141,672,545-142,787,183	q12 - q21.1	Gain	1114638	63.64	7.69	55.94	0.00031
chr1:142,787,183-143,613,581	q21.1	Gain	826398	63.64	15.38	48.25	0.00331
chr1:143,613,581-143,614,341	q21.1	Gain	760	63.64	12.82	50.82	0.00168
chr1:143,614,341-146,342,686	q21.1	Gain	2728345	63.64	15.38	48.25	0.00331
chr1:146,342,686-148,424,834	q21.1 - q21.2	Gain	2082148	63.64	17.95	45.69	0.00602
chr1:148,424,834-154,399,117	q21.2 - q22	Gain	5974283	54.55	17.95	36.60	0.02334
chr1:185,614,023-191,477,703	q31.1 - q31.2	Loss	5863680	27.27	0.00	27.27	0.00842
chr1:192,424,789-197,774,987	q31.3 - q32.1	Loss	5350198	27.27	0.00	27.27	0.00842
chr1:234,285,489-237,780,877	q42.3 - q43	Loss	3495388	27.27	0.00	27.27	0.00842
chr1:241,339,986-247,164,041	q43 - q44	Loss	5824055	27.27	0.00	27.27	0.00842
chr1:25,159,219-29,481,197	p36.11 - p35.3	Gain	4321978	36.36	7.69	28.67	0.03380
chr1:29,481,197-33,046,828	p35.3 - p35.1	Gain	3565631	36.36	5.13	31.24	0.01655
chr1:33,046,828-38,051,746	p35.1 - p34.3	Gain	5004918	36.36	7.69	28.67	0.03380
chr1:38,051,746-39,307,926	p34.3	Gain	1256180	45.45	7.69	37.76	0.00853
chr1:39,307,926-44,062,032	p34.3 - p34.1	Gain	4754106	45.45	5.13	40.33	0.00361
chr1:44,062,032-45,524,938	p34.1	Gain	1462906	45.45	2.56	42.89	0.00116
chr1:45,524,938-50,594,589	p34.1 - p33	Gain	5069651	45.45	5.13	40.33	0.00361
chr1:50,594,589-50,823,305	p33	Gain	228716	36.36	5.13	31.24	0.01655
chr1:50,823,305-53,077,428	p33 - p32.3	Gain	2254123	45.45	5.13	40.33	0.00361
chr1:53,077,428-68,609,865	p32.3 - p31.3	Gain	15532437	45.45	2.56	42.89	0.00116
chr1:68,609,865-73,625,895	p31.3 - p31.1	Gain	5016030	36.36	2.56	33.80	0.00629
chr1:918,164-25,159,219	p36.33 - p36.11	Gain	24241055	36.36	5.13	31.24	0.01655

chr10:103,282,021-104,340,398	q24.32	Loss	1058377	72.73	10.26	62.47	0.00012
chr10:104,340,398-104,813,472	q24.32	Loss	473074	63.64	10.26	53.38	0.00077
chr10:104,813,472-108,400,155	q24.32 - q25.1	Loss	3586683	63.64	12.82	50.82	0.00168
chr10:108,400,155-114,874,404	q25.1 - q25.2	Loss	6474249	63.64	10.26	53.38	0.00077
chr10:114,874,404-116,774,295	q25.2 - q25.3	Loss	1899891	63.64	7.69	55.94	0.00031
chr10:116,774,295-119,495,422	q25.3 - q26.11	Loss	2721127	54.55	7.69	46.85	0.00179
chr10:119,495,422-120,558,865	q26.11	Loss	1063443	54.55	2.56	51.98	0.00018
chr10:120,558,865-123,214,100	q26.11 - q26.13	Loss	2655235	54.55	5.13	49.42	0.00066
chr10:123,214,100-125,057,698	q26.13	Loss	1843598	54.55	2.56	51.98	0.00018
chr10:125,057,698-126,007,431	q26.13	Loss	949733	45.45	2.56	42.89	0.00116
chr10:126,007,431-130,095,088	q26.13 - q26.2	Loss	4087657	45.45	0.00	45.45	0.00022
chr10:130,095,088-131,816,154	q26.2 - q26.3	Loss	1721066	54.55	0.00	54.55	0.00003
chr10:131,816,154-131,982,049	q26.3	Loss	165895	45.45	0.00	45.45	0.00022
chr10:131,982,049-135,247,831	q26.3	Loss	3265782	54.55	0.00	54.55	0.00003
chr10:76,882,526-78,996,385	q22.2 - q22.3	Loss	2113859	36.36	7.69	28.67	0.03380
chr10:78,996,385-80,472,830	q22.3	Loss	1476445	45.45	7.69	37.76	0.00853
chr10:80,472,830-83,636,464	q22.3 - q23.1	Loss	3163634	36.36	7.69	28.67	0.03380
chr10:83,636,464-83,637,155	q23.1	Loss	691	36.36	5.13	31.24	0.01655
chr10:83,637,155-84,577,760	q23.1	Loss	940605	36.36	7.69	28.67	0.03380
chr10:84,577,760-86,390,131	q23.1	Loss	1812371	45.45	7.69	37.76	0.00853
chr10:86,390,131-87,373,214	q23.1	Loss	983083	54.55	7.69	46.85	0.00179
chr10:87,373,214-88,222,653	q23.1 - q23.2	Loss	849439	54.55	10.26	44.29	0.00400
chr10:88,222,653-89,694,469	q23.2 - q23.31	Loss	1471816	63.64	10.26	53.38	0.00077
chr10:89,694,469-89,694,975	q23.31	Loss	506	54.55	10.26	44.29	0.00400
chr10:89,694,975-90,596,444	q23.31	Loss	901469	63.64	10.26	53.38	0.00077
chr10:90,596,444-93,738,544	q23.31 - q23.32	Loss	3142100	63.64	7.69	55.94	0.00031
chr10:93,738,544-94,907,303	q23.32 - q23.33	Loss	1168759	54.55	7.69	46.85	0.00179
chr10:94,907,303-95,924,122	q23.33	Loss	1016819	63.64	7.69	55.94	0.00031
chr10:95,924,122-103,282,021	q23.33 - q24.32	Loss	7357899	63.64	10.26	53.38	0.00077
chr11:107,722,054-108,393,306	q22.3	Loss	671252	36.36	5.13	31.24	0.01655
chr11:108,393,306-110,510,107	q22.3 - q23.1	Loss	2116801	36.36	7.69	28.67	0.03380
chr11:123,449,312-124,487,806	q24.1 - q24.2	Loss	1038494	36.36	7.69	28.67	0.03380
chr11:124,487,806-134,156,487	q24.2 - q25	Loss	9668681	36.36	5.13	31.24	0.01655
chr11:43,020,941-44,879,168	p12 - p11.2	Loss	1858227	45.45	12.82	32.63	0.02990

chr11:44,879,168-46,216,229	p11.2	Loss	1337061	45.45	10.26	35.20	0.01695
chr11:46,216,229-50,013,045	p11.2 - p11.12	Loss	3796816	45.45	7.69	37.76	0.00853
chr11:50,013,045-50,013,069	p11.12	Loss	24	45.45	5.13	40.33	0.00361
chr11:50,013,069-54,839,338	p11.12 - q11	Loss	4826269	36.36	5.13	31.24	0.01655
chr11:54,839,338-59,697,061	q11 - q12.1	Loss	4857723	36.36	0.00	36.36	0.00143
chr11:59,697,061-60,851,894	q12.1 - q12.2	Loss	1154833	36.36	2.56	33.80	0.00629
chr11:68,701,448-69,297,663	q13.2 - q13.3	Gain	596215	45.45	12.82	32.63	0.02990
chr11:69,297,663-69,323,924	q13.3	Gain	26261	45.45	7.69	37.76	0.00853
chr11:69,323,924-69,494,896	q13.3	Gain	170972	45.45	10.26	35.20	0.01695
chr11:69,494,896-70,236,623	q13.3	Gain	741727	45.45	12.82	32.63	0.02990
chr11:79,636,827-81,301,979	q14.1	Gain	1665152	27.27	0.00	27.27	0.00842
chr12:103,714,143-111,697,547	q23.3 - q24.13	Loss	7983404	27.27	0.00	27.27	0.00842
chr12:152,582-153,169	p13.33	Loss	587	27.27	0.00	27.27	0.00842
chr12:16,742,828-25,552,960	p12.3 - p12.1	Loss	8810132	27.27	0.00	27.27	0.00842
chr12:33,333,489-40,716,974	p11.1 - q12	Loss	7383485	27.27	0.00	27.27	0.00842
chr12:40,716,974-42,413,160	q12	Loss	1696186	36.36	0.00	36.36	0.00143
chr12:42,413,160-46,156,911	q12 - q13.11	Loss	3743751	27.27	0.00	27.27	0.00842
chr12:46,299,979-46,573,750	q13.11	Loss	273771	36.36	0.00	36.36	0.00143
chr12:46,573,750-52,417,126	q13.11 - q13.13	Loss	5843376	27.27	0.00	27.27	0.00842
chr13:108,341,331-113,927,980	q33.3 - q34	Gain	5586649	36.36	7.69	28.67	0.03380
chr13:47,964,053-51,243,111	q14.2 - q14.3	Loss	3279058	36.36	5.13	31.24	0.01655
chr13:78,112,209-108,341,331	q31.1 - q33.3	Gain	30229122	36.36	5.13	31.24	0.01655
chr14:25,757,198-26,561,378	q12	Loss	804180	36.36	5.13	31.24	0.01655
chr14:26,744,993-32,835,734	q12 - q13.1	Loss	6090741	36.36	5.13	31.24	0.01655
chr14:32,835,734-33,897,190	q13.1	Loss	1061456	36.36	2.56	33.80	0.00629
chr14:33,897,190-34,061,283	q13.1	Loss	164093	36.36	0.00	36.36	0.00143
chr14:34,061,283-44,957,642	q13.1 - q21.3	Loss	10896359	36.36	2.56	33.80	0.00629
chr14:44,957,642-57,420,120	q21.3 - q23.1	Loss	12462478	36.36	5.13	31.24	0.01655
chr14:57,420,120-58,323,469	q23.1	Loss	903349	45.45	5.13	40.33	0.00361
chr14:58,323,469-58,470,270	q23.1	Loss	146801	36.36	2.56	33.80	0.00629
chr14:58,470,270-59,336,011	q23.1	Loss	865741	45.45	5.13	40.33	0.00361
chr14:59,336,011-65,655,482	q23.1 - q23.3	Loss	6319471	36.36	5.13	31.24	0.01655
chr14:66,870,415-71,308,003	q23.3 - q24.2	Loss	4437588	36.36	7.69	28.67	0.03380
chr14:71,308,003-73,931,005	q24.2 - q24.3	Loss	2623002	45.45	7.69	37.76	0.00853

chr14:73,931,005-74,588,657	q24.3	Loss	657652	45.45	5.13	40.33	0.00361
chr14:74,588,657-81,191,238	q24.3 - q31.1	Loss	6602581	36.36	5.13	31.24	0.01655
chr15:22,736,020-22,894,833	q11.2	Gain	158813	36.36	5.13	31.24	0.01655
chr15:22,894,833-42,756,125	q11.2 - q21.1	Gain	19861292	36.36	7.69	28.67	0.03380
chr15:42,756,125-56,535,071	q21.1 - q22.1	Gain	13778946	45.45	7.69	37.76	0.00853
chr15:56,535,071-63,070,265	q22.1 - q22.31	Gain	6535194	36.36	7.69	28.67	0.03380
chr15:63,070,265-82,907,017	q22.31 - q25.2	Loss	19836752	27.27	0.00	27.27	0.00842
chr15:72,953,319-99,915,007	q24.1 - q26.3	Gain	26961688	36.36	7.69	28.67	0.03380
chr15:83,883,618-85,362,775	q25.3	Loss	1479157	27.27	0.00	27.27	0.00842
chr15:87,338,954-100,022,043	q26.1 - q26.3	Loss	12683089	27.27	0.00	27.27	0.00842
chr16:12,336,699-23,756,350	p13.13 - p12.1	Gain	11419651	27.27	0.00	27.27	0.00842
chr16:23,756,350-24,856,451	p12.1	Gain	1100101	36.36	0.00	36.36	0.00143
chr16:24,856,451-29,550,785	p12.1 - p11.2	Gain	4694334	36.36	2.56	33.80	0.00629
chr16:29,550,785-31,190,651	p11.2	Gain	1639866	36.36	0.00	36.36	0.00143
chr16:31,190,651-45,067,244	p11.2 - q11.2	Gain	13876593	45.45	0.00	45.45	0.00022
chr16:7,019,846-12,014,145	p13.2 - p13.13	Gain	4994299	27.27	0.00	27.27	0.00842
chr19:183,116-211,322	p13.3	Loss	28206	36.36	0.00	36.36	0.00143
chr19:20,458,451-43,004,473	p12 - q13.13	Loss	22546022	27.27	0.00	27.27	0.00842
chr19:21,345,165-22,729,077	p12	Gain	1383912	27.27	0.00	27.27	0.00842
chr19:211,322-5,009,897	p13.3	Loss	4798575	45.45	0.00	45.45	0.00022
chr19:23,732,302-32,891,236	p12 - q12	Gain	9158934	36.36	2.56	33.80	0.00629
chr19:32,891,236-33,399,234	q12	Gain	507998	36.36	0.00	36.36	0.00143
chr19:33,399,234-35,629,568	q12	Gain	2230334	36.36	5.13	31.24	0.01655
chr19:35,629,568-36,171,164	q12	Gain	541596	36.36	2.56	33.80	0.00629
chr19:36,322,238-36,979,850	q12	Gain	657612	36.36	2.56	33.80	0.00629
chr19:36,979,850-37,664,852	q12 - q13.11	Gain	685002	36.36	5.13	31.24	0.01655
chr19:37,664,852-38,091,322	q13.11	Gain	426470	45.45	7.69	37.76	0.00853
chr19:38,091,322-38,091,356	q13.11	Gain	34	45.45	5.13	40.33	0.00361
chr19:38,091,356-38,091,878	q13.11	Gain	522	45.45	2.56	42.89	0.00116
chr19:38,091,878-38,282,890	q13.11	Gain	191012	45.45	5.13	40.33	0.00361
chr19:38,282,890-39,226,664	q13.11	Gain	943774	45.45	7.69	37.76	0.00853
chr19:39,226,664-45,806,715	q13.11 - q13.2	Gain	6580051	45.45	5.13	40.33	0.00361
chr19:45,806,715-46,479,845	q13.2	Gain	673130	36.36	5.13	31.24	0.01655
chr19:46,479,845-51,023,195	q13.2 - q13.32	Gain	4543350	36.36	2.56	33.80	0.00629

chr19:47,423,994-63,771,717	q13.2 - q13.43	Loss	16347723	27.27	0.00	27.27	0.00842
chr19:5,009,897-5,549,421	p13.3	Loss	539524	45.45	2.56	42.89	0.00116
chr19:5,549,421-6,523,485	p13.3	Loss	974064	45.45	0.00	45.45	0.00022
chr19:51,988,000-58,336,597	q13.32 - q13.41	Gain	6348597	27.27	0.00	27.27	0.00842
chr19:59,359,392-59,464,022	q13.42	Gain	104630	27.27	0.00	27.27	0.00842
chr19:6,523,485-20,458,451	p13.3 - p12	Loss	13934966	36.36	0.00	36.36	0.00143
chr19:63,602,791-63,771,717	q13.43	Gain	168926	27.27	0.00	27.27	0.00842
chr2:1,785,220-11,122,011	p25.3 - p25.1	Gain	9336791	45.45	5.13	40.33	0.00361
chr2:11,122,011-20,037,859	p25.1 - p24.1	Gain	8915848	45.45	2.56	42.89	0.00116
chr2:127,253,875-148,009,604	q14.3 - q22.3	Loss	20755729	36.36	2.56	33.80	0.00629
chr2:148,009,604-151,825,968	q22.3 - q23.3	Loss	3816364	36.36	0.00	36.36	0.00143
chr2:151,825,968-153,751,686	q23.3	Loss	1925718	27.27	0.00	27.27	0.00842
chr2:153,751,686-156,410,442	q23.3 - q24.1	Loss	2658756	36.36	0.00	36.36	0.00143
chr2:156,410,442-169,397,061	q24.1 - q24.3	Loss	12986619	27.27	0.00	27.27	0.00842
chr2:157,250,015-159,300,999	q24.1	Gain	2050984	27.27	0.00	27.27	0.00842
chr2:169,397,061-175,231,393	q24.3 - q31.1	Loss	5834332	36.36	0.00	36.36	0.00143
chr2:175,231,393-176,870,358	q31.1	Loss	1638965	45.45	0.00	45.45	0.00022
chr2:176,870,358-183,311,858	q31.1 - q32.1	Loss	6441500	36.36	0.00	36.36	0.00143
chr2:183,311,858-207,861,345	q32.1 - q33.3	Loss	24549487	45.45	0.00	45.45	0.00022
chr2:20,037,859-20,215,537	p24.1	Gain	177678	36.36	2.56	33.80	0.00629
chr2:20,215,537-21,280,646	p24.1	Gain	1065109	45.45	2.56	42.89	0.00116
chr2:207,861,345-208,876,525	q33.3	Loss	1015180	45.45	2.56	42.89	0.00116
chr2:208,876,525-210,331,732	q33.3 - q34	Loss	1455207	63.64	2.56	61.07	0.00002
chr2:21,280,646-25,870,821	p24.1 - p23.3	Gain	4590175	36.36	2.56	33.80	0.00629
chr2:210,331,732-213,347,177	q34	Loss	3015445	63.64	5.13	58.51	0.00010
chr2:213,347,177-216,402,525	q34 - q35	Loss	3055348	63.64	7.69	55.94	0.00031
chr2:216,402,525-225,739,791	q35 - q36.2	Loss	9337266	63.64	10.26	53.38	0.00077
chr2:224,263-1,785,220	p25.3	Gain	1560957	45.45	2.56	42.89	0.00116
chr2:225,739,791-228,542,036	q36.2 - q36.3	Loss	2802245	63.64	12.82	50.82	0.00168
chr2:228,542,036-230,386,971	q36.3	Loss	1844935	72.73	12.82	59.91	0.00028
chr2:230,386,971-230,387,771	q36.3	Loss	800	72.73	10.26	62.47	0.00012
chr2:230,387,771-238,252,220	q36.3 - q37.3	Loss	7864449	72.73	12.82	59.91	0.00028
chr2:238,252,220-239,091,229	q37.3	Loss	839009	72.73	15.38	57.34	0.00061
chr2:239,091,229-241,620,162	q37.3	Loss	2528933	72.73	17.95	54.78	0.00121

chr2:241,620,162-241,796,109	q37.3	Loss	175947	72.73	15.38	57.34	0.00061
chr2:25,870,821-48,938,583	p23.3 - p16.3	Gain	23067762	45.45	2.56	42.89	0.00116
chr2:48,938,583-52,373,212	p16.3	Gain	3434629	45.45	0.00	45.45	0.00022
chr2:52,373,212-64,478,283	p16.3 - p14	Gain	12105071	54.55	0.00	54.55	0.00003
chr2:64,478,283-71,285,149	p14 - p13.3	Gain	6806866	45.45	0.00	45.45	0.00022
chr2:71,285,149-74,335,462	p13.3 - p13.1	Gain	3050313	54.55	0.00	54.55	0.00003
chr2:74,335,462-82,716,433	p13.1 - p12	Gain	8380971	45.45	0.00	45.45	0.00022
chr2:82,716,433-83,447,850	p12	Gain	731417	45.45	2.56	42.89	0.00116
chr2:83,447,850-88,214,979	p12 - p11.2	Gain	4767129	45.45	0.00	45.45	0.00022
chr2:88,214,979-94,782,159	p11.2 - q11.1	Gain	6567180	54.55	0.00	54.55	0.00003
chr2:94,782,159-95,675,764	q11.1	Gain	893605	36.36	0.00	36.36	0.00143
chr2:94,983,765-100,292,273	q11.1 - q11.2	Loss	5308508	27.27	0.00	27.27	0.00842
chr2:96,200,121-97,472,556	q11.2	Gain	1272435	27.27	0.00	27.27	0.00842
chr20:17,961,951-19,322,167	p11.23	Gain	1360216	63.64	10.26	53.38	0.00077
chr20:19,322,167-26,006,126	p11.23 - p11.1	Gain	6683959	63.64	12.82	50.82	0.00168
chr20:26,006,126-26,220,344	p11.1	Gain	214218	63.64	10.26	53.38	0.00077
chr20:26,220,344-28,267,569	p11.1 - q11.1	Gain	2047225	72.73	12.82	59.91	0.00028
chr20:275,014-424,783	p13	Gain	149769	63.64	2.56	61.07	0.00002
chr20:28,267,569-29,503,014	q11.1 - q11.21	Gain	1235445	72.73	23.08	49.65	0.00391
chr20:29,503,014-29,779,350	q11.21	Gain	276336	72.73	20.51	52.21	0.00224
chr20:29,779,350-30,526,698	q11.21	Gain	747348	72.73	23.08	49.65	0.00391
chr20:30,526,698-35,931,146	q11.21 - q11.23	Gain	5404448	72.73	20.51	52.21	0.00224
chr20:35,931,146-36,843,266	q11.23	Gain	912120	81.82	20.51	61.31	0.00036
chr20:36,843,266-37,522,311	q11.23 - q12	Gain	679045	81.82	23.08	58.74	0.00068
chr20:37,522,311-37,666,045	q12	Gain	143734	72.73	23.08	49.65	0.00391
chr20:37,666,045-39,296,098	q12	Gain	1630053	81.82	23.08	58.74	0.00068
chr20:39,296,098-40,680,814	q12	Gain	1384716	81.82	20.51	61.31	0.00036
chr20:40,680,814-40,792,351	q12	Gain	111537	72.73	20.51	52.21	0.00224
chr20:40,792,351-43,889,716	q12 - q13.12	Gain	3097365	72.73	25.64	47.09	0.00995
chr20:424,783-9,340,955	p13 - p12.2	Gain	8916172	63.64	5.13	58.51	0.00010
chr20:43,889,716-44,398,282	q13.12	Gain	508566	72.73	20.51	52.21	0.00224
chr20:44,398,282-45,646,214	q13.12	Gain	1247932	72.73	23.08	49.65	0.00391
chr20:45,646,214-47,243,628	q13.12 - q13.13	Gain	1597414	63.64	23.08	40.56	0.02410
chr20:47,243,628-47,383,084	q13.13	Gain	139456	72.73	23.08	49.65	0.00391

chr20:47,538,301-51,561,551	q13.13 - q13.2	Gain	4023250	72.73	23.08	49.65	0.00391
chr20:51,561,551-59,894,661	q13.2 - q13.33	Gain	8333110	72.73	20.51	52.21	0.00224
chr20:59,894,661-62,393,015	q13.33	Gain	2498354	63.64	20.51	43.12	0.01023
chr20:9,340,955-17,961,951	p12.2 - p11.23	Gain	8620996	63.64	7.69	55.94	0.00031
chr22:15,621,248-15,745,966	q11.1	Loss	124718	36.36	0.00	36.36	0.00143
chr22:15,745,966-16,347,244	q11.1 - q11.21	Loss	601278	54.55	0.00	54.55	0.00003
chr22:16,347,244-16,899,186	q11.21	Loss	551942	45.45	0.00	45.45	0.00022
chr22:16,899,186-18,151,355	q11.21	Loss	1252169	36.36	0.00	36.36	0.00143
chr22:18,151,355-18,151,891	q11.21	Loss	536	27.27	0.00	27.27	0.00842
chr22:18,151,891-20,448,350	q11.21	Loss	2296459	36.36	2.56	33.80	0.00629
chr22:20,448,350-24,286,893	q11.21 - q11.23	Loss	3838543	36.36	5.13	31.24	0.01655
chr22:24,286,893-24,560,716	q11.23 - q12.1	Loss	273823	36.36	7.69	28.67	0.03380
chr22:24,560,716-28,379,404	q12.1 - q12.2	Loss	3818688	36.36	5.13	31.24	0.01655
chr22:28,379,404-30,032,831	q12.2	Loss	1653427	36.36	2.56	33.80	0.00629
chr22:30,032,831-30,535,980	q12.2 - q12.3	Loss	503149	45.45	2.56	42.89	0.00116
chr22:30,535,980-30,623,768	q12.3	Loss	87788	36.36	2.56	33.80	0.00629
chr22:30,623,867-30,646,302	q12.3	Loss	22435	36.36	5.13	31.24	0.01655
chr22:30,646,401-40,803,595	q12.3 - q13.2	Loss	10157194	36.36	2.56	33.80	0.00629
chr22:40,803,595-42,473,589	q13.2	Loss	1669994	45.45	5.13	40.33	0.00361
chr22:42,473,589-44,175,906	q13.2 - q13.31	Loss	1702317	36.36	5.13	31.24	0.01655
chr22:44,175,906-45,618,622	q13.31	Loss	1442716	45.45	5.13	40.33	0.00361
chr22:45,618,622-49,453,810	q13.31 - q13.33	Loss	3835188	45.45	7.69	37.76	0.00853
chr3:111,740,734-121,091,572	q13.13 - q13.33	Gain	9350838	36.36	5.13	31.24	0.01655
chr3:121,091,572-121,205,097	q13.33	Gain	113525	36.36	2.56	33.80	0.00629
chr3:121,205,097-133,822,599	q13.33 - q22.1	Gain	12617502	36.36	5.13	31.24	0.01655
chr3:133,822,599-137,175,189	q22.1 - q22.2	Gain	3352590	36.36	2.56	33.80	0.00629
chr3:137,175,189-137,175,931	q22.2	Gain	742	36.36	0.00	36.36	0.00143
chr3:137,175,931-158,979,197	q22.2 - q25.32	Gain	21803266	36.36	2.56	33.80	0.00629
chr3:158,979,197-181,383,557	q25.32 - q26.33	Gain	22404360	36.36	5.13	31.24	0.01655
chr3:181,383,557-181,436,285	q26.33	Gain	52728	36.36	2.56	33.80	0.00629
chr3:181,436,285-187,914,171	q26.33 - q27.3	Gain	6477886	36.36	5.13	31.24	0.01655
chr3:187,914,171-187,914,682	q27.3	Gain	511	36.36	2.56	33.80	0.00629
chr3:187,914,682-199,160,165	q27.3 - q29	Gain	11245483	36.36	5.13	31.24	0.01655
chr3:54,612,454-71,816,463	p14.3 - p13	Gain	17204009	27.27	0.00	27.27	0.00842

chr3:6,636,703-10,788,431	p26.1 - p25.3	Gain	4151728	36.36	7.69	28.67	0.03380
chr3:74,391,234-77,584,830	p12.3	Gain	3193596	36.36	2.56	33.80	0.00629
chr3:77,584,830-79,097,077	p12.3	Gain	1512247	36.36	0.00	36.36	0.00143
chr3:79,097,077-82,066,186	p12.3 - p12.2	Gain	2969109	36.36	2.56	33.80	0.00629
chr3:82,066,186-82,799,401	p12.2	Gain	733215	36.36	5.13	31.24	0.01655
chr3:82,799,401-83,768,022	p12.2 - p12.1	Gain	968621	45.45	5.13	40.33	0.00361
chr3:83,768,022-87,044,540	p12.1	Gain	3276518	45.45	2.56	42.89	0.00116
chr3:87,044,540-111,740,734	p12.1 - q13.13	Gain	24696194	36.36	2.56	33.80	0.00629
chr3:958,261-6,636,703	p26.3 - p26.1	Gain	5678442	36.36	5.13	31.24	0.01655
chr4:1,065,598-2,865,088	p16.3	Loss	1799490	36.36	2.56	33.80	0.00629
chr4:10,207,878-11,429,778	p16.1 - p15.33	Loss	1221900	36.36	5.13	31.24	0.01655
chr4:113,578,539-152,907,961	q25 - q31.3	Loss	39329422	36.36	0.00	36.36	0.00143
chr4:13,655,289-26,747,433	p15.33 - p15.2	Loss	13092144	36.36	5.13	31.24	0.01655
chr4:152,907,961-179,587,711	q31.3 - q34.3	Loss	26679750	36.36	2.56	33.80	0.00629
chr4:179,587,711-180,006,495	q34.3	Loss	418784	36.36	5.13	31.24	0.01655
chr4:180,006,495-182,025,739	q34.3	Loss	2019244	36.36	7.69	28.67	0.03380
chr4:184,404,421-185,872,338	q35.1	Gain	1467917	27.27	0.00	27.27	0.00842
chr4:184,561,840-185,872,338	q35.1	Loss	1310498	36.36	7.69	28.67	0.03380
chr4:185,872,338-191,020,215	q35.1 - q35.2	Loss	5147877	36.36	5.13	31.24	0.01655
chr4:2,865,088-10,207,878	p16.3 - p16.1	Loss	7342790	36.36	7.69	28.67	0.03380
chr4:207,197-1,065,598	p16.3	Loss	858401	45.45	2.56	42.89	0.00116
chr4:207,197-7,937,465	p16.3 - p16.1	Gain	7730268	36.36	2.56	33.80	0.00629
chr4:26,747,433-38,175,739	p15.2 - p14	Loss	11428306	45.45	5.13	40.33	0.00361
chr4:38,175,739-45,608,190	p14 - p12	Loss	7432451	45.45	2.56	42.89	0.00116
chr4:45,608,190-47,264,023	p12	Loss	1655833	36.36	2.56	33.80	0.00629
chr4:47,264,023-47,677,803	p12	Loss	413780	36.36	0.00	36.36	0.00143
chr4:47,677,803-48,524,316	p12	Loss	846513	27.27	0.00	27.27	0.00842
chr4:55,628-207,197	p16.3	Loss	151569	45.45	0.00	45.45	0.00022
chr4:74,866,776-76,733,068	q13.3 - q21.1	Gain	1866292	27.27	0.00	27.27	0.00842
chr4:77,782,579-78,196,278	q21.1	Gain	413699	27.27	0.00	27.27	0.00842
chr4:80,547,099-81,510,343	q21.21	Loss	963244	27.27	0.00	27.27	0.00842
chr4:82,199,002-113,578,539	q21.21 - q25	Loss	31379537	27.27	0.00	27.27	0.00842
chr5:136,366,234-152,728,888	q31.2 - q33.2	Loss	16362654	36.36	7.69	28.67	0.03380
chr5:152,728,888-154,417,750	q33.2	Loss	1688862	45.45	7.69	37.76	0.00853

chr5:154,417,750-169,611,921	q33.2 - q35.1	Loss	15194171	36.36	7.69	28.67	0.03380
chr5:169,611,921-169,783,365	q35.1	Loss	171444	36.36	5.13	31.24	0.01655
chr5:169,783,365-178,243,610	q35.1 - q35.3	Loss	8460245	36.36	7.69	28.67	0.03380
chr5:178,243,610-178,415,257	q35.3	Loss	171647	36.36	2.56	33.80	0.00629
chr5:178,415,257-180,512,398	q35.3	Loss	2097141	36.36	7.69	28.67	0.03380
chr5:180,512,398-180,626,608	q35.3	Loss	114210	36.36	2.56	33.80	0.00629
chr5:22,468,834-35,388,213	p14.3 - p13.2	Gain	12919379	45.45	10.26	35.20	0.01695
chr5:3,426,805-3,559,003	p15.33	Gain	132198	36.36	7.69	28.67	0.03380
chr5:51,232,444-65,352,862	q11.2 - q12.3	Loss	14120418	45.45	10.26	35.20	0.01695
chr5:99,111,442-107,339,380	q21.1 - q21.3	Loss	8227938	36.36	7.69	28.67	0.03380
chr6:168,121,846-169,488,215	q27	Loss	1366369	45.45	10.26	35.20	0.01695
chr6:169,576,118-170,622,773	q27	Loss	1046655	45.45	10.26	35.20	0.01695
chr6:170,622,773-170,728,000	q27	Loss	105227	45.45	5.13	40.33	0.00361
chr6:20,272,069-22,580,422	p22.3	Gain	2308353	45.45	10.26	35.20	0.01695
chr6:22,580,422-23,499,391	p22.3	Gain	918969	45.45	5.13	40.33	0.00361
chr6:23,499,391-27,152,460	p22.3 - p22.1	Gain	3653069	36.36	5.13	31.24	0.01655
chr7:142,857,956-144,143,399	q35	Gain	1285443	54.55	10.26	44.29	0.00400
chr7:144,143,399-147,259,180	q35	Gain	3115781	54.55	7.69	46.85	0.00179
chr7:147,259,180-148,089,302	q35 - q36.1	Gain	830122	54.55	10.26	44.29	0.00400
chr7:148,089,302-151,558,264	q36.1	Gain	3468962	54.55	12.82	41.72	0.00789
chr7:15,056,488-21,588,275	p21.2 - p15.3	Gain	6531787	45.45	12.82	32.63	0.02990
chr7:151,558,264-153,901,560	q36.1 - q36.2	Gain	2343296	54.55	10.26	44.29	0.00400
chr7:153,901,560-158,625,992	q36.2 - q36.3	Gain	4724432	54.55	12.82	41.72	0.00789
chr7:16,205,630-17,756,921	p21.1	Loss	1551291	27.27	0.00	27.27	0.00842
chr7:188,219-257,533	p22.3	Gain	69314	36.36	7.69	28.67	0.03380
chr7:26,749,335-29,450,068	p15.2 - p15.1	Gain	2700733	45.45	12.82	32.63	0.02990
chr7:50,617,642-52,867,234	p12.2 - p12.1	Gain	2249592	45.45	10.26	35.20	0.01695
chr7:52,867,234-56,264,968	p12.1 - p11.2	Gain	3397734	45.45	12.82	32.63	0.02990
chr7:56,264,968-63,102,874	p11.2 - q11.21	Gain	6837906	45.45	7.69	37.76	0.00853
chr7:63,102,874-67,229,358	q11.21 - q11.22	Gain	4126484	54.55	7.69	46.85	0.00179
chr7:67,229,358-71,274,704	q11.22	Gain	4045346	54.55	10.26	44.29	0.00400
chr7:71,274,704-80,528,144	q11.22 - q21.11	Gain	9253440	54.55	12.82	41.72	0.00789
chr7:80,528,144-81,356,796	q21.11	Gain	828652	54.55	15.38	39.16	0.01410
chr7:81,356,796-142,857,956	q21.11 - q35	Gain	61501160	54.55	12.82	41.72	0.00789

chr8:1,128,443-1,706,678	p23.3	Loss	578235	54.55	17.95	36.60	0.02334
chr8:14,461,142-27,277,284	p22 - p21.2	Loss	12816142	63.64	23.08	40.56	0.02410
chr8:27,277,284-30,816,370	p21.2 - p12	Loss	3539086	63.64	20.51	43.12	0.01023
chr8:37,204,481-38,289,058	p12	Loss	1084577	36.36	7.69	28.67	0.03380
chr8:38,289,058-39,836,613	p12 - p11.22	Loss	1547555	36.36	5.13	31.24	0.01655
chr8:39,836,613-43,315,811	p11.22 - p11.1	Loss	3479198	36.36	2.56	33.80	0.00629
chr8:4,386,741-14,461,142	p23.2 - p22	Loss	10074401	63.64	20.51	43.12	0.01023
chr9:13,729,630-21,157,685	p23 - p21.3	Gain	7428055	27.27	0.00	27.27	0.00842
chr9:140,118,015-140,273,252	q34.3	Loss	155237	0.00	43.59	-43.59	0.00909
chr9:190-336,203	p24.3	Gain	336013	27.27	0.00	27.27	0.00842
chr9:27,417,088-29,639,053	p21.2 - p21.1	Gain	2221965	27.27	0.00	27.27	0.00842
chr9:38,427,196-44,898,290	p13.1 - p11.2	Gain	6471094	27.27	0.00	27.27	0.00842
chr9:45,100,371-70,318,675	p11.2 - q13	Gain	25218304	27.27	0.00	27.27	0.00842
chr9:84,783,002-89,446,315	q21.32 - q21.33	Gain	4663313	27.27	0.00	27.27	0.00842

[1]Physical position is according to hg18/NCBI build 36

Appendix 5.6: Regions showing significant copy number differences in low stage and low grade (TaG1/G2) multifocal (n=11) versus solitary (n=28) tumours.

Region[1]	Cytoband Location	Event	Region Length	Freq. in Multifocal (%)	Freq. in Solitary (%)	Difference	p-value
chr1:119,708,536-153,581,460	p12 - q22	Gain	33872924	27.27	0.00	27.27	0.0181
chr1:157,241,521-157,953,509	q23.1 - q23.2	Gain	711988	36.36	3.57	32.79	0.0169
chr1:157,953,509-167,621,290	q23.2 - q24.2	Gain	9667781	36.36	0.00	36.36	0.0040
chr1:167,621,290-193,197,934	q24.2 - q31.3	Gain	25576644	27.27	0.00	27.27	0.0181
chr10:104,342,397-104,652,460	q24.32	Loss	310063	36.36	7.14	29.22	0.0423
chr10:5,844,781-8,219,578	p15.1 - p14	Gain	2374797	27.27	0.00	27.27	0.0181
chr10:71,487,752-73,834,924	q22.1	Gain	2347172	27.27	0.00	27.27	0.0181
chr10:73,834,924-74,954,700	q22.1 - q22.2	Gain	1119776	36.36	0.00	36.36	0.0040
chr10:74,954,700-89,597,006	q22.2 - q23.2	Gain	14642306	27.27	0.00	27.27	0.0181
chr10:8,346,526-11,805,252	p14	Gain	3458726	27.27	0.00	27.27	0.0181
chr13:19,137,297-19,920,905	q12.11	Gain	783608	45.45	7.14	38.31	0.0122
chr13:19,920,905-20,982,693	q12.11	Gain	1061788	45.45	10.71	34.74	0.0276
chr13:20,982,693-22,108,664	q12.11	Gain	1125971	45.45	7.14	38.31	0.0122
chr13:22,108,664-27,824,701	q12.11 - q12.3	Gain	5716037	45.45	3.57	41.88	0.0041
chr13:27,824,701-31,703,968	q12.3 - q13.1	Gain	3879267	36.36	3.57	32.79	0.0169
chr13:37,218,551-47,794,572	q13.3 - q14.2	Loss	10576021	27.27	0.00	27.27	0.0181
chr13:50,471,832-56,523,630	q14.3 - q21.1	Gain	6051798	36.36	3.57	32.79	0.0169
chr13:56,523,630-56,717,407	q21.1	Gain	193777	36.36	0.00	36.36	0.0040
chr13:56,717,407-66,421,707	q21.1 - q21.32	Gain	9704300	36.36	3.57	32.79	0.0169
chr13:66,421,707-67,895,141	q21.32 - q21.33	Gain	1473434	45.45	3.57	41.88	0.0041
chr13:67,895,141-113,927,980	q21.33 - q34	Gain	46032839	36.36	3.57	32.79	0.0169
chr16:193,278-6,165,969	p13.3	Loss	5972691	27.27	0.00	27.27	0.0181
chr16:82,569,517-84,922,020	q23.3 - q24.1	Loss	2352503	27.27	0.00	27.27	0.0181
chr16:87,260,485-88,421,159	q24.3	Loss	1160674	36.36	3.57	32.79	0.0169
chr16:88,552,007-88,552,722	q24.3	Loss	715	36.36	0.00	36.36	0.0040
chr16:88,552,722-88,643,456	q24.3	Loss	90734	27.27	0.00	27.27	0.0181
chr17:35,227,093-35,920,940	q12 - q21.2	Loss	693847	27.27	0.00	27.27	0.0181

chr19:33,399,234-36,171,164	q12	Gain	2771930	27.27	0.00	27.27	0.0181
chr19:36,322,238-40,876,527	q12 - q13.12	Gain	4554289	27.27	0.00	27.27	0.0181
chr19:41,059,171-51,988,000	q13.12 - q13.32	Gain	10928829	27.27	0.00	27.27	0.0181
chr19:52,342,137-63,602,791	q13.32 - q13.43	Gain	11260654	27.27	0.00	27.27	0.0181
chr20:34,346,661-62,392,510	q11.23 - q13.33	Gain	28045849	45.45	10.71	34.74	0.0276
chr6:162,865,542-162,954,569	q26	Gain	89027	27.27	0.00	27.27	0.0181
chr8:124,550,528-124,718,428	q24.13	Gain	167900	45.45	0.00	45.45	0.0008
chr8:124,718,428-146,003,740	q24.13 - q24.3	Gain	21285312	45.45	3.57	41.88	0.0041
chr8:146,003,740-146,133,884	q24.3	Gain	130144	36.36	3.57	32.79	0.0169
chr8:38,289,058-42,487,636	p12 - p11.21	Loss	4198578	27.27	0.00	27.27	0.0181
chr8:42,674,285-65,551,264	p11.21 - q12.3	Gain	22876979	27.27	0.00	27.27	0.0181
chr8:477,653-658,324	p23.3	Loss	180671	27.27	0.00	27.27	0.0181
chr8:658,324-38,289,058	p23.3 - p12	Loss	37630734	36.36	0.00	36.36	0.0040
chr8:69,616,969-70,378,901	q13.2	Gain	761932	36.36	3.57	32.79	0.0169
chr8:70,378,901-72,600,219	q13.2 - q13.3	Gain	2221318	45.45	3.57	41.88	0.0041
chr8:72,600,219-75,850,345	q13.3 - q21.11	Gain	3250126	36.36	3.57	32.79	0.0169
chr8:96,177,980-124,550,528	q22.1 - q24.13	Gain	28372548	45.45	3.57	41.88	0.0041
chr9:140,118,015-140,273,252	q34.3	Loss	155237	0.00	32.14	-32.14	0.0403
chr9:190-1,340,595	p24.3	Gain	1340405	27.27	0.00	27.27	0.0181
chr9:21,734,602-21,851,433	p21.3	Loss	116831	72.73	21.43	51.30	0.0072
chr9:21,851,433-21,998,414	p21.3	Loss	146981	63.64	21.43	42.21	0.0221
chr9:21,998,414-22,046,818	p21.3	Loss	48404	63.64	17.86	45.78	0.0170
chr9:22,046,818-22,155,847	p21.3	Loss	109029	72.73	17.86	54.87	0.0021
chr9:22,155,847-22,155,946	p21.3	Loss	99	63.64	17.86	45.78	0.0170
chr9:22,155,946-23,376,562	p21.3	Loss	1220616	63.64	21.43	42.21	0.0221
chr9:23,376,562-24,090,721	p21.3	Loss	714159	54.55	17.86	36.69	0.0443
chr9:68,858,635-70,488,655	q12 - q13	Loss	1630020	72.73	28.57	44.16	0.0272
chr9:70,488,655-82,003,000	q13 - q21.31	Loss	11514345	81.82	28.57	53.25	0.0040
chr9:82,003,000-82,148,095	q21.31	Loss	145095	81.82	10.71	71.10	0.0004
chr9:82,148,095-85,485,840	q21.31 - q21.32	Loss	3337745	81.82	28.57	53.25	0.0040
chr9:85,485,840-87,920,679	q21.32 - q21.33	Loss	2434839	81.82	32.14	49.68	0.0107
chr9:87,920,679-88,054,773	q21.33	Loss	134094	81.82	28.57	53.25	0.0040
chr9:88,054,773-88,787,420	q21.33	Loss	732647	81.82	32.14	49.68	0.0107
chr9:88,883,454-88,940,656	q21.33	Loss	57202	63.64	25.00	38.64	0.0331

chr9:88,940,656-89,058,511	q21.33	Loss	117855	81.82	32.14	49.68	0.0107
chr9:89,058,511-132,631,265	q21.33 - q34.12	Loss	43572754	81.82	35.71	46.10	0.0138

[1]Physical position is according to hg18/NCBI build 36

Appendix 5.7: Regions showing significant copy number differences in stage T1 and grade 3 (T1G3) multifocal (n=8) versus solitary (n=29) tumours.

Region[1]	Cytoband Location	Event	Region Length	Freq. in Multifocal (%)	Freq. in Solitary (%)	Difference	p-value
chr1:113,473,675-117,407,078	p13.2 - p13.1	Gain	3933403	37.5	3.45	34.05	0.0256
chr1:119,480,610-141,672,545	p12 - q12	Gain	22191935	62.5	6.90	55.60	0.0023
chr1:141,672,545-142,787,183	q12 - q21.1	Gain	1114638	62.5	10.34	52.16	0.0056
chr1:142,787,183-143,613,581	q21.1	Gain	826398	62.5	17.24	45.26	0.0211
chr1:143,613,581-143,614,341	q21.1	Gain	760	62.5	13.79	48.71	0.0115
chr1:143,614,341-146,342,686	q21.1	Gain	2728345	62.5	17.24	45.26	0.0211
chr1:146,342,686-154,399,117	q21.1 - q22	Gain	8056431	62.5	20.69	41.81	0.0352
chr1:160,195,246-160,195,822	q23.3	Gain	576	62.5	20.69	41.81	0.0352
chr1:185,614,023-191,477,703	q31.1 - q31.2	Loss	5863680	25	0.00	25.00	0.0420
chr1:192,424,789-237,780,877	q31.3 - q43	Loss	45356088	25	0.00	25.00	0.0420
chr1:241,339,986-247,164,041	q43 - q44	Loss	5824055	25	0.00	25.00	0.0420
chr1:38,051,746-39,307,926	p34.3	Gain	1256180	50	10.34	39.66	0.0271
chr1:39,307,926-44,062,032	p34.3 - p34.1	Gain	4754106	50	6.90	43.10	0.0129
chr1:44,062,032-45,524,938	p34.1	Gain	1462906	50	3.45	46.55	0.0048
chr1:45,524,938-53,077,428	p34.1 - p32.3	Gain	7552490	50	6.90	43.10	0.0129
chr1:53,077,428-73,625,895	p32.3 - p31.1	Gain	20548467	50	3.45	46.55	0.0048
chr1:73,625,895-83,494,525	p31.1	Gain	9868630	37.5	3.45	34.05	0.0256
chr10:104,813,472-108,400,155	q24.32 - q25.1	Loss	3586683	75	13.79	61.21	0.0020
chr10:108,400,155-114,874,404	q25.1 - q25.2	Loss	6474249	75	10.34	64.66	0.0008
chr10:114,874,404-116,774,295	q25.2 - q25.3	Loss	1899891	75	6.90	68.10	0.0003
chr10:116,774,295-119,495,422	q25.3 - q26.11	Loss	2721127	62.5	6.90	55.60	0.0023
chr10:119,495,422-120,558,865	q26.11	Loss	1063443	62.5	3.45	59.05	0.0007
chr10:120,558,865-123,214,100	q26.11 - q26.13	Loss	2655235	62.5	6.90	55.60	0.0023
chr10:123,214,100-125,057,698	q26.13	Loss	1843598	62.5	3.45	59.05	0.0007
chr10:125,057,698-126,007,431	q26.13	Loss	949733	50	3.45	46.55	0.0048
chr10:126,007,431-131,816,154	q26.13 - q26.3	Loss	5808723	50	0.00	50.00	0.0011
chr10:131,816,154-131,982,049	q26.3	Loss	165895	37.5	0.00	37.50	0.0072

chr10:131,982,049-135,247,831	q26.3	Loss	3265782	50	0.00	50.00	0.0011
chr10:34,638,996-38,812,575	p11.21 - p11.1	Loss	4173579	25	0.00	25.00	0.0420
chr10:72,803,738-79,687,959	q22.1 - q22.3	Gain	6884221	25	0.00	25.00	0.0420
chr10:78,996,385-80,472,830	q22.3	Loss	1476445	50	6.90	43.10	0.0129
chr10:83,636,464-83,637,155	q23.1	Loss	691	37.5	3.45	34.05	0.0256
chr10:84,577,760-86,390,131	q23.1	Loss	1812371	50	6.90	43.10	0.0129
chr10:86,390,131-87,373,214	q23.1	Loss	983083	62.5	6.90	55.60	0.0023
chr10:87,373,214-88,222,653	q23.1 - q23.2	Loss	849439	62.5	10.34	52.16	0.0056
chr10:88,222,653-89,694,469	q23.2 - q23.31	Loss	1471816	75	10.34	64.66	0.0008
chr10:89,694,469-89,694,975	q23.31	Loss	506	62.5	10.34	52.16	0.0056
chr10:89,694,975-90,596,444	q23.31	Loss	901469	75	10.34	64.66	0.0008
chr10:90,596,444-95,924,122	q23.31 - q23.33	Loss	5327678	75	6.90	68.10	0.0003
chr10:95,924,122-104,813,472	q23.33 - q24.32	Loss	8889350	75	10.34	64.66	0.0008
chr11:50,013,045-54,839,338	p11.12 - q11	Loss	4826293	37.5	3.45	34.05	0.0256
chr11:54,839,338-59,697,061	q11 - q12.1	Loss	4857723	37.5	0.00	37.50	0.0072
chr11:59,697,061-60,851,894	q12.1 - q12.2	Loss	1154833	37.5	3.45	34.05	0.0256
chr11:76,232,396-78,206,791	q13.5 - q14.1	Gain	1974395	25	0.00	25.00	0.0420
chr11:79,636,827-81,301,979	q14.1	Gain	1665152	25	0.00	25.00	0.0420
chr12:152,534-152,582	p13.33	Loss	48	37.5	3.45	34.05	0.0256
chr12:152,582-153,169	p13.33	Loss	587	37.5	0.00	37.50	0.0072
chr12:153,169-16,742,828	p13.33 - p12.3	Loss	16589659	37.5	3.45	34.05	0.0256
chr12:16,742,828-25,552,960	p12.3 - p12.1	Loss	8810132	37.5	0.00	37.50	0.0072
chr12:29,733,366-30,740,646	p11.22 - p11.21	Loss	1007280	25	0.00	25.00	0.0420
chr12:30,939,600-33,333,489	p11.21 - p11.1	Loss	2393889	25	0.00	25.00	0.0420
chr12:33,333,489-46,156,911	p11.1 - q13.11	Loss	12823422	37.5	0.00	37.50	0.0072
chr12:46,156,911-52,417,126	q13.11 - q13.13	Loss	6260215	25	0.00	25.00	0.0420
chr12:68,627,676-71,742,532	q15 - q21.1	Loss	3114856	25	0.00	25.00	0.0420
chr12:91,367,961-121,982,522	q22 - q24.31	Loss	30614561	25	0.00	25.00	0.0420
chr13:47,964,053-51,243,111	q14.2 - q14.3	Loss	3279058	50	6.90	43.10	0.0129
chr14:23,749,068-26,561,378	q12	Loss	2812310	37.5	3.45	34.05	0.0256
chr14:26,744,993-33,897,190	q12 - q13.1	Loss	7152197	37.5	3.45	34.05	0.0256
chr14:33,897,190-34,061,283	q13.1	Loss	164093	37.5	0.00	37.50	0.0072
chr14:34,061,283-57,420,120	q13.1 - q23.1	Loss	23358837	37.5	3.45	34.05	0.0256
chr14:57,420,120-58,323,469	q23.1	Loss	903349	50	3.45	46.55	0.0048

chr14:58,323,469-58,470,270	q23.1	Loss	146801	37.5	0.00	37.50	0.0072
chr14:58,470,270-59,336,011	q23.1	Loss	865741	50	3.45	46.55	0.0048
chr14:59,336,011-66,870,415	q23.1 - q23.3	Loss	7534404	37.5	3.45	34.05	0.0256
chr14:73,931,005-74,588,657	q24.3	Loss	657652	37.5	3.45	34.05	0.0256
chr14:75,833,225-77,328,585	q24.3	Gain	1495360	25	0.00	25.00	0.0420
chr15:20,363,717-31,975,417	q11.2 - q14	Loss	11611700	25	0.00	25.00	0.0420
chr15:62,510,397-63,070,265	q22.31	Loss	559868	37.5	3.45	34.05	0.0256
chr15:63,070,265-82,907,017	q22.31 - q25.2	Loss	19836752	37.5	0.00	37.50	0.0072
chr15:82,907,017-83,883,618	q25.2 - q25.3	Loss	976601	25	0.00	25.00	0.0420
chr15:83,883,618-85,362,775	q25.3	Loss	1479157	37.5	0.00	37.50	0.0072
chr15:85,362,775-87,338,954	q25.3 - q26.1	Loss	1976179	37.5	3.45	34.05	0.0256
chr15:87,338,954-100,022,043	q26.1 - q26.3	Loss	12683089	37.5	0.00	37.50	0.0072
chr16:2,267,343-7,019,846	p13.3 - p13.2	Gain	4752503	25	0.00	25.00	0.0420
chr16:23,756,350-24,856,451	p12.1	Gain	1100101	50	0.00	50.00	0.0011
chr16:24,856,451-29,550,785	p12.1 - p11.2	Gain	4694334	50	3.45	46.55	0.0048
chr16:29,550,785-45,067,244	p11.2 - q11.2	Gain	15516459	50	0.00	50.00	0.0011
chr16:3,918,289-4,131,849	p13.3	Loss	213560	25	0.00	25.00	0.0420
chr16:33,715,230-45,231,075	p11.2 - q11.2	Loss	11515845	25	0.00	25.00	0.0420
chr16:45,231,075-63,462,907	q11.2 - q21	Loss	18231832	37.5	0.00	37.50	0.0072
chr16:63,462,907-88,552,722	q21 - q24.3	Loss	25089815	25	0.00	25.00	0.0420
chr16:7,019,846-23,756,350	p13.2 - p12.1	Gain	16736504	37.5	0.00	37.50	0.0072
chr17:12,108,967-14,364,543	p12	Gain	2255576	25	0.00	25.00	0.0420
chr19:183,116-211,322	p13.3	Loss	28206	25	0.00	25.00	0.0420
chr19:21,345,165-22,729,077	p12	Gain	1383912	25	0.00	25.00	0.0420
chr19:211,322-5,009,897	p13.3	Loss	4798575	37.5	0.00	37.50	0.0072
chr19:23,732,302-32,891,236	p12 - q12	Gain	9158934	37.5	3.45	34.05	0.0256
chr19:32,891,236-33,399,234	q12	Gain	507998	37.5	0.00	37.50	0.0072
chr19:35,629,568-36,171,164	q12	Gain	541596	37.5	3.45	34.05	0.0256
chr19:36,322,238-36,979,850	q12	Gain	657612	37.5	3.45	34.05	0.0256
chr19:37,664,852-38,091,322	q13.11	Gain	426470	50	6.90	43.10	0.0129
chr19:38,091,322-38,282,890	q13.11	Gain	191568	50	3.45	46.55	0.0048
chr19:38,282,890-39,226,664	q13.11	Gain	943774	50	6.90	43.10	0.0129
chr19:39,226,664-45,806,715	q13.11 - q13.2	Gain	6580051	50	3.45	46.55	0.0048
chr19:45,806,715-46,479,845	q13.2	Gain	673130	37.5	3.45	34.05	0.0256

chr19:46,479,845-51,023,195	q13.2 - q13.32	Gain	4543350	37.5	0.00	37.50	0.0072
chr19:5,009,897-5,549,421	p13.3	Loss	539524	37.5	3.45	34.05	0.0256
chr19:5,549,421-6,523,485	p13.3	Loss	974064	37.5	0.00	37.50	0.0072
chr19:51,023,195-58,336,597	q13.32 - q13.41	Gain	7313402	25	0.00	25.00	0.0420
chr19:59,359,392-59,464,022	q13.42	Gain	104630	25	0.00	25.00	0.0420
chr19:6,523,485-20,458,451	p13.3 - p12	Loss	13934966	25	0.00	25.00	0.0420
chr19:63,602,791-63,771,717	q13.43	Gain	168926	25	0.00	25.00	0.0420
chr2:1,785,220-11,122,011	p25.3 - p25.1	Gain	9336791	50	6.90	43.10	0.0129
chr2:109,111,217-109,319,695	q13	Gain	208478	25	0.00	25.00	0.0420
chr2:11,122,011-20,037,859	p25.1 - p24.1	Gain	8915848	50	3.45	46.55	0.0048
chr2:111,491,810-159,300,999	q13 - q24.1	Gain	47809189	25	0.00	25.00	0.0420
chr2:148,009,604-151,825,968	q22.3 - q23.3	Loss	3816364	25	0.00	25.00	0.0420
chr2:153,751,686-169,397,061	q23.3 - q24.3	Loss	15645375	25	0.00	25.00	0.0420
chr2:167,445,852-169,206,769	q24.3	Gain	1760917	25	0.00	25.00	0.0420
chr2:169,397,061-207,861,345	q24.3 - q33.3	Loss	38464284	37.5	0.00	37.50	0.0072
chr2:20,037,859-20,215,537	p24.1	Gain	177678	37.5	3.45	34.05	0.0256
chr2:20,215,537-21,280,646	p24.1	Gain	1065109	50	3.45	46.55	0.0048
chr2:207,861,345-208,876,525	q33.3	Loss	1015180	37.5	3.45	34.05	0.0256
chr2:208,876,525-210,331,732	q33.3 - q34	Loss	1455207	62.5	3.45	59.05	0.0007
chr2:21,280,646-25,870,821	p24.1 - p23.3	Gain	4590175	37.5	3.45	34.05	0.0256
chr2:210,331,732-216,402,525	q34 - q35	Loss	6070793	62.5	6.90	55.60	0.0023
chr2:216,402,525-225,739,791	q35 - q36.2	Loss	9337266	62.5	10.34	52.16	0.0056
chr2:224,263-1,785,220	p25.3	Gain	1560957	50	3.45	46.55	0.0048
chr2:225,739,791-228,542,036	q36.2 - q36.3	Loss	2802245	62.5	13.79	48.71	0.0115
chr2:228,542,036-230,386,971	q36.3	Loss	1844935	75	13.79	61.21	0.0020
chr2:230,386,971-230,387,771	q36.3	Loss	800	75	10.34	64.66	0.0008
chr2:230,387,771-238,252,220	q36.3 - q37.3	Loss	7864449	75	13.79	61.21	0.0020
chr2:238,252,220-239,091,229	q37.3	Loss	839009	75	17.24	57.76	0.0041
chr2:239,091,229-241,620,162	q37.3	Loss	2528933	75	20.69	54.31	0.0077
chr2:241,620,162-241,796,109	q37.3	Loss	175947	75	17.24	57.76	0.0041
chr2:25,870,821-48,938,583	p23.3 - p16.3	Gain	23067762	50	3.45	46.55	0.0048
chr2:48,938,583-52,373,212	p16.3	Gain	3434629	50	0.00	50.00	0.0011
chr2:52,373,212-64,478,283	p16.3 - p14	Gain	12105071	62.5	0.00	62.50	0.0001
chr2:64,478,283-71,285,149	p14 - p13.3	Gain	6806866	50	0.00	50.00	0.0011

chr2:71,285,149-74,335,462	p13.3 - p13.1	Gain	3050313	62.5	0.00	62.50	0.0001
chr2:74,335,462-82,716,433	p13.1 - p12	Gain	8380971	50	0.00	50.00	0.0011
chr2:82,716,433-83,447,850	p12	Gain	731417	50	3.45	46.55	0.0048
chr2:83,447,850-88,214,979	p12 - p11.2	Gain	4767129	50	0.00	50.00	0.0011
chr2:88,214,979-94,782,159	p11.2 - q11.1	Gain	6567180	62.5	0.00	62.50	0.0001
chr2:94,782,159-95,675,764	q11.1	Gain	893605	50	0.00	50.00	0.0011
chr2:94,983,765-100,292,273	q11.1 - q11.2	Loss	5308508	25	0.00	25.00	0.0420
chr2:95,675,764-108,345,037	q11.1 - q12.3	Gain	12669273	25	0.00	25.00	0.0420
chr20:26,006,126-26,220,344	p11.1	Gain	214218	75	3.45	71.55	0.0001
chr20:26,220,344-28,267,569	p11.1 - q11.1	Gain	2047225	75	6.90	68.10	0.0003
chr20:275,014-424,783	p13	Gain	149769	75	3.45	71.55	0.0001
chr20:28,267,569-29,779,350	q11.1 - q11.21	Gain	1511781	75	20.69	54.31	0.0077
chr20:29,779,350-30,526,698	q11.21	Gain	747348	75	24.14	50.86	0.0134
chr20:30,526,698-37,666,045	q11.21 - q12	Gain	7139347	75	20.69	54.31	0.0077
chr20:37,666,045-40,680,814	q12	Gain	3014769	87.5	20.69	66.81	0.0011
chr20:40,680,814-40,792,351	q12	Gain	111537	75	20.69	54.31	0.0077
chr20:40,792,351-43,889,716	q12 - q13.12	Gain	3097365	75	27.59	47.41	0.0345
chr20:424,783-26,006,126	p13 - p11.1	Gain	25581343	75	6.90	68.10	0.0003
chr20:43,889,716-47,383,084	q13.12 - q13.13	Gain	3493368	75	20.69	54.31	0.0077
chr20:47,383,084-47,538,301	q13.13	Gain	155217	62.5	20.69	41.81	0.0352
chr20:47,538,301-62,393,015	q13.13 - q13.33	Gain	14854714	75	20.69	54.31	0.0077
chr22:15,621,248-15,745,966	q11.1	Loss	124718	37.5	0.00	37.50	0.0072
chr22:15,745,966-18,151,355	q11.1 - q11.21	Loss	2405389	50	0.00	50.00	0.0011
chr22:18,151,355-18,151,891	q11.21	Loss	536	37.5	0.00	37.50	0.0072
chr22:18,151,891-24,286,893	q11.21 - q11.23	Loss	6135002	50	3.45	46.55	0.0048
chr22:24,286,893-28,379,404	q11.23 - q12.2	Loss	4092511	50	6.90	43.10	0.0129
chr22:28,379,404-30,623,768	q12.2 - q12.3	Loss	2244364	50	3.45	46.55	0.0048
chr22:30,623,768-30,623,867	q12.3	Loss	99	37.5	3.45	34.05	0.0256
chr22:30,646,302-30,646,401	q12.3	Loss	99	37.5	3.45	34.05	0.0256
chr22:30,646,401-40,803,595	q12.3 - q13.2	Loss	10157194	50	3.45	46.55	0.0048
chr22:40,803,595-42,473,589	q13.2	Loss	1669994	62.5	6.90	55.60	0.0023
chr22:42,473,589-45,618,622	q13.2 - q13.31	Loss	3145033	50	6.90	43.10	0.0129
chr22:45,618,622-49,453,810	q13.31 - q13.33	Loss	3835188	50	10.34	39.66	0.0271
chr3:122,541,183-125,236,945	q13.33 - q21.1	Loss	2695762	25	0.00	25.00	0.0420

chr3:133,822,599-158,979,197	q22.1 - q25.32	Gain	25156598	25	0.00	25.00	0.0420
chr3:140,451,428-140,626,759	q23	Loss	175331	25	0.00	25.00	0.0420
chr3:140,627,376-184,141,428	q23 - q26.33	Loss	43514052	25	0.00	25.00	0.0420
chr3:54,612,454-71,816,463	p14.3 - p13	Gain	17204009	25	0.00	25.00	0.0420
chr3:77,584,830-79,097,077	p12.3	Gain	1512247	25	0.00	25.00	0.0420
chr3:82,799,401-83,768,022	p12.2 - p12.1	Gain	968621	37.5	3.45	34.05	0.0256
chr3:83,768,022-87,044,540	p12.1	Gain	3276518	37.5	0.00	37.50	0.0072
chr3:87,044,540-111,740,734	p12.1 - q13.13	Gain	24696194	25	0.00	25.00	0.0420
chr3:958,261-6,636,703	p26.3 - p26.1	Gain	5678442	37.5	3.45	34.05	0.0256
chr4:113,578,539-152,907,961	q25 - q31.3	Loss	39329422	37.5	0.00	37.50	0.0072
chr4:152,907,961-179,587,711	q31.3 - q34.3	Loss	26679750	37.5	3.45	34.05	0.0256
chr4:184,404,421-185,872,338	q35.1	Gain	1467917	25	0.00	25.00	0.0420
chr4:2,865,088-11,429,778	p16.3 - p15.33	Loss	8564690	37.5	3.45	34.05	0.0256
chr4:26,747,433-47,264,023	p15.2 - p12	Loss	20516590	37.5	3.45	34.05	0.0256
chr4:47,264,023-47,677,803	p12	Loss	413780	37.5	0.00	37.50	0.0072
chr4:47,677,803-48,524,316	p12	Loss	846513	25	0.00	25.00	0.0420
chr4:55,628-2,865,088	p16.3	Loss	2809460	37.5	0.00	37.50	0.0072
chr4:69,912,758-74,866,776	q13.2 - q13.3	Gain	4954018	25	0.00	25.00	0.0420
chr4:74,866,776-78,196,278	q13.3 - q21.1	Gain	3329502	37.5	0.00	37.50	0.0072
chr4:80,547,099-113,578,539	q21.21 - q25	Loss	33031440	25	0.00	25.00	0.0420
chr5:136,366,234-180,626,608	q31.2 - q35.3	Loss	44260374	37.5	3.45	34.05	0.0256
chr5:3,426,805-3,559,003	p15.33	Gain	132198	37.5	3.45	34.05	0.0256
chr5:51,232,444-65,352,862	q11.2 - q12.3	Loss	14120418	50	6.90	43.10	0.0129
chr5:99,111,442-107,339,380	q21.1 - q21.3	Loss	8227938	37.5	3.45	34.05	0.0256
chr6:165,244,688-169,488,215	q27	Loss	4243527	50	10.34	39.66	0.0271
chr6:169,576,118-170,622,773	q27	Loss	1046655	50	10.34	39.66	0.0271
chr6:170,622,773-170,728,000	q27	Loss	105227	50	6.90	43.10	0.0129
chr6:19,131,847-20,272,069	p22.3	Gain	1140222	50	10.34	39.66	0.0271
chr6:20,272,069-22,580,422	p22.3	Gain	2308353	62.5	10.34	52.16	0.0056
chr6:22,580,422-23,499,391	p22.3	Gain	918969	62.5	3.45	59.05	0.0007
chr6:23,499,391-27,152,460	p22.3 - p22.1	Gain	3653069	50	3.45	46.55	0.0048
chr6:27,152,460-32,404,070	p22.1 - p21.32	Gain	5251610	37.5	3.45	34.05	0.0256
chr6:6,382,300-7,427,280	p25.1 - p24.3	Gain	1044980	50	10.34	39.66	0.0271
chr6:62,586,405-69,438,735	q11.1 - q12	Gain	6852330	25	0.00	25.00	0.0420

chr7:142,857,956-144,143,399	q35	Gain	1285443	62.5	13.79	48.71	0.0115
chr7:144,143,399-147,259,180	q35	Gain	3115781	62.5	10.34	52.16	0.0056
chr7:147,259,180-148,089,302	q35 - q36.1	Gain	830122	62.5	13.79	48.71	0.0115
chr7:148,089,302-151,558,264	q36.1	Gain	3468962	62.5	17.24	45.26	0.0211
chr7:151,558,264-153,901,560	q36.1 - q36.2	Gain	2343296	62.5	13.79	48.71	0.0115
chr7:153,901,560-158,625,992	q36.2 - q36.3	Gain	4724432	62.5	17.24	45.26	0.0211
chr7:50,617,642-52,867,234	p12.2 - p12.1	Gain	2249592	50	13.79	36.21	0.0487
chr7:56,264,968-63,102,874	p11.2 - q11.21	Gain	6837906	50	10.34	39.66	0.0271
chr7:63,102,874-67,229,358	q11.21 - q11.22	Gain	4126484	62.5	10.34	52.16	0.0056
chr7:67,229,358-71,274,704	q11.22	Gain	4045346	62.5	13.79	48.71	0.0115
chr7:71,274,704-80,528,144	q11.22 - q21.11	Gain	9253440	62.5	17.24	45.26	0.0211
chr7:80,528,144-81,356,796	q21.11	Gain	828652	62.5	20.69	41.81	0.0352
chr7:81,356,796-142,857,956	q21.11 - q35	Gain	61501160	62.5	17.24	45.26	0.0211
chr8:39,836,613-43,315,811	p11.22 - p11.1	Loss	3479198	37.5	3.45	34.05	0.0256
chr8:4,386,741-14,461,142	p23.2 - p22	Loss	10074401	62.5	20.69	41.81	0.0352
chr9:124,954,691-140,118,015	q33.2 - q34.3	Gain	15163324	25	0.00	25.00	0.0420
chr9:13,729,630-21,157,685	p23 - p21.3	Gain	7428055	25	0.00	25.00	0.0420
chr9:140,118,015-140,273,252	q34.3	Loss	155237	0	48.28	-48.28	0.0148
chr9:190-336,203	p24.3	Gain	336013	37.5	0.00	37.50	0.0072
chr9:27,417,088-29,639,053	p21.2 - p21.1	Gain	2221965	25	0.00	25.00	0.0420
chr9:336,203-991,152	p24.3	Gain	654949	37.5	3.45	34.05	0.0256
chr9:38,427,196-84,783,002	p13.1 - q21.32	Gain	46355806	25	0.00	25.00	0.0420
chr9:84,783,002-89,446,315	q21.32 - q21.33	Gain	4663313	37.5	0.00	37.50	0.0072
chr9:89,446,315-123,651,685	q21.33 - q33.2	Gain	34205370	25	0.00	25.00	0.0420

[1]Physical position is according to hg18/NCBI build 36

Appendix 5.8: Regions showing significant copy number differences in *FGFR3* mutant TaG1/G2 multifocal (n=7) versus solitary (n=19) tumours.

Region[1]	Cytoband Location	Event	Region Length	Freq. in Multifocal (%)	Freq. in Solitary (%)	Difference	p-value
chr1:119,708,536-193,197,934	p12 - q31.3	Gain	73489398	42.86	0.00	42.86	0.013
chr10:104,342,397-104,652,460	q24.32	Loss	310063	57.14	0.00	57.14	0.002
chr10:104,652,460-109,290,751	q24.32 - q25.1	Loss	4638291	42.86	0.00	42.86	0.013
chr10:99,781,492-104,342,397	q24.2 - q24.32	Loss	4560905	42.86	0.00	42.86	0.013
chr13:22,108,664-27,824,701	q12.11 - q12.3	Gain	5716037	42.86	5.26	37.59	0.047
chr13:66,421,707-67,895,141	q21.32 - q21.33	Gain	1473434	42.86	5.26	37.59	0.047
chr16:193,278-6,165,969	p13.3	Loss	5972691	42.86	0.00	42.86	0.013
chr19:33,399,234-36,171,164	q12	Gain	2771930	42.86	0.00	42.86	0.013
chr19:36,322,238-40,876,527	q12 - q13.12	Gain	4554289	42.86	0.00	42.86	0.013
chr19:41,059,171-51,988,000	q13.12 - q13.32	Gain	10928829	42.86	0.00	42.86	0.013
chr19:52,342,137-63,602,791	q13.32 - q13.43	Gain	11260654	42.86	0.00	42.86	0.013
chr20:30,102,016-34,346,661	q11.21 - q11.23	Gain	4244645	42.86	5.26	37.59	0.047
chr20:34,346,661-62,392,510	q11.23 - q13.33	Gain	28045849	57.14	5.26	51.88	0.010
chr20:62,392,510-62,393,015	q13.33	Gain	505	42.86	5.26	37.59	0.047
chr5:162,296,397-171,159,864	q34 - q35.1	Loss	8863467	42.86	0.00	42.86	0.013
chr5:171,159,864-173,800,904	q35.1 - q35.2	Loss	2641040	42.86	5.26	37.59	0.047
chr5:173,800,904-178,243,610	q35.2 - q35.3	Loss	4442706	42.86	0.00	42.86	0.013
chr6:162,865,542-162,954,569	q26	Gain	89027	42.86	0.00	42.86	0.013
chr8:70,378,901-72,600,219	q13.2 - q13.3	Gain	2221318	42.86	0.00	42.86	0.013
chr9:21,734,602-21,851,433	p21.3	Loss	116831	100.00	26.32	73.68	0.001
chr9:21,851,433-21,998,414	p21.3	Loss	146981	85.71	26.32	59.40	0.021
chr9:21,998,414-22,046,818	p21.3	Loss	48404	85.71	21.05	64.66	0.005
chr9:22,046,818-22,155,847	p21.3	Loss	109029	100.00	21.05	78.95	0.001
chr9:22,155,847-22,155,946	p21.3	Loss	99	85.71	21.05	64.66	0.005
chr9:22,155,946-23,376,562	p21.3	Loss	1220616	85.71	26.32	59.40	0.021
chr9:82,003,000-82,148,095	q21.31	Loss	145095	85.71	10.53	75.19	0.001

[1]Physical position is according to hg18/NCBI build 36

Appendix 5.9: Regions showing significant copy number differences in *FGFR3* wildtype TaG1/2 multifocal (n=4) versus solitary (n=9) tumours.

Region[1]	Cytoband Location	Event	Region Length	Freq. in Multifocal (%)	Freq. in Solitary (%)	Difference	p-value
chr8:96,177,980-124,550,528	q22.1 - q24.13	Gain	28372548	100	11.1	88.9	0.007
chr8:124,718,428-146,133,884	q24.13 - q24.3	Gain	21415456	100	11.1	88.9	0.007
chr8:124,550,528-124,718,428	q24.13	Gain	167900	100	0.0	100.0	0.001
chr9:30,699,255-68,858,635	p21.1 - q12	Loss	38159380	75	0.0	75.0	0.014
chr17:35,227,093-35,920,940	q12 - q21.2	Loss	693847	75	0.0	75.0	0.014

[1]Physical position is according to hg18/NCBI build 36

Appendix 5.10: Regions showing significant copy number differences in *FGFR3* wildtype T1G3 multifocal (n=8) versus solitary (n=16) tumours.

Region[1]	Cytoband Location	Event	Region Length	Freq. in Multifocal (%)	Freq. in Solitary (%)	Difference	p-value
chr1:119,480,610-141,672,545	p12 - q12	Gain	22191935	62.5	12.5	50	0.0207
chr1:44,062,032-45,524,938	p34.1	Gain	1462906	50	6.25	43.75	0.0277
chr1:53,077,428-73,625,895	p32.3 - p31.1	Gain	20548467	50	6.25	43.75	0.0277
chr10:116,774,295-125,057,698	q25.3 - q26.13	Loss	8283403	62.5	0	62.5	0.0013
chr10:125,057,698-131,816,154	q26.13 - q26.3	Loss	6758456	50	0	50	0.0066
chr10:131,816,154-131,982,049	q26.3	Loss	165895	37.5	0	37.5	0.0277
chr10:131,982,049-135,247,831	q26.3	Loss	3265782	50	0	50	0.0066
chr10:78,996,385-80,472,830	q22.3	Loss	1476445	50	6.25	43.75	0.0277
chr10:84,577,760-86,390,131	q23.1	Loss	1812371	50	6.25	43.75	0.0277
chr10:86,390,131-88,222,653	q23.1 - q23.2	Loss	1832522	62.5	6.25	56.25	0.0069
chr10:88,222,653-89,694,469	q23.2 - q23.31	Loss	1471816	75	6.25	68.75	0.0013
chr10:89,694,469-89,694,975	q23.31	Loss	506	62.5	6.25	56.25	0.0069
chr10:89,694,975-90,596,444	q23.31	Loss	901469	75	6.25	68.75	0.0013
chr10:90,596,444-116,774,295	q23.31 - q25.3	Loss	26177851	75	0	75	0.0002
chr11:44,879,168-59,697,061	p11.2 - q12.1	Loss	14817893	37.5	0	37.5	0.0277
chr12:152,534-25,552,960	p13.33 - p12.1	Loss	25400426	37.5	0	37.5	0.0277
chr12:33,333,489-46,156,911	p11.1 - q13.11	Loss	12823422	37.5	0	37.5	0.0277
chr13:47,964,053-51,243,111	q14.2 - q14.3	Loss	3279058	50	6.25	43.75	0.0277
chr14:33,897,190-34,061,283	q13.1	Loss	164093	37.5	0	37.5	0.0277
chr14:57,420,120-58,323,469	q23.1	Loss	903349	50	6.25	43.75	0.0277
chr14:58,323,469-58,470,270	q23.1	Loss	146801	37.5	0	37.5	0.0277
chr14:58,470,270-59,336,011	q23.1	Loss	865741	50	6.25	43.75	0.0277
chr15:63,070,265-82,907,017	q22.31 - q25.2	Loss	19836752	37.5	0	37.5	0.0277
chr15:83,883,618-85,362,775	q25.3	Loss	1479157	37.5	0	37.5	0.0277
chr15:87,338,954-100,022,043	q26.1 - q26.3	Loss	12683089	37.5	0	37.5	0.0277
chr16:23,756,350-45,067,244	p12.1 - q11.2	Gain	21310894	50	0	50	0.0066
chr16:45,231,075-63,462,907	q11.2 - q21	Loss	18231832	37.5	0	37.5	0.0277

chr16:7,019,846-23,756,350	p13.2 - p12.1	Gain	16736504	37.5	0	37.5	0.0277
chr19:211,322-6,523,485	p13.3	Loss	6312163	37.5	0	37.5	0.0277
chr19:32,891,236-33,399,234	q12	Gain	507998	37.5	0	37.5	0.0277
chr19:38,091,322-38,282,890	q13.11	Gain	191568	50	6.25	43.75	0.0277
chr19:39,226,664-45,806,715	q13.11 - q13.2	Gain	6580051	50	6.25	43.75	0.0277
chr19:46,479,845-51,023,195	q13.2 - q13.32	Gain	4543350	37.5	0	37.5	0.0277
chr2:1,785,220-20,037,859	p25.3 - p24.1	Gain	18252639	50	6.25	43.75	0.0277
chr2:169,397,061-208,876,525	q24.3 - q33.3	Loss	39479464	37.5	0	37.5	0.0277
chr2:20,215,537-21,280,646	p24.1	Gain	1065109	50	6.25	43.75	0.0277
chr2:208,876,525-210,331,732	q33.3 - q34	Loss	1455207	62.5	0	62.5	0.0013
chr2:210,331,732-228,542,036	q34 - q36.3	Loss	18210304	62.5	6.25	56.25	0.0069
chr2:224,263-1,785,220	p25.3	Gain	1560957	50	0	50	0.0066
chr2:228,542,036-238,252,220	q36.3 - q37.3	Loss	9710184	75	6.25	68.75	0.0013
chr2:238,252,220-241,796,109	q37.3	Loss	3543889	75	12.5	62.5	0.0047
chr2:25,870,821-48,938,583	p23.3 - p16.3	Gain	23067762	50	6.25	43.75	0.0277
chr2:48,938,583-52,373,212	p16.3	Gain	3434629	50	0	50	0.0066
chr2:52,373,212-64,478,283	p16.3 - p14	Gain	12105071	62.5	0	62.5	0.0013
chr2:64,478,283-71,285,149	p14 - p13.3	Gain	6806866	50	0	50	0.0066
chr2:71,285,149-74,335,462	p13.3 - p13.1	Gain	3050313	62.5	0	62.5	0.0013
chr2:74,335,462-82,716,433	p13.1 - p12	Gain	8380971	50	0	50	0.0066
chr2:82,716,433-83,447,850	p12	Gain	731417	50	6.25	43.75	0.0277
chr2:83,447,850-88,214,979	p12 - p11.2	Gain	4767129	50	0	50	0.0066
chr2:88,214,979-94,782,159	p11.2 - q11.1	Gain	6567180	62.5	0	62.5	0.0013
chr2:94,782,159-95,675,764	q11.1	Gain	893605	50	0	50	0.0066
chr20:26,006,126-26,220,344	p11.1	Gain	214218	75	0	75	0.0002
chr20:26,220,344-28,267,569	p11.1 - q11.1	Gain	2047225	75	6.25	68.75	0.0013
chr20:275,014-424,783	p13	Gain	149769	75	0	75	0.0002
chr20:28,267,569-29,779,350	q11.1 - q11.21	Gain	1511781	75	18.75	56.25	0.0215
chr20:29,779,350-30,526,698	q11.21	Gain	747348	75	25	50	0.0324
chr20:30,526,698-37,666,045	q11.21 - q12	Gain	7139347	75	18.75	56.25	0.0215
chr20:37,666,045-40,680,814	q12	Gain	3014769	87.5	18.75	68.75	0.0023
chr20:40,680,814-40,792,351	q12	Gain	111537	75	18.75	56.25	0.0215
chr20:40,792,351-43,889,716	q12 - q13.12	Gain	3097365	75	25	50	0.0324
chr20:424,783-26,006,126	p13 - p11.1	Gain	25581343	75	6.25	68.75	0.0013

chr20:43,889,716-47,383,084	q13.12 - q13.13	Gain	3493368	75	18.75	56.25	0.0215
chr20:47,538,301-62,393,015	q13.13 - q13.33	Gain	14854714	75	18.75	56.25	0.0215
chr22:15,621,248-15,745,966	q11.1	Loss	124718	37.5	0	37.5	0.0277
chr22:15,745,966-18,151,355	q11.1 - q11.21	Loss	2405389	50	0	50	0.0066
chr22:18,151,355-18,151,891	q11.21	Loss	536	37.5	0	37.5	0.0277
chr22:18,151,891-24,286,893	q11.21 - q11.23	Loss	6135002	50	6.25	43.75	0.0277
chr22:28,379,404-30,623,768	q12.2 - q12.3	Loss	2244364	50	6.25	43.75	0.0277
chr22:30,646,401-40,803,595	q12.3 - q13.2	Loss	10157194	50	6.25	43.75	0.0277
chr22:40,803,595-42,473,589	q13.2	Loss	1669994	62.5	12.5	50	0.0207
chr3:83,768,022-87,044,540	p12.1	Gain	3276518	37.5	0	37.5	0.0277
chr4:113,578,539-179,587,711	q25 - q34.3	Loss	66009172	37.5	0	37.5	0.0277
chr4:26,747,433-47,677,803	p15.2 - p12	Loss	20930370	37.5	0	37.5	0.0277
chr4:55,628-11,429,778	p16.3 - p15.33	Loss	11374150	37.5	0	37.5	0.0277
chr4:74,866,776-78,196,278	q13.3 - q21.1	Gain	3329502	37.5	0	37.5	0.0277
chr5:51,232,444-65,352,862	q11.2 - q12.3	Loss	14120418	50	6.25	43.75	0.0277
chr6:170,622,773-170,728,000	q27	Loss	105227	50	6.25	43.75	0.0277
chr6:20,272,069-22,580,422	p22.3	Gain	2308353	62.5	12.5	50	0.0207
chr6:22,580,422-23,499,391	p22.3	Gain	918969	62.5	6.25	56.25	0.0069
chr6:23,499,391-27,152,460	p22.3 - p22.1	Gain	3653069	50	6.25	43.75	0.0277
chr7:142,857,956-147,259,180	q35	Gain	4401224	62.5	12.5	50	0.0207
chr7:63,102,874-67,229,358	q11.21 - q11.22	Gain	4126484	62.5	12.5	50	0.0207
chr9:190-336,203	p24.3	Gain	336013	37.5	0	37.5	0.0277
chr9:84,783,002-89,446,315	q21.32 - q21.33	Gain	4663313	37.5	0	37.5	0.0277

[1]Physical position is according to hg18/NCBI build 36

Appendix 5.11: Details of samples in the four main clusters obtained by hierarchical cluster analysis of copy number data from 22 patients with multifocal tumours and 103 solitary tumours including stage ≥ T2 tumours (n=29).

Tumour	Stage	Grade	Multifocal/Single	FGA group	FGFR3	PIK3CA	RAS	Cluster
1	Ta	G2	Multifocal	B	WT	Mutant	WT	1
9	T1	G3	Multifocal	A	WT	WT	WT	1
17	Ta	G2	Multifocal	B	Mutant	Mutant	WT	1
239	Ta	G1	Single	A	WT	WT	Mutant	1
385	T1	G2	Single	B	Mutant	WT	WT	1
397	Ta	G2	Single	A	Mutant	Mutant	Mutant	1
406	Ta	G2	Single	B	Mutant	WT	WT	1
489	Ta	G3	Single	A	WT	Mutant	WT	1
494	Ta	G2	Single	A	Mutant	WT	WT	1
518	Ta	G2	Single	A	Mutant	Mutant	WT	1
536	Ta	G2	Single	A	Mutant	Mutant	WT	1
575	Ta	G2	Single	B	Mutant	Mutant	WT	1
578	Ta	G2	Single	B	Mutant	WT	WT	1
584	Ta	G3	Single	A	Mutant	WT	WT	1
672	Ta	G2	Single	A	WT	WT	Mutant	1
695	Ta	G2	Single	B	WT	WT	WT	1
701	T2	G3	Single	B	WT	WT	WT	1
811	Ta	G2	Single	A	Mutant	Mutant	WT	1
868	Ta	G2	Single	A	Mutant	WT	WT	1
894	Ta	G1	Single	A	WT	WT	Mutant	1
924	Ta	G2	Single	B	WT	WT	Mutant	1
933	Ta	G2	Single	B	Mutant	Mutant	WT	1
961	Ta	G2	Single	A	Mutant	WT	WT	1
983	T1	G2	Single	B	Mutant	Mutant	WT	1
989	Ta	G3	Single	B	WT	WT	WT	1
1010	T1	G3	Single	B	WT	WT	Mutant	1
1044	Ta	G2	Single	B	WT	WT	WT	1
1103	Ta	G3	Single	A	WT	Mutant	WT	1
1315	T1	G3	Single	A	Mutant	Mutant	WT	1
1317	T2	G3	Single	B	WT	WT	WT	1
2	Ta	G2	Multifocal	C	Mutant	WT	WT	2
4	Ta	G3	Multifocal	C	Mutant	Mutant	WT	2

Tumour	Stage	Grade	Multifocal/Single	FGA group	FGFR3	PIK3CA	RAS	Cluster
7	Ta	G2	Multifocal	C	WT	WT	WT	2
8	Ta	G2	Multifocal	C	Mutant	Mutant	WT	2
11	T1	G3	Multifocal	C	WT	WT	WT	2
15	Ta	G2	Multifocal	C	Mutant	Mutant	WT	2
21	Ta	G2	Multifocal	C	Mutant	WT	WT	2
22	Ta	G2	Multifocal	C	WT	WT	WT	2
140	T1	G3	Single	C	WT	Mutant	WT	2
243	T1	G3	Single	C	WT	WT	WT	2
360	T2	G3	Single	C	WT	WT	WT	2
418	T1	G3	Single	B	WT	Mutant	WT	2
457	T1	G2	Single	C	Mutant	Mutant	WT	2
461	T1	G3	Single	B	Mutant	WT	WT	2
468	T1	G2	Single	B	WT	WT	WT	2
540	Ta	G2	Single	C	Mutant	WT	WT	2
554	T1	G2	Single	B	Mutant	WT	WT	2
572	T1	G3	Single	C	Mutant	WT	WT	2
579	T1	G2	Single	B	Mutant	Mutant	WT	2
675	Ta	G2	Single	B	Mutant	WT	WT	2
718	Ta	G2	Single	C	Mutant	WT	WT	2
736	Ta	G3	Single	B	Mutant	WT	Mutant	2
837	Ta	G1	Single	B	Mutant	WT	WT	2
860	Ta	G2	Single	B	Mutant	Mutant	WT	2
866	T1	G3	Single	B	Mutant	WT	WT	2
934	Ta	G2	Single	B	Mutant	Mutant	WT	2
969	T1	G3	Single	B	Mutant	WT	WT	2
979	T1	G3	Single	C	Mutant	WT	WT	2
1006	Ta	G2	Single	B	Mutant	WT	WT	2
1046	Ta	G2	Single	C	Mutant	WT	WT	2
1079	Ta	G3	Single	C	Mutant	Mutant	WT	2
1082	Ta	G3	Single	C	WT	WT	WT	2
1094	T1	G3	Single	C	Mutant	WT	WT	2
1118	T1	G3	Single	C	Mutant	Mutant	WT	2
1161	T1	G3	Single	C	Mutant	Mutant	WT	2
1210	T1	G3	Single	C	WT	WT	WT	2
1230	T1	G3	Single	C	Mutant	WT	WT	2
1264	T1	G3	Single	C	WT	WT	WT	2

Tumour	Stage	Grade	Multifocal/Single	FGA group	FGFR3	PIK3CA	RAS	Cluster
1342	T1	G2	Single	C	Mutant	WT	WT	2
3	T1	G3	Multifocal	C	WT	WT	Mutant	3
16	Ta	G2	Multifocal	C	WT	WT	Mutant	3
19	Ta	G2	Multifocal	C	Mutant	WT	WT	3
94	T1	G3	Single	C	Mutant	WT	WT	3
271	T2	G3	Single	C	WT	WT	WT	3
291	T2	G3	Single	C	WT	WT	WT	3
358	Ta	G2	Single	C	WT	WT	WT	3
366	Ta	G2	Single	C	WT	WT	WT	3
417	T2	G3	Single	C	WT	Mutant	Mutant	3
438	T2	G3	Single	C	Mutant	WT	WT	3
498	T2	G3	Single	C	WT	WT	WT	3
511	Ta	G3	Single	C	Mutant	WT	WT	3
513	T2	G3	Single	C	WT	Mutant	WT	3
519	T1	G3	Single	D	Mutant	WT	WT	3
561	T1	G3	Single	C	WT	Mutant	Mutant	3
577	T2	G3	Single	C	WT	WT	WT	3
588	T2	G3	Single	D	WT	WT	WT	3
589	T1	G3	Single	C	WT	WT	WT	3
653	T2	G3	Single	D	WT	WT	WT	3
657	Ta	G2	Single	C	WT	Mutant	WT	3
677	T2	G3	Single	C	WT	WT	WT	3
734	Ta	G3	Single	D	WT	WT	WT	3
818	T2	G3	Single	C	WT	WT	WT	3
884	T1	G3	Single	C	WT	WT	WT	3
893	T2	G3	Single	D	WT	WT	WT	3
1021	T1	G3	Single	C	WT	Mutant	WT	3
1049	T2	G3	Single	D	WT	WT	WT	3
1072	Ta	G3	Single	C	WT	WT	WT	3
1109	T2	G3	Single	C	WT	WT	Mutant	3
1126	T2	G3	Single	D	WT	WT	WT	3
1129	T1	G3	Single	C	WT	WT	Mutant	3
1138	T1	G3	Single	C	WT	WT	WT	3
1145	T1	G3	Single	C	WT	WT	WT	3
1148	T2	G3	Single	C	WT	WT	WT	3
1157	T2	G3	Single	C	WT	WT	WT	3

Tumour	Stage	Grade	Multifocal/Single	FGA group	FGFR3	PIK3CA	RAS	Cluster
1229	T1	G3	Single	C	Mutant	WT	WT	3
1267	T2	G3	Single	C	Mutant	Mutant	WT	3
1366	T2	G3	Single	D	WT	WT	WT	3
5	Ta	G2	Multifocal	D	Mutant	WT	WT	4
6	T1	G3	Multifocal	D	WT	WT	WT	4
10	Ta	G3	Multifocal	D	WT	WT	WT	4
12	T1	G3	Multifocal	D	WT	WT	WT	4
13	T1	G3	Multifocal	D	WT	WT	WT	4
14	Ta	G3	Multifocal	D	WT	WT	WT	4
18	T1	G3	Multifocal	D	WT	WT	WT	4
20	T1	G3	Multifocal	D	WT	WT	WT	4
137	T2	G3	Single	D	WT	WT	WT	4
411	T1	G3	Single	D	WT	WT	WT	4
594	T2	G3	Single	D	WT	WT	WT	4
595	T2	G3	Single	D	WT	WT	WT	4
741	T2	G3	Single	D	WT	WT	WT	4
848	T2	G3	Single	D	WT	WT	WT	4
930	T1	G3	Single	D	WT	WT	WT	4
944	T2	G3	Single	D	WT	WT	WT	4
1248	T2	G3	Single	D	WT	WT	WT	4
1320	T1	G3	Single	D	WT	WT	WT	4

Appendix 5.12: Suppliers and manufacturers

Amersham Amersham Place, Little Chalfont, Buckinghamshire, HP7 9NA www.amersham.com

Amity Ltd Libra House, Spring Park, Clayburn Road, Park Springs, Barnsley, South Yorkshire, S72 7FD www.amityinternational.com

Applied Biosystems (AB) Lingley House, 120 Birchwood Boulevard, Warrington, WA3 7QH www.appliedbiosystems.com

BD Biosciences The Danby Building, Edmund Halley Road, Oxford science park, Oxford, OX4 4DQ www.bpeurope.com

Beckman Coulter Oakley Court, Kingsmead Business Park, London Road, High Wycombe, Buckinghamshire, HP11 1JU www.beckmancoulter.com

Bioline Ltd 16 The Edge Business Centre, Humber Road, London, NW62 6EW www.bioline.com

BIO-RAD Bio-Rad house, Maxted Road, Hemel Hempstead, Hertfordshire, HP2 7DX www.bio-rad.com

Cambridge Bioscience Munro House, Trafalgar Way, Cambridge, CB23 8SQ www.bioscience.co.uk

Corning Supplied by Sigma www.corning.com

Falcon Supplied by SLS

Fisher Scientific Ltd Bishop Meadow Road, Loughborough, Leicestershire, LE11 5RG

GE Healthcare Supplied by Fisher Scientific

Guava Technologies 10 Torkington Street, Stamford, Lincolnshire, PE9 2UY www.guavatechnologies.com

Insight Biotechnology Ltd PO Box 520, Wembley, HA9 7YN www.insightbio.com

Integra Biosciences Supplied by SLS www.integra-biosciences.com

Medical Air Technology (MAT) Independent House, Broadway Business Park, Gateway Crescent, Chadderton, Oldham, OL9 9XB www.medicalairtechnology.com

Medichem PO Box 237, Sevenoaks, Kent, TN15 0ZJ www.medi-chem.com

Mirus Supplied by Cambridge Bioscience

Nalgene Unit 1a, Thorn Business Park, Hereford, HR2 6JT www.nalgenelabware.com

National Diagnostics Unit 4 Fleet Business Park, Itlings Lane, Hessle, Yorkshire, HU13 9LX www.nationaldiagnostics.com

New England Biolabs (NEB) 75-77 Knowl Place, Wilbury Way, Hitchin, Hertfordshire, SG4 0TY www.neb.com

NUNC supplied by SLS

PALL Life sciences Europa House, Havant Street, Portsmouth, Hampshire, PO1 3PD www.pall.com

Qiagen Fleming Way, Crawley, West Sussex, RH10 9NQ www.qiagen.com

Santa Cruz Biotechnology Supplied by Insight Biotechnology www.scbt.com

Sarstedt 68 Boston Road, Beaumont Leys, Leicester, LE4 1AW www.sarstedt.com

Scientific Laboratory Supplies (SLS) Ruddington Lane, Wilford Industrial Estate, Nottingham, NG11 7EP www.scientific-labs.com

Sigma-Aldrich Company Ltd. Fancy Road, Poole, Dorset, BH12 4QH www.sigmaaldrich.com

Stratagene Europe Gebouw California, Hogehilweg 15 1101 CB Amsterdam, The Netherlands www.stratagene.com

Thermo Scientific 93-96 Chadwick Road, Astmoor, Runcorn, Cheshire, WA7 1PR www.thermo.com

Zeiss Carl Zeiss Ltd., 5-20 Woodfield Road, Welwyn Garden City, Hertfordshire, AL7 1JQ www.zeiss.co.uk

References

1. Fadl-Elmula, I., *Chromosomal changes in uroepithelial carcinomas.* Cell Chromosome, 2005. **4**: p. 1.
2. Hoglund, M., et al., *Identification of cytogenetic subgroups and karyotypic pathways in transitional cell carcinoma.* Cancer Res, 2001. **61**(22): p. 8241-6.
3. Veltman, J.A., et al., *Array-based comparative genomic hybridization for genome-wide screening of DNA copy number in bladder tumors.* Cancer Res, 2003. **63**(11): p. 2872-80.
4. Blaveri, E., et al., *Bladder cancer stage and outcome by array-based comparative genomic hybridization.* Clin Cancer Res, 2005. **11**(19 Pt 1): p. 7012-22.
5. Hurst, C.D., et al., *High-resolution analysis of genomic copy number alterations in bladder cancer by microarray-based comparative genomic hybridization.* Oncogene, 2004. **23**(12): p. 2250-63.
6. cancerresearchuk.org/bladder-cancer, 2014.
7. Turo, R., W. Cross, and P. Whelan, *Bladder cancer.* Medicine, 2012. **40**(1): p. 14-19.
8. MacLennan, G.T., Z. Kirkali, and L. Cheng, *Histologic grading of noninvasive papillary urothelial neoplasms.* Eur Urol, 2007. **51**(4): p. 889-97; discussion 897-8.
9. Jones, T.D. and L. Cheng, *Papillary urothelial neoplasm of low malignant potential: evolving terminology and concepts.* J Urol, 2006. **175**(6): p. 1995-2003.
10. Soloway, M.S., *Overview of treatment of superficial bladder cancer.* Urology, 1985. **26**(4 Suppl): p. 18-26.
11. Juffs, H.G., M.J. Moore, and I.F. Tannock, *The role of systemic chemotherapy in the management of muscle-invasive bladder cancer.* The Lancet Oncology, 2002. **3**(12): p. 738-747.
12. Botteman, M.F., et al., *The health economics of bladder cancer: a comprehensive review of the published literature.* Pharmacoeconomics, 2003. **21**(18): p. 1315-30.
13. Avritscher, E.B., et al., *Clinical model of lifetime cost of treating bladder cancer and associated complications.* Urology, 2006. **68**(3): p. 549-53.
14. Yabroff, K.R., et al., *Cost of care for elderly cancer patients in the United States.* J Natl Cancer Inst, 2008. **100**(9): p. 630-41.
15. Jacobs, B.L., C.T. Lee, and J.E. Montie, *Bladder cancer in 2010: how far have we come?* CA Cancer J Clin, 2010. **60**(4): p. 244-72.
16. Zehnder, P., et al., *Unaltered oncological outcomes of radical cystectomy with extended lymphadenectomy over three decades.* BJU Int, 2013. **112**(2): p. E51-8.

17. Stein, J.P., et al., *Radical cystectomy in the treatment of invasive bladder cancer: long-term results in 1,054 patients.* J Clin Oncol, 2001. **19**(3): p. 666-75.
18. Herr, H.W., *Superiority of ratio based lymph node staging for bladder cancer.* J Urol, 2003. **169**(3): p. 943-5.
19. Herr, H.W., et al., *Impact of the number of lymph nodes retrieved on outcome in patients with muscle invasive bladder cancer.* J Urol, 2002. **167**(3): p. 1295-8.
20. Kassouf, W., et al., *Lymph node density is superior to TNM nodal status in predicting disease-specific survival after radical cystectomy for bladder cancer: analysis of pooled data from MDACC and MSKCC.* J Clin Oncol, 2008. **26**(1): p. 121-6.
21. Kassouf, W., et al., *Evaluation of the relevance of lymph node density in a contemporary series of patients undergoing radical cystectomy.* J Urol, 2006. **176**(1): p. 53-7; discussion 57.
22. Stein, J.P., *The role of lymphadenectomy in patients undergoing radical cystectomy for bladder cancer.* Curr Oncol Rep, 2007. **9**(3): p. 213-21.
23. Stein, J.P., et al., *Risk factors for patients with pelvic lymph node metastases following radical cystectomy with en bloc pelvic lymphadenectomy: concept of lymph node density.* J Urol, 2003. **170**(1): p. 35-41.
24. Sternberg, C.N., et al., *Methotrexate, vinblastine, doxorubicin, and cisplatin for advanced transitional cell carcinoma of the urothelium. Efficacy and patterns of response and relapse.* Cancer, 1989. **64**(12): p. 2448-58.
25. Chester, J.D., et al., *Systemic chemotherapy for patients with bladder cancer – current controversies and future directions.* Cancer Treatment Reviews, 2004. **30**(4): p. 343-358.
26. Saxman, S.B., et al., *Long-term follow-up of a phase III intergroup study of cisplatin alone or in combination with methotrexate, vinblastine, and doxorubicin in patients with metastatic urothelial carcinoma: a cooperative group study.* J Clin Oncol, 1997. **15**(7): p. 2564-9.
27. von der Maase, H., et al., *Long-term survival results of a randomized trial comparing gemcitabine plus cisplatin, with methotrexate, vinblastine, doxorubicin, plus cisplatin in patients with bladder cancer.* J Clin Oncol, 2005. **23**(21): p. 4602-8.
28. Loehrer, P.J., Sr., et al., *A randomized comparison of cisplatin alone or in combination with methotrexate, vinblastine, and doxorubicin in patients with metastatic urothelial carcinoma: a cooperative group study.* J Clin Oncol, 1992. **10**(7): p. 1066-73.
29. von der Maase, H., et al., *Gemcitabine and cisplatin versus methotrexate, vinblastine, doxorubicin, and cisplatin in advanced or metastatic bladder cancer: results of a large, randomized, multinational, multicenter, phase III study.* J Clin Oncol, 2000. **18**(17): p. 3068-77.
30. Balducci, L., *Evidence-based management of cancer in the elderly.* Cancer Control, 2000. **7**(4): p. 368-76.
31. Nogue-Aliguer, M., et al., *Gemcitabine and carboplatin in advanced transitional cell carcinoma of the urinary tract: an alternative therapy.* Cancer, 2003. **97**(9): p. 2180-6.
32. Sylvester, R.J., et al., *Predicting recurrence and progression in individual patients with stage Ta T1 bladder cancer using EORTC risk tables: a*

combined analysis of 2596 patients from seven EORTC trials. Eur Urol, 2006. **49**(3): p. 466-5; discussion 475-7.
33. Gudjonsson, S., et al., *The value of the UroVysion assay for surveillance of non-muscle-invasive bladder cancer.* Eur Urol, 2008. **54**(2): p. 402-8.
34. Goebell, P.J. and M.A. Knowles, *Bladder cancer or bladder cancers? Genetically distinct malignant conditions of the urothelium.* Urol Oncol, 2010. **28**(4): p. 409-28.
35. Cappellen, D., et al., *Frequent activating mutations of FGFR3 in human bladder and cervix carcinomas.* Nat Genet, 1999. **23**(1): p. 18-20.
36. van Rhijn, B.W., et al., *Molecular grading of urothelial cell carcinoma with fibroblast growth factor receptor 3 and MIB-1 is superior to pathologic grade for the prediction of clinical outcome.* J Clin Oncol, 2003. **21**(10): p. 1912-21.
37. van Rhijn, B.W., et al., *Novel fibroblast growth factor receptor 3 (FGFR3) mutations in bladder cancer previously identified in non-lethal skeletal disorders.* Eur J Hum Genet, 2002. **10**(12): p. 819-24.
38. Bakkar, A.A., et al., *FGFR3 and TP53 gene mutations define two distinct pathways in urothelial cell carcinoma of the bladder.* Cancer Res, 2003. **63**(23): p. 8108-12.
39. Billerey, C., et al., *Frequent FGFR3 mutations in papillary non-invasive bladder (pTa) tumors.* Am J Pathol, 2001. **158**(6): p. 1955-9.
40. Hernandez, S., et al., *FGFR3 and Tp53 mutations in T1G3 transitional bladder carcinomas: independent distribution and lack of association with prognosis.* Clin Cancer Res, 2005. **11**(15): p. 5444-50.
41. Kimura, T., et al., *The incidence of thanatophoric dysplasia mutations in FGFR3 gene is higher in low-grade or superficial bladder carcinomas.* Cancer, 2001. **92**(10): p. 2555-61.
42. Rieger-Christ, K.M., et al., *Identification of fibroblast growth factor receptor 3 mutations in urine sediment DNA samples complements cytology in bladder tumor detection.* Cancer, 2003. **98**(4): p. 737-44.
43. Sibley, K., D. Cuthbert-Heavens, and M.A. Knowles, *Loss of heterozygosity at 4p16.3 and mutation of FGFR3 in transitional cell carcinoma.* Oncogene, 2001. **20**(6): p. 686-91.
44. van Rhijn, B.W., et al., *Combined microsatellite and FGFR3 mutation analysis enables a highly sensitive detection of urothelial cell carcinoma in voided urine.* Clin Cancer Res, 2003. **9**(1): p. 257-63.
45. van Rhijn, B.W., et al., *The fibroblast growth factor receptor 3 (FGFR3) mutation is a strong indicator of superficial bladder cancer with low recurrence rate.* Cancer Res, 2001. **61**(4): p. 1265-8.
46. van Rhijn, B.W., et al., *Frequent FGFR3 mutations in urothelial papilloma.* J Pathol, 2002. **198**(2): p. 245-51.
47. Wallerand, H., et al., *Mutations in TP53, but not FGFR3, in urothelial cell carcinoma of the bladder are influenced by smoking: contribution of exogenous versus endogenous carcinogens.* Carcinogenesis, 2005. **26**(1): p. 177-84.
48. Munro, N.P. and M.A. Knowles, *Fibroblast growth factors and their receptors in transitional cell carcinoma.* J Urol, 2003. **169**(2): p. 675-82.
49. Hafner, C., et al., *High frequency of FGFR3 mutations in adenoid seborrheic keratoses.* J Invest Dermatol, 2006. **126**(11): p. 2404-7.

50. Logie, A., et al., *Activating mutations of the tyrosine kinase receptor FGFR3 are associated with benign skin tumors in mice and humans.* Hum Mol Genet, 2005. **14**(9): p. 1153-60.
51. Hafner, C., et al., *Mosaicism of activating FGFR3 mutations in human skin causes epidermal nevi.* J Clin Invest, 2006. **116**(8): p. 2201-2207.
52. Chesi, M., et al., *Activated fibroblast growth factor receptor 3 is an oncogene that contributes to tumor progression in multiple myeloma.* Blood, 2001. **97**(3): p. 729-36.
53. Knowles, M.A., *Molecular subtypes of bladder cancer: Jekyll and Hyde or chalk and cheese?* Carcinogenesis, 2006. **27**(3): p. 361-73.
54. Wu, X.R., *Urothelial tumorigenesis: a tale of divergent pathways.* Nat Rev Cancer, 2005. **5**(9): p. 713-25.
55. Eswarakumar, V.P., I. Lax, and J. Schlessinger, *Cellular signaling by fibroblast growth factor receptors.* Cytokine Growth Factor Rev, 2005. **16**(2): p. 139-49.
56. Johnson, D.E. and L.T. Williams, *Structural and functional diversity in the FGF receptor multigene family.* Adv Cancer Res, 1993. **60**: p. 1-41.
57. Avivi, A., A. Yayon, and D. Givol, *A novel form of FGF receptor-3 using an alternative exon in the immunoglobulin domain III.* FEBS Lett, 1993. **330**(3): p. 249-52.
58. Chellaiah, A.T., et al., *Fibroblast growth factor receptor (FGFR) 3. Alternative splicing in immunoglobulin-like domain III creates a receptor highly specific for acidic FGF/FGF-1.* J Biol Chem, 1994. **269**(15): p. 11620-7.
59. Ornitz, D.M., et al., *Receptor specificity of the fibroblast growth factor family.* J Biol Chem, 1996. **271**(25): p. 15292-7.
60. Werner, S., et al., *Differential splicing in the extracellular region of fibroblast growth factor receptor 1 generates receptor variants with different ligand-binding specificities.* Mol Cell Biol, 1992. **12**(1): p. 82-8.
61. van Oers, J.M., et al., *Chromosome 9 deletions are more frequent than FGFR3 mutations in flat urothelial hyperplasias of the bladder.* Int J Cancer, 2006. **119**(5): p. 1212-5.
62. Tomlinson, D.C., et al., *FGFR3 protein expression and its relationship to mutation status and prognostic variables in bladder cancer.* J Pathol, 2007. **213**(1): p. 91-8.
63. Jebar, A.H., et al., *FGFR3 and Ras gene mutations are mutually exclusive genetic events in urothelial cell carcinoma.* Oncogene, 2005. **24**(33): p. 5218-25.
64. Hart, K.C., et al., *Transformation and Stat activation by derivatives of FGFR1, FGFR3, and FGFR4.* Oncogene, 2000. **19**(29): p. 3309-20.
65. Oxford, G. and D. Theodorescu, *Ras superfamily monomeric G proteins in carcinoma cell motility.* Cancer Lett, 2003. **189**(2): p. 117-28.
66. Oxford, G. and D. Theodorescu, *The role of Ras superfamily proteins in bladder cancer progression.* J Urol, 2003. **170**(5): p. 1987-93.
67. Adjei, A.A., *Blocking oncogenic Ras signaling for cancer therapy.* J Natl Cancer Inst, 2001. **93**(14): p. 1062-74.
68. Bivona, T.G. and M.R. Philips, *Ras pathway signaling on endomembranes.* Curr Opin Cell Biol, 2003. **15**(2): p. 136-42.

69. Ramjaun, A.R. and J. Downward, *Ras and phosphoinositide 3-kinase: partners in development and tumorigenesis.* Cell Cycle, 2007. **6**(23): p. 2902-5.
70. Burchill, S.A., D.E. Neal, and J. Lunec, *Frequency of H-ras mutations in human bladder cancer detected by direct sequencing.* Br J Urol, 1994. **73**(5): p. 516-21.
71. Cerutti, P., et al., *Mutagenesis of the H-ras protooncogene and the p53 tumor suppressor gene.* Cancer Res, 1994. **54**(7 Suppl): p. 1934s-1938s.
72. Knowles, M.A. and M. Williamson, *Mutation of H-ras is infrequent in bladder cancer: confirmation by single-strand conformation polymorphism analysis, designed restriction fragment length polymorphisms, and direct sequencing.* Cancer Res, 1993. **53**(1): p. 133-9.
73. Saito, S., et al., *Screening of H-ras gene point mutations in 50 cases of bladder carcinoma.* Int J Urol, 1997. **4**(2): p. 178-85.
74. Knowles, M.A., *Role of FGFR3 in urothelial cell carcinoma: biomarker and potential therapeutic target.* World J Urol, 2007. **25**(6): p. 581-93.
75. Cantley, L.C., *The phosphoinositide 3-kinase pathway.* Science, 2002. **296**(5573): p. 1655-7.
76. Carpten, J.D., et al., *A transforming mutation in the pleckstrin homology domain of AKT1 in cancer.* Nature, 2007. **448**(7152): p. 439-44.
77. Eng, C., *PTEN: one gene, many syndromes.* Hum Mutat, 2003. **22**(3): p. 183-98.
78. Launonen, V., *Mutations in the human LKB1/STK11 gene.* Hum Mutat, 2005. **26**(4): p. 291-7.
79. Parsons, D.W., et al., *Colorectal cancer: mutations in a signalling pathway.* Nature, 2005. **436**(7052): p. 792.
80. Philp, A.J., et al., *The phosphatidylinositol 3'-kinase p85alpha gene is an oncogene in human ovarian and colon tumors.* Cancer Res, 2001. **61**(20): p. 7426-9.
81. Samuels, Y. and K. Ericson, *Oncogenic PI3K and its role in cancer.* Curr Opin Oncol, 2006. **18**(1): p. 77-82.
82. Luo, J., B.D. Manning, and L.C. Cantley, *Targeting the PI3K-Akt pathway in human cancer: rationale and promise.* Cancer Cell, 2003. **4**(4): p. 257-62.
83. Shaw, R.J. and L.C. Cantley, *Ras, PI(3)K and mTOR signalling controls tumour cell growth.* Nature, 2006. **441**(7092): p. 424-30.
84. Lopez-Knowles, E., et al., *PIK3CA mutations are an early genetic alteration associated with FGFR3 mutations in superficial papillary bladder tumors.* Cancer Res, 2006. **66**(15): p. 7401-4.
85. Rodriguez-Viciana, P., et al., *Phosphatidylinositol-3-OH kinase as a direct target of Ras.* Nature, 1994. **370**(6490): p. 527-32.
86. Platt, F.M., et al., *Spectrum of phosphatidylinositol 3-kinase pathway gene alterations in bladder cancer.* Clin Cancer Res, 2009. **15**(19): p. 6008-17.
87. Bamford, S., et al., *The COSMIC (Catalogue of Somatic Mutations in Cancer) database and website.* Br J Cancer, 2004. **91**(2): p. 355-8.
88. Sjodahl, G., et al., *A systematic study of gene mutations in urothelial carcinoma; inactivating mutations in TSC2 and PIK3R1.* PLoS One, 2011. **6**(4): p. e18583.
89. Huang, C.H., et al., *The structure of a human p110alpha/p85alpha complex elucidates the effects of oncogenic PI3Kalpha mutations.* Science, 2007. **318**(5857): p. 1744-8.

90. Miled, N., et al., *Mechanism of two classes of cancer mutations in the phosphoinositide 3-kinase catalytic subunit.* Science, 2007. **317**(5835): p. 239-42.
91. Zhao, L. and P.K. Vogt, *Helical domain and kinase domain mutations in p110alpha of phosphatidylinositol 3-kinase induce gain of function by different mechanisms.* Proc Natl Acad Sci U S A, 2008. **105**(7): p. 2652-7.
92. Uchida, T., et al., *p53 mutations and prognosis in bladder tumors.* J Urol, 1995. **153**(4): p. 1097-104.
93. Fujimoto, K., et al., *Frequent association of p53 gene mutation in invasive bladder cancer.* Cancer Res, 1992. **52**(6): p. 1393-8.
94. Spruck, C.H., 3rd, et al., *Two molecular pathways to transitional cell carcinoma of the bladder.* Cancer Res, 1994. **54**(3): p. 784-8.
95. Goebell, P.J., S.G. Groshen, and B.J. Schmitz-Drager, *p53 immunohistochemistry in bladder cancer--a new approach to an old question.* Urol Oncol, 2010. **28**(4): p. 377-88.
96. Malats, N., et al., *P53 as a prognostic marker for bladder cancer: a meta-analysis and review.* Lancet Oncol, 2005. **6**(9): p. 678-86.
97. George, B., et al., *p53 gene and protein status: the role of p53 alterations in predicting outcome in patients with bladder cancer.* J Clin Oncol, 2007. **25**(34): p. 5352-8.
98. Benedict, W.F., et al., *Level of retinoblastoma protein expression correlates with p16 (MTS-1/INK4A/CDKN2) status in bladder cancer.* Oncogene, 1999. **18**(5): p. 1197-203.
99. Shariat, S.F., et al., *p53, p21, pRB, and p16 expression predict clinical outcome in cystectomy with bladder cancer.* J Clin Oncol, 2004. **22**(6): p. 1014-24.
100. Logothetis, C.J., et al., *Altered expression of retinoblastoma protein and known prognostic variables in locally advanced bladder cancer.* J Natl Cancer Inst, 1992. **84**(16): p. 1256-61.
101. Cordon-Cardo, C., et al., *Altered expression of the retinoblastoma gene product: prognostic indicator in bladder cancer.* J Natl Cancer Inst, 1992. **84**(16): p. 1251-6.
102. Hurst, C.D., et al., *Inactivation of the Rb pathway and overexpression of both isoforms of E2F3 are obligate events in bladder tumours with 6p22 amplification.* Oncogene, 2008. **27**(19): p. 2716-27.
103. Steinthorsdottir, V., et al., *A variant in CDKAL1 influences insulin response and risk of type 2 diabetes.* Nat Genet, 2007. **39**(6): p. 770-5.
104. Oeggerli, M., et al., *E2F3 amplification and overexpression is associated with invasive tumor growth and rapid tumor cell proliferation in urinary bladder cancer.* Oncogene, 2004. **23**(33): p. 5616-23.
105. Feber, A., et al., *Amplification and overexpression of E2F3 in human bladder cancer.* Oncogene, 2004. **23**(8): p. 1627-30.
106. Xu, H.J., et al., *Loss of RB protein expression in primary bladder cancer correlates with loss of heterozygosity at the RB locus and tumor progression.* Int J Cancer, 1993. **53**(5): p. 781-4.
107. Takle, L.A. and M.A. Knowles, *Deletion mapping implicates two tumor suppressor genes on chromosome 8p in the development of bladder cancer.* Oncogene, 1996. **12**(5): p. 1083-7.

108. Stoehr, R., et al., *Deletions of chromosome 8p and loss of sFRP1 expression are progression markers of papillary bladder cancer.* Lab Invest, 2004. **84**(4): p. 465-78.
109. Choi, C., et al., *Loss of heterozygosity at chromosome segments 8p22 and 8p11.2-21.1 in transitional-cell carcinoma of the urinary bladder.* Int J Cancer, 2000. **86**(4): p. 501-5.
110. Adams, J., et al., *Loss of heterozygosity analysis and DNA copy number measurement on 8p in bladder cancer reveals two mechanisms of allelic loss.* Cancer Res, 2005. **65**(1): p. 66-75.
111. Kagan, J., et al., *Cluster of allele losses within a 2.5 cM region of chromosome 10 in high-grade invasive bladder cancer.* Oncogene, 1998. **16**(7): p. 909-13.
112. Cappellen, D., et al., *Frequent loss of heterozygosity on chromosome 10q in muscle-invasive transitional cell carcinomas of the bladder.* Oncogene, 1997. **14**(25): p. 3059-66.
113. Aveyard, J.S., et al., *Somatic mutation of PTEN in bladder carcinoma.* Br J Cancer, 1999. **80**(5-6): p. 904-8.
114. Gildea, J.J., et al., *PTEN can inhibit in vitro organotypic and in vivo orthotopic invasion of human bladder cancer cells even in the absence of its lipid phosphatase activity.* Oncogene, 2004. **23**(40): p. 6788-97.
115. Simon, R., et al., *HER-2 and TOP2A coamplification in urinary bladder cancer.* Int J Cancer, 2003. **107**(5): p. 764-72.
116. Sauter, G., et al., *Heterogeneity of erbB-2 gene amplification in bladder cancer.* Cancer Res, 1993. **53**(10 Suppl): p. 2199-203.
117. Miyamoto, H., et al., *C-ERBB-2 gene amplification as a prognostic marker in human bladder cancer.* Urology, 2000. **55**(5): p. 679-83.
118. Lonn, U., et al., *Prognostic value of amplification of c-erb-B2 in bladder carcinoma.* Clin Cancer Res, 1995. **1**(10): p. 1189-94.
119. Coombs, L.M., et al., *Amplification and over-expression of c-erbB-2 in transitional cell carcinoma of the urinary bladder.* Br J Cancer, 1991. **63**(4): p. 601-8.
120. Hirao, S., et al., *Loss of heterozygosity on chromosome 9q and p53 alterations in human bladder cancer.* Cancer, 2005. **104**(9): p. 1918-23.
121. Tsai, Y.C., et al., *Allelic losses of chromosomes 9, 11, and 17 in human bladder cancer.* Cancer Res, 1990. **50**(1): p. 44-7.
122. Linnenbach, A.J., et al., *Characterization of chromosome 9 deletions in transitional cell carcinoma by microsatellite assay.* Hum Mol Genet, 1993. **2**(9): p. 1407-11.
123. Cairns, P., et al., *Rates of p16 (MTS1) mutations in primary tumors with 9p loss.* Science, 1994. **265**(5170): p. 415-7.
124. Williamson, M.P., et al., *p16 (CDKN2) is a major deletion target at 9p21 in bladder cancer.* Hum Mol Genet, 1995. **4**(9): p. 1569-77.
125. Orlow, I., et al., *Deletion of the p16 and p15 genes in human bladder tumors.* J Natl Cancer Inst, 1995. **87**(20): p. 1524-9.
126. Devlin, J., A.J. Keen, and M.A. Knowles, *Homozygous deletion mapping at 9p21 in bladder carcinoma defines a critical region within 2cM of IFNA.* Oncogene, 1994. **9**(9): p. 2757-60.
127. Berggren, P., et al., *Detecting homozygous deletions in the CDKN2A(p16(INK4a))/ARF(p14(ARF)) gene in urinary bladder cancer using real-time quantitative PCR.* Clin Cancer Res, 2003. **9**(1): p. 235-42.

128. Chapman, E.J., et al., *Comprehensive analysis of CDKN2A status in microdissected urothelial cell carcinoma reveals potential haploinsufficiency, a high frequency of homozygous co-deletion and associations with clinical phenotype.* Clin Cancer Res, 2005. **11**(16): p. 5740-7.
129. Luo, J., N.L. Solimini, and S.J. Elledge, *Principles of cancer therapy: oncogene and non-oncogene addiction.* Cell, 2009. **136**(5): p. 823-37.
130. Inoue, K., et al., *Paclitaxel enhances the effects of the anti-epidermal growth factor receptor monoclonal antibody ImClone C225 in mice with metastatic human bladder transitional cell carcinoma.* Clin Cancer Res, 2000. **6**(12): p. 4874-84.
131. Sriplakich, S., S. Jahnson, and M.G. Karlsson, *Epidermal growth factor receptor expression: predictive value for the outcome after cystectomy for bladder cancer?* BJU Int, 1999. **83**(4): p. 498-503.
132. NCT00645593, *Phase II Randomized Trial of Gemcitabine and Cisplatin With or Without Cetuximab in Patients With Urothelial Carcinoma.* 2008.
133. Philips, G.K., et al., *A phase II trial of cisplatin (C), gemcitabine (G) and gefitinib for advanced urothelial tract carcinoma: results of Cancer and Leukemia Group B (CALGB) 90102.* Ann Oncol, 2009. **20**(6): p. 1074-9.
134. Wulfing, C., et al., *A single-arm, multicenter, open-label phase 2 study of lapatinib as the second-line treatment of patients with locally advanced or metastatic transitional cell carcinoma.* Cancer, 2009. **115**(13): p. 2881-90.
135. NCT00949455, *LaMB - maintenance lapatinib versus placebo after first-line chemotherapy in patients with locally advanced or metastatic bladder cancer.* 2011.
136. Matsubara, H., et al., *Potential for HER-2/neu molecular targeted therapy for invasive bladder carcinoma: comparative study of immunohistochemistry and fluorescent in situ hybridization.* Oncol Rep, 2008. **19**(1): p. 57-63.
137. Hansel, D.E., et al., *HER2 overexpression and amplification in urothelial carcinoma of the bladder is associated with MYC coamplification in a subset of cases.* Am J Clin Pathol, 2008. **130**(2): p. 274-81.
138. Park, K., et al., *c-myc amplification is associated with HER2 amplification and closely linked with cell proliferation in tissue microarray of nonselected breast cancers.* Hum Pathol, 2005. **36**(6): p. 634-9.
139. Sonpavde, G., et al., *Sunitinib malate is active against human urothelial carcinoma and enhances the activity of cisplatin in a preclinical model.* Urol Oncol, 2009. **27**(4): p. 391-9.
140. Takeuchi, A., et al., *Sunitinib enhances antitumor effects against chemotherapy-resistant bladder cancer through suppression of ERK1/2 phosphorylation.* Int J Oncol, 2012. **40**(5): p. 1691-6.
141. Gallagher, D.J., et al., *Phase II study of sunitinib in patients with metastatic urothelial cancer.* J Clin Oncol, 2010. **28**(8): p. 1373-9.
142. Multicentre, *A Multicentre Phase II Trial to Determine the Efficacy of the Anti-Tyrosine Kinase Sunitinib (Sutent®) as Second Line Therapy in Patients With Transitional Cell Carcinoma (TCC) of the Urothelium Which Failed or Progressed After First Line Chemotherapy for Advanced or Metastatic Disease.* 2011.

143. Unit, W.C.T., *A Phase II Single-Arm Trial to Evaluate Cisplatin and Gemcitabine Chemotherapy in Combination With Sunitinib for First-Line Treatment of Patients With Advanced Transitional Carcinoma of the Urothelium.* 2010.
144. Galsky, M.D., et al., *Gemcitabine, Cisplatin, and sunitinib for metastatic urothelial carcinoma and as preoperative therapy for muscle-invasive bladder cancer.* Clin Genitourin Cancer, 2013. **11**(2): p. 175-81.
145. Zhu, Z. and L. Witte, *Inhibition of tumor growth and metastasis by targeting tumor-associated angiogenesis with antagonists to the receptors of vascular endothelial growth factor.* Invest New Drugs, 1999. **17**(3): p. 195-212.
146. von Hardenberg, J., et al., *Expression and predictive value of lymph-specific markers in urothelial carcinoma of the bladder.* Urol Oncol, 2014. **32**(1): p. 54.e9-17.
147. Kopparapu, P.K., et al., *Expression of VEGF and its receptors VEGFR1/VEGFR2 is associated with invasiveness of bladder cancer.* Anticancer Res, 2013. **33**(6): p. 2381-90.
148. Henriquez-Hernandez, L.A., et al., *Polymorphisms of glutathione S-transferase mu and theta, MDR1 and VEGF genes as risk factors of bladder cancer: a case-control study.* Urol Oncol, 2012. **30**(5): p. 660-5.
149. Cheng, D., B. Liang, and Y. Li, *Clinical value of vascular endothelial growth factor and endostatin in urine for diagnosis of bladder cancer.* Tumori, 2012. **98**(6): p. 762-7.
150. Bernardini, S., et al., *Serum levels of vascular endothelial growth factor as a prognostic factor in bladder cancer.* J Urol, 2001. **166**(4): p. 1275-9.
151. Bellmunt, J., et al., *Phase II study of sunitinib as first-line treatment of urothelial cancer patients ineligible to receive cisplatin-based chemotherapy: baseline interleukin-8 and tumor contrast enhancement as potential predictive factors of activity.* Ann Oncol, 2011. **22**(12): p. 2646-53.
152. Inoue, K., et al., *Treatment of human metastatic transitional cell carcinoma of the bladder in a murine model with the anti-vascular endothelial growth factor receptor monoclonal antibody DC101 and paclitaxel.* Clin Cancer Res, 2000. **6**(7): p. 2635-43.
153. Sonpavde, G., et al., *Novel agents for muscle-invasive and advanced urothelial cancer.* BJU Int, 2008. **101**(8): p. 937-43.
154. Tomlinson, D.C., et al., *Fibroblast growth factor receptor 1 promotes proliferation and survival via activation of the mitogen-activated protein kinase pathway in bladder cancer.* Cancer Res, 2009. **69**(11): p. 4613-20.
155. Zhu, L., et al., *Fibroblast growth factor receptor 3 inhibition by short hairpin RNAs leads to apoptosis in multiple myeloma.* Mol Cancer Ther, 2005. **4**(5): p. 787-98.
156. Trudel, S., et al., *The inhibitory anti-FGFR3 antibody, PRO-001, is cytotoxic to t(4;14) multiple myeloma cells.* Blood, 2006. **107**(10): p. 4039-46.
157. Qing, J., et al., *Antibody-based targeting of FGFR3 in bladder carcinoma and t(4;14)-positive multiple myeloma in mice.* J Clin Invest, 2009. **119**(5): p. 1216-29.
158. Hadari, Y. and J. Schlessinger, *FGFR3-targeted mAb therapy for bladder cancer and multiple myeloma.* J Clin Invest, 2009. **119**(5): p. 1077-9.

159. di Martino, E., D.C. Tomlinson, and M.A. Knowles, *A Decade of FGF Receptor Research in Bladder Cancer: Past, Present, and Future Challenges.* Adv Urol, 2012. **2012**: p. 429213.
160. Mohammadi, M., et al., *Crystal structure of an angiogenesis inhibitor bound to the FGF receptor tyrosine kinase domain.* EMBO J, 1998. **17**(20): p. 5896-904.
161. Mohammadi, M., et al., *Structures of the tyrosine kinase domain of fibroblast growth factor receptor in complex with inhibitors.* Science, 1997. **276**(5314): p. 955-60.
162. Sarker, D., et al., *A phase I pharmacokinetic and pharmacodynamic study of TKI258, an oral, multitargeted receptor tyrosine kinase inhibitor in patients with advanced solid tumors.* Clin Cancer Res, 2008. **14**(7): p. 2075-81.
163. Lamont, F.R., et al., *Small molecule FGF receptor inhibitors block FGFR-dependent urothelial carcinoma growth in vitro and in vivo.* Br J Cancer, 2011. **104**(1): p. 75-82.
164. Miyake, M., et al., *1-tert-butyl-3-[6-(3,5-dimethoxy-phenyl)-2-(4-diethylamino-butylamino)-pyrido[2,3 -d]pyrimidin-7-yl]-urea (PD173074), a selective tyrosine kinase inhibitor of fibroblast growth factor receptor-3 (FGFR3), inhibits cell proliferation of bladder cancer carrying the FGFR3 gene mutation along with up-regulation of p27/Kip1 and G1/G0 arrest.* J Pharmacol Exp Ther, 2010. **332**(3): p. 795-802.
165. GU12-157, *Dovitinib in BCG Refractory Urothelial Carcinoma With FGFR3 Mutations or Over-expression.* 2012.
166. Andre, F., et al., *Targeting FGFR with Dovitinib (TKI258): Preclinical and Clinical Data in Breast Cancer.* Clin Cancer Res, 2013. **19**(13): p. 3693-3702.
167. NCT00790426, *A Phase II Multi-center, Non-randomized, Open Label Study of TKI258 in FGFR3 Mutated and FGFR3 Wild Type Advanced Urothelial Carcinoma.* 2013.
168. Ciardiello, F. and G. Tortora, *EGFR antagonists in cancer treatment.* N Engl J Med, 2008. **358**(11): p. 1160-74.
169. Sartore-Bianchi, A., et al., *PIK3CA mutations in colorectal cancer are associated with clinical resistance to EGFR-targeted monoclonal antibodies.* Cancer Res, 2009. **69**(5): p. 1851-7.
170. Antonescu, C.R., *Targeted therapy of cancer: new roles for pathologists in identifying GISTs and other sarcomas.* Mod Pathol, 2008. **21 Suppl 2**: p. S31-6.
171. Piccart-Gebhart, M.J., et al., *Trastuzumab after adjuvant chemotherapy in HER2-positive breast cancer.* N Engl J Med, 2005. **353**(16): p. 1659-72.
172. Romond, E.H., et al., *Trastuzumab plus adjuvant chemotherapy for operable HER2-positive breast cancer.* N Engl J Med, 2005. **353**(16): p. 1673-84.
173. Orndal, C., et al., *Cytogenetic evolution in primary tumors, local recurrences, and pulmonary metastases of two soft tissue sarcomas.* Clin Exp Metastasis, 1993. **11**(5): p. 401-8.
174. Levin, N.A., et al., *Identification of novel regions of altered DNA copy number in small cell lung tumors.* Genes Chromosomes Cancer, 1995. **13**(3): p. 175-85.

175. Gagos, S., et al., *Chromosomal markers associated with metastasis in two colon cancer cell lines established from the same patient.* Anticancer Res, 1995. **15**(2): p. 369-78.
176. Baffa, R., et al., *MicroRNA expression profiling of human metastatic cancers identifies cancer gene targets.* J Pathol, 2009. **219**(2): p. 214-21.
177. Bergeron, A., et al., *High frequency of MAGE-A4 and MAGE-A9 expression in high-risk bladder cancer.* Int J Cancer, 2009. **125**(6): p. 1365-71.
178. Bellmunt, J., M. Hussain, and C.P. Dinney, *Novel approaches with targeted therapies in bladder cancer. Therapy of bladder cancer by blockade of the epidermal growth factor receptor family.* Crit Rev Oncol Hematol, 2003. **46 Suppl**: p. S85-104.
179. Dovedi, S.J. and B.R. Davies, *Emerging targeted therapies for bladder cancer: a disease waiting for a drug.* Cancer Metastasis Rev, 2009. **28**(3-4): p. 355-67.
180. Evans, C.P., *Identification of molecular targets in urologic oncology.* World J Urol, 2009. **27**(1): p. 3-8.
181. Fidler, I.J. and M.L. Kripke, *Metastasis results from preexisting variant cells within a malignant tumor.* Science, 1977. **197**(4306): p. 893-5.
182. Clark, E.A., et al., *Genomic analysis of metastasis reveals an essential role for RhoC.* Nature, 2000. **406**(6795): p. 532-5.
183. Ramaswamy, S., et al., *A molecular signature of metastasis in primary solid tumors.* Nat Genet, 2003. **33**(1): p. 49-54.
184. Hovey, R.M., et al., *Genetic alterations in primary bladder cancers and their metastases.* Cancer Res, 1998. **58**(16): p. 3555-60.
185. Bernards, R. and R.A. Weinberg, *A progression puzzle.* Nature, 2002. **418**(6900): p. 823.
186. Weigelt, B., J.L. Peterse, and L.J. van 't Veer, *Breast cancer metastasis: markers and models.* Nat Rev Cancer, 2005. **5**(8): p. 591-602.
187. Klein, C.A., *Parallel progression of primary tumours and metastases.* Nat Rev Cancer, 2009. **9**(4): p. 302-12.
188. Scheel, C., et al., *Adaptation versus selection: the origins of metastatic behavior.* Cancer Res, 2007. **67**(24): p. 11476-9; discussion 11479-80.
189. Jones, T.D., et al., *Clonal origin of lymph node metastases in bladder carcinoma.* Cancer, 2005. **104**(9): p. 1901-10.
190. Cheng, L., et al., *Conserved genetic findings in metastatic bladder cancer: a possible utility of allelic loss of chromosomes 9p21 and 17p13 in diagnosis.* Arch Pathol Lab Med, 2001. **125**(9): p. 1197-9.
191. Miyao, N., et al., *Role of chromosome 9 in human bladder cancer.* Cancer Res, 1993. **53**(17): p. 4066-70.
192. Shariat, S.F., et al., *Cooperative effect of cell-cycle regulators expression on bladder cancer development and biologic aggressiveness.* Mod Pathol, 2007. **20**(4): p. 445-59.
193. Byrne, R.R., et al., *E-cadherin immunostaining of bladder transitional cell carcinoma, carcinoma in situ and lymph node metastases with long-term followup.* J Urol, 2001. **165**(5): p. 1473-9.
194. Malmstrom, P.U., et al., *Early metastatic progression of bladder carcinoma: molecular profile of primary tumor and sentinel lymph node.* J Urol, 2002. **168**(5): p. 2240-4.
195. Jimenez, R.E., et al., *Her-2/neu overexpression in muscle-invasive urothelial carcinoma of the bladder: prognostic significance and*

comparative analysis in primary and metastatic tumors. Clin Cancer Res, 2001. **7**(8): p. 2440-7.
196. Gardmark, T., et al., *Analysis of HER2 expression in primary urinary bladder carcinoma and corresponding metastases.* BJU Int, 2005. **95**(7): p. 982-6.
197. Fleischmann, A., et al., *Her2 amplification is significantly more frequent in lymph node metastases from urothelial bladder cancer than in the primary tumours.* Eur Urol, 2011. **60**(2): p. 350-7.
198. Seiler, R., G.N. Thalmann, and A. Fleischmann, *MMP-2 and MMP-9 in lymph-node-positive bladder cancer.* J Clin Pathol, 2011. **64**(12): p. 1078-82.
199. Seiler, R., et al., *CCND1/CyclinD1 status in metastasizing bladder cancer: a prognosticator and predictor of chemotherapeutic response.* Mod Pathol, 2014. **27**(1): p. 87-95.
200. Kiemeney, L.A., et al., *The clinical epidemiology of superficial bladder cancer. Dutch South-East Cooperative Urological Group.* Br J Cancer, 1993. **67**(4): p. 806-12.
201. Bassi, P., et al., *Prognostic factors of outcome after radical cystectomy for bladder cancer: a retrospective study of a homogeneous patient cohort.* J Urol, 1999. **161**(5): p. 1494-7.
202. Hafner, C., et al., *Evidence for oligoclonality and tumor spread by intraluminal seeding in multifocal urothelial carcinomas of the upper and lower urinary tract.* Oncogene, 2001. **20**(35): p. 4910-5.
203. Sidransky, D., et al., *Clonal origin bladder cancer.* N Engl J Med, 1992. **326**(11): p. 737-40.
204. Li, M. and L.A. Cannizzaro, *Identical clonal origin of synchronous and metachronous low-grade, noninvasive papillary transitional cell carcinomas of the urinary tract.* Hum Pathol, 1999. **30**(10): p. 1197-200.
205. Cheng, L., et al., *Precise microdissection of human bladder carcinomas reveals divergent tumor subclones in the same tumor.* Cancer, 2002. **94**(1): p. 104-10.
206. Takahashi, T., et al., *Distinct microsatellite alterations in upper urinary tract tumors and subsequent bladder tumors.* J Urol, 2001. **165**(2): p. 672-7.
207. Muto, S., et al., *Genetic and epigenetic alterations in normal bladder epithelium in patients with metachronous bladder cancer.* Cancer Res, 2000. **60**(15): p. 4021-5.
208. Hartmann, A., et al., *Clonality and genetic divergence in multifocal low-grade superficial urothelial carcinoma as determined by chromosome 9 and p53 deletion analysis.* Lab Invest, 2000. **80**(5): p. 709-18.
209. Takahashi, T., et al., *Clonal and chronological genetic analysis of multifocal cancers of the bladder and upper urinary tract.* Cancer Res, 1998. **58**(24): p. 5835-41.
210. Denzinger, S., et al., *Improved clonality analysis of multifocal bladder tumors by combination of histopathologic organ mapping, loss of heterozygosity, fluorescence in situ hybridization, and p53 analyses.* Hum Pathol, 2006. **37**(2): p. 143-51.
211. Catto, J.W., et al., *Multifocal urothelial cancers with the mutator phenotype are of monoclonal origin and require panurothelial treatment for tumor clearance.* J Urol, 2006. **175**(6): p. 2323-30.

212. Boland, C.R., et al., *A National Cancer Institute Workshop on Microsatellite Instability for cancer detection and familial predisposition: development of international criteria for the determination of microsatellite instability in colorectal cancer.* Cancer Res, 1998. **58**(22): p. 5248-57.
213. Shibata, D. and L.A. Aaltonen, *Genetic predisposition and somatic diversification in tumor development and progression.* Adv Cancer Res, 2001. **80**: p. 83-114.
214. van Tilborg, A.A., et al., *Molecular evolution of multiple recurrent cancers of the bladder.* Hum Mol Genet, 2000. **9**(20): p. 2973-80.
215. Parmar, M.K., et al., *Prognostic factors for recurrence and followup policies in the treatment of superficial bladder cancer: report from the British Medical Research Council Subgroup on Superficial Bladder Cancer (Urological Cancer Working Party).* J Urol, 1989. **142**(2 Pt 1): p. 284-8.
216. Steidl, C., et al., *Patterns of chromosomal aberrations in urinary bladder tumours and adjacent urothelium.* J Pathol, 2002. **198**(1): p. 115-20.
217. Hartmann, A., et al., *Frequent genetic alterations in simple urothelial hyperplasias of the bladder in patients with papillary urothelial carcinoma.* Am J Pathol, 1999. **154**(3): p. 721-7.
218. Nowell, P.C., *The clonal evolution of tumor cell populations.* Science, 1976. **194**(4260): p. 23-8.
219. Nowell, P.C., *Mechanisms of tumor progression.* Cancer Res, 1986. **46**(5): p. 2203-7.
220. Hittelman, W.N., *Clones and subclones in the lung cancer field.* J Natl Cancer Inst, 1999. **91**(21): p. 1796-9.
221. Hittelman, W.N., et al., *Detection of chromosome instability of tissue fields at risk: in situ hybridization.* J Cell Biochem Suppl, 1996. **25**: p. 57-62.
222. Lee, J.J., et al., *Predicting cancer development in oral leukoplakia: ten years of translational research.* Clin Cancer Res, 2000. **6**(5): p. 1702-10.
223. Mao, L., et al., *Clonal genetic alterations in the lungs of current and former smokers.* J Natl Cancer Inst, 1997. **89**(12): p. 857-62.
224. Simon, R., et al., *Cytogenetic analysis of multifocal bladder cancer supports a monoclonal origin and intraepithelial spread of tumor cells.* Cancer Res, 2001. **61**(1): p. 355-62.
225. Albertson, D.G., et al., *Quantitative mapping of amplicon structure by array CGH identifies CYP24 as a candidate oncogene.* Nat Genet, 2000. **25**(2): p. 144-6.
226. Wilhelm, M., et al., *Array-based comparative genomic hybridization for the differential diagnosis of renal cell cancer.* Cancer Res, 2002. **62**(4): p. 957-60.
227. Weigelt, B., et al., *Challenges translating breast cancer gene signatures into the clinic.* Nat Rev Clin Oncol, 2012. **9**(1): p. 58-64.
228. Andre, F., S. Delaloge, and J.C. Soria, *Biology-driven phase II trials: what is the optimal model for molecular selection?* J Clin Oncol, 2011. **29**(10): p. 1236-8.
229. Fearon, E.R. and B. Vogelstein, *A genetic model for colorectal tumorigenesis.* Cell, 1990. **61**(5): p. 759-67.
230. Lurkin, I., et al., *Two multiplex assays that simultaneously identify 22 possible mutation sites in the KRAS, BRAF, NRAS and PIK3CA genes.* PLoS One, 2010. **5**(1): p. e8802.

231. Hurst, C.D., et al., *A SNaPshot assay for the rapid and simple detection of four common hotspot codon mutations in the PIK3CA gene.* BMC Res Notes, 2009. **2**: p. 66.
232. van Oers, J.M., et al., *A simple and fast method for the simultaneous detection of nine fibroblast growth factor receptor 3 mutations in bladder cancer and voided urine.* Clin Cancer Res, 2005. **11**(21): p. 7743-8.
233. Dean, F.B., et al., *Rapid amplification of plasmid and phage DNA using Phi 29 DNA polymerase and multiply-primed rolling circle amplification.* Genome Res, 2001. **11**(6): p. 1095-9.
234. Fiegler, H., et al., *DNA microarrays for comparative genomic hybridization based on DOP-PCR amplification of BAC and PAC clones.* Genes Chromosomes Cancer, 2003. **36**(4): p. 361-74.
235. Hurst, C.D., et al., *Novel tumor subgroups of urothelial carcinoma of the bladder defined by integrated genomic analysis.* Clin Cancer Res, 2012. **18**(21): p. 5865-77.
236. Jong, K., et al., *Breakpoint identification and smoothing of array comparative genomic hybridization data.* Bioinformatics, 2004. **20**(18): p. 3636-7.
237. Letouze, E., et al., *Analysis of the copy number profiles of several tumor samples from the same patient reveals the successive steps in tumorigenesis.* Genome Biol, 2010. **11**(7): p. R76.
238. Studer, U.E., et al., *Experience in 100 patients with an ileal low pressure bladder substitute combined with an afferent tubular isoperistaltic segment.* J Urol, 1995. **154**(1): p. 49-56.
239. Fleischmann, A., et al., *Extracapsular extension of pelvic lymph node metastases from urothelial carcinoma of the bladder is an independent prognostic factor.* J Clin Oncol, 2005. **23**(10): p. 2358-65.
240. Sobin, L.H., P. Hermanek, and R.V. Hutter, *TNM classification of malignant tumors. A comparison between the new (1987) and the old editions.* Cancer, 1988. **61**(11): p. 2310-4.
241. Kononen, J., et al., *Tissue microarrays for high-throughput molecular profiling of tumor specimens.* Nat Med, 1998. **4**(7): p. 844-7.
242. Richter, J., et al., *High-throughput tissue microarray analysis of cyclin E gene amplification and overexpression in urinary bladder cancer.* Am J Pathol, 2000. **157**(3): p. 787-94.
243. Simon, R., et al., *Patterns of chromosomal imbalances in muscle invasive bladder cancer.* Int J Oncol, 2000. **17**(5): p. 1025-9.
244. Simon, R., et al., *Chromosomal aberrations associated with invasion in papillary superficial bladder cancer.* J Pathol, 1998. **185**(4): p. 345-51.
245. Richter, J., et al., *Marked genetic differences between stage pTa and stage pT1 papillary bladder cancer detected by comparative genomic hybridization.* Cancer Res, 1997. **57**(14): p. 2860-4.
246. Voorter, C., et al., *Detection of chromosomal imbalances in transitional cell carcinoma of the bladder by comparative genomic hybridization.* Am J Pathol, 1995. **146**(6): p. 1341-54.
247. Kallioniemi, A., et al., *Identification of gains and losses of DNA sequences in primary bladder cancer by comparative genomic hybridization.* Genes Chromosomes Cancer, 1995. **12**(3): p. 213-9.
248. Turo, R., et al., *FGFR3 expression in primary invasive bladder cancers and matched lymph node metastases.* J Urol, 2015. **193**(1): p. 325-30.

249. Conconi, D., et al., *DNA copy number alterations and PPARG amplification in a patient with multifocal bladder urothelial carcinoma.* BMC Res Notes, 2012. **5**: p. 607.
250. Zuiverloon, T.C., et al., *Fibroblast growth factor receptor 3 mutation analysis on voided urine for surveillance of patients with low-grade non-muscle-invasive bladder cancer.* Clin Cancer Res, 2010. **16**(11): p. 3011-8.
251. Lindgren, D., et al., *Recurrent and multiple bladder tumors show conserved expression profiles.* BMC Cancer, 2008. **8**: p. 183.
252. Knowles, M.A., *Molecular pathogenesis of bladder cancer.* Int J Clin Oncol, 2008. **13**(4): p. 287-97.
253. Hoglund, M., *Bladder cancer, a two phased disease?* Semin Cancer Biol, 2007. **17**(3): p. 225-32.
254. Hoglund, M., *On the origin of syn- and metachronous urothelial carcinomas.* Eur Urol, 2007. **51**(5): p. 1185-93; discussion 1193.
255. Richter, J., et al., *Patterns of chromosomal imbalances in advanced urinary bladder cancer detected by comparative genomic hybridization.* Am J Pathol, 1998. **153**(5): p. 1615-21.
256. von Knobloch, R., et al., *Allelic changes at multiple regions of chromosome 5 are associated with progression of urinary bladder cancer.* J Pathol, 2000. **190**(2): p. 163-8.
257. Bohm, M., et al., *Deletion analysis at the DEL-27, APC and MTS1 loci in bladder cancer: LOH at the DEL-27 locus on 5p13-12 is a prognostic marker of tumor progression.* Int J Cancer, 1997. **74**(3): p. 291-5.
258. Miyamoto, H., et al., *Loss of heterozygosity at the p53, RB, DCC and APC tumor suppressor gene loci in human bladder cancer.* J Urol, 1996. **155**(4): p. 1444-7.
259. Koo, S.H., et al., *Detection of genetic alterations in bladder tumors by comparative genomic hybridization and cytogenetic analysis.* Cancer Genet Cytogenet, 1999. **110**(2): p. 87-93.
260. Knowles, M.A., M.E. Shaw, and A.J. Proctor, *Deletion mapping of chromosome 8 in cancers of the urinary bladder using restriction fragment length polymorphisms and microsatellite polymorphisms.* Oncogene, 1993. **8**(5): p. 1357-64.
261. Hodgson, J.G., et al., *Genome amplification of chromosome 20 in breast cancer.* Breast Cancer Res Treat, 2003. **78**(3): p. 337-45.
262. Bruch, J., et al., *Chromosomal changes during progression of transitional cell carcinoma of the bladder and delineation of the amplified interval on chromosome arm 8q.* Genes Chromosomes Cancer, 1998. **23**(2): p. 167-74.
263. Bruch, J., et al., *Delineation of the 6p22 amplification unit in urinary bladder carcinoma cell lines.* Cancer Res, 2000. **60**(16): p. 4526-30.
264. Wu, Q., et al., *Amplification and overexpression of the ID4 gene at 6p22.3 in bladder cancer.* Mol Cancer, 2005. **4**(1): p. 16.
265. Evans, A.J., et al., *Defining a 0.5-mb region of genomic gain on chromosome 6p22 in bladder cancer by quantitative-multiplex polymerase chain reaction.* Am J Pathol, 2004. **164**(1): p. 285-93.
266. Knowles, M.A., *Bladder cancer subtypes defined by genomic alterations.* Scand J Urol Nephrol Suppl, 2008(218): p. 116-30.

267. Louhelainen, J., H. Wijkstrom, and K. Hemminki, *Allelic losses demonstrate monoclonality of multifocal bladder tumors.* Int J Cancer, 2000. **87**(4): p. 522-7.
268. Chern, H.D., et al., *Clonal analysis of human recurrent superficial bladder cancer by immunohistochemistry of P53 and retinoblastoma proteins.* J Urol, 1996. **156**(5): p. 1846-9.
269. Stoehr, R., et al., *Deletions of chromosomes 9 and 8p in histologically normal urothelium of patients with bladder cancer.* Eur Urol, 2005. **47**(1): p. 58-63.
270. Chow, N.H., et al., *Papillary urothelial hyperplasia is a clonal precursor to papillary transitional cell bladder cancer.* Int J Cancer, 2000. **89**(6): p. 514-8.
271. Obermann, E.C., et al., *Frequent genetic alterations in flat urothelial hyperplasias and concomitant papillary bladder cancer as detected by CGH, LOH, and FISH analyses.* J Pathol, 2003. **199**(1): p. 50-7.
272. Matsumoto, M., et al., *Fibroblast growth factor receptor 3 protein expression in urothelial carcinoma of the urinary bladder, exhibiting no association with low-grade and/or non-invasive lesions.* Oncol Rep, 2004. **12**(5): p. 967-71.
273. Mhawech-Fauceglia, P., et al., *FGFR3 and p53 protein expressions in patients with pTa and pT1 urothelial bladder cancer.* Eur J Surg Oncol, 2006. **32**(2): p. 231-7.
274. Gomez-Roman, J.J., et al., *Fibroblast growth factor receptor 3 is overexpressed in urinary tract carcinomas and modulates the neoplastic cell growth.* Clin Cancer Res, 2005. **11**(2 Pt 1): p. 459-65.
275. Wolff, A.C., et al., *Recommendations for human epidermal growth factor receptor 2 testing in breast cancer: american society of clinical oncology/college of american pathologists clinical practice guideline update.* J Clin Oncol, 2013. **31**(31): p. 3997-4013.
276. Yaziji, H., et al., *HER-2 testing in breast cancer using parallel tissue-based methods.* JAMA, 2004. **291**(16): p. 1972-7.
277. Sauter, G., et al., *Guidelines for human epidermal growth factor receptor 2 testing: biologic and methodologic considerations.* J Clin Oncol, 2009. **27**(8): p. 1323-33.
278. Guancial, E.A., et al., *FGFR3 expression in primary and metastatic urothelial carcinoma of the bladder.* Cancer Med, 2014. **3**(4): p. 835-44.
279. Sung, J.Y., et al., *FGFR3 overexpression is prognostic of adverse outcome for muscle-invasive bladder carcinoma treated with adjuvant chemotherapy.* Urol Oncol, 2014. **32**(1): p. 49 e23-31.
280. Navin, N., et al., *Inferring tumor progression from genomic heterogeneity.* Genome Res, 2010. **20**(1): p. 68-80.
281. Wood, H.M., et al., *Using next-generation sequencing for high resolution multiplex analysis of copy number variation from nanogram quantities of DNA from formalin-fixed paraffin-embedded specimens.* Nucleic Acids Res, 2010. **38**(14): p. e151.